ATTACHMENT (1)

BACKGROUND AND ANALYSIS

Calvert Cliffs Nuclear Power Plant, Inc.
September 30, 2003

BACKGROUND

The primary purpose of the spent fuel pool (SFP) is to maintain the spent fuel assemblies in a safe storage condition. Per 10 CFR 50.68, if no credit for soluble boron is taken, the k-effective of the spent fuel storage racks loaded with fuel of the maximum fuel assembly reactivity must not exceed 0.95, at a 95% probability, 95% confidence level, if flooded with unborated water. If credit is taken for soluble boron, the k-effective of the spent fuel storage racks loaded with fuel of the maximum fuel assembly reactivity must not exceed 0.95, at a 95% probability, 95% confidence level, if flooded with borated water, and the k-effective must remain below 1.0 (subcritical) at a 95% probability, 95% confidence level, if flooded with unborated water. In addition, the maximum nominal U-235 enrichment of the fresh fuel assemblies is limited to 5.0 weight percent.

The current Technical Specifications limit the maximum enrichment for standard fuel assemblies based on an older pellet design utilizing smaller pellet diameters and stack densities to 4.52 weight percent U-235. The corresponding maximum enrichment for value added pellet (VAP) fuel assemblies utilizing larger pellet diameters and stack densities is limited to 4.30 weight percent U-235 with the present storage configuration and with no credit for soluble boron. Note that VAP fuel is more reactive than similarly enriched standard fuel, thus any analysis performed for VAP fuel conservatively bounds that for standard fuel.

The current analyses for the Unit 2 SFP assume the presence of Boraflex poison sheets with 4" staggered gaps. However, possible boraflex degradation in the Unit 2 SFP was calculated using the Racklife software package. The Racklife results indicated that at certain highly-irradiated locations the degradation could be as high as 70%. An evaluation was performed to determine Calvert Cliffs' compliance with Technical Specification 4.3.1.1, which states that k-effective must be less than or equal to 0.95 if fully flooded with unborated water including an allowance for uncertainties and biases as described in the Calvert Cliffs Updated Final Safety Analysis Report. Crediting burnup in lieu of Boraflex assures that the Technical Specification k-effective limit of 0.95 is maintained. Each assembly offloaded from either reactor or from an Independent Spent Fuel Storage Installation dry shielded canister must be evaluated against the burnup restrictions to determine if it can be safely stored in the Unit 2 SFP. No similar restrictions exist on the Unit 1 SFP.

This submittal documents the Calvert Cliffs SFP Rack Criticality Methodology that was used to ensure k-effective for the Unit 2 SFP is less than the 10 CFR 50.68 regulatory limit for VAP fuel. The soluble boron credit will be limited to 300 ppm per the restrictions of the Unit 1 criticality analysis documented in Reference (1). Note that 300 ppm is a minimum boron concentration requirement. The proposed change to Technical Specification 4.3.1 adds approximately 15 percent to this value to account for any unknown uncertainties. This increases the boron level to 350 ppm required to safely store 5.0 weight percent VAP fuel in the SFP.

Several checkerboard fuel patterns were modeled in an effort to determine if more reactive fuel can be stored in the Unit 2 SFP while meeting the requirements of 10 CFR 50.68. This will require that a fuel assembly that does not have sufficient burnup to satisfy the reactivity requirements must be surrounded on all four adjacent faces by empty rack cells or other non-reactive materials (e.g., wall, water, etc.).

The calculation contained in Attachment (5) documents the Calvert Cliffs SFP Rack Criticality Methodology. This calculation shows that the spent fuel pool rack multiplication factor, k-effective, is less than the 10 CFR 50.68 regulatory limit with 5.0 weight percent VAP fuel and with credit for soluble boron and burnup in the Unit 2 SFP. The proposed change will add Technical Specification 3.7.17

"Spent Fuel Pool Storage" to provide the necessary configuration controls. The proposed Technical Specification conforms to the Improved Standard Technical Specifications.

An additional consideration needed to allow the credit of the soluble boron is the negative reactivity required to ensure that acceptable levels of subcriticality are maintained, assuming a design basis event occurs. For spent fuel storage, we must consider credible boron dilution events. The analysis for the boron dilution events determined what the minimum SFP boron concentration needs to be at the start of a credible event in order to ensure the boron concentration does not go below 350 ppm. The proposed changes will add Technical Specification 3.7.16, "Spent Fuel Pool Boron Concentration," to the Unit 2 Technical Specifications to provide sufficient negative reactivity to ensure acceptable levels of subcriticality for spent fuel storage assuming a dilution event. Technical Specification 3.7.16 was proposed for the Unit 1 Technical Specifications as part of the proposed change described in Reference (1). A minimum SFP boron concentration of 2000 ppm supports the normal and accident boron assumptions in the required calculations (see Attachment 6). With credit being taken for soluble boron in the SFP, a Surveillance Requirement will be included in Technical Specification 3.7.16 to ensure the appropriate minimum concentration of soluble boron is maintained in the SFP for both normal and accident conditions. The proposed Surveillance Requirement to verify the SFP boron concentration is appropriate because no major replacement of pool water is expected to take place over a short period of time. This proposed Surveillance Requirement Frequency conforms to the Improved Standard Technical Specification Frequency.

SYSTEM DESIGN

The SFP is a large rectangular structure that holds the spent fuel assemblies from the reactors in both units. Each half of the pool is 54 feet long, 25 feet wide, and approximately 39 feet deep (the floor elevation varies). Borated water fills the SFP and completely covers the spent fuel assemblies. The SFP is constructed of reinforced concrete 5-1/2 to 6 feet in thickness and is lined with a 3/16-inch stainless steel liner that serves as a leakage barrier. A 3-1/2 foot dividing wall separates the SFP, with the north half being associated with Unit 1 and the south half associated with Unit 2. A slot in the dividing wall has a removable gate that allows movement of fuel assemblies between the two halves of the pool. The SFP is located in the Auxiliary Building between the two containment structures. Each half of the SFP is equipped with vertical spent fuel racks installed on the pool bottom. The fuel rack cells are individual double-walled containers approximately 14 feet high. The inner wall of each cell is made from a 0.06-inch thick sheet of stainless steel formed into a square cross-section container, indented on the corners, with an inside dimension of 8.56 inches. The outer or external wall is also formed from a stainless steel sheet 0.06 inches thick.

Plates of borated, neutron absorbing material are inserted between the two cell walls, in each of the four spaces formed by the indentations in the inner wall. The plates are made of a composite material (Boraflex) consisting mainly of boron carbide (B_4C) and are 6.5 inches wide by 0.08 inches thick. Each plate originally contained at least 0.020 grams of boron-10 per square centimeter of plate. Although Calvert Cliffs has a coupon surveillance program that confirms the integrity of the Boraflex material, possible Boraflex degradation in the Unit 2 SFP was calculated using the Racklife software package. Therefore, Boraflex was not credited in the Unit 2 criticality analysis. The spacing between the cells is maintained at 10 3/32 inches, center-to-center, by external sheets and welded spacers. The original SFP design used boron plate inserts and assembly spacing to help maintain the SFP assemblies in a subcritical condition. The Unit 2 SFP racks are vertical cells grouped in ten 10x10 modules.

The racks are designed to withstand all anticipated loadings. Structural deformations are limited to preclude any possibility of criticality. The Seismic Category 1 racks are supported in such a manner as to

preclude a reduction in separation under either the Operating Basis or Safe Shutdown Earthquake. The racks are designed not to collapse or bow under the force of a fuel assembly dropped into an empty cavity or dropped horizontally across the top of the racks assuming no drag resistance from the water. Heavy loads in excess of 1600 lbs are prohibited from travel over spent fuel assemblies in the SFP unless such loads are handled by a single-failure proof device. The Spent Fuel Cask Handling Crane, which is designed in accordance with the single-failure proof criteria of NUREG-0554 and NUREG-0612, is used to handle heavy loads in the SFP area. Thus, a cask or heavy object drop accident is not a credible event.

CRITICALITY ANALYSIS

The fuel assemblies contain uranium dioxide (UO_2) over the entire length of the active fuel region in each fuel rod and a uniform distribution of enrichments both radially and axially. The fuel and 14x14 assembly parameters for Westinghouse/Combustion Engineering standard and VAP fuel designs are detailed in the Calvert Cliffs Updated Final Safety Analysis Report. Since the VAP fuel design is more limiting, all calculations performed in this work will model VAP assemblies.

The VAP fuel is contained in a 14x14 assembly array. The VAP fuel rods were modeled with six different clad materials (Zirlo, Optin, Zirc-4, low tin Zirlo, Alloy A, and M5) to maximize assembly reactivity. No shims were modeled in the fuel assemblies.

Burnable Absorbers

NUREG/CR-6760 details the effect of Integral Burnable Absorbers (IBAs) on reactivity as a function of burnup, fuel enrichment, IBA number and loading, and cooling time. Integral Burnable Absorbers are burnable poisons that are an integral part of the fuel assembly. Two types are detailed. The first is the Westinghouse Integral Fuel Burnable Absorber (IFBA), which has a coating of zirconium diboride (ZrB_2) on the fuel pellets and which does not displace fuel. The second includes UO_2-Gd_2O_3 rods, UO_2-Er_2O_3 rods, and Al_2O_3-B_4C rods, which do displace fuel. For pressurized water reactor (PWR) fuels without IBAs, reactivity decreases with burnup in a nearly linear fashion. For PWR fuel assembly designs that make significant use of IBAs, reactivity actually increases as fuel burnup increases, reaching a maximum at a burnup where the IBA is nearly depleted (approximately one third of the assembly life), and then decreases with burnup almost linearly. The presence of IBAs during depletion hardens the neutron spectrum, resulting in lower U-235 depletion and higher production of fissile plutonium isotopes. Enhanced plutonium production and the concurrent diminished fission of U-235 can increase the reactivity of the fuel at later burnups. However, the analyses of NUREG/CR-6760 conclusively demonstrate that with the exception of the Westinghouse IFBA rods, k-effective for an assembly without IBAs is always greater (throughout burnup) than k-effective for an assembly with IBAs, including UO_2-Gd_2O_3 rods, UO_2-Er_2O_3 rods, and Al_2O_3-B_4C rods. The negative reactivity effect of the IBAs was found to increase with increasing poison loading (the number of poison rods and the absorber content) and with increasing initial fuel enrichment. This is due to the negative residual effect associated with the neutron-absorbing isotopes and with the reduced reactivity due to the reduction in fissile isotopes. Therefore, for those IBAs other than IFBAs, burnup credit criticality safety analyses may conservatively neglect the presence of the IBAs by assuming non-poisoned equivalent enrichment fuel. Two-dimensional radially-infinite calculations have demonstrated that the neutron multiplication factor is slightly greater for assembly designs with IFBA rods (maximum of 0.4%Δk). Similar reactivity behavior as a function of IBA loading is observed for Calvert Cliffs-specific VAP fuel. Since the non-poisoned equivalent enriched fuel is more reactive than the poisoned fuel, our burnup criticality safety analysis assumed non-poisoned equivalent enriched fuel to assure conservative results.

Reactivity Equivalency

The spent fuel inventory subsequent to the decay of the short-lived Xe-135 isotope is typically used within the storage pool geometry to determine a fresh fuel enrichment that provides the same reactivity as the spent fuel inventory. This Reactivity Equivalent Fresh Fuel Enrichment (REFFE) is then used within a criticality safety analysis code to perform the actual safety analysis. The acceptability of this practice can be demonstrated, provided the environment in which the REFFE is determined remains unchanged (e.g., an infinite array of identical storage rack cells in unborated water). However, if the REFFE is determined based on a reference configuration and employed in the analysis of another condition, erroneous estimations of reactivity may result. The use of REFFE can be shown to produce nonconservative results when used in the presence of soluble boron. These results show increasing nonconservatism with increasing soluble boron concentration and with increasing burnup. The soluble boron in the water is an effective thermal neutron absorber. Because of its negative reactivity worth, the presence of soluble boron reduces the relative reactivity worth of the fission products and actinide absorbers. The fission product and actinide absorbers have greater negative reactivity worth in the unborated reference condition in which the REFFE was determined, resulting in a lower prediction of the REFFE reactivity value. When a REFFE assembly is placed in a checkerboard configuration with a more reactive assembly, the REFFE approach yields nonconservative results. When comparing the reference infinite configuration to a configuration in which the reference assembly is stored with higher-reactivity fuel, the reactivity of the latter configuration is controlled by the higher-reactivity fuel. Physically, the maximum reactivity or fission density for this latter configuration occurs in the higher-reactivity fuel, with the lower-reactivity fuel acting in a supplementary manner. Therefore, the fission products and actinide absorbers have less relative negative reactivity worth in this configuration (as compared to the reference configuration), because they are not physically located where the fission density is maximum. Because of the possible nonconservatisms referenced above, reactivity equivalence was not used in this evaluation.

Source Terms

The source-term portion of this evaluation employs SAS2H, a functional module in the SCALE system, to calculate the burnup-dependent source terms for the Unit 2 SFP system. The SAS2H control module performs the depletion/decay analysis using well-established codes and data libraries provided in the SCALE system. Problem-dependent resonance processing of neutron cross-sections is performed using the Bondarenko resonance self-shielding module BONAMI-S and the Nordheim Integral Treatment resonance self-shielding module NITAWL-II. The XSDRNPM-S module is used to produce spectral weighted and collapsed cross-sections for the fuel depletion calculations. COUPLE updates the cross-section constants included in an ORIGEN-S nuclear data library with data from the cell-weighted cross-section library produced by XSDRNPM-S. The weighting spectrum computed by XSDRNPM-S is applied to update all nuclides in the ORIGEN-S library that were not specified in the XSDRNPM-S analysis. The point-depletion ORIGEN-S module is used to compute time-dependent concentrations and source terms for isotopes simultaneously generated and depleted through neutronic transmutation, fission, and radioactive decay. The cross-section library 44GROUPNDF5 was utilized in this evaluation. The cross-section 44GROUPNDF5 is a 44-energy group library derived from the latest ENDF/B-V files with the exception of O-16, Eu-154, and Eu-155, which were taken from the more improved ENDF/B-VI files.

Regulatory guidance dictates that a reactivity uncertainty, due to uncertainty in the fuel depletion calculation, should be developed and combined with other calculational uncertainties. Although SAS2H is benchmarked to the Calvert Cliffs Unit 2 Cycle 14 environmental qualification radioactive source terms and to the measured data in ORNL/TM-12667, no reactivity biases or uncertainties were determined. In the absence of any other determination of the depletion uncertainty, an uncertainty equal to 5% of the reactivity decrement to the burnup of interest is an acceptable assumption. Thus, for 5.0 weight percent

fuel burned to 70 GWD/MTU, a worst case uncertainty value of 0.02089 was calculated and was used in all burnup related reactivity calculations. Comparisons against the radiochemical assay (RCA) data of Calvert Cliffs fuel presented in ORNL/TM-12667 and PNNL-13667 were also performed. The results indicate that the isotopic compositions predicted for Calvert Cliffs fuel by SAS2H produce conservative values of k-effective [k(SAS2H) > k(RCA)]. The reactivity of a SAS2H-generated system is more conservative by 0.358% Δk than an RCA-normalized system. An independent comparison performed by Bechtel SAIC and reported at the 2002 ANS Winter Meeting, also shows a similar result. Thus, use of the 0.02089 uncertainty was extremely conservative.

The SAS2H employs multiple steps (paths) at specified burnup intervals to produce a burnup dependent cross-section library for use in the ORIGEN-S depletion. The model used in SAS2H Path A represents the fuel as an infinite lattice of fuel pins. Cell-weighted cross-sections are produced by this model and are then applied to the fuel zone of the Path B model.

The model applied to SAS2H Path B is a larger unit cell model used to represent part of an assembly within an infinite lattice. The concept of using cell-weighted data in the 1-D XSDRNPM-S analysis of Path B is an appropriate method for evaluating heterogeneity effects found in fuel pin lattices. The Path B model is used by SAS2H to generate few-group, cell-weighted cross-sections for ORIGEN-S, and to calculate the neutron flux for an assembly-averaged fuel region that is used to update the ORIGEN-S spectral parameters for isotopes not explicitly included in the cell model. The essential rule in deriving the zone radii is to maintain the relative volumes in the actual assembly.

Additional conservative assumptions utilized in the SAS2H isotopics generation are as follows:

1) A decrease in refueling downtime results in less Pu-241 decay to Am-241, which results in increased reactivity. A 100 hour decay time at end-of-life per Technical Specifications is conservatively assumed.

2) A significant spatial variation exists in the fuel temperature because of the low thermal conductivity of UO_2. The fuel temperature is highest at the pellet centerline and lowest at the pellet outside diameter. In addition, the fuel temperature varies axially due to different linear heat generation rates at different axial positions. An increase in fuel temperature increases the resonance capture of neutrons in U-238 due to Doppler effect, which results in increased production of fissile plutonium and actinide absorbers. This, in turn, causes more fissions in fissile plutonium and leads to less depletion in U-235. The net effect is increased reactivity with an increase in fuel temperature. It is thus desirable to select a value for fuel temperature that estimates the highest average temperature that an assembly has experienced. The fuel temperature used is the highest axially-averaged fuel temperature, based on the rated linear power multiplied by the radial peaking factor limit. The bounding fuel temperature was calculated as a function of burnup for a T_{hot} value of 601°F, a core thermal power of 2970 MWt (2700 MWt times a 10% power uprate), and a radial peaking factor of 1.65. The peak fuel temperature value of 1285.42°K at zero burnup was conservatively employed in all SAS2H calculations.

3) The moderator temperature is lowest at the reactor inlet and increases monotonically as it reaches the reactor outlet. This increase in moderator temperature is greater in a hot channel where the heat generation is higher than the average. Neutron spectral hardening occurs with an increase in moderator temperature due to fewer hydrogen nuclides that thermalize fast neutrons past the resonance region. An increase in resonance capture of neutrons in U-238 due to the hardened spectrum results in increased production of fissile plutonium and actinide absorbers. This, in turn, causes more fissions in fissile plutonium and leads to less depletion in U-235. The net effect is

increased reactivity with an increase in moderator temperature. The moderator temperature increases from the bottom to the top of the reactor core. Thus, the use of the average core outlet temperature conservatively bound the moderator temperature. Applying the average core outlet temperature over the entire fuel length and for the entire depletion time provides adequate assurance of bounding treatment. An average core outlet temperature of 601°F or 589.26°K with a corresponding water density of 0.6905 gm/cc was conservatively employed in all SAS2H calculations.

4) The concentration of soluble boron is adjusted to maintain core criticality. The soluble boron concentration is gradually decreased as the burnup increases and reaches a minimum value at the end-of-cycle. The soluble boron present in the moderator increases the thermal absorption cross-section, decreases the thermal flux, and results in a hardened neutron spectrum. An increase in resonance capture of neutrons in U-238 due to the hardened spectrum results in increased production of fissile plutonium and actinide absorbers. This, in turn, causes more fissions in fissile plutonium and leads to less depletion in U-235. The net effect is increased reactivity with an increase in soluble boron concentration. The maximum average boron concentration is to be identified and used in the SAS2H depletion analysis. The maximum beginning-of-cycle soluble boron concentration is less than 1820 ppm. Thus a bounding beginning-of-cycle soluble boron concentration of 1900 ppm was conservatively assumed with a linear letdown curve, resulting in a maximum average soluble boron concentration of 950 ppm.

5) The reactivity results were shown to be only slightly power-dependent. The reactivity tends to increase slightly with decreasing assembly power. Thus the core-averaged assembly power of 12.442 MW (2700 MWt/217 assemblies) was utilized in this work.

6) Per regulatory guidance, the SFP storage rack should be evaluated with spent fuel at the highest reactivity following removal from the reactor (usually after the decay of Xe-135). Thus the SAS2H-generated Xe-135 concentration was conservatively set to zero.

The edited actinides include the important nuclides included in the benchmark comparisons.

U-234	U-235	U-238	NP-237	PU-238	PU-239	PU-240
PU-241	PU-242	AM-241	CM-242	CM-243	CM-244	

The edited fission products include the important nuclides included in the benchmark comparisons.

KR-83	KR-84	KR-86	MO-95	TC-99	RU-101	RH-103	
AG-109	SN-126	I-129	XE-131	XE-132	CS-133	XE-134	
CS-134	CS-135	CS-137	ND-143	ND-144	ND-145	ND-146	
PM-147	SM-147	ND-148	SM-148	SM-149	ND-150	SM-150	
SM-151	EU-151	SM-152	EU-153	EU-154	GD-154	EU-155	GD-155

The SCALE 4.4 CSAS25 code module with the 44 group ENDF/B-V cross-section library, 44GROUPNDF5, was utilized in this work to perform the KENO criticality calculations. CSAS25 uses the SCALE Material Information Process and the associated material composition library to calculate material number densities, to prepare geometry data for resonance self-shielding, and to create data input files for the cross-section processing codes, BONAMI and NITAWL-II. The CSAS25 sequence then invokes the KENO-Va Monte Carlo criticality code. The lattice-type is LATTICECELL

SQUAREPITCH, assuming cylindrical rods in a square pitch and using the VAP dimensions. The number of generations per case is 1010, while the number of particles per generation and the number of skipped generations are 600 and 10, respectively. This is identical to the modeling methodology used in the validation effort.

Most of the criticality computations model a single assembly in a storage cell with reflective boundary conditions on all surfaces to simulate an array of infinite axial and radial extent. Eccentric positioning uncertainties were modeled with a ten-by-ten array of storage cells with mirror boundary conditions on all surfaces to simulate a ten-by-ten array of infinite axial and radial extent. The assembly drop accident was simulated with a model of the entire Unit 2 SFP in both the normal and reconstitution configuration.

Benchmarking

Regulatory guidance dictates the analysis methods and neutron cross-section data shall be benchmarked by comparison with critical experiment data for similar configurations. The benchmarking process should establish a calculational bias and uncertainty of the mean with a one-sided tolerance factor of 95% probability at a 95% confidence level. The maximum k-effective value for the SFP is obtained by summing the calculated value, the calculational bias, the total uncertainty (defined as a statistical combination of the calculational and mechanical uncertainties), and the burnup axial distribution bias. A bias that reduces the calculated value of k-effective should not be applied. Mechanical and material uncertainties may be treated by assuming worst case conditions or by performing sensitivity studies and obtaining worst case uncertainties. Uncertainties may be combined statistically provided that they are independent variations.

NUREG/CR-6361, "Criticality Benchmark Guide for Light-Water-Reactor Fuel in Transportation and Storage Packages" provides documentation for 180 criticality experiments with geometries, materials, and neutron interaction characteristics representative of LWR fuel in core, storage, and cask arrangements. NUREG/CR-6361 was used as design input and as the primary reference for the validation calculation package. Statistical evaluations included calculating the range of calculated k-effective, the mean k-effective, standard deviation of the mean, bias, 95/95 uncertainty in the bias, and the average Monte Carlo error for the whole group of experiments as well as categories within a data base. Trending of k-effective with physical parameters, i.e., fuel rod pitch, fuel enrichment, moderator-to-fuel ratio, soluble boron concentration, assembly separation, and average energy group causing fission, was evaluated by creating scatter plots of k-effective versus each physical parameter and then performing linear regression on the data. The strength of a trend was evaluated by the magnitude of the correlation coefficient from the linear regression. In addition, the validation results were organized into three groupings: reactor core-type experiments, storage rack-type experiments, and cask-type experiments. For each of these groupings, a bias and 95/95 uncertainty is also specified for use in criticality safety evaluations.

The storage rack-type category combines the results of 123 critical experiments, including the results for the core-type, separator plate, separator plate-soluble boron, and flux trap-void experiments, but excluding the reflector wall categories. This experimental data is sufficiently diverse to establish that the method bias and uncertainty applies to the Calvert Cliffs storage rack conditions. The storage rack-type category exhibits a bias of 0.0008 and a 95/95 one sided uncertainty of 0.0076.

A histogram for the frequency of k-effective values shows a tight clustering of k-effective values near k-effective equal to 1 and a near normal distribution. Scatter plots were constructed of k-effective versus fuel rod pitch, k-effective versus fuel enrichment, k-effective versus water/fuel volume ratio, k-effective versus $H/^{235}U$ atom ratio, k-effective versus soluble boron concentration, k-effective versus assembly separation, and k-effective versus average energy group of fission, respectively. Also included in each

plot is the associated regression line and equation with correlation coefficient. Review of these plots indicates all the trend lines are nearly horizontal, with very small correlation coefficients. Thus, there are no significant trends indicated.

Uncertainty Calculations

The evaluation of normal storage should be done at the temperature (water density) corresponding to the highest reactivity. In poisoned racks, the highest reactivity will usually occur at a water density of 1.0000 (i.e., at ~40°F or 277.15°K). However, if the temperature coefficient of reactivity is positive, the evaluation should be done at the highest temperature expected during normal operation: i.e., equilibrium temperature under normal refueling conditions (including full-core offload), with one coolant train out-of-service and the pool filled with spent fuel from previous reloads. In the event that any one loop is lost, the remaining two loops [either two spent fuel pool cooling (SFPC) loops or one SFPC loop and one shutdown cooling loop] can continue to maintain the pool temperature at or below 155°F (341.48°K @ 0.9785 gm/cc) for 1830 fuel assemblies in the SFP including a full core offload. An infinite axial and radial array of storage cells of nominal dimensions containing the maximum enrichment of 5.0 weight percent fuel was modeled as a function of temperature (40°F and 155°F) and as a function of fuel clad material (Zirlo, Optin, Zirc-4, Alloy A, low tin Zirlo, and M5). The Zirc-4 clad cases at 155°F were the most reactive for all conditions (unborated, borated, unburned, burned). This worst case condition was assumed in all calculations.

The mechanical design of the fuel racks is such that the average pitch between cells is maintained by structural members at 10.09375 ± 0.03125 inches. Thus a nominal pitch of 10.09375 inches was assumed, and an uncertainty value to ± 0.03125 inches was included in the mechanical and material uncertainty value. A storage cell pitch of 10.0625 inches results in the highest reactivity value (0.358% Δk at zero boron/zero burnup, 0.449% Δk at 300 ppm/zero burnup, and 0.454 % Δk at 300 ppm/finite burnup), and the resulting uncertainty values were used in the uncertainty calculations.

The maximum stack height density is 10.31 gm/cc (<94.5% theoretical density). For VAP fuel, the stack height density can range between 94.0% and 96.5% of theoretical density. Thus a nominal stack height density of 94.5% of theoretical density was assumed, and an uncertainty value to 96.5% of theoretical density was included in the mechanical and material uncertainty value. The higher stack height density results in the higher reactivity values, and the resulting uncertainty values (0.090%Δk at zero boron/zero burnup, 0.340% Δk at 300 ppm/zero burnup, and 0.841% Δk at 300 ppm/finite burnup) were used in the uncertainty calculations

Per 10 CFR 50.68, the maximum nominal U-235 enrichment of the fresh fuel assemblies is limited to 5.0 weight percent. An uncertainty of 0.05 weight percent enrichment was assumed. The higher enrichment value results in the higher reactivity values, and the resulting uncertainty values (0.155%Δk at zero boron/zero burnup, 0.210% Δk at 300 ppm/zero burnup, and 0.304% Δk at 300 ppm/finite burnup) were used in the uncertainty calculations.

The mechanical design of the fuel racks is such that the average wall thickness is 0.060 ± 0.010 inches. Thus a nominal wall thickness of 0.060 inches was assumed, and an uncertainty value to ± 0.010 inches was included in the mechanical and material uncertainty value. A storage cell steel thickness of 0.1270 cm results in the highest reactivity values. The above uncertainty values (1.346% Δk at zero boron/zero burnup, 0.775% Δk at 300 ppm/zero burnup, and 0.698% Δk at 300 ppm/finite burnup) were used in the uncertainty calculations.

It is possible for a fuel assembly not to be positioned centrally within a storage cell, because of clearance between the assembly and the cell wall. Calculations have been performed to determine the effects of eccentrically located fuel. It was assumed that the fuel assemblies were displaced diagonally within their storage cells as far as possible towards and away from each other. This generated an uncertainty value, which was included in the mechanical and material uncertainty value. The cases modeled an infinite axial and radial array of 10x10 storage cells of nominal dimensions containing the maximum enrichment of 5.0 weight percent fuel as a function of eccentric positioning within the storage cell at the worst case temperature of 155°F for a fuel clad material composed of Zirc-4. The larger of the above uncertainty values (0.961% Δk at zero boron/zero burnup, 1.112% Δk at 300 ppm/zero burnup, and 0.800% Δk at 300 ppm/finite burnup) were used in the uncertainty calculations.

The soluble boron credit is limited to a maximum value of 300 ppm per the restrictions of the Unit 1 criticality analysis. Note that 300 ppm is a minimum boron concentration requirement. The proposed change to the Technical Specification 4.3.1 adds 15 percent to this value to account for any unknown uncertainties, which increases the boron level to 350 ppm required to safely store 5.0 weight percent VAP fuel in the SFP.

Nominally, all of the cases in this evaluation assume that the pellet-to-clad gap contains void, which it normally does. However, failed fuel rods may exist and the gap may be filled with water of the same composition as that exterior to the fuel rod. The uncertainty values (0.000% Δk at zero boron/zero burnup, 0.356% Δk at 300 ppm/zero burnup, and 0.267% Δk at 300 ppm/finite burnup) were used in the uncertainty calculations.

In addition, fuel clad failure would indicate that certain fission gases and highly soluble nuclides (noble gases, halogens, cesiums, and technetiums) could escape the affected fuel pins and increase system reactivity. Pin failure occurs infrequently (much less than 1% of the rods inserted into the core fail). When failure does occur, not all of the gases escape from the fuel matrix. Assuming that the pin is at or near centerline melting temperature and assuming that a fuel pin fails for 1 of the 3 cycles of insertion (it is the policy at Calvert Cliffs not to reinsert failed fuel back into the core without reconstitution), approximately 9% of the noble gases, 33% of the halogens and cesiums, and 99.9% of the technetiums would remain. Conservatively assuming that 5% of all fuel pins fail and that all of the gaseous fission products from the failed fuel would be lost, the change in reactivity would only amount to 0.00084 Δk. Treating this as a component in the uncertainty analysis, the total bias and uncertainty would only increase by 0.001% Δk. In addition, part of this reactivity increase would be negated by a smaller two-dimensional to three-dimensional burnup bias. Thus, this effect is negligible and will be neglected.

Burnup Effects

The dynamics of reactor operation results in non-uniform axial-burnup profiles in fuel with any significant burnup. At the beginning-of-life in a PWR, a near-cosine axial-shaped flux will begin depleting fuel near the axial center of a fuel assembly at a greater rate than at the ends. As the reactor continues to operate, the cosine flux shape will flatten because of the fuel depletion and fission product buildup that occurs near the center. However, because of the high leakage near the ends of the fuel, burnup will drop off rapidly near the ends. The majority of PWR fuel assemblies have similar axial-burnup shapes - relatively flat in the axial mid-section (with peak burnup from 1.1 to 1.2 times the assembly average burnup) and significantly underburned fuel at the ends (with burnup of 50 to 60% of the assembly average). Note that due to a difference in the moderator density, the burnup is slightly higher at the bottom of the assembly than at the top. The cooler higher-density water at the assembly inlet results in a higher reactivity and thus, higher burnup than the warmer moderator at the assembly outlet. An assumed single average burnup incorrectly weights the calculation of k-effective by placing the flux

profile toward the center of the rod. Thus, leakage is artificially minimized, and burnup in the driving region is artificially reduced. In reality, the most reactive region of spent fuel is towards the assembly ends, where there exists a balance between reactivity due to lower burnup and increased leakage. The reactivity difference between the neutron multiplication factor (k-effective) calculated with explicit representation of the axial burnup distribution and k-effective calculated assuming a uniform axial burnup is referred to as the "end effect". The "end effect" is dependent on the axial burnup profile, total accumulated burnup, cooling time, initial enrichment, assembly design, and the isotopics considered (i.e., actinide-only or actinide plus fission products).

A reactivity bias was included in the overall k-effective calculations, to account for differences between two-dimensional and three-dimensional modeling. A conservative set of biases was developed that account for the reactivity difference between a fuel assembly with an explicit axial three-dimensional burnup profile and one with a uniform two-dimensional profile at the same average burnup. The biases were computed and tabulated as a function of both burnup and initial enrichment. The conservative axial bias corresponding to the highest enrichment/burnup storage limit was employed, since among all enrichment/burnup combinations, the highest yields the largest positive axial bias. Worst-case 18-node axial profiles were extracted from ORNL/TM-1999/246 and NUREG/CR-ORNL/TM-2001/33 as a function of burnup. Two-dimensional to three-dimensional comparisons were performed as a function of enrichment and soluble boron. The reactivity bias results indicate that the worst-case reactivity bias (0.03226 Δk) is for the unborated highest enrichment and highest burnup fuel. A worst-case bias of 3.25% Δk was utilized in all calculations.

Actual Calvert Cliffs end-of-cycle 26-node burnups were generated for a complete core's assemblies. Two-dimensional to three-dimensional comparisons were performed at the highest enrichment value of 5.0 weight percent and at zero soluble boron. The reactivity bias results indicate that the worst-case reactivity bias is -0.00579 Δk. Thus, for Calvert Cliffs specific fuel, use of 26-node axial burnup profiles is less conservative than uniform axial burnups at all values of burnup.

All three dimensional KENO executions assumed that the upper end fitting and lower end fitting of each assembly are composed of moderator. This was verified to be conservative.

Worst case values of moderator temperature, clad composition, soluble boron concentration, and fixed poison loading were assumed in all reactivity calculations. Most of the uncertainties and biases were determined at three state points: zero soluble boron and zero burnup, 300 ppm soluble boron and zero burnup, and 300 ppm soluble boron and 40 GWD/MTU average burnup. The calculational methodology and axial burnup distribution biases and uncertainties were independent of soluble boron concentration and average burnup and were bounding for all cases, while the fuel depletion uncertainty was a function of soluble boron only. The composite bias and uncertainty values as a function of state point were determined. The worst case composite bias and uncertainty value was 0.06129 Δk for zero soluble boron and zero burnup. This value was conservatively applied to all calculated reactivity values.

The uncertainty in measured burnup was extracted from the Asea Brown Boveri, Inc./Combustion Engineering, Inc. Methodology Manual for Physics Biases and Uncertainties for Asea Brown Boveri, Inc./Combustion Engineering, Inc. Fuel Assemblies. For burnups less then 30 GWD/MTU, the burnup must be increased by 2.5%. For burnups in excess of 30 GWD/MTU, the burnup must be increased by 750 MWD/MTU.

Reactivity was determined as a function of burnup, enrichment, and soluble boron concentration. Note that at zero soluble boron, all of the reactivity values are less than 0.998, while at 300 ppm soluble boron, all of the reactivity values are much less than 0.95. This is in accordance with 10 CFR 50.68, if credit is

taken for soluble boron. The above burnup values must then be increased by the measured burnup uncertainty. The burnups required to store fuel in the Unit 2 SFP crediting 350 ppm of soluble boron including all biases and uncertainties are detailed in the following table:

Enrichment (weight percent)	Burnup (GWD/MTU)
2.0	6.00
2.5	13.75
3.0	20.50
3.5	27.00
4.0	32.75
4.5	38.25
5.0	43.75

Several checkerboard patterns were modeled in an effort to store more reactive fuel (i.e., fuel with less burnup than required by the above table) in the Unit 2 SFP. To store any fuel with burnups less than those indicated in the above table, that fuel assembly must be surrounded on all four adjacent faces by empty rack cells or other non-reactive materials (e.g., wall, water, etc.). Note that this checkerboard pattern meets the requirements of 10 CFR 50.68.

A finite radial and axial model of the Unit 2 SFP of nominal dimensions containing the maximum enrichment of 5.0 weight percent VAP fuel at a soluble boron concentration of 0, 300, and 2000 ppm was modeled with sequential assemblies in the row closest to the SFP wall on 20.5" spacers to simulate the reconstitution/inspection process. There is no reactivity difference between reconstituting an entire row of assemblies or normal storage of said assemblies. Since Boraflex is not credited in this analysis, placing assemblies on spacers has no reactivity effect.

Accident Conditions

Regulatory guidance dictates subcriticality must be maintained under accident conditions. Since assemblies must possess sufficient burnup to be placed in the Unit 2 SFP to counteract the loss of Boraflex, placement of an assembly with insufficient burnup in the SFP would constitute a fuel misloading accident. However, per regulatory guidance and ANSI-N16.1-1975, the double contingency principle allows the crediting of the soluble boron in the SFP during such an event. A criticality accident would require two unlikely, independent, concurrent events to occur. The Technical Specification boron concentration must be 2000 ppm or greater without biases and uncertainties. Assuming that the Unit 2 SFP is completely misloaded with fresh fuel of the indicated enrichments, k-effective is maintained below 0.95. Thus there are no adverse consequences for a worst-case fuel misloading accident in this analysis.

The top opening of the SFP racks has angled lead-in guides, which effectively block the spaces between the cavities, as well as guide the fuel assembly into the open tube. Also to avoid the possibility of inadvertently placing a fuel assembly between the outermost storage cell and the pool wall, the top rack surface is extended to cover this space. Thus the abnormal placement of a fuel assembly in the SFP racks is not a credible event.

Dropping an assembly horizontally onto the top of the SFP racks from the Spent Fuel Handling Machine is not possible at Calvert Cliffs due to the design of the Spent Fuel Handling Machine and due to the height of the SFP racks. The bottom of the outer mast assembly is at elevation 49'6", while the top of the SFP racks is at elevation 45'0". Dropping an assembly on top of the SFP racks from the Cask Handling Crane or the new fuel elevator is also not a credible accident. The Cask Handling Crane is designed in

accordance with the single-failure proof criteria of NUREG-0554 and NUREG-0612 and is used to move assemblies into the new fuel elevator. Assuming a dropped assembly during normal operation and during reconstitution/inspection activities, k-effective is maintained below 0.95 in both cases. Thus, there are no adverse consequences for a worst-case horizontal assembly drop accident in this analysis.

Dropping an assembly and having it stand upright atop another assembly in the SFP racks is less limiting than the current analysis, which assumes infinite axial extent. Thus, there are no adverse consequences for a vertical assembly drop accident in this analysis.

Criticality Conservatisms

The reactivity calculations include the following conservatisms that result in appreciable reactivity margin:

1) SAS2H isotopics were modeled with conservative fuel temperature, moderator temperature, soluble boron concentration, specific power, and refueling downtime inputs. For 5.0 weight percent fuel at 50 GWD/MTU, the conservatism was in excess of 0.4% Δk for T_{fuel}, 0.5% Δk for T_{mod}, and 2.6% Δk for cooling time (100 hours vs 5 years). The conservatisms were higher for lower enrichments but lower for lower burnups.

2) Integral burnable absorbers, boraflex poison sheets, and control element assemblies were conservatively neglected in this evaluation.

3) A reactivity uncertainty due to uncertainty in the fuel depletion calculation must be developed and combined with other calculational uncertainties. An uncertainty equal to 5% of the reactivity decrement to the burnup of interest is an acceptable alternative. Based on computations presented in this evaluation, a worst case uncertainty value of 2.089% was used in all burnup related reactivity calculations, even though SAS2H generated isotopic were determined to be 0.358% more reactive than those adjusted to radiochemical assay isotopics. Thus for Calvert Cliffs specific fuel, use of SAS2H generated isotopics is more conservative than use of isotopics normalized to radiochemical assay isotopics.

4) For conservatism, an axial burnup bias of 3.25% Δk was utilized for all burnup cases. The most conservative Calvert Cliffs specific reactivity bias was calculated to be -0.579% Δk. Thus for Calvert Cliffs specific fuel, use of 26-node axial burnup profiles is less conservative than uniform axial burnups.

5) Inclusion of additional isotopes in the SAS2H and KENO executions can add significantly more margin to the reactivity results. While no benchmarks exist for these additional isotopes, comparison of existing benchmark cases to SAS2H/KENO computations indicates that the computation results are conservative. Note that the additional margin provided by an expanded list of isotopes (101 vs 50) generally increases as a function of burnup and enrichment, exceeding 1.5% Δk for high enrichments (4-5 weight percent) and high burnup (60 GWD/MTU) fuel.

6) The worst case composite bias and uncertainty value was 0.06129 Δk for zero soluble boron and zero burnup. This value was conservatively applied to all calculated reactivity values.

7) The conservatism in reactivity for a two-dimensional infinite array versus a three-dimensional Unit 2 specific model increases from 1.56% Δk at 0 ppm, to 10.18% Δk at 300 ppm, to 21.87% Δk

at 2000 ppm. In addition, for the zero burnup cases, an additional reactivity conservatism of 4.185% Δk exists.

DILUTION ANALYSIS

The objective of the evaluation in Attachment (6) was to confirm that design features, instrumentation, administrative procedures, and sufficient time are available to detect and mitigate boron dilution in the SFP before the boron concentration is reduced below the value assumed in the SFP criticality analyses that credit boron to remain below the design basis criticality limit of 0.95 k-effective. Attachment (6) identifies the potential boron dilution sources and dilution events, the instrumentation available for detection of dilution, and the operating and administrative procedures available for the detection and mitigation of dilution. The report also identifies the potential events that could dilute the soluble boron contained in the Units 1 and 2 SFPs and quantifies the dilution rates and response times of each event.

Flooding

Spent fuel pool flooding by tsunami, hurricane, and storms are not credible events at Calvert Cliffs. Since there has been no record of tsunamis on the northeastern United States coast, it is not believed that the site will be subjected to a significant tsunami effect. The relative frequency of hurricane occurrence for the Calvert Cliffs site is slightly more than one hurricane per year. For the Probable Maximum Hurricane it is assumed that the peak hurricane surge is coincident with normal high tide and with a 99th percentile wave height. The total predicted wave run-up is to Elevation 27.1', which is considerably less than the Elevation 69' of the top of the SFP. Thus the maximum hypothetical flood level is below the top of the SFP elevation. The Auxiliary Building is a concrete structure and qualified for high winds. Therefore, severe storms with high winds are not expected to cause sufficient damage to the roof to allow a large volume of rain to enter the building and become an unborated source of water to the pool. The 6" lip around the SFP should cause the bulk of any entering rain water to flow out of the SFP area via the 13 floor drains, 13 doors, and 2 tendon end cap shafts.

The onsite water sources that can flood the SFP and possibly cause dilution below the minimum boron concentration are the two pretreated water storage tanks of 500,000 gallons each, the two condensate storage tanks of 315,000 gallons each, the demineralized water storage tank of 350,000 gallons, and the two refueling water tanks of 420,000 gallons each. The large volume of water necessary to dilute the pool to the boron endpoint precludes many small tanks as potential dilution sources. No tanks containing any significant amount of water are stored in the vicinity of the SFPs. The large unborated water sources, such as reactor makeup water and demineralized water, are in tanks at elevations below the SFP, so that gravity feed from these tanks to the SFP is not possible. It is very unlikely that the large volumes of water necessary to substantially dilute the SFP (i.e., to the boron endpoint) could be transferred from these tanks to the SFP without being detected by plant personnel.

The possibility of a fire in the SFP area leading to a boron dilution event is not a credible event. Typically, combustible loadings around the pool area are minor. If the fire hose stations were used to extinguish a fire, the volume of water required to extinguish a local fire is not expected to be of sufficient magnitude to dilute the pool such that a several hundred ppm reduction in the pool boron concentration would occur. Water for the Fire Protection System is supplied by two 2,500 gpm full-capacity fire pumps. The fire pumps take suction from the two 500,000 gallon capacity pretreated water storage tanks. Fire in the fuel handling building could result in unborated water entering the SFP while attempting to extinguish the fire. However, the rate of addition of unborated water from a fire would be insufficient to exceed the minimum boron level of 350 ppm, since sufficient time would exist to take compensatory measures (i.e., add additional boron to the SFP).

In addition, the discussion that follows on incomplete boron mixing indicates that the unborated water would tend to float on the surface of the pool and overflow the SFP as water continues to flow into the SFP. Thus the fuel assemblies should remain surrounded by borated water. Finally, assuming that the fire is not directly over the SFP, the 6" lip around the SFP should cause the bulk of the water used to extinguish the fire to flow out of the SFP area via the 13 floor drains, 13 doors, and 2 tendon end cap shafts. At a dilution rate of 2,500 gpm directly into the SFP, it will take 6.95 hours to dilute the SFP from 2000 to 350 ppm. It is not credible that dilution could occur for this length of time without operator notice, since this event would activate the SFP high level alarm and initiate Auxiliary Building flooding. In addition, in excess of 1,043,000 gallons of pretreated water must be added to the SFP to reach 350 ppm soluble boron concentration. Assuming that a fire hose was inserted into the SFP and discharged at the maximum rate of 2500 gpm, it would exhaust the pretreated water storage tank that it was aligned to in approximately 3.45 hours. Two well water pumps would automatically actuate and pump 600 gpm into the pretreated water storage tank. An additional 13 hours would be required for the SFP to be diluted to 350 ppm boron at this rate. Note that this dilution by flooding scenario bounds all others. Even in the unlikely event that the SFP is completely diluted of boron, the SFP will remain subcritical by a design margin of k-effective not to exceed 0.998.

The unlikely probability of an inadvertent boron dilution event reducing the SFP boron concentration to less than 350 ppm is based on the assumption of complete mixing of the boron in the SFP. The complete mixing assumption may not always be valid, if the circulation flow in the SFP is insufficient to prevent stratification. Where stratification has occurred (Robinson 2 December 20, 1988 and San Onofre 1 January 23, 1989), it was observed that the diluted water floated on the higher borated water. This suggests that if stratification does occur, the water with the higher boron concentration will tend to be in the lower level of the SFP where the fuel assemblies are located. Circulating the SFP water via the SFP cooling or purification systems can eliminate the possibility of boron stratification in the SFP.

Another type of incomplete boron mixing is a ribbon effect, where a channel of unborated water bores its way to a SFP assembly location. If the SFP cooling or purification systems are in operation, mixing will occur in the piping systems eliminating any ribbon effects. Assuming that the SFP cooling and purification systems are not in operation, an analysis using turbulent jet and diffusion theory was performed to determine the extent of any ribbon effect. For an initial SFP concentration of 2000 ppm and an unborated discharge from a 10" diameter pipe (the largest discharge pipe in the SFP is from an 8" diameter pipe, use of a 10" is conservative), the boron concentration will reach 350 ppm within 29" of the nozzle discharge. The active fuel region of the fuel assembly is more than 29" from the nozzle discharge. Thus, it is not credible that a diluted ribbon flow of less than 350 ppm could reach the fuel.

The SFP instrumentation is not powered from the emergency diesel generators, thus, a loss-of-offsite power would affect the plant's ability to respond to a dilution event. However, the loss-of-offsite power would also affect electric pumps involved in the dilution event. The large unborated water sources such as reactor makeup water and demineralized water are in tanks at elevations below the SFP, so that gravity feed from these tanks to the SFP is not possible.

Loss of SFP Inventory

Structural failures, where makeup can compensate for the loss-of-coolant, can also initiate a dilution event.

The SFP is designed to preclude the loss of structural integrity. A 3/16" solid stainless steel liner plate was used on the inside face of both pools for leak tightness, and all of the field welds have leak-test channels welded to the outer side of the liner plates. The channels are grouped into ten zones, each

with its own detector pipe to localize leaks in the liner seams. Even with the precautions described, small leaks may still occur in the SFP. Early leakage detection is assured by a Surveillance Requirement (SR 3.7.13.1), which requires that the minimum pool level be verified at least once every seven days. In practice, the level is checked once every 12 hours as required by the Auxiliary Building log sheets. In addition, a level alarm keeps the Control Room Operator aware of level changes.

The likelihood of a fuel handling incident is minimized by administrative controls and physical limitations imposed on fuel handling operations. All refueling operations are conducted in accordance with prescribed procedures under direct surveillance of a qualified supervisor. Mechanical interlocks prevent inadvertent disengagement of a fuel assembly from the fuel handling machine; consequently, the possibility of dropping and damaging of a fuel assembly is remote. Even though the assembly drop is an unlikely event, the SFP concrete plus liner plate are stronger than the assembly bottom casting, fuel, and guide tubes for impact of a fresh or irradiated VAP fuel assembly with an inserted control element assembly (1350-1360 lbm). The bottom casting is, in turn, stronger than the fuel and guide tubes. Essentially all impact kinetic energy absorption will take place in the fuel and guide tubes. Interface forces between the bottom assembly and the liner plate would be limited by the buckling of the fuel and guide tubes. In addition, for impact over the collection trenches in the SFP, the interface forces between the bottom assembly and the liner plate would be limited by the buckling of the fuel and guide tubes. The interface forces, therefore, will be of insufficient magnitude to cause perforation of the liner plate. Therefore, for both full contact impact and impact over the collection trenches of a fresh or irradiated VAP fuel assembly with an inserted control element assembly (1350-1360 lbm), the liner plate would not be perforated.

The most serious failure to the system is the loss of SFP water. This is avoided by routing all SFP piping connections and penetrations above the water level and providing them with siphon breakers to prevent gravity drainage. The SFP inlets to the SFP cooling and purification systems are above the spent fuel racks and penetrate the SFP liner at 65' 11" elevation. The SFP discharge pipes from the shutdown cooling system, purification system, refueling water tank, and demineralized water tank are also above the spent fuel racks and penetrate the SFP liner at 65' 11" elevation. The SFP does not contain any permanent drains, thereby, preventing accidental drain down.

Loss of Spent Fuel Pool Cooling

The SFPC system is common to both units. The SFPC system is a closed-loop system consisting of two half-capacity 1,390 gpm pumps and two half-capacity heat exchangers in parallel, a bypass 128 gpm cartridge-type filter which removes insoluble particulates, and a bypass 128 gpm mixed bed resin demineralizer which removes soluble ions. The SFPC heat exchangers are cooled by service water. The normal configuration for the cooling system is one pump/one cooler loop in operation on each half of the SFP to cool the water. However, the purity and clarity of the water is maintained by passing a portion of the flow through the purification system. The purification system consists of a filter to remove insoluble particulates and a demineralizer (ion exchanger) which removes soluble ions. Ten skimmers are provided in the spent fuel pools to remove accumulated dust and debris from the surface of the water. Connections are provided for tie-in to the shutdown cooling system to provide for 2,000 gpm of additional heat removal in the event that the reactor cores are off-loaded resulting in 1,830 fuel assemblies contained in the pool. A total loss-of-cooling is not part of the system's design basis for the SFPC system and pool structural components (e.g., pool liner plate, SFPC piping, and pumps). The entire SFPC system is tornado-protected and is located in a Seismic Category I structure.

Even though loss of SFP cooling is not part of the system's design basis, because the SFPC system is a Class III system, the effect of that event was analyzed. Assuming that the Units' 1 and 2 SFPs contain

1,830 assemblies generating the maximum possible heat load, and assuming the worst case initial SFP temperature of 155°F, then the time to boil can be calculated as 7.34 hours. Time to uncover the fuel assemblies is 79.0 hours. However, loss of the pool water via boiling will not result in a loss of soluble boron, since the soluble boron is not volatile. Thus, loss of SFPC system without makeup flow is not a mechanism for boron dilution. A worst-case scenario involves adding sufficient unborated water to the SFP to just keep the water from boiling and letting the excess fluid flow down the Auxiliary Building gravity drains associated with the SFP overflow level. It would take 24.88 hours to dilute the SFP to 350 ppm under this scenario. It is not credible that dilution could occur for this length of time without operator notice, since this event would activate the high level alarm and initiate Auxiliary Building flooding. In addition, in excess of 1,043,000 gallons of demineralized water must be added to the SFP to reach 350 ppm soluble boron concentration. This is three times more water volume than is contained in the demineralized water tank.

CONCLUSION

The proposed change would allow the maximum fresh fuel enrichment with the VAP fuel design to be increased to 5.0 weight percent, assuming credit for soluble boron, burnup, and configuration control in maintaining acceptable margins of subcriticality in the SFP. The analyses contained in Attachments (5) and (6) demonstrate that the requirements of 10 CFR 50.68 are met.

Allowing the maximum enrichment for fresh fuel to be increased to 5.0 weight percent, assuming partial credit for soluble boron, credit for burnup, and configuration control will allow the number of fresh fuel assemblies per cycle to be decreased. This will decrease Independent Spent Fuel Storage Installation storage requirements, decrease permanent Department of Energy storage requirements and decrease fuel cycle costs.

REFERENCE

1. Letter from Mr. P. E. Katz (CCNPP) to Document Control Desk (NRC), dated May 1, 2003, License Amendment Request: Increase to the Unit 1 Spent Fuel Pool Maximum Enrichment Limit with Soluble Boron Credit

ATTACHMENT (2)

DETERMINATION OF SIGNIFICANT HAZARDS

Calvert Cliffs Nuclear Power Plant, Inc.
September 30, 2003

ATTACHMENT (2)

DETERMINATION OF SIGNIFICANT HAZARDS

The proposed change has been evaluated against the standards in 10 CFR 50.92 and has been determined to not involve a significant hazards consideration in operation of the facility in accordance with the proposed amendment:

1. *Would not involve a significant increase in the probability or consequences of an accident previously evaluated.*

   The proposed change will increase the maximum enrichment limit of the fuel assemblies that can be stored in the Unit 2 spent fuel pool (SFP) by taking credit for soluble boron, burnup and configuration control in maintaining acceptable margins of subcriticality. The proposed change will modify Technical Specification 4.3.1 "Criticality," add Technical Specification 3.7.16, "Spent Fuel Pool Boron Concentration" and add Technical Specification 3.7.17 "Spent Fuel Pool Storage." The postulated accidents for the SFP are basically four types; 1) dropped fuel assembly on top of the storage rack, 2) a misloading accident, 3) an abnormal location of a fuel assembly, and 4) loss-of-normal cooling to the SFP.

   There is no increase in the probability of a fuel assembly drop accident in the SFP when considering the higher enriched fuel or the presence of soluble boron in the SFP water. Dropping a fuel assembly on top of the SFP storage racks is not credible at Calvert Cliffs due to the design of the spent fuel handling machine and the height of the SFP storage racks. The handling of fuel assemblies has always been performed in borated water and will not change as a result of crediting soluble boron in the SFP criticality analysis. The proposed change does not change the general design or characteristics of the fuel assemblies. Therefore, the proposed change does not increase the probability of a fuel assembly drop accident.

   There is no increase in the probability of the accidental misloading of irradiated fuel assemblies into the SFP storage racks when considering the higher enriched fuel or the presence of soluble boron in the SFP water for criticality control. Fuel assembly placement will continue to be controlled pursuant to approved fuel handling procedures.

   Due to the design of the SFP storage racks, an abnormal placement of a fuel assembly into the SFP storage racks is not possible. Also, the design of the SFP prevents an inadvertent placement of a fuel assembly between the outer most storage cell and the pool wall. The proposed change does not make any change to the design of SFP. Therefore, there is no increase in the probability of abnormal placement of a fuel assembly into the SFP storage racks.

   The proposed change will not result in any changes to the SFP cooling system, and the fuel assembly design and characteristics are not changed by an increase in fuel enrichment. Therefore, there is no increase in the probability of a loss of SFP cooling. Also, since a high concentration of soluble boron has always been maintained in the SFP water, there is no increase in the probability of the loss of normal cooling to the SFP water considering the presence of soluble boron in the pool water for criticality control.

   There is no increase in the consequences of an accidental drop, accidental misloading, or abnormal placement of a maximum enriched fuel assembly into the SFP storage racks, because the criticality analysis demonstrates that the pool will remain subcritical following either event. The Technical Specification limit for SFP boron concentration will ensure that an adequate SFP boron concentration will be maintained.

There is no increase in the consequences of a loss-of-normal SFP cooling because the Technical Specification boron concentration provides significant negative reactivity. Loss of the SFP water via boiling will not result in a loss of soluble boron, since the soluble boron is not volatile. Therefore, loss of SFP cooling system, without makeup flow, is not a mechanism for boron dilution. Even in the unlikely event that soluble boron in the SFP is completely diluted via unborated makeup flow, a pool completely filled with maximum enriched unburned assemblies will remain subcritical by a design margin that meets the requirements of 10 CFR 50.68.

Therefore, the proposed change does not involve a significant increase in the probability or consequences of an accident previously evaluated.

2. *The proposed change does not create the possibility of a new or different kind of accident from any accident previously evaluated.*

The proposed change will increase the maximum enrichment limit of the fuel assemblies that can be stored in the Unit 2 SFP by taking credit for soluble boron, burnup and configuration control in maintaining acceptable margins of subcriticality. Increasing the maximum enrichment limit does not create a new type of criticality accident.

Soluble boron has been maintained in the SFP water and is currently required by procedures. Therefore, crediting soluble boron in the SFP criticality analysis will have no effect on normal pool operation and maintenance. Crediting soluble boron will only result in increased sampling to verify the boron concentration in accordance with the proposed Technical Specification Surveillance Requirement. This increased sampling will not create the possibility of a new or different kind of accident.

A dilution of the SFP soluble boron has always been a possibility. However, the boron dilution event previously had no consequences, since boron was not previously credited in the accident analysis. The initiating events that were considered for having the potential to cause dilution of the boron in the SFP to a level below that credited in the criticality analyses fall into three categories: dilution by flooding, dilution by loss-of-coolant induced makeup, and dilution by loss-of-cooling system induced makeup. The SFP dilution analysis demonstrates that a dilution event that could increase k-effective in the SFP to greater than 0.95 is not a credible event. It is not credible that dilution could occur for the required length of time without operator notice, since this event would activate the high level alarm and initiate Auxiliary Building flooding. In addition, in excess of 1,043,000 gallons of unborated water must be added to the SFP to reach the minimum soluble boron concentration. This is more water volume than is contained in both pretreated water storage tanks and also more water volume than is contained in the demineralized water storage tank and both condensate storage tanks combined. Even in the unlikely event that soluble boron in the SFP is completely diluted, the SFP will remain subcritical by a design margin that meets the requirements of 10 CFR 50.68.

Burned assemblies have been stored in the SFP for many cycles. Therefore, crediting burnup in the SFP criticality analysis will have no effect on normal pool operation and maintenance. Fuel assembly placement, although more complex, will continue to be controlled pursuant to approved fuel handling procedures and in accordance with Technical Specification spent fuel rack storage configuration limitations.

The proposed change will not result in any other change in the plant configuration or equipment design. Therefore, the proposed change does not create the possibility of a new or different kind of accident from any previously evaluated.

3. *The proposed change does not involve a significant reduction in a margin of safety.*

The Technical Specification changes proposed by this license amendment request will provide an adequate safety margin to ensure that the stored fuel assembly array of maximum enriched fuel will always remain subcritical. Those limits are based on a plant specific criticality analysis performed for the Calvert Cliffs Unit 2 SFP, that include technically supported margins.

Soluble boron is used to provide subcritical margin such that the SFP k-effective is maintained less than or equal to 0.95. Since k-effective is less than or equal to 0.95, the current margin of safety is maintained. In addition, while the criticality analysis utilized credit for soluble boron, the fuel in the SFP rack will remain subcritical with no soluble boron with a 95 percent probability at a 95 percent confidence level as required by 10 CFR 50.68. This substantial reduction in the SFP soluble boron concentration was evaluated and shown not to be credible.

Therefore, the proposed change does not involve a significant reduction in a margin of safety.

ATTACHMENT (3)

TECHNICAL SPECIFICATIONS

MARKED-UP PAGES

iii

3.7.16-1

3.7.17-1

3.7.17-2

3.7.17-3

4.0-2

3.7 PLANT SYSTEMS

3.7.16 Spent Fuel Pool (SFP) Boron Concentration

LCO 3.7.16 Boron concentration of the SFPs shall be ≥ 2000 ppm.

APPLICABILITY: When fuel assemblies are stored in the SFPs.

ACTIONS

CONDITION	REQUIRED ACTION	COMPLETION TIME
A. Spent Fuel Pool boron concentration not within limit.	---------- NOTE ---------- LCO 3.0.3 is not applicable. ----------	
	A.1 Suspend movement of fuel assemblies in the SFPs.	Immediately
	AND	
	A.2 Initiate action to restore boron concentration to within limit.	Immediately

SURVEILLANCE REQUIREMENTS

SURVEILLANCE		FREQUENCY
SR 3.7.16.1	Verify boron concentration is greater than 2000 ppm.	7 days

New TS page

3.7 PLANT SYSTEMS

3.7.17 Spent Fuel Pool (SFP) Storage

LCO 3.7.17 The combination of initial nominal enrichment and burnup of each fuel assembly stored in the Unit 2 Spent Fuel Pool shall be in accordance with the following:

(a) Irradiated fuel assemblies may be stored in any rack location in the Unit 2 Spent Fuel Pool provided the combination of burnup and initial nominal enrichment is in the acceptable range of Figure 3.7.17-1, and

(b) Irradiated or unirradiated fuel assemblies with a combination of burnup and initial nominal enrichment that are not in the acceptable range of Figure 3.7.17-1 may be stored in the Unit 2 Spent Fuel Pool if surrounded on all four adjacent faces by empty rack cells or other non-reactive materials.

APPLICABILITY: Whenever any fuel assembly is stored in the Unit 2 Spent Fuel Pool.

ACTIONS

CONDITION	REQUIRED ACTION	COMPLETION TIME
A. Requirements of the LCO not met.	---------- NOTE ---------- LCO 3.0.3 is not applicable. ----------	
	A.1 Initiate action to move the non-complying fuel assembly to an acceptable storage location.	Immediately

New TS Page

SURVEILLANCE REQUIREMENTS

SURVEILLANCE		FREQUENCY
SR 3.7.17.1	Verify by administrative means that the initial enrichment, burnup and storage location of the fuel assembly is in accordance with Figure 3.7.17-1.	Prior to storing the fuel assembly in the Unit 2 Spent Fuel Pool

New TS Page

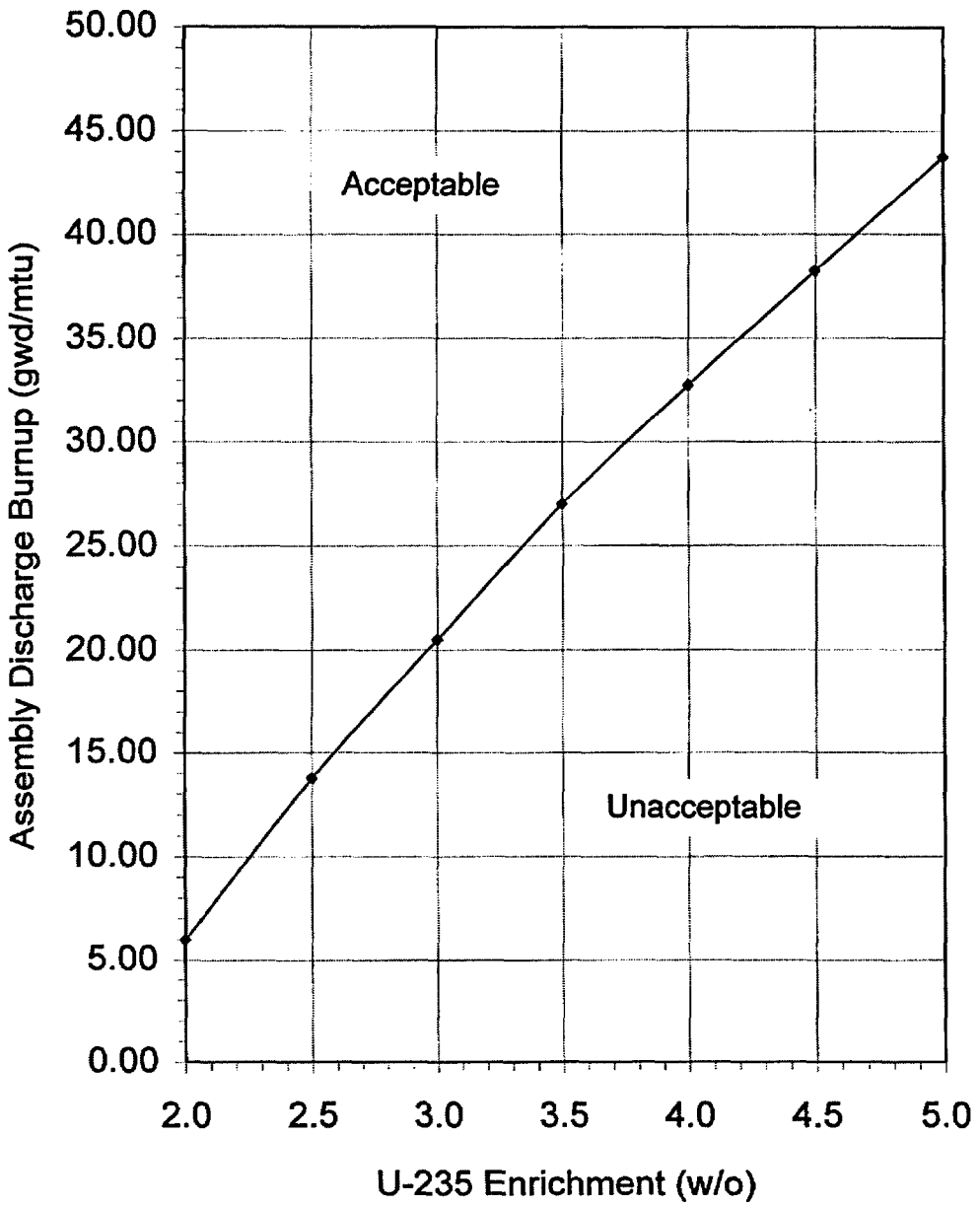

Figure 3.7.17-1
Discharge Burnup vs. Initial Enrichment for Unit 2 SFP

4.0 DESIGN FEATURES

4.2.2 Control Element Assemblies

The reactor core shall contain 77 control element assemblies.

4.3 Fuel Storage

4.3.1 Criticality

4.3.1.1 The spent fuel storage racks are designed and shall be maintained with:

a. Fuel assemblies having a maximum U-235 enrichment of 5.00 weight percent ~~for the Unit 1 pool and 4.52 weight percent for the Unit 2 pool~~;

b. ~~For Unit 1,~~ $k_{eff} < 1.00$ if fully flooded with unborated water, which includes an allowance for uncertainties as described in Section 9.7.2 of the Updated Final Safety Analysis Report (UFSAR) and $k_{eff} \leq 0.95$ if fully flooded with water borated to 350 ppm, which includes an allowance for uncertainties as described in Section 9.7.2 of the UFSAR;

~~c. For Unit 2, $k_{eff} \leq 0.95$ if fully flooded with unborated water, which includes an allowance for uncertainties as described in Section 9.7.2 of the UFSAR;~~

c d. A nominal 10-3/32-inch center-to-center distance between fuel assemblies placed in the high density fuel storage racks;

4.3.1.2 The new fuel storage racks are designed and shall be maintained with:

a. Fuel assemblies having a maximum U-235 enrichment of 5.0 weight percent;

ATTACHMENT (4)

FINAL TECHNICAL SPECIFICATIONS PAGES

iii

iv

v

3.7.16-1

3.7.17-1

3.7.17-2

3.7.17-3

4.0-2

4.0-3

3.7 PLANT SYSTEMS

3.7.16 Spent Fuel Pool (SFP) Boron Concentration

LCO 3.7.16 Boron concentration of the SFPs shall be ≥ 2000 ppm.

APPLICABILITY: When fuel assemblies are stored in the SFPs.

ACTIONS

CONDITION	REQUIRED ACTION	COMPLETION TIME
A. Spent Fuel Pool boron concentration not within limit.	---------- NOTE ---------- LCO 3.0.3 is not applicable. ----------	
	A.1 Suspend movement of fuel assemblies in the SFPs.	Immediately
	AND	
	A.2 Initiate action to restore boron concentration to within limit.	Immediately

SURVEILLANCE REQUIREMENTS

SURVEILLANCE		FREQUENCY
SR 3.7.16.1	Verify boron concentration is greater than 2000 ppm.	7 days

3.7 PLANT SYSTEMS

3.7.17 Spent Fuel Pool (SFP) Storage

LCO 3.7.17 The combination of initial nominal enrichment and burnup of each fuel assembly stored in the Unit 2 Spent Fuel Pool shall be in accordance with the following:

(a) Irradiated fuel assemblies may be stored in any rack location in the Unit 2 Spent Fuel Pool provided the combination of burnup and initial nominal enrichment is in the acceptable range of Figure 3.7.17-1, and

(b) Irradiated or unirradiated fuel assemblies with a combination of burnup and initial nominal enrichment that are not in the acceptable range of Figure 3.7.17-1 may be stored in the Unit 2 Spent Fuel Pool if surrounded on all four adjacent faces by empty rack cells or other non-reactive materials.

APPLICABILITY: Whenever any fuel assembly is stored in the Unit 2 Spent Fuel Pool.

ACTIONS

CONDITION	REQUIRED ACTION	COMPLETION TIME
A. Requirements of the LCO not met.	---------- NOTE ---------- LCO 3.0.3 is not applicable. ----------	
	A.1 Initiate action to move the non-complying fuel assembly to an acceptable storage location.	Immediately

SURVEILLANCE REQUIREMENTS

SURVEILLANCE		FREQUENCY
SR 3.7.17.1	Verify by administrative means that the initial enrichment, burnup and storage location of the fuel assembly is in accordance with Figure 3.7.17-1.	Prior to storing the fuel assembly in the Unit 2 Spent Fuel Pool

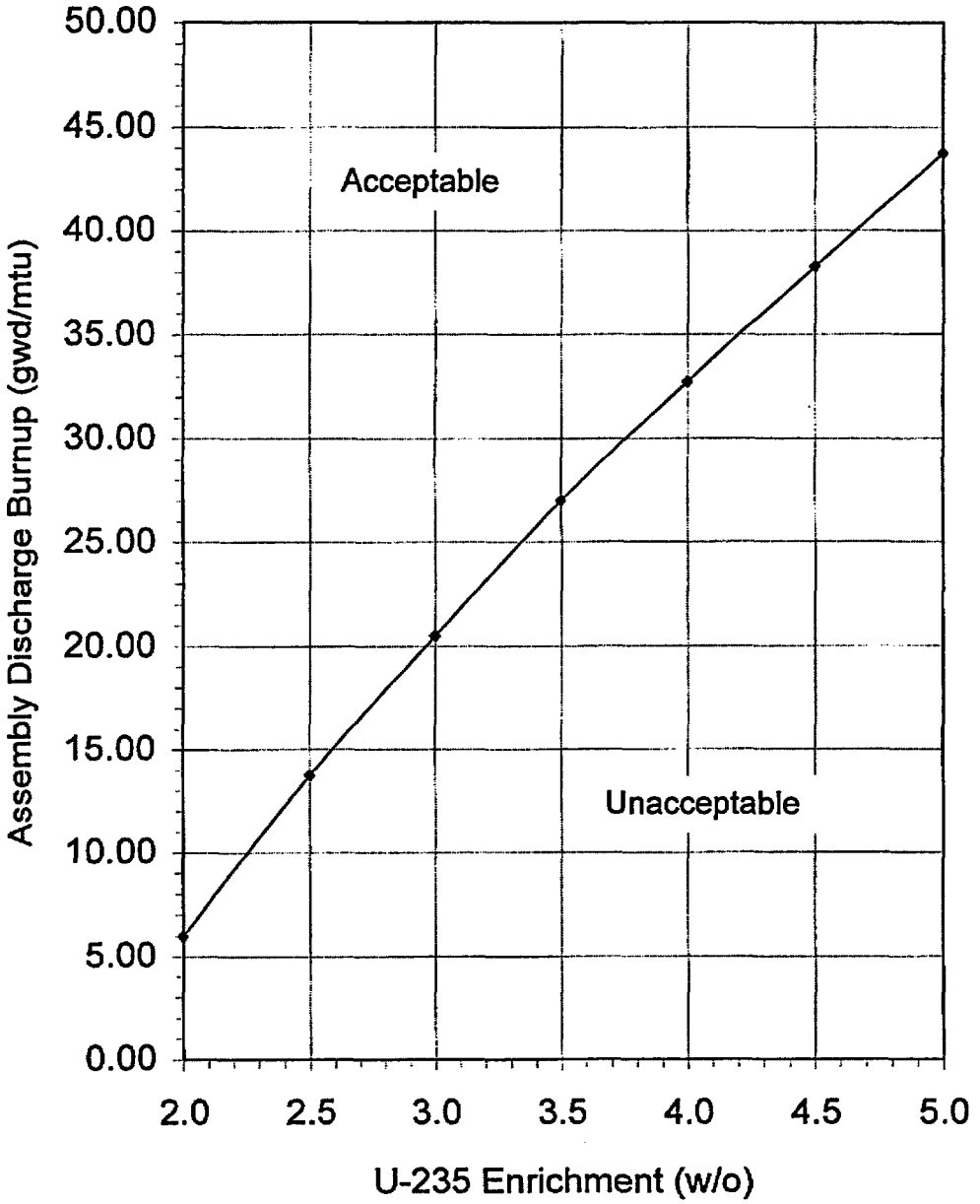

Figure 3.7.17-1
Discharge Burnup vs. Initial Enrichment for Unit 2 SFP

4.0 DESIGN FEATURES

4.2.2 Control Element Assemblies

The reactor core shall contain 77 control element assemblies.

4.3 Fuel Storage

4.3.1 Criticality

4.3.1.1 The spent fuel storage racks are designed and shall be maintained with:

a. Fuel assemblies having a maximum U-235 enrichment of 5.00 weight percent;

b. $k_{eff} < 1.00$ if fully flooded with unborated water, which includes an allowance for uncertainties as described in Section 9.7.2 of the Updated Final Safety Analysis Report (UFSAR) and $k_{eff} \leq 0.95$ if fully flooded with water borated to 350 ppm, which includes an allowance for uncertainties as described in Section 9.7.2 of the UFSAR;

c. A nominal 10-3/32-inch center-to-center distance between fuel assemblies placed in the high density fuel storage racks;

4.3.1.2 The new fuel storage racks are designed and shall be maintained with:

a. Fuel assemblies having a maximum U-235 enrichment of 5.0 weight percent;

b. $k_{eff} \leq 0.95$ if fully flooded with unborated water, which includes an allowance for uncertainties as described in Section 9.7.1 of the UFSAR;

4.0 DESIGN FEATURES

c. $k_{eff} \leq 0.95$ if moderated by aqueous foam, which includes an allowance for uncertainties as described in Section 9.7.1. of the UFSAR; and

d. A nominal 18-inch center-to-center distance between fuel assemblies placed in the storage racks.

4.3.2 Drainage

The spent fuel storage pool is designed and shall be maintained to prevent inadvertent draining of the pool below elevation 63 ft.

4.3.3 Capacity

The spent fuel storage pool is designed and shall be maintained with a storage capacity, for both Units 1 and 2, limited to no more than 1830 fuel assemblies.

ATTACHMENT (5)

CALVERT CLIFFS UNIT 2

SFP CRITICALITY ANALYSIS

Calvert Cliffs Nuclear Power Plant, Inc.
September 30, 2003

ESP No.:	ES200100780	Supp No.	0	Rev. No.	0	Page 1 of 1

FORM 19, CALCULATION COVER SHEET

INITIATION (Control Doc Type - DCALC) Page 1 of 191

DCALC No.: CA06015 Revision No.: 0

Vendor Calculation (Check one): ☐ Yes ☒ No

Responsible Group: NEU

Responsible Engineer: Gerard E. Gryczkowski

CALCULATION

ENGINEERING DISCIPLINE:
☐ Civil ☐ Instr & Controls ☒ Nuc Engrg
☐ Electrical ☐ Mechanical ☐ Diesel Gen Project
☐ Life Cycle Mngmt ☐ Reliability Engrg ☐ Nuc Fuel Mngmt
☐ Other:

Title: UNIT 2 SPENT FUEL POOL CRITICALITY ANALYSIS WITH SOLUBLE BORON AND BURNUP CREDIT BUT WITHOUT BORAFLEX CREDIT

Unit ☐ UNIT 1 ☒ UNIT 2 ☐ COMMON

Proprietary or Safeguards Calculation ☐ YES ☒ NO

Comments:

Vendor Calc No.: REVISION NO.:

Vendor Name:

Safety Class (Check one): ☒ SR ☐ AQ ☐ NSR

There are assumptions that require Verification during walkdown: AIT #:

This calculation **SUPERSEDES:**

REVIEW AND APPROVAL:

Responsible Engineer: Gerard E. Gryczkowski Date: 5/14/03

Independent Reviewer: John R. Massari Date: 5/15/03

Approval: M.T.Finley Date: 6/10/03

2. LIST OF EFFECTIVE PAGES

Page	Latest Rev	Page	Latest Rev	Page	Latest Rev	Page	Latest Rev	Page	Latest Rev
001	0	002	0	003	0	004	0	005	0
006	0	007	0	008	0	009	0	010	0
011	0	012	0	013	0	014	0	015	0
016	0	017	0	018	0	019	0	020	0
021	0	022	0	023	0	024	0	025	0
026	0	027	0	028	0	029	0	030	0
031	0	032	0	033	0	034	0	035	0
036	0	037	0	038	0	039	0	040	0
041	0	042	0	043	0	044	0	045	0
046	0	047	0	048	0	049	0	050	0
051	0	052	0	053	0	054	0	055	0
056	0	057	0	058	0	059	0	060	0
061	0	062	0	063	0	064	0	065	0
066	0	067	0	068	0	069	0	070	0
071	0	072	0	073	0	074	0	075	0
076	0	077	0	078	0	079	0	080	0
081	0	078	0	083	0	084	0	085	0
086	0	087	0	088	0	089	0	090	0
091	0	092	0	093	0	094	0	095	0
096	0	097	0	098	0	099	0	100	0
101	0	102	0	103	0	104	0	105	0
106	0	107	0	108	0	109	0	110	0
111	0	112	0	113	0	114	0	115	0
116	0	117	0	118	0	119	0	120	0
121	0	122	0	123	0	124	0	125	0
126	0	127	0	128	0	129	0	130	0
131	0	132	0	133	0	134	0	135	0
136	0	137	0	138	0	139	0	140	0
141	0	142	0	143	0	144	0	145	0
146	0	147	0	148	0	149	0	150	0
151	0	152	0	153	0	154	0	155	0
156	0	157	0	158	0	159	0	160	0
161	0	162	0	163	0	164	0	165	0
166	0	167	0	168	0	169	0	170	0
171	0	172	0	173	0	174	0	175	0
176	0	177	0	178	0	179	0	180	0
181	0	182	0	183	0	184	0	185	0
186	0	187	0	188	0	189	0	190	0
191	0								

3. REVIEWER COMMENTS

Comments on CA06015 from J. R. Massari

(01) The document has no page numbers, which makes the TOC useless.
Response: Page numbers will be add after incorporation of comments.

(02) **Section 5, second page.** The first paragraph on this page (just below the table) indicates that no unburned fuel may be stored in the Unit 2 spent fuel pool. However, on the same page, the fourth paragraph provides an acceptable checkerboard pattern for storing unburned fuel in the Unit 2 pool. This inconsistancy is also repeated in Section 13. If Pattern 1 is to be permitted, then the initial statement should be modified to reflect this condition.
Response: Done

(03) **Section 5, third page.** The first paragraph indicates a 2.6% Δk for cooling time from 100 days vs. 5 years. This should be 100 hours vs. 5 years. This error is also repeated in Sections 9.B.3.a and 13.
Response: Done

(04) **Section 6.A.** Change "theVAP" to "the VAP" in the last sentence.
Response: Done

(05) **Section 6.B.** Change "thet" to "that" in the sentence before the last paragraph.
Response: Done

(06) **Section 6.C.4.(e).** Change "kenetic" to "kinetic" in the last sentence.
Response: Done

(07) **Section 6.D.1.** In item (2)(f) for M5 cladding material, the phrase "Refs. and 22" should be changed to "Ref. 22", or the second reference should be added. Also, items (7) and (8) should probably indicate that the material info for the upper and lower endfittings comes from Refs. 25 and 26. Finally, the statement in item (12) does not appear to be true in all cases. The SAS2HED50 cases specify the fuel region as material 1, not 101.
Response: Done

(08) **Section 6.D.2.** This section indicates that the Boraflex panel is 0.09" thick, while the Unit 2 rack design report, NES 81A0704 Rev. 0 page 8, indicates that the panels are 0.08" thick. The Unit 1 panels are 0.09" thick. Since the KENO models replace the Boraflex with water, a few cases were run to quanitfy the effect of this small discrepancy. The results indicate a very small negative uncertainty (in the noise in one case), which indicates that the existing model is conservative and no changes to the model or uncertainties are warranted.

KENO Case	Enr w/o	Burnup gwd/t	"Poison Sheet" H_2O Thickness	Boron ppm	Clad	Unbiased K-eff	Delta K-eff	Uncertainty
K500000B6	*5*	*0*	*0.09"*	*0*	*zirc4*	*1.21112*	*0.00091*	
K500000BZ	5	0	0.08"	0	zirc4	1.20794	0.00093	-0.00318
K504000C6	*5*	*40*	*0.09"*	*300*	*zirc4*	*0.89089*	*0.00077*	
K504000CZ	5	40	0.08"	300	zirc4	0.89013	0.00085	-0.00076

Response: Noted. Also note that our current design basis CE calculation assumes 0.09".

(09) **Section 6.D.2.iii.** Provide a reference for the height of moderator above the active fuel region. I get 22.77 feet based on the TS requirement of 21.5 feet of water above the top of the fuel assembly, and 15.293 inches from the top of the active fuel region to the top of the assembly

(Ref. 13). This small discrepancy will have absolutely no impact on the results of the calculation.
Response: The 23.619' of water above the active fuel region and 17.871" of water below the active fuel region comes from Attachment G with appropriate references.

(10) **Section 7.A.** This assumption should probably also mention that the KENO model assumed that the boraflex was completely replaced by pool water and this representation is based on the fact that the silica matrix is dissolved by the water and transported away from the vicinity of the panel. Section 3.2.1 of Reference 14 provides a good description of the dissolution process.
Response: Done

(11) **Section 8, Reference 15.** Instead of the Unit 1 rack design report, the correct reference should probably be the report for the Unit 2 racks, NES Report 81A0704 Rev. 0.
Response: Done

(12) **Section 8, References 36 and 37.** These are both the same.
Response: Ref.37 has been changed.

(13) **Section 8, Reference 38.** To ensure that this reference can be obtained in the future, you should probably indicate that the paper was published in the ANS Transactions for the 2002 Winter Meeting (Vol. 87, pp. 105-107).
Response: Done

(14) **Section 9.B.2.** This section included a brief comparison with Calvert Cliffs radiochemical assay data from Ref. 10 that was used in the SAS2H Validation (CA05780). Recently, an independent radiochemical assay of Calvert Cliffs assembly BT03, performed by the V.G. Khlopin Radium Institute in Russia, was published in Ref. 11. This radiochemical assay included isotopes that were not included in the Oak Ridge doucment. An analysis similar to that performed at the end of section 9.B.2 was performed using this data. The results provided below show that the new data still supports the conclusion that the SAS2H generated isotopics produce conservative k_{eff} results for Calvert Cliffs fuel.

Case 08: Calvert Cliffs Assembly BT03 Rod NBD107, 37.27 GWD/MTU

Nuclide	measured mg/g UO2	Measured Ci/g UO2	SAS2H mg/g UO2	SAS2H Ci/g UO2	Percent Difference
U234	1.270E-01		1.070E-01		-15.75
U235	2.710E+00		2.590E+00		-4.43
U236	3.030E+00		3.000E+00		-0.99
U238	8.438E+02		8.330E+02		-1.28
Pu238	1.947E-01		1.890E-01		-2.93
Pu239	3.835E+00		3.990E+00		4.04
Pu240	2.321E+00		2.280E+00		-1.77
Pu241	8.130E-01		7.840E-01		-3.57
Pu242	7.753E-01		7.450E-01		-3.91
Np237		2.260E-07		2.690E-07	19.03
Am241		1.460E-03		1.250E-03	-14.38
Cm243-Cm244		4.110E-03		3.950E-03	-3.89
Se79		5.630E-08		6.500E-08	15.45
Sr90		5.180E-02		5.520E-02	6.56
Cs133		Used Average from CA05780			2.50
Cs134		Used Average from CA05780			-11.21
Tc99		8.960E-06		1.300E-05	45.09
Sn126		1.60E-07		6.13E-07	283.13

Cs135		4.15E-07	4.63E-07	11.57	
Cs137		8.56E-02	8.81E-02	2.92	
I129		Used Average from CA05780		-10.75	
Rh103	5.98E-01	4.53E-01		-24.28	
Nd143	6.69E-01	6.39E-01		-4.49	
Nd144	1.49E+00	1.38E+00		-7.63	
Nd145	6.74E-01	6.29E-01		-6.69	
Nd146	7.39E-01	6.94E-01		-6.15	
Nd148	3.91E-01	3.60E-01		-7.86	
Nd150	1.95E-01	1.83E-01		-6.12	
Sm147	2.47E-01	2.32E-01		-6.19	
Sm148	1.59E-01	1.51E-01		-5.26	Ref. 11
Sm149	1.87E-03	1.77E-03		-5.20	
Sm150	2.79E-01	2.76E-01		-0.97	
Sm151	7.30E-03	9.22E-03		26.33	
Sm152	1.13E-01	1.31E-01		16.41	14.9 years
Eu151	1.23E-03	1.14E-03		-7.62	
Eu153	1.38E-01	1.28E-01		-7.21	after
Eu154	6.58E-03	6.79E-03		3.17	
Eu155	1.04E-03	6.67E-04		-36.05	discharge
Gd154	1.17E-02	2.00E-02		71.48	
Gd155	6.46E-03	5.47E-03		-15.36	

KENO Case	SAS2H Case	Enr (w%)	Burnup (gwd/t)	Unbiased k_{eff}	Delta k_{eff}	Uncertainty
K506000D1	S560	5.0	60	0.84339	0.00071	-0.00196
K506000R1	Hand	5.0	60	0.84143	0.00074	

Response: OK

(15) **Section 9.B.3.a – d.** In the tables in these sections, the cases indicating that isotopics from SAS2H case S550 were used actually utilized those from case S550A.
Response: Done

(16) **Section 9.B.3.c.** This section addressed the effect of varying the average RCS boron concentration used during the SAS2H depletion, but did not address the manner in which the letdown was modeled during the depletion. If more than one library is requested per cycle (you used 1 long cycle with 20 libraries) SAS2H models boron letdown by varying the boron concentration linearly from 1.9 to 0.1 times the average during the time interval of the cycle. This is appropriate for an assembly with only 20 gwd/t burnup, but is not realistic for an assembly with 50 gwd/t burnup. To examine the sensitivity to variations in boron letdown, two SAS2H depletions were run with the same assembly power and EFPD as the 50 gwd/t case, but with varying boron letdown assumptions. The resulting k_{eff} values are provided in the table below. It seems that the letdown method currently used during the depletion provides the least conservative results for high burnup fuel. Options to fix this include applying a bias on the order of 0.35% Δk (possibly making it burnup dependent), or demonstrating that there is sufficient margin in other parts of the model to off-set this effect.

KENO Case	SAS2H Case	Enr w/o	Burnup gwd/t	Avg. Boron ppm	SAS2H Depletion Boron Letdown Method	Unbiased K-eff	delt
K505000AN	S550N	5.0	50	950	One 1649 EFPD Cycle (20 lib/cyc) w/ B linearly varying from 1.9 to 0.1 avg.	0.88363	-
K5050ANC3	S550C3	5.0	50	950	Three 549.7 EFPD Cycles (7 lib/cyc) w/ B linearly varying from 1.9 to 0.1 avg. each cycle	0.88712	0.002
K5050ANCB	S550CB	5.0	50	950	Twenty 82.45 EFPD Cycles (1 lib/cyc) w/ B constant at 950 ppm each cycle	0.88915	0.005

Response: In this analysis, where burnups ranged from 0 to 70 gwd/mtu, a single consistent methodology was employed to model soluble boron letdown. The single depletion model with one library per 2.5 gwd/mtu step minimizes any discontinuity due to arbitrary cycle lengths.

Three cases were executed to determine the effect of using three cycles per depletion instead of one:

KENO Case	SAS2H Case	Enr w/o	Burnup gwd/t	Avg. Boron ppm	SAS2H Depletion Boron Letdown Method	Unbiased K-eff	delt
K505000D1	S550N	5.0	50	950	One 1649 EFPD Cycle (20 lib/cyc) w/ B linearly varying from 1.9 to 0.1 avg.	0.89641	-
K5050ANC4	S550C4	5.0	50	950	Three 549.7 EFPD Cycles (7 lib/cyc) w/ B linearly varying from 1.9 to 0.1 avg. each cycle	0.89663	0.00(
K5050ANC3	S550C3	5.0	50	950	Same as prevuious case except with 180 down days between cycles	0.89717	0.00(

The difference between the three executions are within one sigma of each other and thus statistically equivalent. Note that these cases use zirc4 as the clad material, while the above use zirlo. Modification of the calculation results to incorporate multiple cycles per depletion is not warranted and would unnecessarily complicate the calculations, since cycle length and downtime between cycles would theoreticall have to be optimized.

(17)**Section 9.B.** The analyses in References 4 through 8 utilized 2-D depletion codes such as CASMO-4, and Reference 9 does not specifically mention SAS2H/ORIGEN-S (a point/quasi-1D code) as an acceptable depletion method. To allay any possible concerns, a comparison of k_{eff} values calculated from isotopics obtained from SAS2H and CASMO-4 was performed. The CASMO-4 depletion utilized identical input conditions and materials as those used in SAS2H. This comparison used the same set of actinides, but only 20 of the 36 fission products (for both the SAS2H and CASMO4 cases). The 16 fission products not available from CASMO-4 were: KR-84, KR-86, MO-95, TC-99, RU-101, SN-126, I-129, XE-132, XE-134, ND-144, ND-146, ND-148, SM-148, ND-150, EU-151, and GD-154. The KENO results are provided in the table below, and indicate that for the 34 isotopes considered, isotopics from SAS2H are more conservative than from CASMO-4 by average of 0.675% Δk. This conservatism is larger than the worth of the 16 isotopes that were not considered in this comparison.

KENO Case	SAS2H Case	Enr w/o	Burnup gwd/t	Avg. Boron ppm	SAS2H Depletion Boron Letdown Method	Unbiased K-eff	Delta 50 vs. 34	Delta SAS2H vs.
K505000AN33	S550N	5.0	50	950	Same as above but with 34 isotopes	0.89216	-0.00853	0.006
K5050ANC3-33	S550C3	5.0	50	950	Same as above but with 34 isotopes	0.89482	-0.00770	0.00866
K5050ANCB33	S550CB	5.0	50	950	Same as above but with 34 isotopes	0.89175	-0.00260	0.00559
K5050ANCB33cas	CASMO4	5.0	50	950	34 isotopes from CASMO4 depletion	0.88616	N/a	N/a
					Average worth of 16 remaining fission products w/ SAS2H	-0.00628		
					Average delta between SAS2H and CASMO4 for 34 isotopes	0.00675		

Response: OK

(18) **Section 9.C.** In the first sentence, remove the first "i" from "iisotopics."
Response: Done

(19) **Section 9.C.** The analysis credited a number of fission product absorbers that might not be present at 100% of their predicted values in failed fuel. Examples include Kr, Xe, I, Cs, and Mo isotopes. Reference 1 provides the design basis release rates for these isotopes from a failed rod while at power (6.5E-8 sec^{-1} for noble gases, 2.3E-8 sec^{-1} for I and Cs, and 1.4E-9 sec^{-1} for Mo) for use in calculating the RCS specific activity for 1% failed fuel. These release rates indicate that for a 24-month cycle, only 2% of the noble gases, 25% of the I and Cs, and 90% of the Mo would remain from BOC (see figure below) in a failed rod. In addition, any remaining noble gases and highly soluble isotopes, such as I and Cs (Ref. 3, p. 6-28), would continue to be lost while the failed rod was in the spent fuel pool. Three possible options to correct this deficiency are: 1) expand the moderator-in-gap uncertainty to be a failed fuel uncertainty that also considers reduction/loss of the above mentioned isotopes, 2) restrict failed fuel from the Unit 2 pool, in which case you could argue that it was bounded by the fresh fuel misload accident, 3) demonstrate that there is sufficient margin in other parts of the model to off-set this effect. As a side note, none of the other evaluations in References 4 through 8 addressed this.

Response: See Section 9.E.2.j.

(20) **Section 9.C.** There appears to be a bug in the SAS2HED50 code. The SAS2H output contains moles of U-236, but the SAS2HED50 code supplied KENO input section contains a number density of 1E-20 for U-236. However, the code correctly calculates the number density, as is shown at the top of the output. To determine the impact of this bug, one of the previous KENO cases was rerun with the correct U-236 number density. The results suggest a reactivitiy bias of –0.61%, which indicates that the existing method used in the calc is conservative (and compensates for some of the errors noted above).

Case K5050ANCB without U-236	0.88915
Case K5050ANCB236 with U-236 added in	0.88305

Response: OOPS. But conservative. SAS2HED50 corrected for later use.

(21) **Section 9.D.** In the paragraph just below the table, the first sentence indicates that Figures 8 – 11 depict various isotopic quantities as a function of burnup. This needs to be changed to Figures 9 – 11. Figure 8 looks like a loading curve but it could use a better title since the current one is not very descriptive.
Response: Done

(22) **Section 9.E.2.b.** For case K50400C8, change ",89004" to "0.89004".
Response: Done

(23) **Sections 9.E.c & d.** It would be helpful if the baseline k_{eff} cases (K500000B6, K500000C6, and K504000C6) were listed in these tables as was done in the other sections, to make it easy for the reader to see how the uncertainties were determined.
Response: The data is listed in many places including a master listing in Appendix A.

(24) **Section 9.E.2.k.** No problems were found with this section. However, it seems worth noting some new information that further demonstrates the conservatism of the 3.3% axial profile bias used. Reference 15 performed an even more detailed review of the PWR Axial Profile Database (YAEC-1937) than did References 33 and 34 of CA06015. Of particular interest is the plots in Ref. 15 (pp. 44-49) for each of the 12 burnup groups by fuel type, which indicate that the axial bias for CE 14x14 assemblies (544 of 3169 assemblies in the database) is never greater than 1% for any of the burnup groups. The profiles which result in high axial profile biases occur only in fuel designs where control and axial power shaping rods are utilized for flux shaping (11 of the 12 bounding designs are from B&W 15x15 assemblies). Axial power shaping rods are not used at CCNPP and a review of cycles back to U1C8 and U2C7 confirmed all rods are generally fully withdrawn (any insertion that does occur is typically on the order of a few inches for a total of 3% or less of the cycle duration). In addition, another conservatism worth noting is that the axial bias is generated by comparing axial vs. average burnup profiles in an axially finite assembly model, but is applied to calculations using average burnup profiles in an axially infinite assembly model.
Response: OK. Some additional information was added from Ref.37.

(25) **Section 12.C.** For clarity, you may wish to add a column indicating the SAS2H case that the isotopics used in the KENO run came from.
Response: Done

REFERENCES

(01) "Fission Product Activity in the Reactor Coolant," CE Report SE-69-971, NORMS Doc ID #77330, October 9, 1969

(02) CCNPP Calculation CA05994, "RC Waste Processing System Incident and Waste Gas Incident Dose Analysis," October 4, 2002.
(03) "Evaluation of the Candidate High-Level Radioactive Waste Repository at Yucca Mountain Using Total System Performance Assessment," EPRI TR-1000802, November 2000.
(04) Docket 50-247, Indian Point Unit 2, "License Amendment Request for Spent Fuel Storage Pit Rack Criticality Analysis with Soluble Boron Credit," Entergy Nuclear Northeast, September 20, 2001.
(05) Docket 50-336, Millstone Power Station Unit 2, "Technical Specification Change Request 2-10-01, Fuel Pool Requirements," Dominion Nuclear Connecticut, November 6, 2001.
(06) Docket 50-335, St. Lucie Unit 1, "Proposed License Amendment: Spent Fuel Pool Soluble Boron Credit," Florida Power and Light Corporation, November 25, 2002.
(07) Docket 50-368, Arkansas Nuclear One Unit 2, "License Amendment Request to Change Spent Fuel Pool Loading Restrictions," Entergy Operations, January 29, 2003.
(08) Docket 50-250 & 251, Turkey Point Units 3 & 4, "Soluble Boron Credit for Spent Fuel Pool and Fresh Fuel Rack Criticality Analyses," Florida Power and Light Corporation, November 30, 1999.
(09) "Guidance on the Regulatory Requirements for Criticality Analysis of Fuel Storage at LWR Power Plants", NRC Memorandum L. Kopp to T. Collins, 8/19/98
(10) "Validation of the Scale System for PWR Spent Fuel Isotopic Analyses," ORNL/TM-12667, Oak Ridge National Laboratory, March 1995.
(11) "Compilation of Radiochemical Analyses of Spent Nuclear Fuel Samples," PNNL-13667, Pacific Northwest National Laboratory, September 2001.
(12) "Nuclear Design Analysis Report for the Calvert Cliffs Unit 2 Nuclear Plant High Density Spent Fuel Storage Racks," NES Report 81A0704 Rev. 0, October 28, 1980.
(13) "Fuel Bundle Assembly," CCNPP Drawing 12131-0342SH0001, Rev. 1, November 17, 1999.
(14) "The RACKLIFE Boraflex Rack Life Extension Code: Theory and Numerics," EPRI TR-107333, Electric Power Research Institute, August 1997.
(15) "Recommendation for Addressing Axial Burnup in PWR Burnup Credit Analyses," ORNL/TM-2001/273, November 2002.

4. TABLE OF CONTENTS

5. PURPOSE

The primary purpose of the spent fuel pool is to maintain the spent fuel assemblies in a safe storage condition. Per 10 CFR 50 App.A GDC 62 (Ref.1), criticality in the fuel storage and handling system shall be prevented by physical systems or processes, preferably by use of geometrically safe configurations. Per 10 CFR 50.68 (Ref.2), if no credit for soluble boron is taken, the k-effective of the spent fuel storage racks loaded with fuel of the maximum fuel assembly reactivity must not exceed 0.95, at a 95% probability, 95% confidence level, if flooded with unborated water. If credit is taken for soluble boron, the k-effective of the spent fuel storage racks loaded with fuel of the maximum fuel assembly reactivity must not exceed 0.95, at a 95% probability, 95% confidence level, if flooded with borated water, and the k-effective must remain below 1.0 (subcritical) at a 95% probability, 95% confidence level, if flooded with unborated water. In addition, the maximum nominal U-235 enrichment of the fresh fuel assemblies is limited to five percent by weight.

The existing analysis of record for the Unit 2 SFP (Ref.28) allows the storage of standard fresh fuel assemblies with a maximum fresh fuel enrichment of 4.52 w/o U-235, based on the older pellet design utilizing smaller pellet diameters and stack densities; a k-effective less than 0.95 including uncertainties and biases, and no soluble boron credit. Ref.29 determined the maximum fresh fuel enrichment with VAP fuel with the present storage configuration, such that, K-effective is less than 0.95 with uncertainties and biases and assuming no soluble boron credit. VAP fuel with enrichments less than or equal to 4.30 w/o U-235 can now be safely stored in the CCNPP Spent Fuel Pools. Note that VAP fuel is more reactive than similarly enriched standard fuel, thus any analysis performed for VAP fuel conservatively bounds that for standard fuel. The analyses of record for the Unit 2 SFP assume the presence of Boraflex poison sheets with 4" staggered gaps.

Issue Reports IR3-045-938, IR3-045-939, and IR3-052-199 documented possible boraflex degradation in the Unit 2 Spent Fuel Pool, based on calculations using the Racklife software package. The Racklife results indicated that at certain highly-irradiated locations the degradation could be as high as 70%. Since the Unit 2 design basis areal B-10 loading is 0.020 gm/cm^2 and since the initial loading was a minimum of 0.020 gm/cm^2, insufficient margin exists to cover the degradation. The evaluation in Ref.42 was performed to determine CCNPP's compliance with Technical Specification 4.3.1.1, which states that K-effective must be less than or equal to 0.95 if fully flooded with unborated water, which includes an allowance for uncertainties and biases as described in Section 9.7.2 of the UFSAR. Crediting burnup in lieu of boraflex assures that the Technical Specification K-effective limit of 0.95 is maintained.

The purpose of this report is to document the Calvert Cliffs Nuclear Power Plant (CCNPP) Spent Fuel Pool (SFP) Rack Criticality Methodology that ensures that the spent fuel rack multiplication factor, k-eff, is less than the 10 CFR 50.68 (Ref.2) regulatory limit with Value Added Pellet (VAP) fuel ranging in enrichment from 2.0 to 5.0 w/o with burnup credit and with partial credit for soluble boron in the Unit 2 SFP. The soluble boron credit will be limited to 300 ppm per the restrictions of the Unit 1 criticality analysis in Ref.43. Note that 300 ppm is a minimum boron concentration requirement. 15% should be added to this value to account for all uncertainties. Thus a boron level of 350 ppm with uncertainties is required to credit soluble boron in the SFP.

The burnups required to store fuel in the Unit 2 SFP crediting 350 ppm of soluble boron including all biases and uncertainties are the following:

Enrichment (w/o)	Burnup (GWD/MTU)
2.0	6.00
2.5	13.75
3.0	20.50
3.5	27.00
4.0	32.75
4.5	38.25
5.0	43.75

A graphical representation of the above is presented in Figure 8, while a second-order regression analysis is listed in Attachment S. Note that these minimum burnup values are less than those reported in Ref.42 Thus, all assemblies currently qualified to be stored in the Unit 2 Spent Fuel Pool may continue to be safely stored in the Unit 2 Spent Fuel Pool. In addition, each assembly offloaded from either reactor or from an ISFSI DSC must be evaluated against the above burnup restrictions to determine if it can be safely stored in the Unit 2 SFP. No similar restrictions exist on the Unit 1 SFP.

A finite radial and axial model of the Unit 2 SFP of nominal dimensions containing the maximum enrichment of 5.0 w/o VAP fuel at a soluble boron concentration of 0, 300, and 2000 ppm was modeled with sequential assemblies in the row closest to the SFP wall on spacers to simulate the reconstitution/inspection process. There is no reactivity difference between reconstituting an entire row of assemblies or normal storage of said assemblies. Since Boraflex is not credited in this analysis, placing assemblies on spacers has no reactivity effect.

Dropping an assembly of 5.0 w/o VAP fuel onto the SFP racks was analyzed, even though it is not a credible accident. Per Ref.4, the double contingency principle was applied. It required two unlikely, independent, concurrent events to produce a criticality accident. The double contingency principle means that realistic conditions may be assumed. For example, if soluble boron is normally present in the SFP water, the loss of soluble boron is considered as one accident condition and a second concurrent accident need not be assumed. Therefore, total credit for the presence of soluble boron may be assumed in evaluating this accident condition. Per Technical Assumption 7.H, the normal SFP boron concentration is conservatively assumed to be 2000 ppm. A finite radial and axial configuration of the Unit 2 SFP of nominal dimensions containing the maximum enrichment of 5.0 w/o fuel was modeled as a function of soluble boron concentration (0, 300, 2000 ppm) for the dropped assembly accident with and without reconstitution. The dropped assembly is effectively decoupled from the assemblies stored in the SFP storage racks as was previously noted in Ref.32. Taking credit for 2000 ppm per the double contingency principle drops the k-effective value to well below the regulatory requirement for all cases.

Several checkerboard patterns were modeled in an effort to store more reactive fuel in the Unit 2 SFP. Note that only one pattern meets the requirements of 10 CFR 50.68 (Ref.2). If credit is taken for soluble boron, the k-effective of the spent fuel storage racks loaded with fuel of the maximum fuel assembly reactivity must not exceed 0.95, at a 95% probability, 95% confidence level, if flooded with borated water, and the k-effective must remain below 1.0 (subcritical) at a 95% probability, 95% confidence level, if flooded with unborated water. Thus to store any fuel with insufficient burnup to satisfy reactivity requirements, that fuel assembly must be surrounded on all four adjacent faces by empty rack cells or other nonreactive materials (e.g., wall, water,...).

The above results include the following conservatisms:

(01) SAS2H isotopics were modeled with conservative fuel temperature, moderator temperature, soluble boron concentration, specific power, and refueling downtime inputs. For 5 w/o fuel at 50

GWD/MTU, the conservatism was in excess of 0.4% Δk for Tfuel, 0.5% Δk for Tmod, and 2.6% Δk for cooling time (100 hours vs 5 years). The conservatisms were higher for lower enrichments but lower for lower burnups.

(02) Integral burnable absorbers, boraflex poison sheets, and control element assemblies were conservatively neglected in this work.

(03) A reactivity uncertainty due to uncertainty in the fuel depletion calculation should be developed and combined with other calculational uncertainties. An uncertainty equal to 5% of the reactivity decrement to the burnup of interest is an acceptable assumption. Based on computations presented in this work, a worst case uncertainty value of 0.02089 was used in all burnup related reactivity calculations, even though SAS2H generated reactivity was determined to be 0.358% more reactive than those adjusted to radiochemical assay isotopics.

(04) For conservatism, an axial burnup bias of 3.3% Δk was utilized for all burnup cases. The most conservative Calvert Cliffs specific reactivity bias was calculated to be -0.579% Δk. Thus for Calvert Cliffs specific fuel, use of 26-node axial burnup profiles is less conservative than uniform axial burnups

(05) Inclusion of additional isotopes in the SAS2H and KENO executions can add significantly more margin to the reactivity results. While no benchmarks exist for these additional isotopes, comparison of existing benchmark cases to SAS2H/KENO computations indicates that the computation results are conservative. Note that the additional margin provided by an expanded list of isotopes (101 vs 50) generally increases as a function of burnup and enrichment, exceeding 1.5% Δk for high enrichments (4-5 w/o) and high burnup (60 gwd/mtu) fuel.

(06) The worst case composite bias and uncertainty value was 0.06129 ΔK for zero soluble boron and zero burnup. This value was conservatively applied to all calculated reactivity values.

(07) The conservatism in reactivity for a two-dimensional infinite array versus a three-dimensional Unit 2 specific model increases from 1.56% Δk at 0 ppm, to 10.18% Δk at 300 ppm, to 21.87% Δk at 2000 ppm. In addition, for the zero burnup cases, an additional reactivity conservatism of 4.185% Δk exists. Thus for the three-dimensional Unit 2 specific model, an entire SFP of 5.0 w/o fresh fuel becomes subcritical (k-effective < 1) for soluble boron concentrations in excess of 500 ppm assuming no credit for boraflex in the Unit 2 SFP racks and no credit for burnup. For the two-dimensional infinite array model, ~1600 ppm would be required to maintain subcriticality under the same conditions.

6. INPUT DATA

Inputs and assumptions have been developed conservatively consistent with applicable safety analysis guidance.

(6.A) Fuel and Assembly Parameters

The fuel assemblies contain uranium dioxide (UO_2) over the entire length of the active fuel region in each fuel rod and a uniform distribution of enrichments both radially and axially. The fuel and 14x14 assembly parameters for standard and VAP fuel designs are detailed in Z2INP.XLS(Fuel) (Attachment D). Note that per Ref.28 the Unit 2 SFP enrichment limit is 4.52 w/o for the standard fuel design, while per Ref.29 the Unit 2 SFP enrichment limit is 4.30 w/o for the VAP fuel design. Thus since the VAP fuel design is more limiting, all calculations performed in this work will model VAP assemblies.

(6.B) Integral Burnable Absorbers

Ref.35 details the effect of Integral Burnable Absorbers (IBAs) on reactivity as a function of burnup, fuel enrichment, IBA number and loading, and cooling time. IBAs are burnable poisons that are an integral part of the fuel assembly. Two types are detailed. The first is the Westinghouse Integral Fuel Burnable Absorber (IFBA), which has a coating of zirconium diboride (ZrB_2) on the fuel pellets and which does not displace fuel. The second includes UO_2-Gd_2O_3 rods, UO_2-Er_2O_3 rods, and Al_2O_3-B_4C rods, which do displace fuel.

For PWR fuels without IBAs, reactivity decreases with burnup in a nearly linear fashion. For PWR fuel assembly designs that make significant use of IBAs, reactivity actually increases as fuel burnup increases, reaching a maximum at a burnup where the IBA is nearly depleted (approximately a third into the assembly life), and then decreasing with burnup almost linearly. The presence of IBAs during depletion hardens the neutron spectrum, resulting in lower U-235 depletion and higher production of fissile plutonium isotopes. Enhanced plutonium production and the concurrent diminished fission of U-235 can increase the reactivity of the fuel at later burnups.

The analyses of Ref.35 conclusively demonstrate that with the exception of the Westinghouse IFBA rods, k-eff for an assembly without IBAs is always greater (throughout burnup) than k-eff for an assembly with IBAs, including UO_2-Gd_2O_3 rods, UO_2-Er_2O_3 rods, and Al_2O_3-B_4C rods. The negative reactivity effect of the IBAs was found to increase with increasing poison loading (the number of poison rods and the B-10 content) and with increasing initial fuel enrichment. This is due to the negative residual effect associated with the neutron-absorbing isotopes and with the reduced reactivity due to the reduction in fissile isotopes. Therefore, for those IBAs other than IFBAs, burnup credit criticality safety analyses may conservatively neglect the presence of the IBAs by assuming non-poisoned equivalent enrichment fuel.

For assembly designs with IFBA rods, two-dimensional radially-infinite calculations have demonstrated that the neutron multiplication factor is slightly greater for assembly designs with IFBA rods (maximum of 0.4% Δk). Three-dimensional cask calculations showed that when the axial burnup is included, assemblies with full-axial length IFBA coatings are less reactive than corresponding assemblies without IFBA rods, because of the residual absorber in the low-burnup end regions. However, the results also indicated that the effect of the IFBA rods is dependent on the axial length of the poison loading and that for typical IFBA coating lengths, there is a small positive effect associated with the IFBA rods. For a fixed initial fuel enrichment, the positive reactivity effect was shown to increase with increasing poison loading. For a fixed poison loading, the positive reactivity effect was shown to increase with decreasing initial fuel enrichment. This increase in reactivity for assemblies with IFBAs is due to a lack of residual reactivity effects associated with IFBAs and due to no reduction in fissile isotopes.

The Ref.35 results indicate that the calculated effects are not sensitive to cooling time.

Similar reactivity behavior as a function of IBA loading is observed for Calvert Cliffs specific VAP fuel. Ref.36 and the tables and graphs of Attachment J detail k-infinity versus burnup for 3.8 and 4.8 w/o VAP fuel for 2.0 w/o UO_2-Er_2O_3 rods of 0, 20, 44, and 68 quantity. In all cases, the non-poisoned equivalent enrichment fuel is more reactive than the poisoned fuel, and the negative reactivity effect of the IBAs was found to increase with increasing poison loading Therefore, burnup credit criticality safety analyses may conservatively neglect the presence of the IBAs by assuming non-poisoned equivalent enrichment fuel.

(6.C) SAS2H Depletion Inputs
(6.C.1) Isotopics
(a) Per Ref.4, the SFP storage rack should be evaluated with spent fuel at the highest reactivity following removal from the reactor (usually after the decay of Xe-135). Thus the SAS2H-generated Xe-135 concentration will be set to zero.
(b) Per Ref.4, subsequent decay of longer-life nuclides, such as Pu-241 to Am-241, over the rack storage time may be accounted for to reduce the minimum burnup required to meet the reactivity requirements. In this work, the minimum of 100 hours of decay time will be assumed per Ref.45.

(6.C.2) Cross Section Library
The SAS2H executions utilize the 44GROUPNDF5 cross section library as recommended in Ref.9 and validated in Ref.8. 44GROUPNDF5 is a 44-energy group library derived from the latest ENDF/B-V files with the exception of O-16, Eu-154, and Eu-155, which were taken from the more improved ENDF/B-VI files.

(6.C.3) Lattice Type
Per Ref.9, SAS2H always requires LATTICECELL.

(6.C.4) Material Specifications
(a) The UO_2 weight percentages for 5.0, 4.5, 4.0, 3.5, 3.0, 2.5, and 2.0 w/o enriched fuel are derived in the EXCEL spreadsheet (Densities)z2inp.xls, which is listed in Attachment C. The methodology for calculating the weight percentages is as follows:

U5w = U235 w/o enrichment of total U (given)
U8w = (100-U5w) = U238 w/o enrichment of total U
Ow = 32*(U5w/235+U8w/238)
U5x = U5w/(U5w+U8w+Ow)=U235 w/o of UO_2
U8x = U8w/(U5w+U8w+Ow) =U238 w/o of UO_2
Ox = Ow/(U5w+U8w+Ow) =O16 w/o of UO_2

(b) Per UFSAR Tables 3.3-1 and 3.3-2, the maximum stack height density is 10.31 gm/cc (<94.5% theoretical density). Thus a nominal stack height density of 94.5% of theoretical density (10.3572 gm/cc) will be assumed.

(c) Per Refs.9 and 40, trace elements of selected nuclides are automatically included by SAS2H to assure appropriate cross sections are available for important nuclides that accumulate in the fuel during depletion. These include

Xe-135	Cs-133	U-234	U-235	U-236
U-238	Np-237	Pu-238	Pu-239	Pu-240
Pu-241	Pu-242	Am-241	Am-242m	Am-243
Cm-242	Cm-243	Cm-244	1/v-absorber	

(d) Per Ref.9, trace elements of additional nuclides (trace density $1x10^{-20}$ atoms/b-cm) may be added by the user to assure appropriate cross sections are available for important nuclides that

accumulate in the fuel during depletion. The additional nuclides used in this work corresponds to a set generated by ORNL in Ref.40. These isotopes represent the highest worth fission products or the precursors for the highest worth fission products and include the following:

Moderator region:	Co-59			
Fuel region:	Zr-94	Mo-94	Nb-95	Mo-95
Tc-99	Rh-103	Rh-105	Ru-106	Sn-126
Xe-131	Cs-134	Cs-135	Cs-137	Pr-143
Nd-143	Ce-144	Nd-144	Nd-145	Nd-146
Nd-147	Pm-147	Sm-147	Nd-148	Pm-148
Sm-148	Pm-149	Sm-149	Nd-150	Sm-150
Sm-151	Eu-151	Sm-152	Eu-153	Eu-154
Gd-154	Eu-155	Gd-155	Gd-157	Gd-158
Gd-160				

(e) Light elements are used in the calculation of the average energy per fission. Since most of the energy released per fission is in the kinetic energy of the fission products, the correction for capture energy with light element absorption is small. ORNL in Ref.40 has been in the practice of estimating the light element content of PWRs by use of a constant content. Assembly light element masses were taken from Reference 40 and are summarized below.

Assembly Light Element Masses

Element	Kg/assy
O	119
Fe	11
Zr	195
Cr	5.2
Co	0.066
Nb	0.63
Mn	0.29
Ni	8.7
Sn	3.2

(6.C.5) Fuel Temperature

A significant spatial variation exists in the fuel temperature because of the low thermal conductivity of UO_2. The fuel temperature is highest at the pellet centerline and lowest at the pellet outside diameter. In addition, the fuel temperature varies axially due to different linear heat generation rates at different axial positions. An increase in fuel temperature increases the resonance capture of neutrons in U-238 due to Doppler effect, which results in increased production of fissile plutonium and actinide absorbers. This, in turn, causes more fissions in fissile plutonium and leads to less depletion in U-235. The net effect is increased reactivity with an increase in fuel temperature.

Per Ref.48, it is desirable to select a value for fuel temperature that estimates the highest average temperature that an assembly has experienced. The fuel temperature determined, based on the rated linear power multiplied by the radial peaking factor limit, is the highest axially-averaged fuel temperature. Since the radial peaking factor limit is established on fuel pins, not on assemblies, application of the radial peaking factor throughout the entire assembly provides a layer of conservatism. It is still possible that parts of assemblies could experience higher fuel temperatures for a period of time because of axial variations; however, decreased end effects should compensate for higher mid-region effects. Thus the nominal average pellet temperature

should be calculated based on a reactor rated linear power multiplied by the radial peaking factor limit. A sufficiently conservative value can be obtained using a uniform axial power distribution and taking the average pellet temperature from the top of the fuel assembly. The burnup that results in the highest fuel temperature should be used.

Fuel temperature used in the SAS2H cases was calculated using the fuel temperature correlation from the CORD model for Unit 1 Cycle 16, as documented in file gbnszsoq.cdf of Refs,49-50. The correlation is:

$$T_{fuel} = T_{mod} + (-2.34607E\text{-}7*B^2 + 1.10995E\text{-}3*B + 130.08)*L + (-9.505119E\text{-}13*B^3 + 5.13836E\text{-}8*B^2 - 5.11639E\text{-}4*B - 1.67177)*L^2$$

where, T_{fuel} = fuel temperature in °F
T_{mod} = moderator temperature in °F
B = burnup in MWd/MTU
L = linear power density in kW/ft.

As in the CORD model, the actual burnup is used up to 20,000 MWd/MTU, above which it is fixed at 20,000 MWd/MTU.

Attachment K (EXCEL Spreadsheet SAS2H-Tfuel(X2inp.xls)) details the calculation of the bounding fuel temperature as a function of burnup for a T_{hot} value of 601°F per UFSAR Figure 4-9, a core thermal power of 2970 MWt (2700 MWt times a 10% power uprate), and a radial peaking factor of 1.65 per Refs.51-52. Note that the peak fuel temperature value of 1285.42°K at zero burnup will be conservatively employed in all SAS2H calculations.

Note that the fuel, moderator, and clad temperatures are defined on the material cards; however, they may also be specified on the power cards via the TMPFUEL, TMPCLAD, and TMPMOD inputs. If the temperatures are specified on the power cards, all must be specified or none must be specified. If none are specified, the temperatures on the material cards will be utilized. If all are specified, the temperatures on the power cards will be utilized. If only some are specified on the power cards, the remaining will be set to zero.

(6.C.6) Moderator Temperature

The moderator temperature is lowest at the reactor inlet and increases monotonically as it reaches the reactor outlet. This increase in moderator temperature is greater in a hot channel where the heat generation is higher than the average. Neutron spectral hardening occurs with an increase in moderator temperature due to fewer hydrogen nuclides that thermalize fast neutrons past the resonance region. An increase in resonance capture of neutrons in U-238 due to the hardened spectrum results in increased production of fissile plutonium and actinide absorbers. This, in turn, causes more fissions in fissile plutonium and leads to less depletion in U-235. The net effect is increased reactivity with an increase in moderator temperature.

The moderator temperature increases from the bottom to the top of the reactor core. Thus per Ref.48, the use of the average core outlet temperature appears to conservatively bound the moderator temperature. In fact, the use of the average core outlet temperature ($T_{in} + \Delta T_{ave}$) is more conservative than the use of the peak average moderator temperature ($T_{in} + \Delta T_{ave}*P_{radial}/2$). Applying the average core outlet temperature over the entire fuel length and for the entire depletion time provides adequate assurance of bounding treatment.

Per UFSAR Figure 4-9, an average core outlet temperature of 601°F or 589.26°K will be conservatively employed in all SAS2H calculations. The corresponding water density of 0.6905 gm/cc is derived in Attachment L (H2ODEN(x2inp.xls)) from data extracted from Ref.9.

(6.C.7) Soluble Boron Concentration
The concentration of soluble boron is adjusted to maintain core criticality. The soluble boron concentration is gradually decreased as the burnup increases and reaches a minimum value at the end of cycle. The soluble boron present in the moderator increases the thermal absorption cross section, decreases the thermal flux, and results in a hardened neutron spectrum. An increase in resonance capture of neutrons in U-238 due to the hardened spectrum results in increased production of fissile plutonium and actinide absorbers. This, in turn, causes more fissions in fissile plutonium and leads to less depletion in U-235. The net effect is increased reactivity with an increase in soluble boron concentration.

The limit on moderator temperature coefficient (MTC) restricts the level of soluble boron concentration in a given reactor cycle, which is the reason that many plants with long cycle lengths resort to the use of burnable absorbers in fuel assemblies. The average soluble boron concentration can be calculated from the critical boron letdown curve generated as a result of fuel reload analysis. The average boron concentration can be found by integrating the boron letdown curve with respect to time and dividing by the cycle length. Per Ref.48, the maximum average boron concentration is to be identified and used in the SAS2H depletion analysis.

Per Refs.53-55, the maximum BOC soluble boron concentration is less than 1820 ppm, where Ref.55 models a cycle at the MTC Technical Specification limit. The boron letdown curves in these cycles are approximately linear with exposure. Thus a bounding BOC soluble boron concentration of 1900 ppm will be assumed with a linear letdown curve, resulting in a maximum average soluble boron concentration of 950 ppm. Note that the use of IFBAs would result in a nonlinear soluble boron letdown curve and is thus not bounded by this work.

(6.C.8) Specific Power
An increase in specific power results in an increase in neutron flux and a decrease in fuel depletion time to achieve the same burnup. The decrease in fuel depletion time has a negligible effect on the majority of the actinides because of their long half-lives; however, Pu-241 has less time to β-decay to Am-241 because of its short half-life of 14.4 years. Therefore, the concentration of Pu-241 increases and that of Am-241 decreases as the specific power increases. The equilibrium concentration of Xe-135 increases as the neutron flux increases, which results in neutron spectral hardening. An increase in resonance capture of neutrons in U-238 due to the hardened spectrum results in increased production of fissile plutonium and actinide absorbers. This, in turn, causes more fissions in fissile plutonium and leads to less depletion in U-235. The net effect is increased reactivity with an increase in specific power.

Per Ref.48, multiplying the specific power by the radial peaking factor limit assures the highest axially averaged specific power. Since the radial peaking factor limit is established on fuel pins, not on assemblies, application of the radial peaking factor throughout the entire assembly provides a layer of conservatism. It is still possible that parts of assemblies could experience higher specific powers for a period of time because of axial variations; however, decreased end effects should compensate for higher mid-region effects.

The specific power (SP) and assembly power (AP) are calculated from the VAP fuel data detailed in Attachment D.

$M=\pi*(0.96774/2cm)^2*(347.218cm)*(10.96gm/cc)*(0.945)*(176)*(238/270)/(10^6 gm/MTU)$
$=0.410372MTU$

$SP=(2700\ MWt)*(1.1)*(1.65)/217/M$
$=55.03\ MW/MTU$

$AP=(2700\ MWt)*(1.1)*(1.65)/217$

= 22.583 MW

which assumes a 10% power uprate and a radial peaking factor of 1.65 per Refs.51-52. The correspondence between burnup and EFPD for the above powers are listed in Attachment K (EXCEL Spreadsheet SAS2H-Tfuel(X2inp.xls)).

It was attempted to verify this behavior for the current work via the SAS2H and KENO executions of Section 9.B.3.e (also see Figure 6). Examination of the results of that section indicates that the reactivity results are only slightly power-dependent, the maximum and minimum values within 2 sigma at high burnups and within 3 sigma at low burnups. The reactivity tends to increase slightly with decreasing assembly power not with increasing assembly power as indicated in Ref.48. Since Ref.48 was applicable to actinide credit only, inclusion of fission products in the reactivity calculations tends to reverse the actinide only reactivity behavior as a function of assembly power. This is most probably due to the increased time required to attain the same burnup at a lower assembly power level, which allows more decay of the neutron parasitic fission products. Thus the core-averaged assembly power of 12.442 MW will be utilized in this work.

SP= (2700 MWt)/217/M
= 30.32 MW/MTU

AP = (2700 MWt)/217
= 12.442 MW

Note that the fuel irradiation period 'BURN' in days can be readily calculated as the desired burnup in MWD/MTU divided by the specific power in MW/MTU per Attachment K and EXCEL spreadsheet X2INP.XLS(SAS2H-Tfuel(2)).

(6.C.9) Refueling Downtime
A decrease in refueling downtime results in less Pu-241 decay to Am-241, which results in increased reactivity. Per Ref.48, fuel cycles modeled with no reactor downtime are a conservative approach. In this work, only a 100 hour decay time at end-of-life per Ref.45 is conservatively assumed.

(6.C.10) Clad Material and Temperature
The clad was assumed to be composed of zircaloy-4 (ZIRC4) as defined in the Standard Composition Library of Ref. 9. Current fuel pin clad composition includes zirlo, optin, low tin zirlo, alloy A, and M5 (Refs.5, 6, 17, 18, 22, and 30); however, ~98% of these materials are composed of zirconium, thus the use of zirc4 should be representative of the clad. Also note that only fission products and actinides will be extracted from the SAS2H executions for use in the criticality calculations. A clad temperature of 620°F or 599.82°K was utilized in this work consistent with Refs.8 and 40.

(6.C.11) Path A Geometry
The model used in Path A represents the fuel as an infinite lattice of fuel pins. Cell-weighted cross sections are produced by this model and are then applied to the fuel zone of the Path B model. The VAP fuel rod pitch (1.4732 cm), pellet outer diameter (0.96774 cm), clad outer diameter (1.1176 cm), and clad inner diameter (0.98552 cm) are extracted from Attachment D (Z2INP.XLS(Fuel)).

(6.C.12) Path B Geometry
The model applied to Path B is a larger unit cell model used to represent part of an assembly within an infinite lattice. The concept of using cell-weighted data in the 1-D XSDRNPM-S analysis of Path B is an appropriate method for evaluating heterogeneity effects found in fuel pin

lattices. The Path B model is used by SAS2H to generate few-group, cell-weighted cross sections for ORIGEN-S and to calculate the neutron flux for an assembly-averaged fuel region that is used to update the ORIGEN-S spectral parameters for isotopes not explicitly included in the cell model. The essential rule in deriving the zone radii is to maintain the relative volumes in the actual assembly. The effective radii for the SAS2H Path B model for 176 pin VAP CE 14x14 assemblies were taken from Attachment D (Z2INP.XLS(Fuel)).

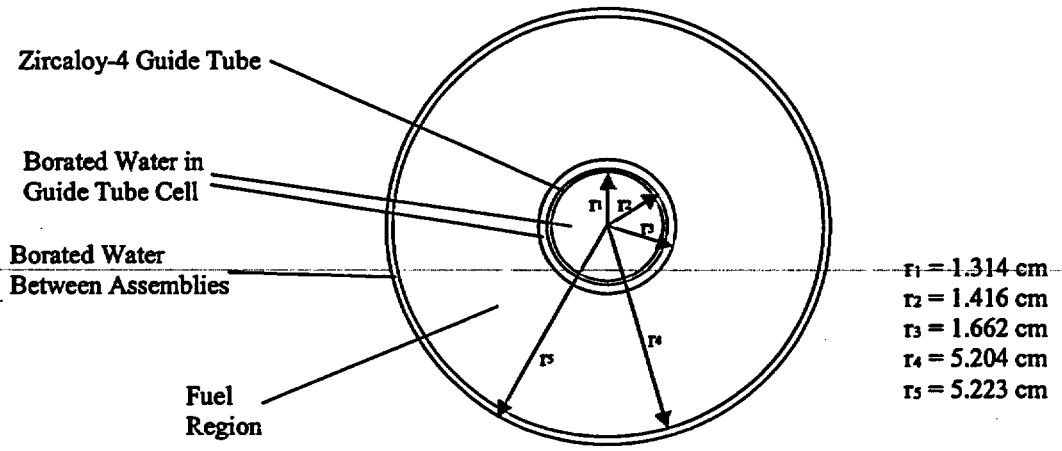

Figure 1: Path B Model for SAS2H

(6.C.13) Additional Inputs

		Definition	Reference
NPIN/ASSM	176	Number of fuel rods/assembly	Attachment D
FUELNGTH	347.218	Fuel rod active length in cm	Attachment D
NCYCLES	1	Number of cycles	
NLIB/CYC	1/2.5 gwd/mtu	Number of libraries made per cycle	
PRINTLEVEL	9	Print level	Ref.9 S2.5.19
LIGHTEL	9	Number of light elements	Section 6.C.4.e
INPLEVEL	2	Input level	Ref.9 S2.5.14
NUMHOLES	5	Number of guide tubes per assembly	Attachment D
NUMINSTR	0	Number of instrument tubes per assembly	Attachment D
MXTUBE	2	Mixture number of guide tubes	
ORTUBE	1.41605	Outside radius of guide tubes in cm	Attachment D
SRTUBE	1.31445	Inside radius of guide tubes in cm	Attachment D
ASMPITCH	20.7772	Assembly pitch in cm	Attachment D
NUMZTOTAL	5	Number of zones in Path B cell	Attachment D
MXREPEATS	1	Mixes and radius required only once	Ref.9 S2.5.5
MIXMOD	3	Mixture number of moderator	
FACMESH	1.0	Mesh size factor	

(6.D) Keno Criticality Inputs

All KENO calculations are LATTICECELL calculations using the 44GROUPNDF5 library. The lattice type is SQUAREPITCH, assuming cylindrical rods in a square pitch and using the VAP dimensions detailed in Attachment D.

(6.D.1) Materials
The following material designations are used in the KENO input decks.

(1) Material 1 is UO_2 at the indicated enrichment, stack height density, and temperature per Z2INP.XLS(CALCLIST) (Attachment A).
(2) Material 2 is fuel clad. Three materials are modeled:
(a) Zirlo fuel clad is detailed in Z2INP.XLS(DENSITIES) (Attachment C).
(b) Optin fuel clad is detailed in Z2INP.XLS(DENSITIES) (Attachment C).
(c) Zirc4 fuel clad is a standard composition of Ref.21.
(d) Alloy A fuel clad is detailed in Refs. 5 and 6.
(e) Low tin zirlo fuel clad is detailed in Refs. 5 and 6.
(f) M5 fuel clad is detailed in Refs. 5 and 22.
(3) Material 3 is borated moderator as detailed in Z2INP.XLS(DENSITIES) (Attachment C).
(4) Material 4 is SS304. a standard composition of Ref.21.
(5) Material 5 is borated moderator as detailed in Z2INP.XLS(DENSITIES) (Attachment C). Note that borated moderator is used in lieu of boraflex in the rack structure.
(6) Material 6 is guide tube clad and is composed of ZIRC4, standard composition of Ref.21.
(7) Material 7 comprises the upper end fitting or moderator as detailed in Z2INP.XLS(DENSITIES) (Attachment C – Refs.25-26).
(8) Material 8 comprises the lower end fitting or moderator as detailed in Z2INP.XLS(DENSITIES) (Attachment C – Refs.25-26).
(9) Material 9 is the SS304 SFP liner, a standard composition of Ref.21.
(10) Material 10 is the SFP concrete structure, a standard composition of Ref.21.
(11) Material 11 is a second UO_2 enrichment for some configuration control cases.
(12) For material densities generated by SAS2HLIN, and SAS2HLAG, material designations starting with material 101 are employed, similar to the nomenclature of Ref.34.

The single assembly and 10x10 assembly array of infinite axial extent calculations use material types 1-6. The 1-node, 18-node, and 26-node axial burnup bias calculations use material types 11 for fuel, 2 for clad, 3 for moderator, 4-5 for rack, 6 for guide tube, 7 for UEF and LEF, 8 for SFP SS304 liner, and 9 for SFP concrete. The whole core, reconstitution, dropped assembly, and configuration controlled models use materials 1-10 as described above.

(6.D.2) Geometry
The SFP is a large rectangular structure which holds the spent fuel assemblies from the reactors of both units. Borated water fills the SFP and completely covers the spent fuel assemblies. The SFP is constructed of reinforced concrete and is lined with a stainless steel plate which serves as a leakage barrier. A dividing wall separates the SFP, with the north half being associated with Unit 1 and the south half associated with Unit 2. A slot in the dividing wall has removable gates which allow movement of fuel assemblies between the two halves of the pool. The SFP is located in the Auxiliary Building between the two containment structures.

Each half of the SFP is equipped with vertical spent fuel racks installed on the pool bottom. The fuel rack cells are individual double-walled containers approximately 14 feet long. The inner wall of each cell is made from a 0.06 inch thick sheet of stainless steel formed into a square cross-section container, indented on the corners, with an inside dimension of 8.56 inches. The outer, or external, wall is also formed from a stainless steel sheet 0.06 inches thick. Plates of borated, neutron absorbing material are inserted between the two walls, in each of the four spaces formed by the indentations in the inner wall. The plates are made of a boron carbide (B_4C) composite material (boraflex) and are 6.5 inches wide by 0.09 inches thick. Issue Reports IR3-045-938, IR3-045-939, and IR3-052-199 documented possible boraflex degradation in the Unit 2 Spent Fuel Pool, based on calculations using the Racklife software package. The Racklife results indicated that at certain highly-irradiated locations the degradation could be as high as 70%. Since the Unit 2 design basis areal B-10 loading is 0.020 gm/cm^2 and since the initial loading

was a minimum of 0.020 gm/cm^2, insufficient margin exists to cover the degradation. No boraflex is credited in this work. Attachments E and G display a single SFP planar and axial storage cell geometry. The spacing between the cells is maintained at 10 3/32 inches, center to center, by external sheets and welded spacers.

(6.D.2.i) Single Assembly Model of Infinite Axial Extent
Geometric regions designated as Units 1-8 in each of the KENO input decks define an assembly seated in a fuel rack cell. For the single assembly model of infinite axial extent, Units 1-8 are sufficient to completely define the problem.

Storage Cell Pitch = 10.09375" (Ref.15)
Storage Cell Inner Dimension = 8.5625" (Ref.15)
Poison Sheet = 6.5" * 0.09" (Ref.15)
Inner Steel Wall = 0.06" (Ref.15)
Outer Steel Wall = 0.06" (Ref.15)

Unit 1: Fuel pin cell (Z2INP.XLS(FUEL))
Unit 2: Guide tube cell (Z2INP.XLS(FUEL))
Unit 3: Storage rack wall section 6.5" * (0.06" SS + 0.09" B_4C + 0.06" SS)
Unit 4: Storage rack wall section (0.06" SS + 0.09" B_4C + 0.06" SS) * 6.5"
Unit 5: Storage rack wall section 1.15125" * 0.12" SS
Unit 6: Storage rack wall section 0.12" * 1.03125" SS
Unit 7: 2 * 2 fuel cell
Unit 8: 14 * 14 assembly in fuel rack cell

(6.D.2.ii) 10x10 Assembly Array of Infinite Axial Extent
In addition to the Units 1-8 geometric regions in 6.D.2.i, a Unit 9 geometric region is required to model the 10x10 assembly array of infinite axial extent.

(6.D.2.iii) Single Assembly Axial Burnup Models
The 1-node, 18-node, and 26-node axial burnup bias calculations model an infinite array of assemblies in the lateral directions. In addition to the Units 1-8 geometric regions in 6.D.2.i, Unit 9 is employed to model 23.619 feet of moderator above the active fuel region and 17.871 inches of moderator below the active fuel region followed by 3/16 inch stainless steel liner and 6 feet of concrete wall.

(6.D.2.iv) Complete Unit 2 SFP, Reconstitution/Inspection, and Dropped Assembly Models
During inspection/reconstitution activities in the SFP, assemblies are put on 20.5" spacers (Ref. 25) adjacent to the SFP wall. This process lifts the active fuel region of the affected assembly above the boraflex poison plates (Attachment G) and thus could affect reactivity. In this work, the boraflex plates are replaced with moderator and are not credited, thus the reactivity effect of inspection/reconstitution should be minimal. In addition to the Units 1-8 geometric regions in 6.D.2.i, Units 11-18 in the KENO input decks define an assembly seated on a rack spacer in a fuel rack cell.

Unit 11: Fuel pin cell on spacer (Z2INP.XLS(FUEL))
Unit 12: Guide tube cell on spacer (Z2INP.XLS(FUEL))
Unit 13: Storage rack wall section 6.5" * (0.06" SS + 0.09" B_4C + 0.06" SS)
Unit 14: Storage rack wall section (0.06" SS + 0.09" B_4C + 0.06" SS) * 6.5"
Unit 15: Storage rack wall section 1.15125" * 0.12" SS
Unit 16: Storage rack wall section 0.12" * 1.03125" SS
Unit 17: 2 * 2 fuel cell on spacer
Unit 18: 14 * 14 assembly on spacer in fuel rack cell

For accident analysis, an assembly dropped across the top of the SFP racks must be modeled. Units 21-24 in the KENO input decks define an assembly in the horizontal position.

Unit 21: Horizontal fuel pin cell (Z2INP.XLS(FUEL))
Unit 22: Horizontal guide tube cell (Z2INP.XLS(FUEL))
Unit 23: Horizontal 2 * 2 fuel cell
Unit 24: Horizontal 14 * 14 assembly

The Unit 2 SFP racks are vertical cells grouped in 10 10x10 modules. Units 30-32 in the KENO decks define these arrays.

Unit 30: 10x10 array
Unit 31: 10x9 array
Unit 32: 10x1 array on spacers

The SFP is located in the Auxiliary Building between the two containment structures. Designed in two identical sections separated by a 3 1/2 foot thick dividing wall, the pool is constructed of reinforced concrete and lined with 3/16 inch stainless steel. Each half of the pool is 54 feet long, 25 feet wide and approximately 39 feet deep (the floor elevation varies). The SFP walls and floor are 5 1/2 or 6 feet thick, depending on the location. Unit 40 is the entire Unit 2 SFP structure to the outside concrete boundary (Attachment F) and includes any reconstitution and/or dropped assembly details.

Unit 40: Unit 2 SFP

(6.D.2.v) Configuration Control Models with Empty Rack Spaces and Fresh Fuel
For the some configuration control models (KU2CONA-C), Units 30-34 define a rack space filled only with moderator, while Unit 40 is a 10x10 array of assemblies and empty rack spaces and Unit 50 is the entire Unit 2 SFP filled with the Unit 40 10x10 arrays. Units 1-24 are as detailed in Section 6.D.2.iv.

(6.D.2.vi) Configuration Control Models with Burned and Fresh Fuel
For the configuration control models (KU2COND1-3 and KU2CONE1-3), Units 1-8 define a burned assembly in a rack space, and Units 11-18 a fresh assembly in a rack space. Unit 40 is a 10x10 array of fresh and burned assemblies, while Unit 50 is the entire Unit 2 SFP filled with the Unit 40 10x10 arrays.

Verification that the input geometries are constructed correctly can be seen by an inspection of the KENO generated plots in Attachment H.

(6.D.3) Parameters
(1) Maximum execution time is set at 500 minutes.
(2) Number of generations is 1010
(3) Number of particles per generation is 600
(4) Number of skipped generations is 10
(5) The NB8 parameter on the PARAM card and the DAB parameter on the DATA card must be set to at least 500 to accommodate the increased storage requirements of axial burnup profile isotopics.

(6.D.4) MORE DATA
(1) The NB8 parameter on the PARAM card and the DAB parameter on the DATA card must be set to at least 500 to accommodate the increased storage requirements of axial burnup profile isotopics.
(2) For multiple fuel types in the same model, enter

RES=Mixture Number
CYL=Fuel pellet radius (0.48387 cm)
DAN(Mixture Number)=Dancoff Factor
for each fuel type not specified in the SQUAREPITCH card.

From multiple KENO outputs, it was determined that the Dancoff Factor is independent of enrichment and burnup and is only a function of soluble boron concentration.

Dancoff Factor (0 ppm) =0.24337743
Dancoff Factor (300 ppm) =0.24314851
Dancoff Factor (2000 ppm) =0.24185666

(6.D.5) Boundary Conditions

Per Ref.4, the SFP storage racks should be assumed to be infinite in the lateral dimension or to be surrounded by a water reflector and concrete or structural material as appropriate to the design. The fuel may be assumed to be infinite in the axial dimension, or the effect of a reflector on the top and bottom of the fuel may be evaluated. Thus reflective boundary conditions are modeled on all sides and on top and bottom.

7. TECHNICAL ASSUMPTIONS

The following technical assumptions were utilized in this work:

(7.A) No Boraflex was credited in this work. In addition, the KENO model assumes that the boraflex is completely replaced by SFP water, which is based on the fact that the silica matrix is completely dissolved by by the water.

(7.B) No CEA insertion was credited in these evaluations.

(7.C) No shims were modeled in the fuel assemblies. The analyses in Refs.35-37 demonstrate that, with the exception of Westinghouse IFBA rods, the neutron multiplication factor for an assembly without Integral Burnable Absorbers (IBAs) is always greater (throughout burnup) than the k-eff for an assembly with IBAs, including UO_2-Gd_2O_3, UO_2-Er_2O_3, and Al_2O_3-B_4C rods.

(7.D) The following assumptions are consistent with the validation methodology of Ref.8 and are necessitated by the methodology biases and uncertainties used in this work.
(7.D.1) All criticality calculations were run with 1010 generations and 600 neutrons per generation to improve statistics.
(7.D.2) The first ten generations are omitted when calculating the average eigenvalue of the system.
(7.D.3) The default value was used for the start option of flat neutron distribution.
(7.D.4) No albedo boundary conditions were applied.
(7.D.5) No neutron biasing in the water reflection region was used.
(7.D.6) Structural components such as control and safety rod guides, support angles and channels, and tanks were neglected. This is conservative, since they are parasitic neutron absorbers.
(7,D.7) Trace chemical elements were neglected.
(7.D.8) The 44 group ENDF-B/V cross section library is utilized.

(7.E) This work does not address encapsulated fuel stored in assembly guide tubes, which would increase total reactivity. Thus encapsulated fuel can not be stored in the guide tubes of fuel assemblies stored in the Unit 2 Spent Fuel Pool. Encapsulated fuel can be stored in empty grid cages in the Unit 2 Spent Fuel Pool, since that would constitute a decrease in reactivity.

(7.F) The most reactive fuel type, 5.0 w/o VAP fuel, is modeled.

(7.G) U234 and U236 are conservatively not modeled in the fresh fuel pellet.

(7.H) Per Refs.53 and 54, the Technical Specification Refueling Boron Concentration is greater than 2150 ppm. 2000 ppm will be conservatively used in this work.

(7.I) Per Refs.53 and 54, the Refueling Boron Concentration uncertainty is 7.5%. 15% will conservatively assumed in this work.

8. REFERENCES

(1) "Prevention of Criticality in Fuel Storage and Handling", 10 CFR 50 App.A GDC 62

(2) "Criticality Accident Requirements", 10 CFR 50.68

(3) "Review and Acceptance of Spent Fuel Storage and Handling Applications", B.K.Grimes (NRC) to All Power Reactor Licensees, 4/14/78

(4) "Guidance on the Regulatory Requirements for Criticality Analysis of Fuel Storage at LWR Power Plants", NRC Memorandum L. Kopp to T. Collins, 8/19/98

(5) "Chemistry Review of New Fuel Cladding Materials in Westinghouse and Framatome LFAs", RL0092

(6) "Safety Analysis Report for Use of Improved Zirconium Based Cladding in Calvert Cliffs Unit 2 Batch T LFAs", WCAP-15874-P, Rev.0

(7) "SCALE 4.4 Verification and Validation for BGE's CCNPP", CA04910

(8) "SCALE 4.4 CSAS Validation Computations", CA04911

(9) "SCALE: A Modular Code System for Performing Standardized Computer Analyses for Licensing Evaluation," NUREG/CR-0200, Rev. 6 (ORNL/NUREG/CSD-2/R6), Vols. I, II, and III September 1998.

(10) ANSI/ANS-8.1, "American National Standard for Nuclear Criticality Safety in Operations with Fissionable Materials Outside Reactors."

(11) ANSI/ANS-8.17, "American National Standard for Criticality Safety Criteria for the Handling, Storage, and Transportation of LWR Fuel Outside of Reactors."

(12) NUREG/CR-6361, "Criticality Benchmark Guide for Light-Water-Reactor Fuel in Transportation and Storage Packages," J. J. Lichtenwalter, S. M. Bowman, M. D. DeHart and C. M. Hopper, March 1997.

(13) NEA/NSC/DOC(95)03, International Handbook of Evaluated Criticality Safety Benchmark Experiments, Volume IV, Low Enriched Uranium Systems, September 1999 Edition.

(14) NTIS PB93-196-038, "Experimental Statistics Handbook 91", August 1963.

(15) "Nuclear Design Analysis Report for the CCNPP Unit 2 High Density Spent Fuel Storage Racks", NES Report 81A0704 Rev.0.

(16) 1967 Steam Tables, New York St. Martin's press, 1967

(17) "Impact of Zirlo on the Reactivity Bias", Westinghouse Interoffice Correspondence CA-2001-0026

(18) "Implementation of Zirlo Cladding Material in CE Nuclear Power Fuel Assembly Designs", CENPD-404-P Rev.0

(19) "Nuclides and Isotopes, Chart of the Nuclides", GE Nuclear 14th Edition.

(20) "Introduction to Nuclear Engineering", J.R.Lamarsh, 12/77.

(21) "Standard Composition Library", NUREG/CR-0200 Rev.6 Volume 3 Section M8

(22) "M5 Alloy Topical", Framatome

(23) "Auxiliary Building SFP Liner Plan and Sections Sheet 1", BGE Drawing 61-706-E Rev.18.

(24) " Fuel Storage Rack Installation in Pool", BGE Drawing 13939-0038 Rev.2

(25) "Fuel Handling Accident during Reconstitution", CA04048

(26) "Design Input Data for CCNPP ISFSI", NEU-01-016.

(27) "Guide Tube Assembly Details", BGE Drawing E-STD-701-303 Rev.5.

(28) "Reanalysis of Calvert Cliffs Unit 2 Spent Fuel Pool Criticality Calculations", ABB/CE Calculation A-CC2-FE-0003 Rev.2, 7/2/92.

(29) "Spent Fuel Pool Enrichment Limit with Value Added Pellets", CA04662.

(30) "Calvert Cliffs Lead Fuel Assemblies Fuel Design and Safety Analysis Report", Volume 1, EMF-2807(P) Rev.0, RL00101.

(31) "Westinghouse Spent Fuel Rack Criticality Analysis Methodology", WCAP-14416-NP-A. Rev.1

(32) "Separation Distance to Neutronically Decouple Fresh Fuel Assemblies in the Spent Fuel Pool", P.F.O'Donnell to P.H.Gavin, CC-FE-0130 Rev.0, 3/5/98.

(33) "Review of Axial Burnup Distribution Considerations for Burnup Credit Calculations", ORNL/TM-1999/246

(34) "STARBUCS: A Prototype SCALE Control Module for Automated Criticality Safety Analyses Using Burnup Credit", NUREG/CR-ORNL/TM-2001/33. 9/2001

(35) "Study of the Effect of Integral Burnable Absorbers for PWR Burnup Credit", NUREG/CR-6760, ORNL/TM-2000-321, March 200.

(36) "Cross Section Generation for 2.00 w/o Erbia Pins for VAP Using ENDF/B-VI Library", CA04732.

(37) "Recommendations for Addressing Axial Burnup in PWR Burnup Credit Analyses", NUREG/CR-ORNL/TM-2001/273.

(38) Isotopic Bias and Uncertainty for Burnup Credit Applications", J.M.Scaglione (Bechtel SAIC), ANS Transactions for the 2002 Winter Meeting (Vol. 87, pp. 105-107)

(39) "Calvert Cliffs Unit 2 Cycle 14 EQ Source Term Verification", CA05653.

(40) "Validation of the SCALE System for PWR Spent Fuel Isotopic Composition Analyses", ORNL/TM-12667.

(41) "SAS2H Validation", CA05780.

(42) "Unit 2 Spent Fuel Pool Boraflex Degradation Operability Evaluation", CA05883

(43) "Unit 1 Spent Fuel Pool Enrichment Limit with Soluble Boron Credit", CA06011.

(44) "A Critical Review of the Practice of Equating the Reactivity of Spent Fuel to Fresh Fuel in Burnup Credit Criticality Safety Analyses for PWR SFP Storage", NUREG/CR-6683, 9/2000.

(45) "CCNPP Technical Requirements Manual Section 15.9.1: Refueling Operations Decay Time", Rev.8

(46) "Non-conservatisms in Axial Burnup Biases for Spent Fuel Rack Criticality Analysis Methodology", USNRC 7/27/2001

(47) "Axial Burnup Shape Reactivity Bias", NSAL-00-015, 11/2/2000.

(48) "Depletion and Package Modeling Assumptions for Actinide-Only Burnup Credit", DOE/RW-0495, May 1997.

(49) "Calvert Cliffs Unit 1 Cycle 16 CORD/ROCS Design Models and Depletions," CCNPP Calculation CA05735, Westinghouse Calculation A-CC1-FE-0128, Rev. 0.

(50) "RC Waste Processing System Incident and Waste Gas Incident - Dose Analysis", CA05994

(51) Calvert Cliffs Unit 1 Cycle 16 COLR, Rev.0

(52) Calvert Cliffs Unit 2 Cycle 14 COLR, Rev.2

(53) "Unit 1 Technical Data Book", NEOP-13, Rev.18

(54) "Unit 2 Technical Data Book", NEOP-23, Rev.14

(55) "Calvert Cliffs Unit 1 Cycle 15 CORD and ROCS Design Models and Depletions", ABB/CE Calculation A-CC1-FE-0090 Rev.01

(56) "Applied Numerical Methods", Brice Carnahan, H. A. Luther, and James O. Wilkes, John Wiley & Sons, N.Y., 1969.

(57) "Calvert Cliffs Unit 1 Cycle 16 CORD and ROCS Asbuilt Models and Depletions", CA05743.

(58) "CE Response to NRC Questions on Enrichment Limit Upgrade at Calvert Cliffs", Combustion Engineering Letter J.E.Baum (CE) to J.A.Mihalcik (BGE), B-88-128,.

(59) "Specification for UO2 Fuel Pellets", Specification Number 00000-PD-110, Rev.11, 4/24/97.

(60) "BGE Criticality Analysis for Units 1 and 2 Spent Fuel Pools", CA04166

(61) "ABB/CE Methodology Manual Physics Biases and Uncertainties", CE-CES-129 Rev.8-P

(62) "Fission Product Activity in the Reactor Coolant", CE Report SE-69-971, NORMS Doc. ID #77330, 10/9/69.

9. METHOD OF ANALYSIS

(9.A) Reactivity Equivalencing

Per Ref.44, the spent nuclear fuel inventory subsequent to the decay of the short-lived Xe-135 isotope is typically used within the storage pool geometry to determine a fresh fuel enrichment that provides the same reactivity (neutron multiplication factor k_{inf}) as the spent nuclear fuel inventory. This Reactivity Equivalent Fresh Fuel Enrichment (REFFE) is then used within a criticality safety analysis code to perform the actual safety analysis. The acceptability of this practice can be demonstrated, provided the environment in which the REFFE is determined remains unchanged (e.g., an infinite array of identical storage rack cells in unborated water). However, if the REFFE is determined based on a reference configuration and employed in the analysis of another condition, erroneous estimations of reactivity may result.

The use of REFFE can be shown to produce nonconservative results when used in the presence of soluble boron. These results show increasing nonconservatism with increasing soluble boron concentration and with increasing burnup. The soluble boron in the water is an effective thermal neutron absorber. Because of its negative reactivity worth, the presence of soluble boron reduces the relative reactivity worth of the fission products and actinide absorbers. The fission product and actinide absorbers have greater negative reactivity worth in the unborated reference condition in which the REFFE was determined, resulting in a lower prediction of the REFFE reactivity value.

When a REFFE assembly is placed in a checkerboard configuration with a more reactive assembly, the REFFE approach yields nonconservative results. When comparing the reference infinite configuration to a configuration in which the reference assembly is stored with higher-reactivity fuel, the reactivity of the latter configuration is controlled by the higher-reactivity fuel. Physically, the maximum reactivity or fission density for this latter configuration occurs in the higher-reactivity fuel, with the lower-reactivity (reference) fuel acting in a supplementary manner. Therefore, the fission products and actinide absorbers have less relative negative reactivity worth in this configuration (as compared to the reference configuration), because they are not physically located where the fission density is maximum.

Because of the possible nonconservatisms referenced above, reactivity equivalencing will not be employed in this work.

(9B) SAS2H Method of Analysis

(9.B.1) Calculational Methodology

The source term portion of this work employs SAS2H, a functional module in the SCALE system, to calculate the burnup-dependent source terms for the CCNPP Unit 2 SFP system. Ref.9 documents the SCALE 4.4 modular code system SAS2H for computing the isotopic content of PWR spent fuel. The SAS2H control module performs the depletion/decay analysis using the well-established codes and data libraries provided in the SCALE system. Problem-dependent resonance processing of neutron cross sections is performed using the Bondarenko resonance self-shielding module BONAMI-S and the Nordheim Integral Treatment resonance self-shielding module NITAWL-II. The XSDRNPM-S module is used to produce spectral weighted and collapsed cross sections for the fuel depletion calculations. COUPLE updates the cross section constants included on an ORIGEN-S nuclear data library with data from the cell-weighted cross section library produced by XSDRNPM-S. The weighting spectrum computed by XSDRNPM is applied to update all nuclides in the ORIGEN-S library that were not specified in the XSDRNPM analysis. The point-depletion ORIGEN-S module is used to compute time-dependent concentrations and source terms for isotopes simultaneously generated and depleted through neutronic transmutation, fission, and radioactive decay. The cross section library 44GROUPNDF5 was utilized in this work. 44GROUPNDF5 is a 44-energy group library

derived from the latest ENDF/B-V files with the exception of O-16, Eu-154, and Eu-155, which were taken from the more improved ENDF/B-VI files. Note that the SAS2H/ORIGEN-S libraries include 689 light elements, such as clad and structural materials, 129 actinides, including fuel nuclides and their decay and activation products, and 879 fission product nuclides.

(9.B.2) Calculation of Biases and Uncertainties

Per Ref.4, a reactivity uncertainty due to uncertainty in the fuel depletion calculation should be developed and combined with other calculational uncertainties. Although SAS2H is benchmarked in Ref.41 to the Calvert Cliffs Unit 2 Cycle 14 EQ radioactive source terms of Ref.39 and to the measured data in ORNL/TM-12667 (Ref.40), no reactivity biases or uncertainties were determined. Per Ref.4, in the absence of any other determination of the depletion uncertainty, an uncertainty equal to 5% of the reactivity decrement to the burnup of interest is an acceptable assumption.

KENO Case	Boron ppm	Enr w/o	Burnup gwd/t	Unbiased K-eff	Delta K-eff	Uncertainty
K200000D1	0	2.0	0	0.97726	0.00082	
K207000D1	0	2.0	70	0.69082	0.00060	0.01439
K300000D1	0	3.0	0	1.09184	0.00091	
K307000D1	0	3.0	70	0.71073	0.00063	0.01913
K400000D1	0	4.0	0	1.15989	0.00096	
K407000D1	0	4.0	70	0.74660	0.00070	0.02075
K500000D1	0	5.0	0	1.21112	0.00091	
K507000D1	0	5.0	70	0.79503	0.00072	0.02089
K200000D2	300	2.0	0	0.89457	0.00083	
K207000D2	300	2.0	70	0.63731	0.00056	0.01293
K300000D2	300	3.0	0	1.00921	0.00081	
K307000D2	300	3.0	70	0.65791	0.00058	0.01763
K400000D2	300	4.0	0	1.08296	0.00085	
K407000D2	300	4.0	70	0.69218	0.00069	0.01962
K500000D2	300	5.0	0	1.13444	0.00094	
K507000D2	300	5.0	70	0.73910	0.00068	0.01985

Based on the above computations, a worst case uncertainty value of 0.02089 will be used in all burnup related reactivity calculations.

Ref.38 includes additional benchmarking of SAS2H to Calvert Cliffs radiochemical assays. Radiochemical assays (RCAs) are the destructive post-irradiation examination of nuclear fuel. Note that there are compensating effects by the over/under-prediction of different isotopes. Therefore, when evaluating a code's ability to accurately predict the isotopic composition of irradiated fuel, the effect on reactivity is the important result. The results for CCNPP fuel indicate that the isotopic compositions predicted by SAS2H produce conservative values of k-effective (k(SAS2H)>k(RCA)).

Additional calculations in this work verified that the reactivity of a SAS2H generated system is more conservative than an RCA based system.

KENO Case	SAS2H Case	Enr w/o	Burnup gwd/t	Unbiased K-eff	Delta K-eff	Uncertainty
K506000D1	S560	5.0	60	0.84339	0.00071	-0.00358
K506000G1	Hand	5.0	60	0.83981	0.00071	

The isotopics for Case K506000D1 were generated via a SAS2H execution, while those for K506000G1 used the same SAS2H isotopics but were modified by the SAS2H to RCA biases

determined in Attachment R from the validation data of Ref.41. Note that the SAS2H generated reactivity is 0.358% more reactive than those adjusted to the RCA isotopics.

(9.B.3) Calculations
(9.B.3.a) Reactivity vs Refueling Downtime
Per Section 6.C.9, a decrease in refueling downtime results in less Pu-241 decay to Am-241, which results in increased reactivity. This was verified for the current work via the following SAS2H and KENO executions (also see Figure 2):

KENO Case	SAS2H Case	Enr w/o	Burnup gwd/t	Cooling Time	Unbiased K-eff
K205000AA	S250A	2.0	50	100 hours decay	0.70641
K205000AB	S250B	2.0	50	1 year decay	0.69684
K205000AC	S250C	2.0	50	2 year decay	0.69026
K205000AD	S250D	2.0	50	5 year decay	0.67068
K502000AA	S520A	5.0	20	100 hours decay	1.05935
K502000AB	S520B	5.0	20	1 year decay	1.05345
K502000AC	S520C	5.0	20	2 year decay	1.05450
K502000AD	S520D	5.0	20	5 year decay	1.05015
K505000AA	S550A	5.0	50	100 hours decay	0.88271
K505000AB	S550B	5.0	50	1 year decay	0.87514
K505000AC	S550C	5.0	50	2 year decay	0.87105
K505000AD	S550D	5.0	50	5 year decay	0.85665

Thus using the Technical Specification cooling time of 100 hours is conservative in all cases.

(9.B.3.b) Reactivity vs Fuel Temperature
Per Section 6.C.5, an increase in fuel temperature increases the resonance capture of neutrons in U-238 due to Doppler effect, which results in increased production of fissile plutonium and actinide absorbers. This, in turn, causes more fissions in fissile plutonium and leads to less depletion in U-235. The net effect is increased reactivity with an increase in fuel temperature. This was verified for the current work via the following SAS2H and KENO executions (also see Figure 3):

KENO Case	SAS2H Case	Enr w/o	Burnup gwd/t	Notes	Unbiased K-eff
K205000AA	S250A	2.0	50	Tfuel=1285.42K	0.70641
K205000AE	S250E	2.0	50	Tfuel=1085.42K	0.69927
K205000AF	S250F	2.0	50	Tfuel=885.42K	0.69036
K502000AA	S520A	5.0	20	Tfuel=1285.42K	1.05935
K502000AE	S520E	5.0	20	Tfuel=1085.42K	1.05864
K502000AF	S520F	5.0	20	Tfuel=885.42K	1.05793
K505000AA	S550A	5.0	50	Tfuel=1285.42K	0.88271
K505000AE	S550E	5.0	50	Tfuel=1085.42K	0.87832
K505000AF	S550F	5.0	50	Tfuel=885.42K	0.87249

Thus using a fuel temperature of 1285.42K should be conservative in all cases.

(9.B.3.c) Reactivity vs Soluble Boron Concentration
Per Section 6.C.7, the soluble boron present in the moderator increases the thermal absorption cross section, decreases the thermal flux, and results in a hardened neutron spectrum. An increase in resonance capture of neutrons in U-238 due to the hardened spectrum results in increased production of fissile plutonium and actinide absorbers. This, in turn, causes more fissions in fissile plutonium and leads to less depletion in U-235. The net effect is increased reactivity with an increase in soluble boron concentration. This was verified for the current work via the following SAS2H and KENO executions (also see Figure 4):

KENO Case	SAS2H Case	Enr w/o	Burnup gwd/t	Boron PPM	Unbiased K-eff
K205000AH	S250H	2.0	50	800	0.70343
K205000AA	S250A	2.0	50	950	0.70641
K205000AG	S250G	2.0	50	1100	0.71116
K502000AH	S520H	5.0	20	800	1.05837
K502000AA	S520A	5.0	20	950	1.05935
K502000AG	S520G	5.0	20	1100	1.05882
K505000AH	S550H	5.0	50	800	0.88274
K505000AA	S550A	5.0	50	950	0.88271
K505000AG	S550G	5.0	50	1100	0.88656

Per Refs.53-55, the maximum BOC soluble boron concentration is less than 1820 ppm, where Ref.55 models a cycle at the MTC Technical Specification limit. The boron letdown curves in these cycles are approximately linear with exposure. Thus a bounding BOC soluble boron concentration of 1900 ppm will be assumed with a linear letdown curve, resulting in a maximum average soluble boron concentration of 950 ppm.

(9.B.3.d) Reactivity vs Moderator Temperature
Per Section 6.C.6, neutron spectral hardening occurs with an increase in moderator temperature due to fewer hydrogen nuclides that thermalize fast neutrons past the resonance region. An increase in resonance capture of neutrons in U-238 due to the hardened spectrum results in increased production of fissile plutonium and actinide absorbers. This, in turn, causes more fissions in fissile plutonium and leads to less depletion in U-235. The net effect is increased reactivity with an increase in moderator temperature. This was verified for the current work via the following SAS2H and KENO executions (also see Figure 5):

KENO Case	SAS2H Case	Enr w/o	Burnup gwd/t	Density-mod gm/cc	Tmod F	Unbiased K-eff
K205000AA	S250A	2.0	50	0.6905	601	0.70641
K205000AI	S250I	2.0	50	0.7177	580	0.69791
K205000AJ	S250J	2.0	50	0.7404	560	0.69044
K502000AA	S520A	5.0	20	0.6905	601	1.05935
K502000AI	S520I	5.0	20	0.7177	580	1.05764
K502000AJ	S520J	5.0	20	0.7404	560	1.05770
K505000AA	S550A	5.0	50	0.6905	601	0.88271
K505000AI	S550I	5.0	50	0.7177	580	0.87720
K505000AJ	S550J	5.0	50	0.7404	560	0.87276

Thus the HFP value of Thot (601°F) was conservatively utilized in this work.

(9.B.3.e) Reactivity vs Assembly Power

Per Section 6.C.8, an increase in specific power results in an increase in neutron flux and a decrease in fuel depletion time to achieve the same burnup. The decrease in fuel depletion time has a negligible effect on the majority of the actinides because of their long half-lives; however, Pu-241 has less time to β-decay to Am-241 because of its short half-life of 14.4 years. Therefore, the concentration of Pu-241 increases and that of Am-241 decreases as the specific power increases. The equilibrium concentration of Xe-135 increases as the neutron flux increases, which results in neutron spectral hardening. An increase in resonance capture of neutrons in U-238 due to the hardened spectrum results in increased production of fissile plutonium and actinide absorbers. This, in turn, causes more fissions in fissile plutonium and leads to less depletion in U-235. The net effect is increased reactivity with an increase in specific power. It was attempted to verify this behavior for the current work via the following SAS2H and KENO executions (also see Figure 6):

KENO Case	SAS2H Case	Enr w/o	Burnup gwd/t	Assembly Power (MW)	EFPD	Unbiased K-eff
K205000AA	S250A	2.0	50	22.583	908.590	0.70641
K205000AK	S250K	2.0	50	20.000	1025.930	0.70793
K205000AL	S250L	2.0	50	17.500	1172.490	0.70753
K205000AM	S250M	2.0	50	15.000	1367.910	0.70754
K205000AN	S250N	2.0	50	12.442	1649.090	0.70774
K502000AA	S520A	5.0	20	22.583	363.440	1.05935
K502000AK	S520K	5.0	20	20.000	410.370	1.05903
K502000AL	S520L	5.0	20	17.500	469.000	1.05801
K502000AM	S520M	5.0	20	15.000	547.160	1.05983
K502000AN	S520N	5.0	20	12.442	659.640	1.06091
K505000AA	S550A	5.0	50	22.583	908.590	0.88271
K505000AK	S550K	5.0	50	20.000	1025.930	0.88415
K505000AL	S550L	5.0	50	17.500	1172.490	0.88372
K505000AM	S550M	5.0	50	15.000	1367.910	0.88420
K505000AN	S550N	5.0	50	12.442	1649.090	0.88363

Examination of the above results indicates that the reactivity results are only slightly power-dependent, the maximum and minimum values within 2 sigma at high burnups and within 3 sigma at low burnups. The reactivity tends to increase slightly with decreasing assembly power not with increasing assembly power as indicated in Ref.48. Since Ref.48 was applicable to actinide credit only, inclusion of fission products in the reactivity calculations tends to reverse the actinide only reactivity behavior as a function of assembly power. This is most probably due to the increased time required to attain the same burnup at a lower assembly power level, which allows more decay of the neutron parasitic fission products. Thus the core-averaged assembly power of 12.442 MW will be utilized in this work.

(9.C) SAS2H Edit Code

It was necessary to generate SAS2H isotopics as a function of enrichment, burnup, cooling time, moderator temperature, fuel temperature, and soluble boron concentration; to edit each output for the specified number of actinide and fission product values; to convert the isotopic content from moles to atoms/b-cm; and then to put the results in KENO format prior to insertion into the

KENO input decks. This laborious task was simplified by writing the FORTRAN programs SAS2HED50 and SAS2HED101, which accomplished all of the above.

The FORTRAN code listing for SAS2HED50.FOR is included in Attachment M, while that for SAS2HED101.FOR is included in Attachment N. The programs can be compiled and linked via the FORT51 and LINK51 batch files. A copy of FORT51.BAT and LINK51.BAT are included on the accompanying CDROM. The program executable files SAS2HED50.EXE and SAS2HED101.EXE are executed on DOS. The program queries the user for the SAS2H output file and prints the results to the SAS2HED.OUT output file. The fuel portion of the KENO material cards is included in SAS2HED.OUT and may be manually copied into the KENO input deck.

The SAS2HED program performs the following functions:

(1) SAS2HED101 edits the number of moles for the following 28 actinides at the end of the final decay period. The edited actinides include the important nuclides delineated in Section 6.C.4.

TH-232	U-232	U-233	U-234	U-235	U-236	U-237	U-238
NP-237	NP-238	PU-236	PU-237	PU-238	PU-239	PU-240	PU-241
PU-242	AM-241	AM-242	AM-242M	AM-243	CM-242	CM-243	CM-244
CM-245	CM-246	CM-247	CM-248				

Note that if any of the above nuclides are not included in the SAS2H output listing, SAS2HED101 assigns a molar value of 1.E-20 to that nuclide.

SAS2HED101 also edits the number of moles for the following 73 fission products at the end of the final decay period. The edited fission products include the important nuclides delineated in Section 6.C.4.

KR-83	KR-84	KR-85	KR-86	ZR-91	ZR-92	ZR-93	ZR-94
NB-95	MO-95	ZR-96	MO-97	MO-98	TC-99	RU-100	RU-101
RU-102	RU-103	RH-103	RU-104	PD-104	RH-105	PD-105	RU-106
PD-106	PD-107	PD-108	AG-109	CD-113	SN-126	I-127	I-129
XE-131	XE-132	XE-133	CS-133	XE-134	CS-134	XE-135	CS-135
CS-137	LA-139	PR-141	PR-143	ND-143	CE-144	ND-144	ND-145
ND-146	ND-147	PM-147	SM-147	ND-148	PM-148	PM-148M	SM-148
PM-149	SM-149	ND-150	SM-150	SM-151	EU-151	SM-152	EU-153
EU-154	GD-154	EU-155	GD-155	EU-156	GD-156	GD-157	GD-158
GD-160							

Note that if any of the above nuclides are not included in the SAS2H output listing, SAS2HED assigns a molar value of 1.E-20 to that nuclide.

(2) SAS2HED50 edits the number of moles for the following 14 actinides at the end of the final decay period. The edited actinides include the important nuclides included in the benchmark comparisons of Refs. 38 and 41.

U-234	U-235	U-236	U-238	NP-237	PU-238	PU-239
PU-240	PU-241	PU-242	AM-241	CM-242	CM-243	CM-244

Note that if any of the above nuclides are not included in the SAS2H output listing, SAS2HED50 assigns a molar value of 1.E-20 to that nuclide.

SAS2HED50 also edits the number of moles for the following 36 fission products at the end of the final decay period. The edited fission products include the important nuclides included in the benchmark comparisons of Refs. 38 and 41.

KR-83	KR-84	KR-86	MO-95	TC-99	RU-101	RH-103
AG-109	SN-126	I-129	XE-131	XE-132	CS-133	XE-134
CS-134	CS-135	CS-137	ND-143	ND-144	ND-145	ND-146
PM-147	SM-147	ND-148	SM-148	SM-149	ND-150	SM-150

SM-151 EU-151 SM-152 EU-153 EU-154 GD-154 EU-155 GD-155
Note that if any of the above nuclides are not included in the SAS2H output listing, SAS2HED assigns a molar value of 1.E-20 to that nuclide.

(3) The edited molar quantities are converted to atoms/b-cm via the following algorithm:

N(atoms/b-cm) = N(moles) * (6.023E+23 atoms/mole)*(1.E-24 cm^2/b)/(44949.183 cc)

where 44949.183 cc is the fuel volume per assembly as calculated in Attachment K.

(4) Per Ref.4, the SFP storage racks should be evaluated with spent fuel at the highest reactivity following removal from the reactor (usually after the decay of Xe-135). Thus the quantity of Xe-135 is set equal to 1.E-20 moles.

(5) The nuclide designation and the quantity of each nuclide in moles and in atoms/b-cm are printed for the actinides and fission products.

(6) Finally, the fuel portion of the KENO material cards is printed, assuming that the fuel is material 1 in the KENO input file.

Verification that the program performs its intended function properly was checked as follows:

(1) The edited molar actinide and fission product values were verified to be identical to those in the SAS2H output file.

(2) The resultant Xe-135 value was verified as correct.

(3) The conversion from moles to atoms/b-cm was verified.

(4) The KENO material input cards were verified.

(9.D) SAS2H Interpolation Codes
It was necessary to generate the SAS2H isotopic data for the 14 actinides and 36 fission products as a function of axial burnup for a given enrichment value for the 3D-to-2D KENO biasing calculations and then to put the results in KENO format prior to insertion into the KENO input decks. This process was simplified by writing two FORTRAN programs SAS2HLIN and SAS2HLAG, which interpolated on burnup to generate isotopic data and which created the fuel portion of the 3D KENO input decks..

The FORTRAN code listing for SAS2HLIN.FOR is included in Attachment O. The program can be compiled and linked via the FORT51 and LINK51 batch files. A copy of FORT51.BAT and LINK51.BAT are included on the accompanying CDROM. The program executable file SAS2HLIN.EXE is executed on DOS. The program queries the user for an enrichment-specific SAS2HED50-generated isotopic file(S2xx.ed for 2.0 w/o fuel, S3xx.ed for 3.0 w/o fuel, S4xx.ed for 4.0 w/o fuel, and S5xx.ed for 5.0 w/o fuel), the burnup profile file (SAX18.INP for 18 axial nodes and SAX26.INP for 26 axial nodes), the profile number, and a switch for single/multiple axial nodes (1 for single and 2 for multiple). The program linearly interpolates on burnup to generate the required isotopic data and prints the results to the SAS2HLIN.XXX output file. The fuel portion of the KENO material cards may be manually copied into the KENO input deck.

The FORTRAN code listing for SAS2HLAG.FOR is included in Attachment P. The program can be compiled and linked via the FORT51 and LINK51 batch files. A copy of FORT51.BAT and LINK51.BAT are included on the accompanying CDROM. The program executable file SAS2HLAG.EXE is executed on DOS. The program queries the user for an enrichment-specific

SAS2HED50-generated isotopic file(S2xx.ed for 2.0 w/o fuel, S3xx.ed for 3.0 w/o fuel, S4xx.ed for 4.0 w/o fuel, and S5xx.ed for 5.0 w/o fuel), the burnup profile file (SAX18.INP for 18 axial nodes and SAX26.INP for 26 axial nodes), the profile number, and a switch for single/multiple axial nodes (1 for single and 2 for multiple). The program interpolates on burnup via a second-order Lagrangian algorithm (Ref.56) to generate the required isotopic data and prints the results to the SAS2HLAG.XXX output file. The fuel portion of the KENO material cards may be manually copied into the KENO input deck.

The codes were verified by manual calculations and comparisons.

The isotopic data as a function of burnup and enrichment were generated from the following SAS2H and SAS2HED50 executions:

	2.0 w/o		3.0 w/o		4.0 w/o		5.0 w/o	
Burnup	SAS2H	SAS2HED50	SAS2H	SAS2HED50	SAS2H	SAS2HED50	SAS2H	SAS2HED50
0	s200.out	s200.ed	s300.out	s300.ed	s400.out	s400.ed	s500.out	s500.ed
5	s205.out	s205.ed	s305.out	s305.ed	s405.out	s405.ed	s505.out	s505.ed
10	s210.out	s210.ed	s310.out	s310.ed	s410.out	s410.ed	s510.out	s510.ed
15	s215.out	s215.ed	s315.out	s315.ed	s415.out	s415.ed	s515.out	s515.ed
20	s220.out	s220.ed	s320.out	s320.ed	s420.out	s420.ed	s520.out	s520.ed
25	s225.out	s225.ed	s325.out	s325.ed	s425.out	s425.ed	s525.out	s525.ed
30	s230.out	s230.ed	s330.out	s330.ed	s430.out	s430.ed	s530.out	s530.ed
35	s235.out	s235.ed	s335.out	s335.ed	s435.out	s435.ed	s535.out	s535.ed
40	s240.out	s240.ed	s340.out	s340.ed	s440.out	s440.ed	s540.out	s540.ed
45	s245.out	s245.ed	s345.out	s345.ed	s445.out	s445.ed	s545.out	s545.ed
50	s250.out	s250.ed	s350.out	s350.ed	s450.out	s450.ed	s550.out	s550.ed
55	s255.out	s255.ed	s355.out	s355.ed	s455.out	s455.ed	s555.out	s555.ed
60	s260.out	s260.ed	s360.out	s360.ed	s460.out	s460.ed	s560.out	s560.ed
65	s265.out	s265.ed	s365.out	s365.ed	s465.out	s465.ed	s565.out	s565.ed
70	s270.out	s270.ed	s370.out	s370.ed	s470.out	s470.ed	s570.out	s570.ed
input		s2xx.ed		s3xx.ed		s4xx.ed		s5xx.ed

Figures 9-11 depict various isotopic quantities as a function of burnup for 2 w/o fuel (EXCEL spreadsheet s2xx.xls). The curves are smooth and well-behaved, as expected. While a first-order interpolation would probably be of sufficient accuracy for the 5 gwd/mtu burnup intervals, a second-order Lagrangian interpolation technique was developed and implemented to assure accuracy. The isotope file S5xx.ed is listed in Attachment Q.

Worst case 18-node axial burnup profiles as a function of average burnup were imported from Refs.33-34 (Attachment I). The Ref.33 axial profiles were designated as 06AL, 10AK, ..., where the first two digits indicate average burnup and the last two profile. The Ref.34 axial profiles were designated as 06BL, 10BK, ..., where the first two digits indicate average burnup and the last two profile. These 24 files are stored in the input file SAX18.INP (Attachment Q). Actual 26-node axial burnup profiles as a function of average burnup were imported from Ref.57 and represent actual Calvert Cliffs Unit 1 Cycle 16 end-of-cycle profiles. The Ref.57 axial profiles were designated 01S0, 02S0, 03S1,..., where the first two digits indicate the quartercore assembly number and the last two the fuel type. The 43 files are stored in the input file SAX26.INP (Attachment Q). Note that 26 nodes were utilized for the Calvert Cliffs profiles, since the data was provided in that format, while 18 nodes were utilized for the worst-case profiles, since that data was provided in that format. Also note that while a quartercore encompasses 62 assemblies, only 43 axial profiles were modeled. Credit was taken for eighthcore symmetry.

Comparison of reactivities generated with isotopics generated from SAS2HLAG (K5006ALG1) and isotopics generated from SAS2H (K5006ALH1) indicates reactivity values within two-sigma of each other. Note that the interpolated isotopics were only employed to calculate biases between axial and uniform burnup profiles. Any bias in the interpolation process itself should cancel out.

(9E) KENO Method of Analysis
(9.E.1) Calculational Methodology
The SCALE 4.4 CSAS25 code module (Ref.9) with the 44 group ENDF/B-V cross section library was utilized in this work to perform the KENO criticality calculations. CSAS25 uses the SCALE Material Information Process (MIP) and the associated material composition library to calculate material number densities, to prepare geometry data for resonance self-shielding, and to create data input files for the cross section processing codes, BONAMI and NITAWL-II. The CSAS25 sequence then invokes the KENO-Va Monte Carlo criticality code.

(9.E.2) Calculation of Biases and Uncertainties
Per Refs.3-4, the analysis methods and neutron cross-section data shall be benchmarked by comparison with critical experiment data for similar configurations. The benchmarking process should establish a calculational bias and uncertainty of the mean with a one-sided tolerance factor of 95% probability at a 95% confidence level. The maximum k-eff value for the SFP shall be obtained by summing the calculated value, the calculational bias, the total uncertainty defined as a statistical combination of the calculational and mechanical uncertainties, and the burnup axial distribution bias. A bias that reduces the calculated value of k-eff should not be applied. Mechanical and material uncertainties may be treated by assuming worst case conditions or by performing sensitivity studies and obtaining worst case uncertainties. Uncertainties may be combined statistically provided that they are independent variations.

(9.E.2.a) Methodology Bias and Uncertainty
The SCALE 4.4 nuclear analysis software package (Ref.9) was verified on a dedicated CCNPP computer (Ref.7). The Ref.8 calculation package documented the validation of SCALE 4.4 for Light-Water Reactor (LWR) fuel criticality analysis.

Criticality safety standards ANSI/ANS-8.1 (Ref.10) and ANSI/ANS-8.17 (Ref.11) apply to criticality methods validation and to criticality evaluations, respectively. ANSI/ANS-8.1 requires that a validation be performed on the method used to calculate criticality safety margins. The validation shall be documented in a written report describing the method, computer program and cross section libraries used, the experimental data, the areas of applicability and the bias and margins of safety. ANSI/ANS-8.17 prescribes the criteria to establish sub-criticality safety margins.

The USNRC has issued NUREG/CR-6361, "Criticality Benchmark Guide for Light-Water-Reactor Fuel in Transportation and Storage Packages" (Ref.12). This guide provides documentation for 180 criticality experiments with geometries, materials, and neutron interaction characteristics representative of LWR fuel in core, storage and cask arrangements. NUREG/CR-6361 was used as design input and as the primary reference for the validation calculation package.

The objective of the Ref.8 calculation package was to satisfy the intent of ANSI/ANS-8.1 (Ref.10) with respect to LWR fuel criticality evaluations in reactor core, spent fuel rack, and cask environments and to satisfy the intent of ANSI/ANS-8.17 (Ref.11) with respect to a determination of the bias and uncertainty in the bias. The Ref.8 calculation package validates the SCALE 4.4 code package (Ref.9) with the 44 neutron energy group ENDF/B-V based cross section library for use in light-water-reactor (LWR) type fuel criticality evaluations. Estimates are made for the bias, uncertainty in the bias and trending with important physical parameters.

Criticality evaluations were performed with the CSAS25 sequence of the SCALE 4.4 code package and with the 44 neutron energy group ENDF/B-V based cross section library. CSAS25 uses the SCALE Material Information Process (MIP) and the associated material composition library to calculate material number densities, to prepare geometry data for resonance self-shielding and to create data input files for the cross section processing codes. The BONAMI and NITAWL-II codes are then used to perform problem dependent cross section processing and resonance correction. The CSAS25 sequence then invokes the KENO-V.a Monte Carlo criticality code. KENO-Va is capable of modeling each critical experiment in three dimensions including explicit representation of the fuel rod array and any associated water or metal reflector regions.

Statistical evaluations included calculating the range of calculated k-eff, the mean k-eff, standard deviation of the mean, bias, 95/95 uncertainty in the bias, and the average Monte Carlo error for the whole group of experiments as well as categories within a data base. Trending of k-eff with physical parameters, i.e. fuel rod pitch, fuel enrichment, moderator to fuel ratio, soluble boron concentration, assembly separation, and average energy group causing fission, was evaluated by creating scatter plots k-eff versus each physical parameter and then performing linear regression on the data. The strength of a trend was evaluated by the magnitude of the correlation coefficient from the linear regression.

In addition, the validation results were organized into three groupings: reactor core type experiments, storage rack type experiments and cask type experiments. For each of these groupings, a bias and 95/95 uncertainty is also specified for use in criticality safety evaluations. The bias and 95/95 uncertainty statistics are determined as follows. For any group or category of k-eff results, the bias is defined as $\beta = \langle k\text{-eff} \rangle - 1$ where <k-eff> is the average for the category or group of critical experiments. According to this definition of bias, the bias is negative if $k < 1$ and positive if $k > 1$. ANSI/ANS-8.17 (Ref.11) requires that the total uncertainty in the mean k-eff or equivalently the bias should include uncertainties for the computation of <k-eff>, the statistical convergence (Monte Carlo error) in computed k-eff and experimental uncertainty. Thus, the total uncertainty in the bias is the square root of the pooled variance of the variance in <k-eff> (σ_{keff}^2) plus the average Monte Carlo variance of the category of critical experiments (σ_{mc}^2) plus the average variance of the experimental uncertainty (σ_{exp}^2), i.e.,

$$\sigma_\beta = \text{sqrt}(\sigma_{keff}^2 + \sigma_{mc}^2 + \sigma_{exp}^2)$$

The average Monte Carlo variance is approximately $(0.0017)^2$ in these criticality evaluations. NUREG/CR-6361 (Ref.12) does not provide an estimate of experimental uncertainty, but the International Handbook of Evaluated Criticality Safety Benchmark Experiments, Volume IV, Ref.13 provides extensive analysis of the experimental uncertainty associated with the benchmark experiments referenced in NUREG/CR-6361 as well as others. Review of the experimental uncertainties associated with the LWR type critical experiments provides an average experimental uncertainty of ±0.0024. Per Ref.8, σ_{keff} is 0.0035 for the storage rack type experiments. Thus, the total uncertainty in the bias becomes:

$$\sigma_\beta = \text{sqrt}(0.0017^2 + 0.0024^2 + 0.0035^2)$$

The 95/95 uncertainty in the bias is the standard deviation, σ_β, times one-sided 95% confidence factor from a Student "t" distribution with n-2 degrees of freedom or:

$$\sigma_{95/95} = t_{05} * \sigma_\beta$$

where n is the number of k_{eff} results in the category or group of critical experiment. For large samples, $t_{.05}$ approaches 1.645 (Ref.14).

The storage rack type category combines the results for the 123 critical experiments including the results for the core-type, separator plate, separator plate-soluble boron, and flux trap-void experiments but excluding the reflector wall categories. This experimental data is sufficiently diverse to establish that the method bias and uncertainty will apply to the Calvert Cliffs storage rack conditions. The storage rack type category exhibits a bias of -0.0008 and a 95/95 one sided uncertainty of 0.0076.

A histogram for the frequency of k-eff values shows a tight clustering of k-eff values near k-eff= 1 and a near normal distribution. Scatter plots were constructed of k-eff versus fuel rod pitch, k-eff versus fuel enrichment, k-eff versus H_2O/fuel volume ratio, k-eff versus H/^{235}U atom ratio, k-eff versus soluble boron concentration, k-eff versus assembly separation, and k-eff versus average group of fission, respectively. Also included in each plot is the associated regression line and equation with correlation coefficient. Review of these plots indicates all the trend lines are nearly horizontal with very small correlation coefficients. Thus, there are no significant trends indicated.

(9.E.2.b) Temperature and Clad Composition Bias

Per Ref.4, the evaluation of normal storage should be done at the temperature (water density) corresponding to the highest reactivity. In poisoned racks, the highest reactivity will usually occur at a water density of 1.0000 (i.e., at 4°C or ~40°F or 277.15°K). However, if the temperature coefficient of reactivity is positive, the evaluation should be done at the highest temperature expected during normal operation: i.e., equilibrium temperature under normal refueling conditions (including full-core offload), with one coolant train out of service and the pool filled with spent fuel from previous reloads. Per UFSAR 9.4.1, in the event that any one loop is lost, the remaining two loops (either two SFPC loops or one SFPC loop and one SDC loop) can continue to maintain the pool temperature at or below 155°F (68°C or 341.48°K @ 0.9785 gm/cc per Ref. 16) for 1830 fuel assemblies in the SFP including a full core offload.

Cases K500000B1-9, K500000C1-9, and K504000C1-9 model an infinite axial and radial array of storage cells of nominal dimensions containing the maximum enrichment of 5.0 w/o fuel as a function of temperature (40°F and 155°F) and as a function of fuel clad material (zirlo, optin, zirc4, alloy a, low tin zirlo, and m5).

KENO Case	Enr w/o	Burnup gwd/t	Tmod K	Boron ppm	Clad	Unbiased K-eff
K500000B1	5.0	0	277.15	0	zirlo	1.19925
K500000B2	5.0	0	277.15	0	optin	1.19707
K500000B3	5.0	0	277.15	0	zirc4	1.19639
K500000B4	5.0	0	341.48	0	zirlo	1.20803
K500000B5	5.0	0	341.48	0	optin	1.20813
K500000B6	*5.0*	*0*	*341.48*	*0*	*zirc4*	*1.21112*
K500000B7	5.0	0	341.48	0	alloy a	1.20980
K500000B8	5.0	0	341.48	0	lt zirlo	1.20870
K500000B9	5.0	0	341.48	0	m5	1.20890
K500000C1	5.0	0	277.15	300	zirlo	1.12220
K500000C2	5.0	0	277.15	300	optin	1.12203
K500000C3	5.0	0	277.15	300	zirc4	1.12104
K500000C4	5.0	0	341.48	300	zirlo	1.13323
K500000C5	5.0	0	341.48	300	optin	1.13396
K500000C6	*5.0*	*0*	*341.48*	*300*	*zirc4*	*1.13444*
K500000C7	5.0	0	341.48	300	alloy a	1.13241
K500000C8	5.0	0	341.48	300	lt zirlo	1.13259
K500000C9	5.0	0	341.48	300	m5	1.13359
K504000C1	5.0	40	277.15	300	zirlo	0.87878
K504000C2	5.0	40	277.15	300	optin	0.87862
K504000C3	5.0	40	277.15	300	zirc4	0.87750

K504000C4	5.0	40	341.48	300	zirlo	0.89027
K504000C5	5.0	40	341.48	300	optin	0.89083
K504000C6	*5.0*	*40*	*341.48*	*300*	*zirc4*	*0.89089*
K504000C7	5.0	40	341.48	300	alloy a	0.89039
K504000C8	5.0	40	341.48	300	lt zirlo	0.89004
K504000C9	5.0	40	341.48	300	m5	0.89018

The zirc4 clad cases at 155°F are the most reactive for all conditions (unborated, borated, unburned, burned). This worst case condition will be assumed in all calculations.

(9.E.2.c) Storage Cell Pitch Uncertainty

Per Ref.4, mechanical and material uncertainties may be treated by assuming worst case conditions or by performing sensitivity studies and obtaining worst case uncertainties. Per Ref.15, the mechanical design of the fuel racks is such that the average pitch between boxes is maintained by structural members at 10.09375 ± 0.03125 inches. Thus a nominal pitch of 10.09375 inches will be assumed, and an uncertainty value to ± 0.03125 inches will be included in the mechanical and material uncertainty value. See Attachment E.

Cases K500000BB-C, K500000CB-C, and K504000CB-C model an infinite axial and radial array of storage cells of nominal dimensions containing the maximum enrichment of 5.0 w/o fuel as a function of storage cell pitch (10.0625, 10.09375, and 10.125 in) at the worst case temperature of 155°F for a fuel clad material composed of zirc4.

KENO Case	Enr w/o	Burnup gwd/t	Tmod K	Boron ppm	Pitch inch	Unbiased K-eff	Delta K-eff	Uncertainty
K500000BB	5.0	0	341.48	0	10.125	1.20356	0.00088	-0.00577
K500000BC	5.0	0	341.48	0	10.0625	1.21278	0.00101	0.00358
K500000CB	5.0	0	341.48	300	10.125	1.12857	0.00091	-0.00402
K500000CC	5.0	0	341.48	300	10.0625	1.13705	0.00094	0.00449
K504000CB	5.0	40	341.48	300	10.125	0.88473	0.00077	-0.00462
K504000CC	*5.0*	*40*	*341.48*	*300*	10.0625	0.89382	0.00084	0.00454

A storage cell pitch of 10.0625 in results in the highest reactivity value, and the resulting uncertainty values will be used in the uncertainty calculations

(9.E.2.d) Stack Height Density Uncertainty

Per Ref.4, mechanical and material uncertainties may be treated by assuming worst case conditions or by performing sensitivity studies and obtaining worst case uncertainties. Per UFSAR Tables 3.3-1 and 3.3-2, the maximum stack height density is 10.31 gm/cc (<94.5% theoretical density). Per Ref.58 for standard fuel pellets, the stack height density can range between 93.5% and 96.0% of theoretical density, while per Ref.59 for value added fuel pellets, the stack height density can range between 94.0% and 96.5% of theoretical density. Thus a nominal stack height density of 94.5% of theoretical density will be assumed, and an uncertainty value to 96.5% of theoretical density will be included in the mechanical and material uncertainty value.

KENO Case	Enr w/o	Burnup gwd/t	Tmod K	Boron ppm	SHD	Unbiased K-eff	Delta K-eff	Uncertainty
K500000BA	5.0	0	341.48	0	0.965	1.21021	0.00090	0.00090
K500000CA	5.0	0	341.48	300	0.965	1.13606	0.00084	0.00340
K504000CA	5.0	40	341.48	300	0.965	0.89768	0.00085	0.00841

The higher stack height density results in the higher reactivity values, and the resulting uncertainty values will be used in the uncertainty calculations

(9.E.2.e) Enrichment Uncertainty
Per Ref.4, mechanical uncertainties may be treated by assuming worst case conditions or by performing sensitivity studies and obtaining worst case uncertainties. Per 10 CFR 50.68 (Ref.2), the maximum nominal U-235 enrichment of the fresh fuel assemblies is limited to five percent by weight. Per the methodology of Ref.60, an uncertainty of 0.05 w/o enrichment was assumed.

KENO Case	Enr w/o	Burnup gwd/t	Tmod K	Boron ppm	Clad	Unbiased K-eff	Delta K-eff	Uncertainty
K500000B6	*5.0*	*0*	*341.48*	*0*	*zirc4*	*1.21112*	*0.00091*	
K500000BI	5.05	0	341.48	0	zirc4	1.21080	0.00096	0.00155
K500000C6	*5.0*	*0*	*341.48*	*300*	*zirc4*	*1.13444*	*0.00094*	
K500000CI	5.05	0	341.48	300	zirc4	1.13474	0.00086	0.00210
K504000C6	*5.0*	*40*	*341.48*	*300*	*zirc4*	*0.89089*	*0.00077*	
K504000CI	5.05	40	341.48	300	zirc4	0.89238	0.00078	0.00304

The above uncertainty values will be used in the uncertainty calculations.

(9.E.2.f) Steel Thickness Uncertainty
Per Ref.4, mechanical and material uncertainties may be treated by assuming worst case conditions or by performing sensitivity studies and obtaining worst case uncertainties. Per Ref.15, the mechanical design of the fuel racks is such that the average wall thickness is 0.060 ± 0.010 inches. Thus a nominal wall thickness of 0.060 inches will be assumed, and an uncertainty value to ± 0.010 inches will be included in the mechanical and material uncertainty value. See Attachment E.

KENO Case	Enr w/o	Burnup gwd/t	Tmod K	Boron ppm	Steel cm	Unbiased K-eff	Delta K-eff	Uncertainty
K500000B6	*5.0*	*0*	*341.48*	*0*	*0.1524*	*1.21112*	*0.00091*	
K500000BD	5.0	0	341.48	0	0.1270	1.22267	0.00100	0.01346
K500000BE	5.0	0	341.48	0	0.1778	1.19742	0.00109	-0.01170
K500000C6	*5.0*	*0*	*341.48*	*300*	*0.1524*	*1.13444*	*0.00094*	
K500000CD	5.0	0	341.48	300	0.1270	1.14037	0.00088	0.00775
K500000CE	5.0	0	341.48	300	0.1778	1.12599	0.00098	-0.00653
K504000C6	*5.0*	*40*	*341.48*	*300*	*0.1524*	*0.89089*	*0.00077*	
K504000CD	5.0	40	341.48	300	0.1270	0.89639	0.00071	0.00698
K504000CE	5.0	40	341.48	300	0.1778	0.88471	0.00083	-0.00458

The above cases model an infinite axial and radial array of storage cells of nominal dimensions containing the maximum enrichment of 5.0 w/o fuel as a function of storage cell steel thickness (0.1270, 0.1524, and 0.1778 cm) at the worst case temperature of 155°F for a fuel clad material composed of zirc4. A storage cell steel thickness of 0.1270 cm results in the highest reactivity values The above uncertainty values will be used in the uncertainty calculations.

(9.E.2.g) Poison Loading Uncertainty
Per Refs.3-4, mechanical uncertainties may be treated by assuming worst case conditions or by performing sensitivity studies and obtaining worst case uncertainties. Although the Unit 2

storage rack cells contain sheets of Boraflex neutron absorber, Issue Reports IR3-045-938, IR3-045-939, and IR3-052-199 documented possible boraflex degradation in the Unit 2 SFP, based on calculations using the Racklife software package. Thus the worst case assumption of no Boraflex credit is assumed in this work.

(9.E.2.h) Eccentric Positioning Uncertainty

Per Ref.4, mechanical uncertainties may be treated by assuming worst case conditions or by performing sensitivity studies and obtaining worst case uncertainties. It is possible for a fuel assembly not to be positioned centrally within a storage cell, because of clearance between the assembly and the cell wall. Calculations will be performed to determine the effects of eccentrically located fuel. It will be assumed that the fuel assemblies will be displaced diagonally within their storage cells as far as possible towards and away from each other. This will generate an uncertainty value, which will be included in the mechanical and material uncertainty value. See Attachment E.

KENO Case	Enr w/o	Burnup gwd/t	Tmod K	Boron ppm		Unbiased K-eff	Delta K-eff	Uncertainty
K500000B6	*5.0*	*0*	*341.48*	*0*	Single assembly	*1.21112*	*0.00091*	
K500000BF	5.0	0	341.48	0	10x10	1.20934	0.00095	-0.00178
K500000BG	5.0	0	341.48	0	10x10 eccentric in	1.21883	0.00099	0.00961
K500000BH	5.0	0	341.48	0	10x10 eccentric out	1.21889	0.00092	0.00960
K500000C6	*5.0*	*0*	*341.48*	*300*	Single assembly	*1.13444*	*0.00094*	
K500000CF	5.0	0	341.48	300	10x10	1.13528	0.00096	0.00084
K500000CG	5.0	0	341.48	300	10x10 eccentric in	1.14187	0.00104	0.00941
K500000CH	5.0	0	341.48	300	10x10 eccentric out	1.14386	0.00086	0.01122
K504000C6	*5.0*	*40*	*341.48*	*300*	Single assembly	*0.89089*	*0.00077*	
K504000CF	5.0	40	341.48	300	10x10	0.89070	0.00077	-0.00019
K504000CG	5.0	40	341.48	300	10x10 eccentric in	0.89731	0.00081	0.00800
K504000CH	5.0	40	341.48	300	10x10 eccentric out	0.89682	0.00088	0.00758

Cases K500000BF, K500000CF, and K504000CF models an infinite axial and radial array of 10x10 storage cells of nominal dimensions containing the maximum enrichment of 5.0 w/o fuel at the worst case temperature of 155°F for a fuel clad material composed of zirc4. The purpose of these cases was to verify that the reactivity of the infinite axial and radial array of 10x10 storage cells is equivalent to the infinite axial and radial array of single storage cells. The resultant k-effective values are well within the two-sigma error margins of the calculations.

The remaining cases modeled an infinite axial and radial array of 10x10 storage cells of nominal dimensions containing the maximum enrichment of 5.0 w/o fuel as a function of eccentric positioning within the storage cell at the worst case temperature of 155°F for a fuel clad material composed of zirc4. The larger of the above uncertainty values will be used in the uncertainty calculations.

(9.E.2.i) Soluble Boron Uncertainty

Per Ref.4, mechanical uncertainties may be treated by assuming worst case conditions or by performing sensitivity studies and obtaining worst case uncertainties. The soluble boron credit will be limited to a maximum value of 300 ppm per the restrictions of the Unit 1 criticality analysis in Ref.43. Note that 300 ppm is a minimum boron concentration requirement. 15% should be added to this value to account for all uncertainties. Thus a boron level of 350 ppm with uncertainties is required to credit soluble boron in the SFP.

(9.E.2.j) Moderator in Gap Uncertainty
Per Ref.4, mechanical uncertainties may be treated by assuming worst case conditions or by performing sensitivity studies and obtaining worst case uncertainties. Nominally, all of the cases in this work assume that the pellet-to-clad gap contains void, which it normally does. However, failed fuel rods may exist and the gap may be filled with water of the same composition as that exterior to the fuel rod. This is an NRC requirement for cask criticality safety analysis (NUREG-1536, p. 6-3).

KENO Case	Enr w/o	Burnup gwd/t	Tmod K	Boron ppm		Unbiased K-eff	Delta K-eff	Uncertainty
K500000B6	*5.0*	*0*	*341.48*	*0*	*No mod in gap*	*1.21112*	*0.00091*	
K500000BJ	5.0	0	341.48	0	Mod in gap	1.20915	0.00089	-0.00017
K500000C6	*5.0*	*0*	*341.48*	*300*	*No mod in gap*	*1.13444*	*0.00094*	
K500000CJ	5.0	0	341.48	300	Mod in gap	1.13618	0.00088	0.00356
K504000C6	*5.0*	*40*	*341.48*	*300*	*No mod in gap*	*0.89089*	*0.00077*	
K504000CJ	5.0	40	341.48	300	Mod in gap	0.89204	0.00075	0.00267

The above uncertainty values will be used in the uncertainty calculations.

In addition, fuel clad failure would indicate that certain fission gases (noble gases, halogens, cesiums, and technetiums) could escape the affected fuel pins and increase system reactivity. Pin failure occurs infrequently (much less than 1% of the rods inserted into the core fail). When failure does occur, not all of the gases escape from the fuel matrix. Assuming that the pin is at or near centerline melting temperature, the fission product pellet-to-coolant escape rates can be extracted from Ref.62 (6.50E-08/sec for noble gases, 2.30E-08/sec for halogens and cesiums, and 1.40E-11 for technetium). Assuming that a fuel pin fails for 1 of the 3 cycles of insertion (It is the policy at CCNPP not to reinsert failed fuel back into the core without reconstitution.), approximately 9% of the noble gases, 33% of the halogens and cesiums, and 99.9% of the technetiums would remain. Conservatively assuming that 5% of all fuel pins fail and that all of the gaseous fission products from the failed fuel would be lost, the change in reactivity would only amount to 0.00084 Δk. Treating this as a component in the uncertainty analysis, the total bias and uncertainty would only increase by 0.00001 Δk. In addition, part of this reactivity increase would be negated by a smaller two-dimensional to three-dimensional burnup bias. Thus, this effect is negligible and will be neglected in this work.

(9.E.2.k) Axial Distribution Burnup Bias
The dynamics of reactor operation results in non-uniform axial-burnup profiles in fuel with any significant burnup. At the beginning of life in a PWR, a near-cosine axial-shaped flux will begin depleting fuel near the axial center of a fuel assembly at a greater rate than at the ends. As the reactor continues to operate, the cosine flux shape will flatten because of the fuel depletion and fission product buildup that occurs near the center. However, because of the high leakage near the ends of the fuel, burnup will drop off rapidly near the ends. The majority of PWR fuel assemblies have similar axial-burnup shapes - relatively flat in the axial mid-section (with peak burnup from 1.1 to 1.2 times the assembly average burnup) and significantly underburned fuel at the ends (with burnup of 50 to 60% of the assembly average). Note that due to a difference in the moderator density, the burnup is slightly higher at the bottom of the assembly than at the top. The cooler higher-density water at the assembly inlet results in a higher reactivity and thus higher burnup than the warmer moderator at the assembly outlet.

An assumed single average burnup incorrectly weights the calculation of k-effective by placing the flux profile toward the center of the rod. Thus, leakage is artificially minimized, and burnup at the driving region of a uniform problem (center) is artificially reduced. In reality, the most

reactive region of spent fuel is towards the assembly ends, where there exists a balance between reactivity due to lower burnup and increased leakage.

Depletion and criticality models cannot exactly represent the continuous burnup distribution that occurs in spent fuel. Discretization is required. Very fine axial discretization is possible, but is computationally expensive. In addition, real burnup data is generally available on a relatively coarse grid. Ref.37 ndicates that using more than 18 equally-spaced axial regions has no significant impact on the calculated end effect.

The reactivity difference between the neutron multiplication factor (k-effective) calculated with explicit representation of the axial burnup distribution and k-effective calculated assuming a uniform axial burnup is referred to as the "end effect". The "end effect" is dependent on the axial burnup profile, total accumulated burnup, cooling time, initial enrichment, assembly design, and the isotopics considered (i.e., actinide-only or actinide plus fission products).

Studies have shown that assuming a uniform axial distribution is usually conservative for low burnups, but becomes increasingly nonconservative as burnup increases. The transition between conservatism and nonconservatism depends on several factors, including the initial enrichment, the cooling time, and the nuclide composition.

Per Ref.4, a correction for the effect of the axial distribution in burnup should be determined and, if positive, added to the reactivity calculated for uniform axial burnup distribution. Per Ref.46, WCAP-14416 (Ref.31) can no longer be relied upon as approved methodology by the NRC staff or licensees due to larger (non-conservative) two-dimensional (2D) to three-dimensional (3D) axial burnup biases than Westinghouse had reported in WCAP-14416. For future licensing actions, licensees need to submit plant-specific criticality calculations for SFP configurations that include technically supported margins. This issue was further addressed in Ref.47.

A reactivity bias was included in the overall k-effective calculations, to account for differences between two-dimensional and three-dimensional modeling. A conservative set of biases was developed that account for the reactivity difference between a fuel assembly with an explicit axial three-dimensional burnup profile and one with a uniform two-dimensional profile at the same average burnup. The biases were computed and tabulated as a function of both burnup and initial enrichment. The conservative axial bias corresponding to the highest enrichment / burnup storage limit was employed, since among all enrichment / burnup combinations on the reactivity equivalence curve, the highest yields the largest positive axial bias.

Burnup profiles change with burnup - tending to flatten with increasing burnup. Consequently, if an axial burnup profile from a low burnup assembly is used in a calculation involving high burnup, the end-effect is over-estimated. Hence, for determination of bounding profiles, it is common to sort the profiles into burnup ranges, Worst-case axial profiles were extracted from Ref.33 as a function of burnup (The 12 burnup profiles are listed in Attachment I.). Two-dimensional to three-dimensional comparisons were performed as a function of enrichment and soluble boron.

Three-Dimensional to Two Dimensional Reactivity Bias							
		5.0 w/o	4.0 w/o	3.0 w/o	5.0 w/o	4.0 w/o	3.0 w/o
Gwd/mtu	Profile	0 ppm	0 ppm	0 ppm	300 ppm	300 ppm	300 ppm
62	AA	0.03226	0.03046	0.01704	0.03047	0.02898	0.01423
46	AB	0.01751	0.02128	0.01459	0.01656	0.02062	0.01619
42	AC	0.01060	0.01195	0.01380	0.00944	0.01367	0.01345
38	AD	0.01623	0.02367	0.02465	0.02030	0.02418	0.02391
34	AE	0.01255	0.01739	0.01684	0.01245	0.01549	0.01495

30	AF	0.00918	0.01559	0.01609	0.00996	0.01475	0.01616
26	AG	0.00688	0.01089	0.01730	0.00789	0.00858	0.01544
22	AH	0.00193	0.00479	0.00914	0.00109	0.00863	0.00869
18	AI	0.01682	0.02645	0.02942	0.01528	0.02703	0.02705
14	AJ	-0.00834	-0.00135	-0.00052	-0.00236	-0.00250	0.00036
10	AK	-0.00294	-0.00241	-0.00079	-0.00409	-0.00208	-0.00224
6	AL	-0.00360	-0.00406	-0.00169	-0.00286	-0.00290	-0.00331

The above reactivity bias results indicate that the worst-case reactivity bias (0.03226 Δk) is for the unborated highest enrichment and highest burnup fuel.

Worst-case axial profiles were extracted from Ref.34 as a function of burnup (Attachment I). Two-dimensional to three-dimensional comparisons were performed as a function of enrichment and soluble boron.

Three-Dimensional to Two Dimensional Reactivity Bias							
		5.0 w/o	4.0 w/o	3.0 w/o	5.0 w/o	4.0 w/o	3.0 w/o
Gwd/mtu	Profile	0 ppm	0 ppm	0 ppm	300 ppm	300 ppm	300 ppm
62	BA	0.03054	0.03061	0.01470	0.02955	0.02802	0.01271
46	BB	0.01381	0.01803	0.01373	0.01598	0.01744	0.01542
42	BC	0.00643	0.01066	0.01006	0.00773	0.00791	0.01041
38	BD	0.01073	0.01842	0.01912	0.01285	0.01650	0.01842
34	BE	0.01013	0.01499	0.01453	0.00603	0.01217	0.01249
30	BF	0.00850	0.01648	0.01584	0.01083	0.01359	0.01612
26	BG	0.00741	0.00923	0.01401	0.00678	0.01002	0.01499
22	BH	-0.00008	0.00461	0.00909	0.00154	0.00430	0.00891
18	BI	0.01989	0.02704	0.02853	0.01519	0.02669	0.02753
14	BJ	0.00644	0.00963	0.01008	0.00767	0.00811	0.00814
10	BK	-0.00337	-0.00151	0.00102	-0.00235	-0.00023	-0.00244
6	BL	-0.00254	-0.00247	-0.00109	-0.00081	-0.00091	0.00010

The above reactivity bias results indicate that the worst-case reactivity bias (0.03054 Δk) is for the unborated highest enrichment and highest burnup fuel.

A statistical evaluation was performed in Ref.37 on the neutron multiplication factors resulting from the profiles contained in the database to assess the likelihood of the existence of axial profiles that have significantly higher reactivity. Comparison of the individual k-effective values to the mean and standard deviation for each burnup group reveals that the bounding profiles provide a significant increase in reactivity compared with the average. For all but one of the 12 burnup groups, the k-effective value associated with the bounding axial profile, is more than 3 standard deviations above the mean and in most cases is more than 4 standard deviations above the mean. The only exception is burnup group 12 (burnup < 6 GWd/MTU), which has relatively few profiles and is of little interest to burnup credit, since the burnup profiles in group 12 yield a negative end effect. Nevertheless, the k-effective value associated with the bounding axial profile in group 12 is 2.2 standard deviations above the mean. Thus the bounding profiles can be considered statistical outliers, as opposed to representative of typical spent nuclear fuel profiles. Consequently, the probability that other axial profiles exist that are notably more reactive than the bounding profiles is very small.

Also note that per Ref.37 some evidence exists that some plants may have selectively submitted their most reactive profiles. This would introduce a conservative bias into the database.

Actual Calvert Cliffs end-of-cycle burnups were extracted from Ref.57 (Attachment I). Two-dimensional to three-dimensional comparisons were performed at the highest enrichment value of 5.0 w/o and at zero soluble boron.

Calvert Cliffs Three-Dimensional to Two Dimensional Reactivity Bias							
Assm	Batch	gwd/mtu	ΔK	Assm	Batch	gwd/mtu	ΔK
01	S0	48.013	-0.01135	26	V1	27.861	-0.00680
02	S0	46.688	-0.00875	27	T2	50.026	-0.01105
03	S1	49.523	-0.00838	28	V1	27.664	-0.00847
04	V0	14.895	-0.00649	33	V2	27.782	-0.00699
05	T0	35.696	-0.01075	34	T2	49.939	-0.01008
06	V1	20.408	-0.00934	35	V2	27.639	-0.00797
07	V0	22.090	-0.00761	36	T2	49.592	-0.00679
08	S2	51.485	-0.00863	42	V2	27.667	-0.00660
09	V0	18.880	-0.00579	43	T2	49.325	-0.00952
10	T0	35.485	-0.01080	44	V2	27.779	-0.00864
11	V1	25.651	-0.00581	52	V2	27.236	-0.00780
12	T0	41.171	-0.01016	53	T0	40.843	-0.00914
13	T1	42.997	-0.01064	54	S0	46.417	-0.01068
14	T2	35.350	-0.01111	55	V0	22.094	-0.00777
15	V0	19.296	-0.00902	56	T1	42.987	-0.01120
16	T2	46.518	-0.00887	57	T2	48.568	-0.01021
17	V1	26.726	-0.00914	58	V1	27.667	-0.00667
18	T2	49.829	-0.01169	59	T2	49.583	-0.00905
19	V1	27.257	-0.00765	60	V2	27.735	-0.00956
20	T2	48.874	-0.00977	61	T0	43.765	-0.01120
24	V1	26.492	-0.00935	62	J0	50.648	-0.00700
25	T2	47.452	-0.00864				

The above reactivity bias results indicate that the worst-case reactivity bias is -0.00579 Δk. Thus for Calvert Cliffs specific fuel, use of 26-node axial burnup profiles is less conservative than uniform axial burnups. Note that per Ref.37, CE fuel types tend to exhibit a smaller end effect on average.

For conservatism, an axial burnup bias of 3.25% Δk will be utilized for all burnup cases.

(9.E.2.l) Effect of UEF/LEF Composition on Reactivity
All three dimensional KENO executions in this work assume that the Upper End Fitting (UEF) and Lower End Fitting (LEF) of each assembly are composed of moderator. This was verified to be conservative.

KENO Case	Enr w/o	Burnup gwd/t	Tmod K	Boron ppm	UEF/LEF	Unbiased K-eff
K5U2SFPA	5.0	0	341.48	0	Water	1.19548
KU2SFPX	5.0	0	341.48	0	Actual	1.19449

(9.E.3) KENO Calculations
(9.E.3.a) The reactivity of an infinite array of fuel as a function of enrichment, burnup, and soluble boron to determine compliance with 10 CFR 50.68.
(9.E.3.b) The reactivity of an infinite array and of the whole Unit 2 SFP as a function of soluble boron.

(9.E.3.c) Reactivity as a function of soluble boron and burnup using checkerboard patterns in a whole Unit 2 SFP model.
(9.E.3.d) Reactivity of the whole Unit 2 SFP model with reconstitution.
(9.E.3.e) Comparison of reactivity of an infinite array of fuel as a function of burnup and enrichment for 50 and 101 isotope models.

(9.E.4) Accident Conditions
Per Ref.3, for accident conditions, the following assumptions apply: (i) The double contingency principle of ANSI N 16.1-1975 shall be applied. It shall require two unlikely, independent, concurrent events to produce a criticality accident. (ii) Realistic initial conditions (e.g., the presence of soluble boron) may be assumed. (iii) Accidents shall include dropping of a fuel assembly on top of the racks, abnormal placement of a fuel assembly in the SFP, a cask or heavy object drop onto the SFP racks, effect of tornado or earthquake on the deformation and relative position of the fuel racks, and loss of cooling systems or flow unless single failure proof.

(9.E.4.a) Fuel Misloading Accident:
Since assemblies must possess sufficient burnup to be placed in the Unit 2 SFP to counteract the loss of Boraflex, placement of an assembly with insufficient burnup in the SFP would constitute a fuel misloading accident. However, the double contingency principle allows the crediting of the soluble boron in the SFP during such an event. Per Refs. 53 and 54, the Technical Specification Refueling Boron Concentration is greater than 2150 ppm. 2000 ppm will be conservatively used in this work.

KENO Case	Enr w/o	Burnup gwd/t	Tmod K	Boron ppm	Unbiased K-eff	Delta K-eff	Biased K-eff
K200000D3	*2.0*	*0*	*341.48*	*2000*	0.62679	0.00066	0.68808
K300000D3	3.0	0	341.48	2000	0.74302	0.00073	0.80431
K400000D3	*4.0*	*0*	*341.48*	*2000*	0.82161	0.00096	0.88290
K500000D3	5.0	0	341.48	2000	0.87907	0.00094	0.94036

The above accident cases assume that the Unit 2 SFP is completely misloaded with fresh fuel of the indicated enrichments. K-effective is maintained below 0.95 in all cases. Thus there are no adverse consequences for a worst-case fuel misloading accident in this analysis.

(9.E.4.b) Abnormal Placement of a Fuel Assembly in the SFP Racks:
The top opening of the SFP racks has angled lead-in guides, which effectively block the spaces between the cavities, as well as guide the fuel assembly into the open tube. Also to avoid the possibility of inadvertently placing a fuel assembly between the outermost storage cell and the pool wall, the top rack surface is extended to cover this space. Thus the abnormal placement of a fuel assembly in the SFP racks is not a credible event.

(9.E.4.c) Horizontal Assembly Drop Accident:
Dropping an assembly on top of the SFP racks from the Spent Fuel Handling Machine (SFHM) is not possible at CCNPP due to the design of the SFHM and due to the height of the SFP racks. The bottom of the outer mast assembly is at elevation 49'5", while the top of the SFP racks is at elevation 45'0". While not a credible accident, this accident will be explicitly analyzed in this work.

Dropping an assembly on top of the SFP racks from the Cask Handling Crane (CHC) or the New Fuel Elevator (NFE) is also not a credible accident. The CHC is designed in accordance with the single-failure proof criteria of NUREG-0554 and NUREG-0612 and is used to move assemblies into the new fuel elevator. The NFE is utilized to lower new fuel from the operating floor to the

bottom of the SFP, where it is then grappled by the Spent Fuel Handling Machine. The elevator is powered by a cable winch, and the assembly is contained in a simple support structure whose wheels are captured on two rails. Dropping an assembly from the NFE would require a catastrophic failure of the NFE, which is not a credible event and which has never occurred to date.

Per Ref.4, the double contingency principle shall be applied. It shall require two unlikely, independent, concurrent events to produce a criticality accident. The double-contingency principle means that realistic conditions may be assumed. For example, if soluble boron is normally present in the SFP water, the loss of soluble boron is considered as one accident condition and a second concurrent accident need not be assumed. Therefore, total credit for the presence of soluble boron may be assumed in evaluating this accident condition.

During inspection/reconstitution activities in the SFP, assemblies are put on 20.5" spacers (Ref. 25) adjacent to the SFP wall. This process lifts the active fuel region of the affected assembly above the boraflex poison plates (Attachment G) and thus could affect reactivity. In this work, the boraflex plates are replaced with moderator and are not credited, thus the reactivity effect of inspection/reconstitution should be minimal. However, a horizontal dropped assembly in the vicinity of assemblies on rack spacers may affect reactivity.

KENO Case	Enr w/o	Burnup gwd/t	Boron ppm		Unbiased K-eff	Delta K-eff	Biased K-eff
KU2SFPCD	5.0	0	2000	Dropped assm	0.65990	0.00085	0.72119
KU2SFPCRD	5.0	0	2000	Dropped assm during recon	0.66264	0.00068	0.72393

The above accident cases assume a dropped assembly during normal operation and a dropped assembly during reconstitution/inspection activities. K-effective is maintained below 0.95 in both cases. Thus there are no adverse consequences for a worst-case horizontal assembly drop accident in this analysis.

(9.E.4.d) Vertical Assembly Drop Accident:
Dropping an assembly vertically will not cause abnormal placement of a fuel assembly in the SFP racks since the top opening of the SFP racks has angled lead-in guides, which effectively block the spaces between the cavities, as well as guide the fuel assembly into the open tube. Also to avoid the possibility of inadvertently dropping a fuel assembly between the outermost storage cell and the pool wall, the top rack surface is extended to cover this space. Dropping an assembly and having it stand upright atop another assembly in the SFP racks is less limiting than the current analysis, which assumes infinite axial extent. Thus there are no adverse consequences for a vertical assembly drop accident in this analysis.

(9.E.4.e) Cask or Heavy Object Drop onto the SFP Racks:
The racks are designed to withstand all anticipated loadings. Structural deformations are limited to preclude any possibility of criticality. The Seismic Category 1 racks are supported in such a manner as to preclude a reduction in separation under either the Operating Basis or Safe Shutdown Earthquake. The racks are designed not to collapse or bow under the force of a fuel assembly dropped into an empty cavity or dropped horizontally across the top of the racks assuming no drag resistance from the water. Heavy loads in excess of 1600 lbs are prohibited from travel over spent fuel assemblies in the SFP unless such loads are handled by a single-failure proof device. The Spent Fuel Cask Handling Crane, which is designed in accordance with the single-failure proof criteria of NUREG-0554 and NUREG-0612, is used to handle heavy loads in the SFP area. Thus the cask or heavy object drop accident is not a credible event.

(9.E.4.f) Boron Dilution Accident:

This proposed criticality design basis for the SFP racks assumes that the k-effective of the spent fuel storage racks loaded with fuel of the maximum fuel assembly reactivity will not exceed 0.95, at a 95% probability, 95% confidence level, if flooded with borated water, and the k-effective will remain below 0.998 (subcritical) at a 95% probability, 95% confidence level, if completely flooded with unborated water. Dilution events that have the potential to dilute the SFP boron concentration to a value less than the minimum required are not credible events based on existing level alarms and the stored inventory of demineralized water in the systems interfacing with the SFP. Even in the unlikely event that the SFP is completely diluted of boron, the SFP will remain subcritical by a design margin of k-eff not to exceed 0.998. Thus boron dilution to less than the required minimum is not a credible event; however, in the unlikely event of complete dilution, no adverse consequences would result.

(9.E.4.g) Loss of Coolant Accident:
The most serious failure to the system is the loss of SFP water. This is avoided by routing all SFP piping connections above the water level and providing them with siphon breakers to prevent gravity drainage (UFSAR 9.4.4).

The SFP is designed to preclude the loss of structural integrity. The SFP is designed in two identical sections separated by a 3 1/2 foot thick dividing wall, the pool is constructed of reinforced concrete and lined with 3/16 inch stainless steel. Each half of the pool is 54 feet long, 25 feet wide and approximately 39 feet deep (the floor elevation varies). The SFP walls and floor are 5 1/2 or 6 feet thick, depending on the location.

Even with the precautions described, small leaks may still occur in the SFP. Early detection of pool leakage and prompt replacement of water is essential. Early leakage detection is assured by a surveillance which requires that the minimum pool level be verified at least once every 7 days. In practice, level is checked one every 12 hours as required by the Auxiliary Building log sheets. In addition, a level alarm keeps the Control Room Operator aware of level changes. PEO 0-067-02-O-M (SFP Leakage Test) requires a regular check for leakage, as well.

(9.E.4.h) Loss of Cooling Accident:
The design of the SFP Cooling System and pool structural components (e.g., pool liner plate, SFPC piping and pumps) for total loss of cooling is not part of the system's design basis (UFSAR 9.4.4). The entire Spent Fuel Pool Cooling System is tornado-protected and is located in a Seismic Category I structure.

(9.E.4.i) Natural Phenomena Incident:
The racks are designed to withstand all anticipated loadings. Structural deformations are limited to preclude any possibility of criticality. The Seismic Category 1 racks are supported in such a manner as to preclude a reduction in separation under either the Operating Basis or Safe Shutdown Earthquake.

Since there has been no record of tsunamis on the northeastern United States coast, it is not believed that the site will be subjected to a significant tsunami effect (UFSAR 2.6.6).

The relative frequency of hurricane occurrence for the CCNPP site is slightly more than one hurricane per year. For the Probable Maximum Hurricane (PMH), it is assumed that the peak hurricane surge is coincident with normal high tide and with a 99th percentile wave height. The total predicted wave run-up is to Elevation 27.1', which is considerably less than the 69' elevation of the top of the SFP. Thus the maximum hypothetical flood level is below the top of the SFP elevation (UFSAR 2.8.3).

Missiles generated externally to the plant could be from high winds (tornadoes or hurricanes). Missiles generated internally to the plant could be from the malfunction or structural failure of

plant equipment, such as the turbine generator. Internal and external missile protection is provided by the 6 foot thick SFP walls. In addition, a 2 foot thick concrete missile barrier positioned at the 118-foot elevation protects the SFP from a high trajectory missile generated by a turbine overspeed incident.

(9.F) Burnup Measurement Uncertainty
The uncertainty in measured burnup was extracted from Ref. 61 for ABB/CE fuel assemblies. For burnups less then 30 gwd/mtu, the burnup must be increased by 2.5%. For burnups in excess of 30 gwd/mtu, the burnup must be increased by 750 mwd/mtu.

Note that per Ref.37, these burnup measurement uncertainties are conservative. The uncertainty in burnup, evaluated over three cycles of operation, decreases with increasing burnup. For assemblies discharged after one cycle of operation the uncertainty was estimated to be 1.90%; after two cycles of burnup the uncertainty was 0.98%; and after three cycles of burnup the uncertainty was 1.02%.

Figure 2: Reactivity vs Cooling Time

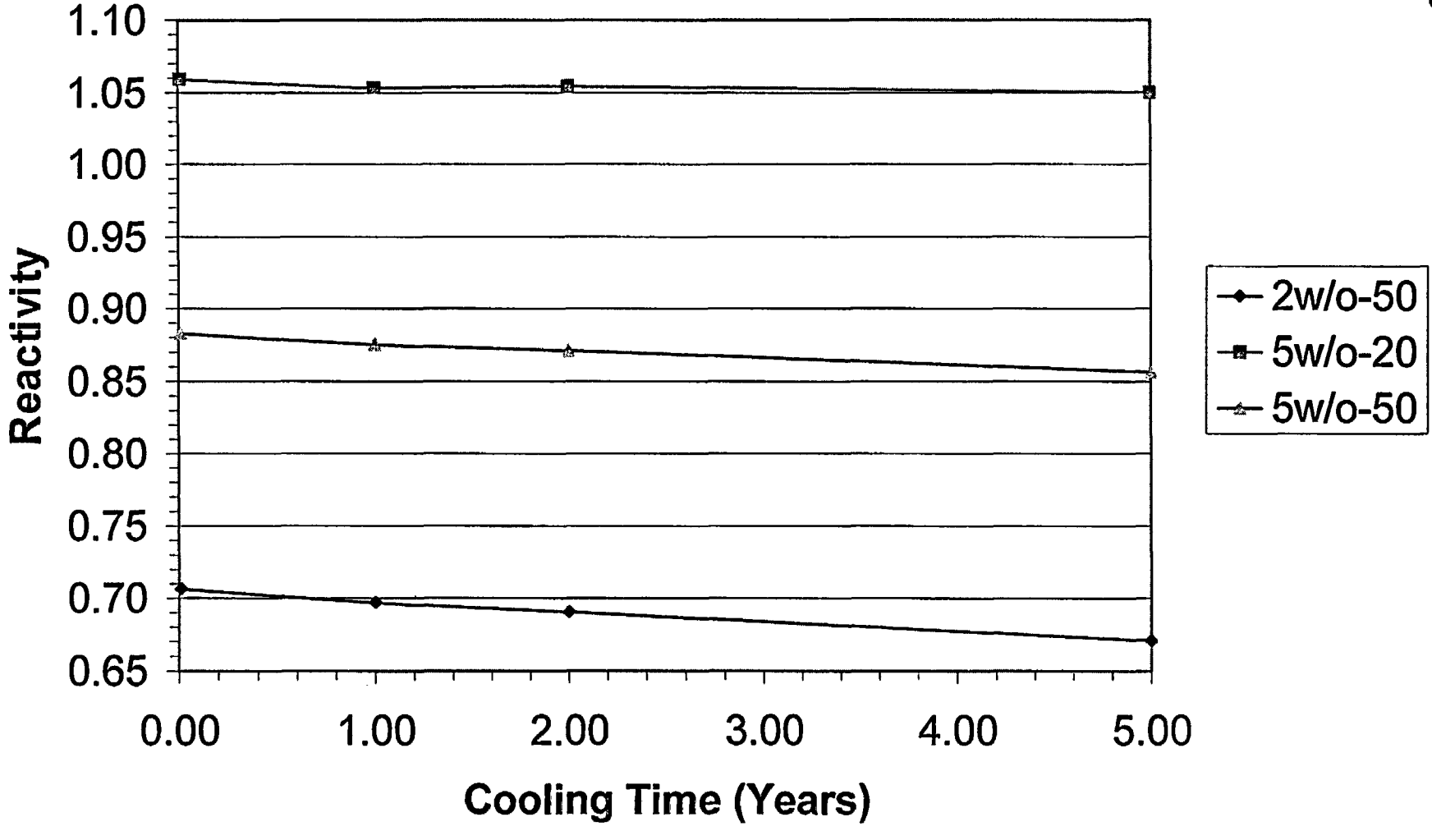

Figure 3: Reactivity vs Tfuel

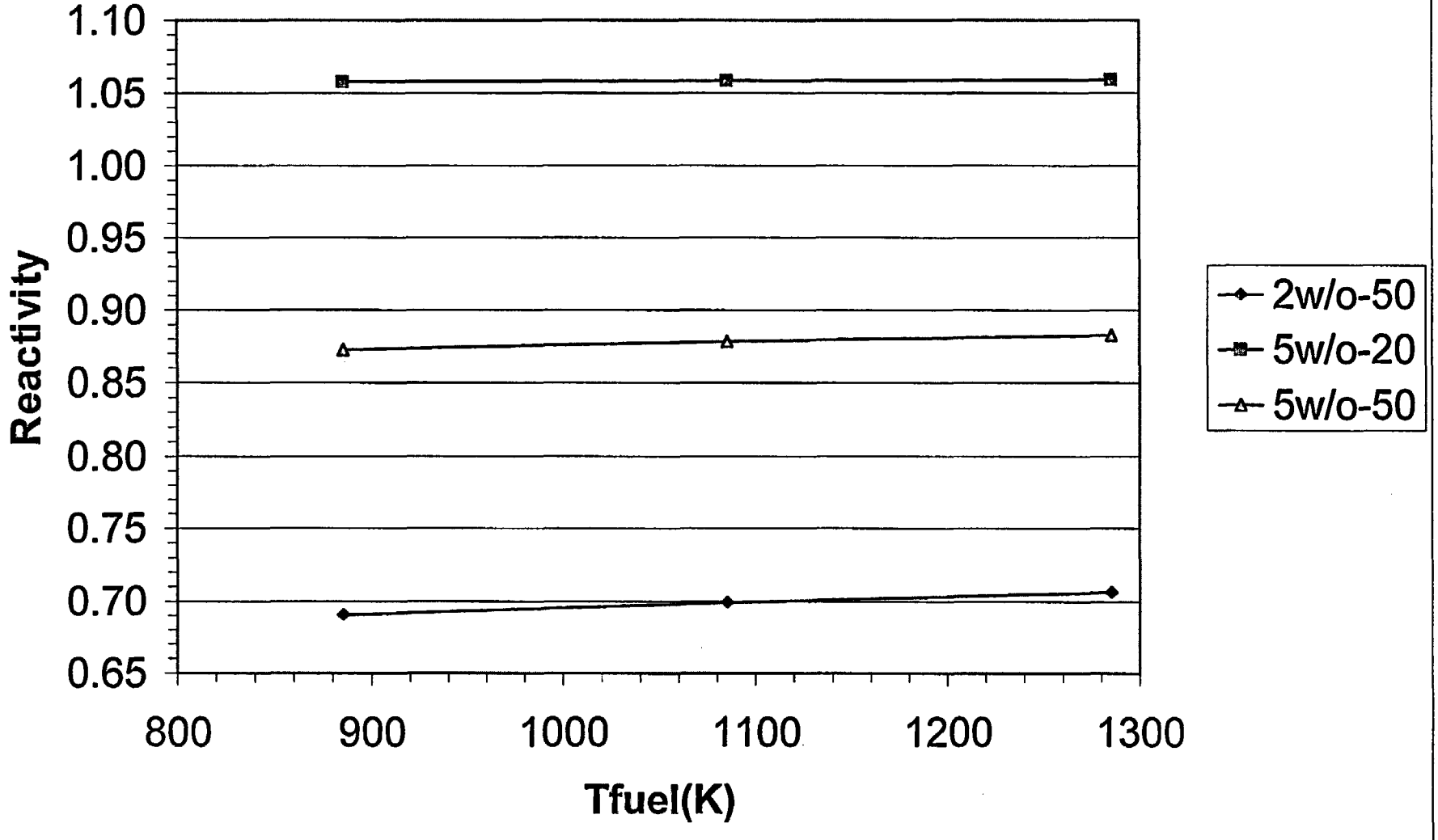

Figure 4: Reactivity vs Soluble Boron

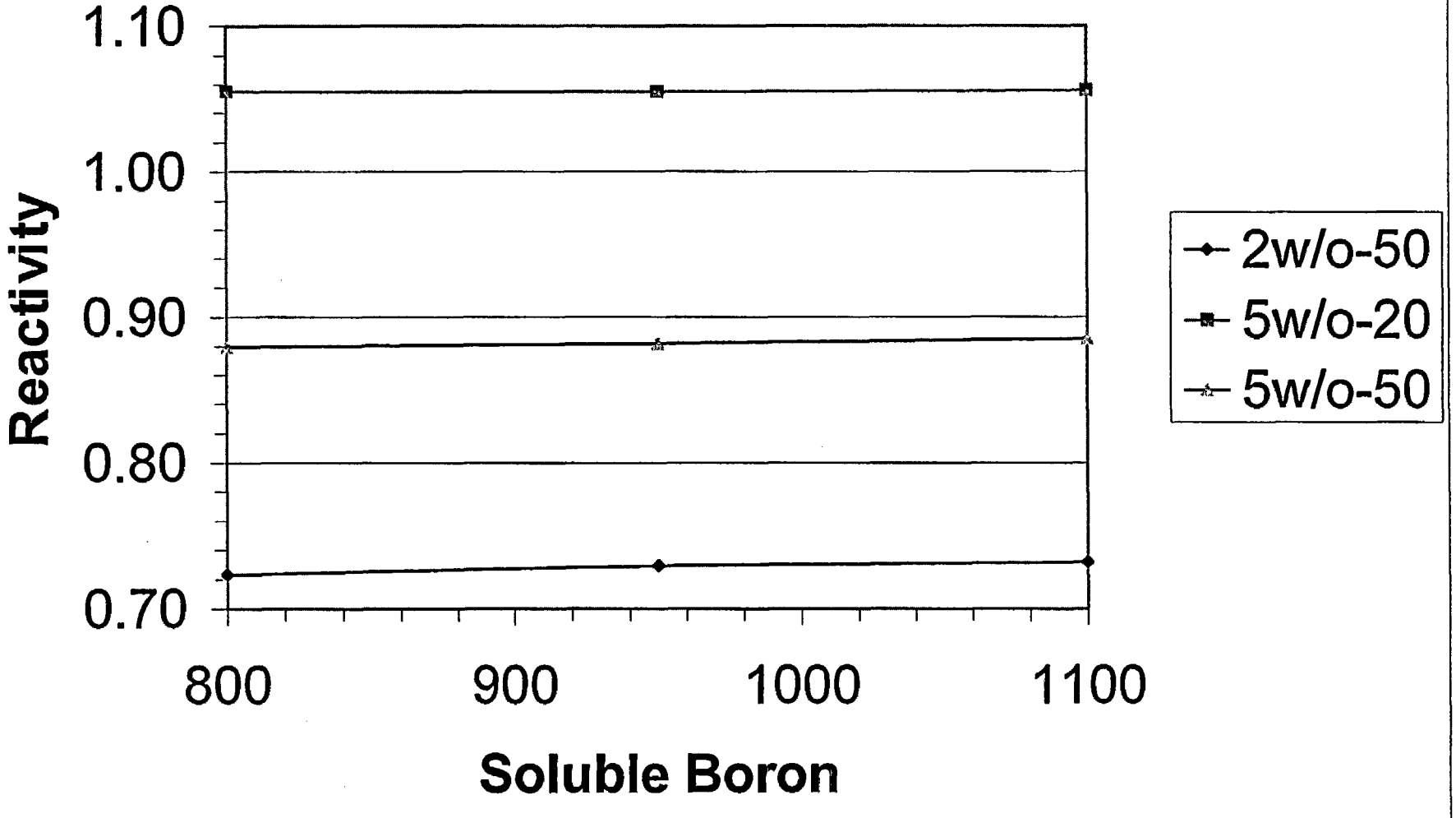

Figure 5: Reactivity vs Tmod

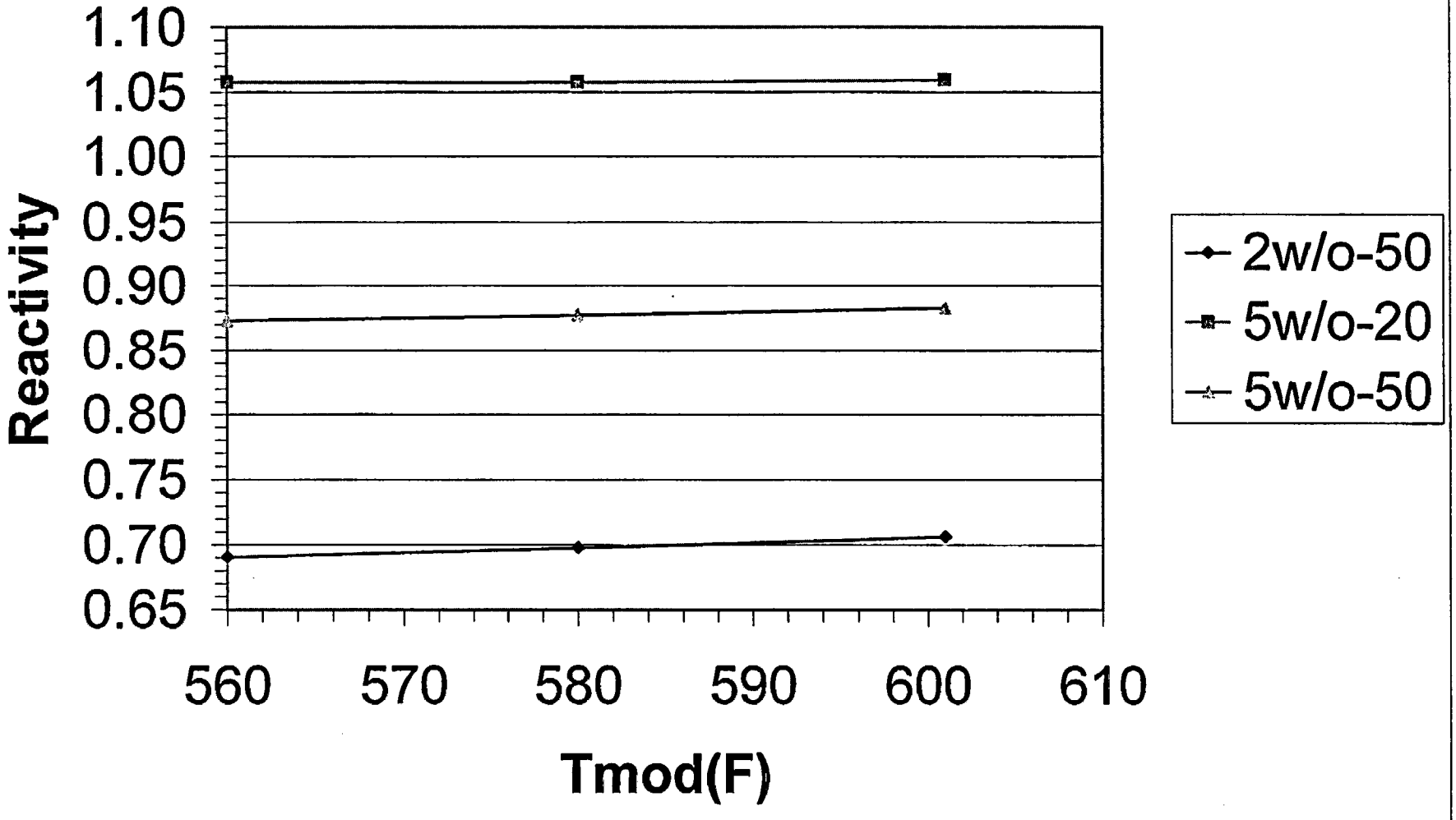

Figure 6: Reactivity vs Assm Power

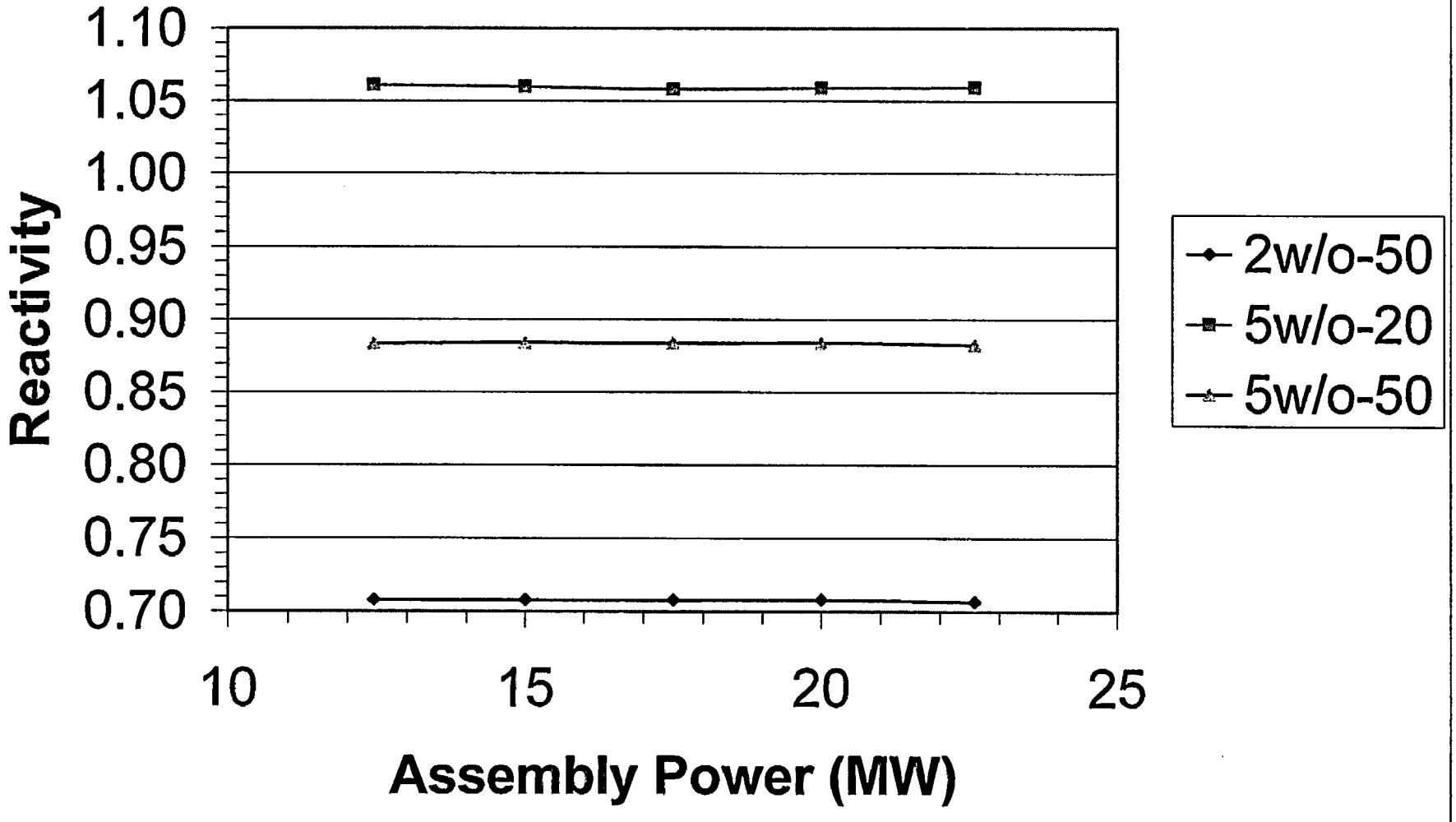

Figure 7: U2SFP K-eff vs Boron

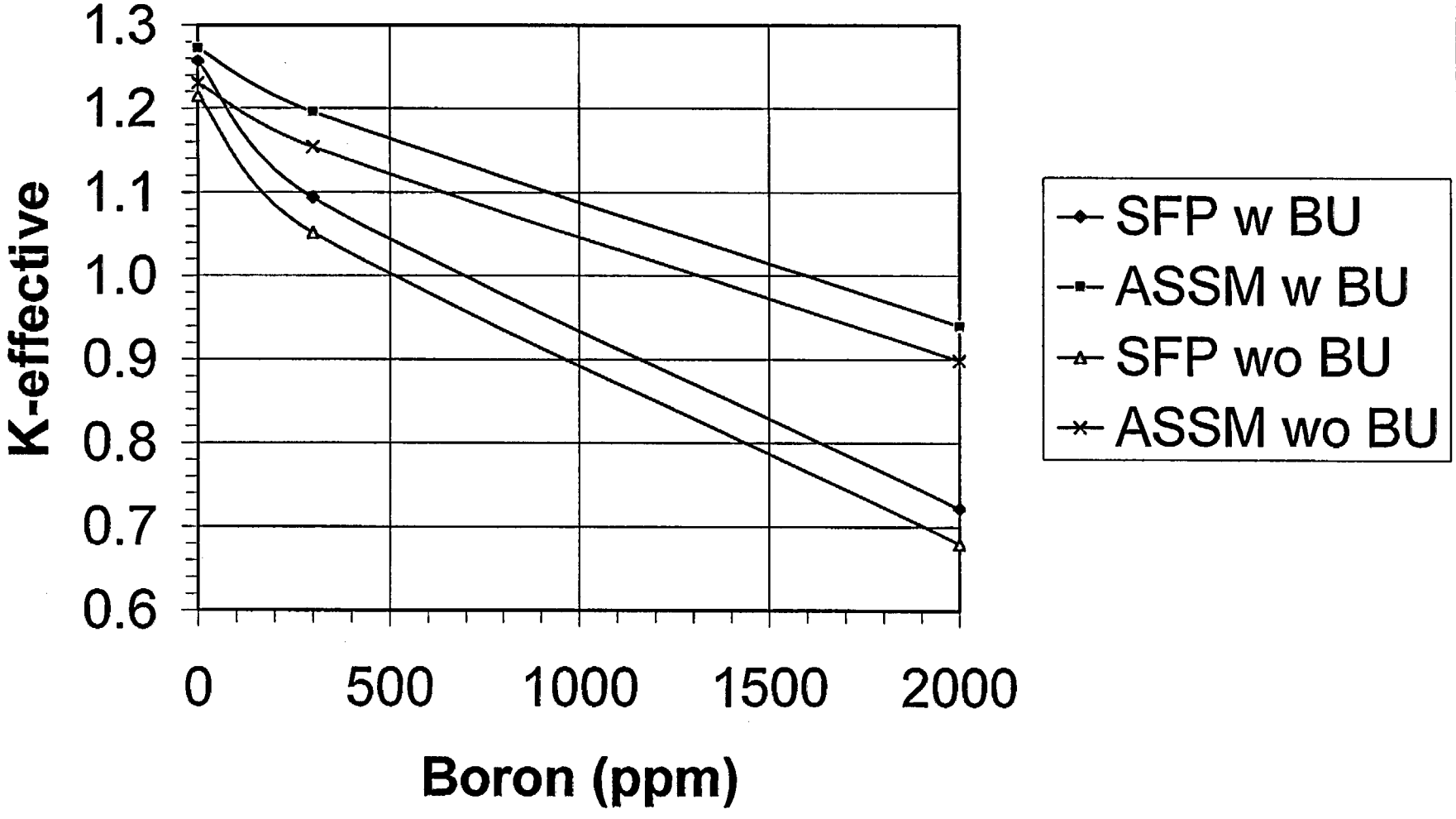

Figure 8: Enrichment vs Burnup

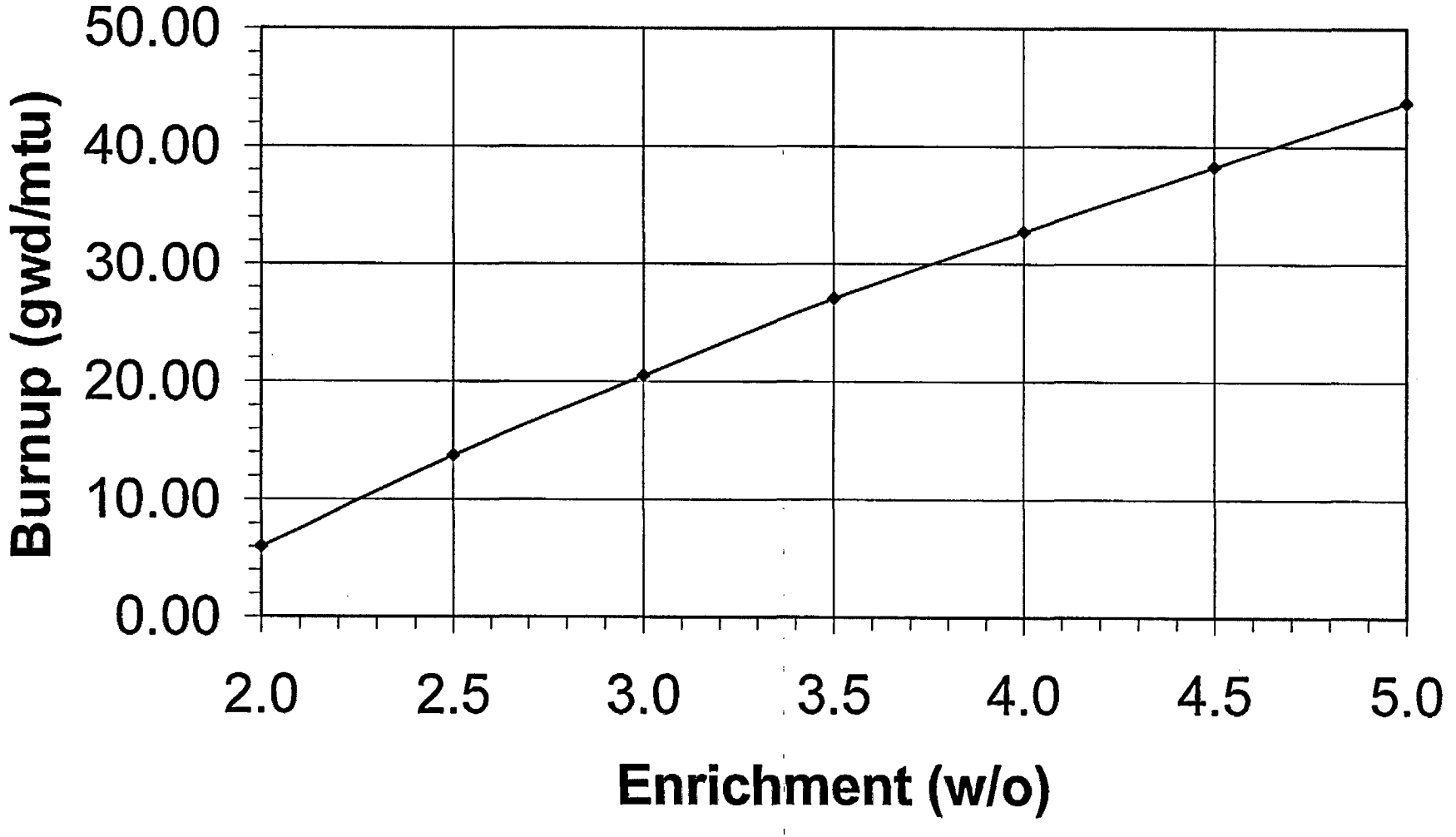

Figure 9: Isotopics Vs. Burnup

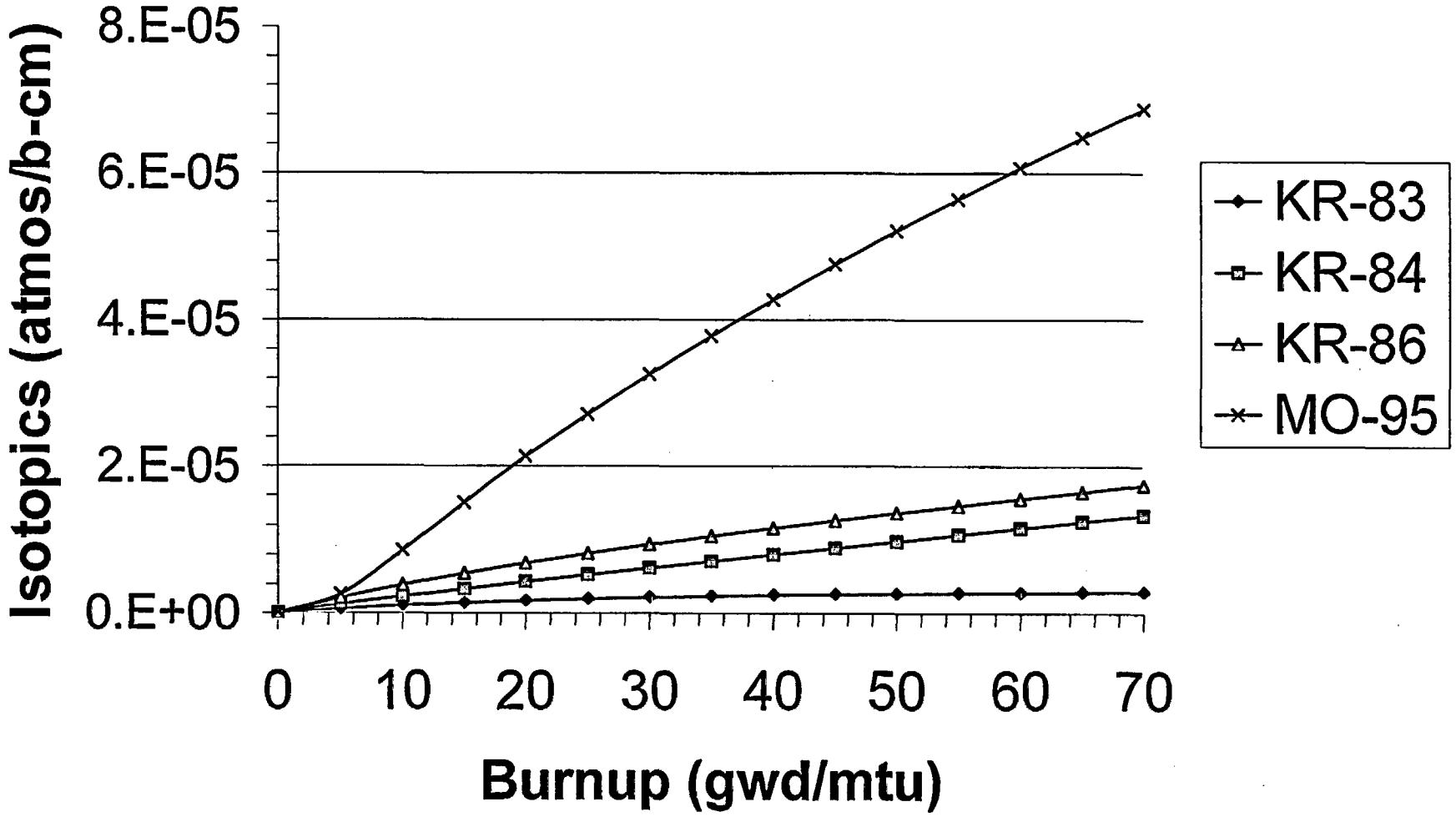

Fugure 10: Isotopics Vs Burnup

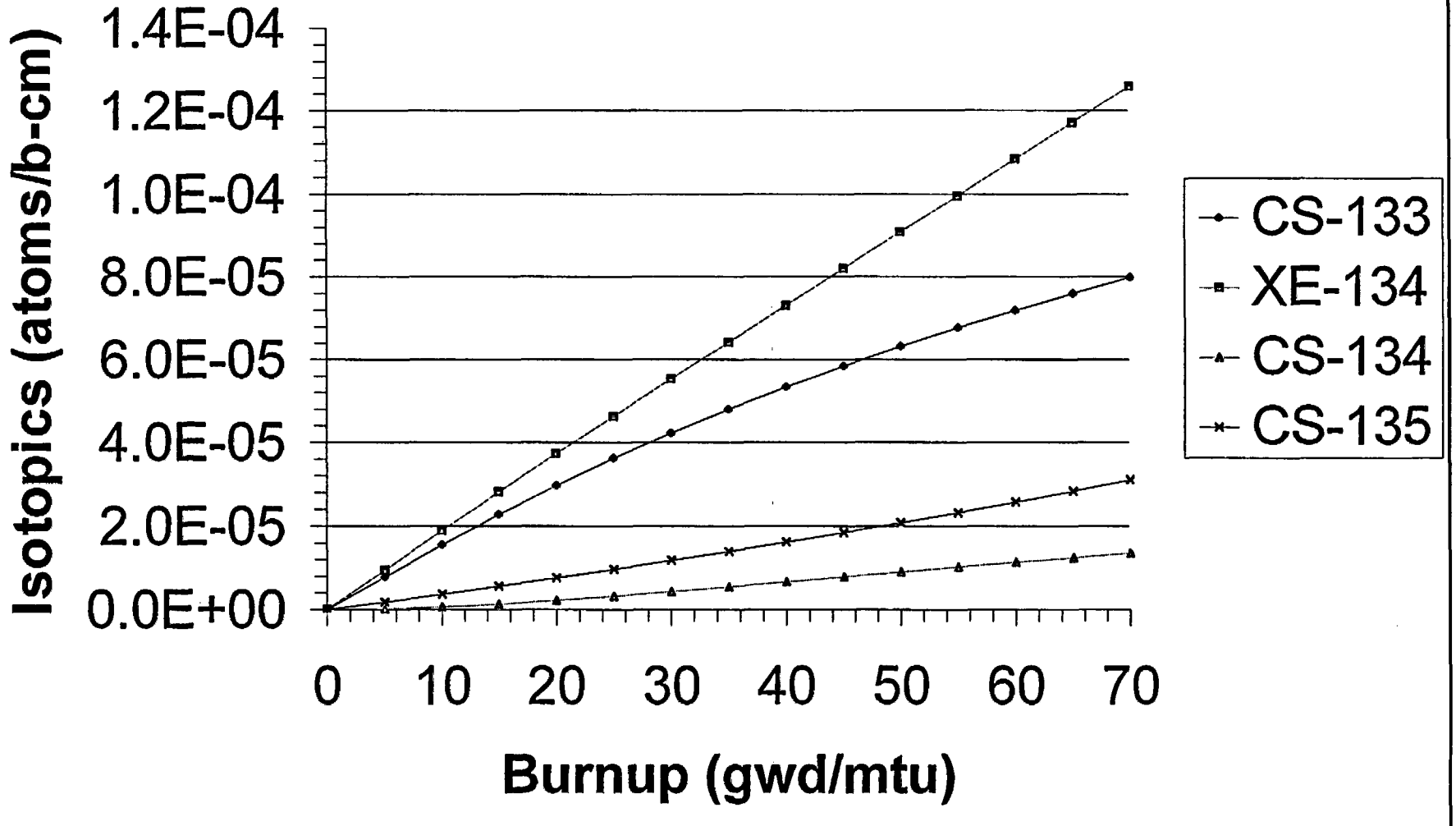

Figure 11: Isotopics Vs Burnup

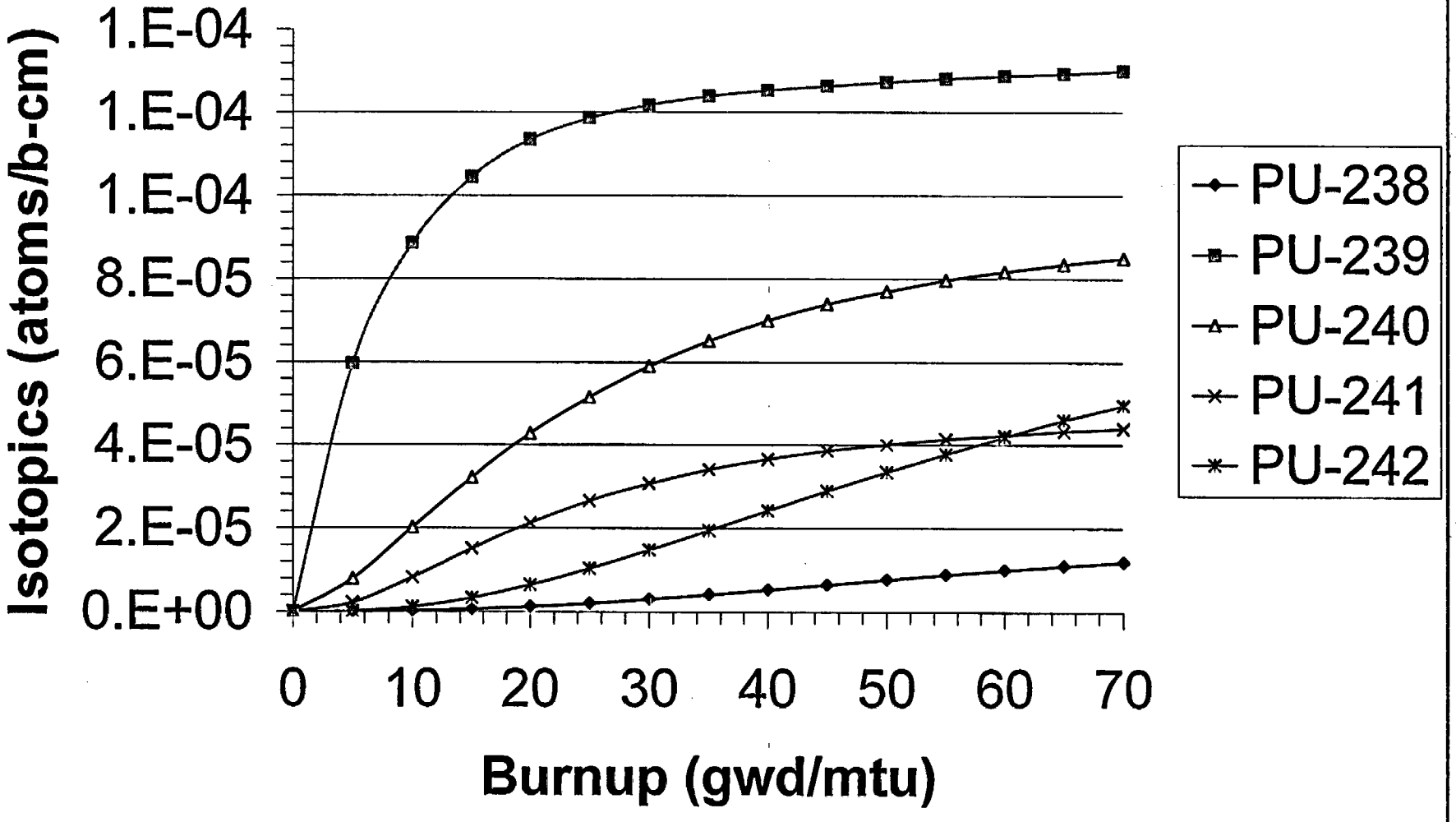

Figure 12: Reactivity vs Burnup (0 ppm)

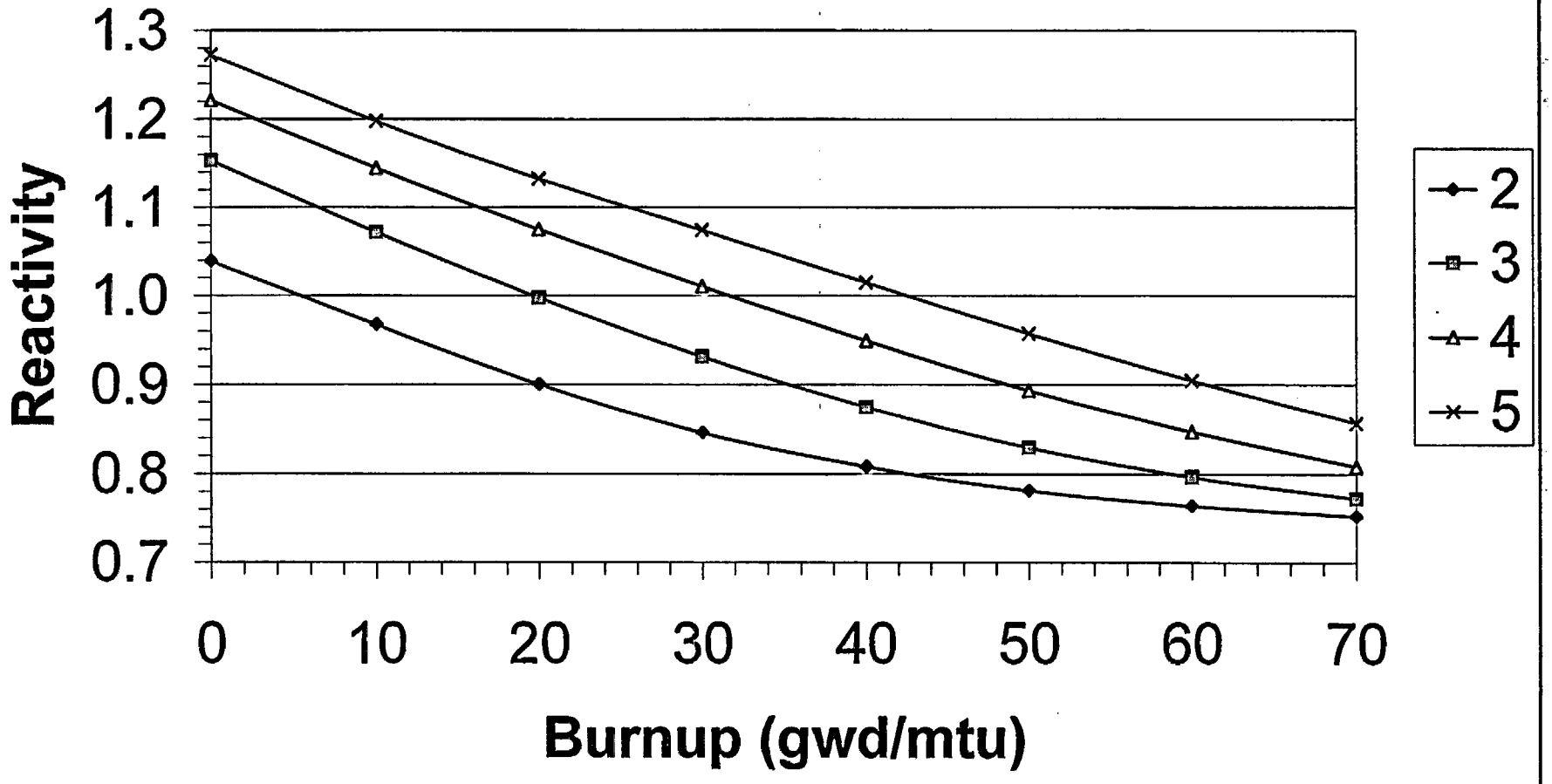

Figure 13: Reactivity vs Burnup (300 ppm)

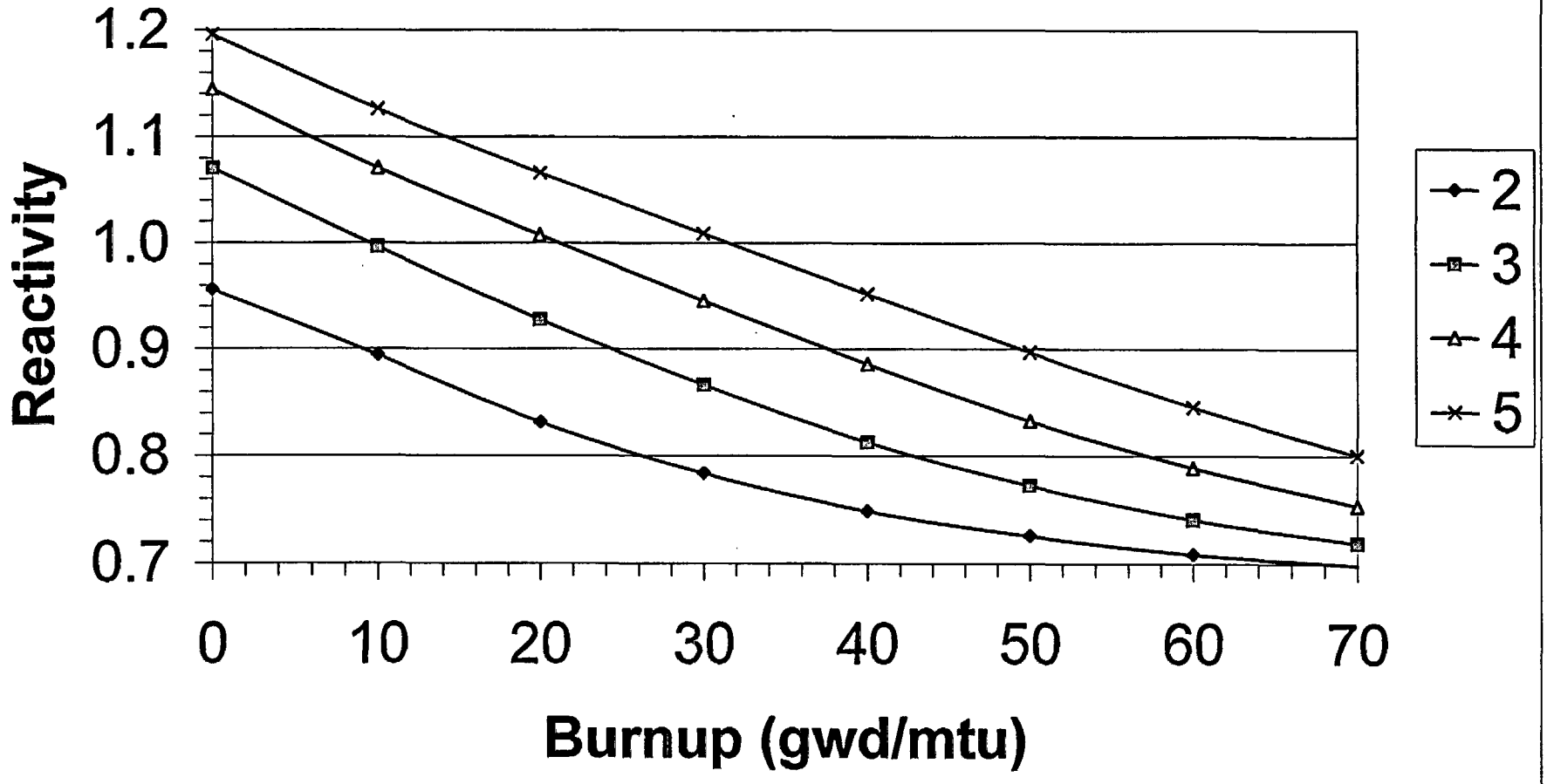

10. CALCULATIONS

A list of all of the SAS2H and KENO calculations is included in Attachment A.

11. DOCUMENTATION OF COMPUTER CODES

The source term portion of this work employs SAS2H, a functional module in the SCALE system, to calculate the burnup-dependent source terms for the CCNPP Unit 2 SFP system. Ref.9 documents the SCALE 4.4 modular code system SAS2H for computing the isotopic content of PWR spent fuel. The SAS2H control module performs the depletion/decay analysis using the well-established codes and data libraries provided in the SCALE system. Problem-dependent resonance processing of neutron cross sections is performed using the Bondarenko resonance self-shielding module BONAMI-S and the Nordheim Integral Treatment resonance self-shielding module NITAWL-II. The XSDRNPM-S module is used to produce spectral weighted and collapsed cross sections for the fuel depletion calculations. COUPLE updates the cross section constants included on an ORIGEN-S nuclear data library with data from the cell-weighted cross section library produced by XSDRNPM-S. The weighting spectrum computed by XSDRNPM is applied to update all nuclides in the ORIGEN-S library that were not specified in the XSDRNPM analysis. The point-depletion ORIGEN-S module is used to compute time-dependent concentrations and source terms for isotopes simultaneously generated and depleted through neutronic transmutation, fission, and radioactive decay. The cross section library 44GROUPNDF5 was utilized in this work. 44GROUPNDF5 is a 44-energy group library derived from the latest ENDF/B-V files with the exception of O-16, Eu-154, and Eu-155, which were taken from the more improved ENDF/B-VI files. Note that the SAS2H/ORIGEN-S libraries include 689 light elements, such as clad and structural materials, 129 actinides, including fuel nuclides and their decay and activation products, and 879 fission product nuclides.

Ref. 7 constitutes a verification that the computer codes of SCALE 4.4 have been successfully installed on the NEU computer PCB386 with the Windows NT operating system and with a PENTIUM II XEON processor. SCALE 4.4 includes the codes CSAS, SAS1, SAS2H, SAS3, SAS4, QADS, HTAS1, ARP, and CSAS6, which codes calculate nuclear criticality, source term, radiation shielding, heat transfer, and cross section processing.

SAS2H is benchmarked to the Calvert Cliffs Unit 2 Cycle 14 EQ radioactive source terms of Ref.39 and to the measured data in ORNL/TM-12667 (Ref.40). Ref.39 constitutes a safety-related source term calculation performed by Westinghouse/Combustion Engineering (W/CE). Ref.40 documents radiological assays of PWR spent fuel conducted by the Material Characteristics Center (MCC) at Pacific Northwest Laboratory (PNL) using discharged PWR fuel from Calvert Cliffs Unit 1 and H. B. Robinson Unit 2. Additional spent fuel characteristics were conducted by four research laboratories in Europe using fuel from the Obrigheim (KWO) PWR. Even though not exhaustive in scope, the validation included comparison of predicted and measured concentrations for 14 actinides and 37 fission and activation products. Ref.41 validates SAS2H for general and safety related use in calculating isotopics and thermal power. The SAS2H results with cross section file 44GROUPNDF5 agrees well with the W/CE safety-related results of Ref.39 and the ORNL/TM-12667 results of Ref.40.

Per Ref.4, acceptable computer codes for criticality applications include, but are not necessarily limited to the following: NITAWL-KENO5a.

The criticality portion of this work employs KENO.Va, a functional module in the SCALE system, and the Criticality Safety Analysis Sequence Number 25 (CSAS25) to calculate the k-effective of a three-dimensional system (Ref.9). CSAS25 uses the SCALE Material Information Process (MIP) and the associated material composition library to calculate material number densities, to prepare geometry data for resonance self-shielding, and to create data input files for the cross section processing codes, BONAMI, NITAWL-II, and XSDRNPM. BONAMI performs resonance self-shielding calculations for nuclides that have Bondarenko data associated with their cross sections. NITAWL-II applies a Nordheim resonance self-shielding correction to nuclides having resonance parameters.

XSDRNPM provides cell-weighted cross sections based on the specified unit cell and can calculate k-effective for a one-dimensional system. The CSAS25 sequence then invokes the KENO-Va Monte Carlo criticality code.

The SCALE 4.4 CSAS module with the 44 group ENDF/B-V cross section library for criticality safety evaluations of LWR fuel in spent fuel rack, in-core, and cask type environments is validated in Ref.8 via comparison of the computational CSAS outputs with the 180 criticality experiments documented in Ref.12. The validation is performed in compliance with the standards of ANSI/ANS-8.1 (Ref.10) and ANSI/ANS-8.17 (Ref.11). ANSI/ANS-8.1 requires that a validation be performed on the method used to calculate criticality safety margins. The validation shall be documented in a written report describing the method, computer program, and cross section libraries used, the experimental data, the areas of applicability, the uncertainties and biases, and the margins of safety. ANSI/ANS-8.17 prescribes the criteria to establish sub-criticality safety margins.

Additional input calculations and result compilations were performed manually in the Excel spreadsheet X2inp.xls.

12. RESULTS

(12.A) Biases and Uncertainties

Worst case values of moderator temperature, clad composition, soluble boron concentration, and fixed poison loading were assumed in all reactivity calculations. The bias and uncertainty determinations were detailed in Section 9 and are summarized in Attachment 2. Note that most of the uncertainties and biases were determined at three state points: zero soluble boron and zero burnup, 300 ppm soluble boron and zero burnup, and 300 ppm soluble boron and 40 gwd/mtu average burnup. The calculational methodology and axial burnup distribution biases and uncertainties were independent of soluble boron concentration and average burnup and were bounding for all cases, while the fuel depletion uncertainty was a function of soluble boron only. The composite bias and uncertainty values as a function of state point were determined. The worst case composite bias and uncertainty value was 0.06129 ΔK for zero soluble boron and zero burnup. This value was conservatively applied to all calculated reactivity values.

(12.B) Accident Conditions

The accident determinations were also detailed in Section 9 and pose no reactivity challenge.

(12.C) Enrichment vs Burnup Loading Limits

Multiple cases were executed to determine reactivity as a function of burnup, enrichment, and soluble boron concentration. The results are summarized in Figures 12 and 13 and in the following table:

KENO Case	SAS2H Files	Enr w/o	Burnup gwd/t	Tmod K	Boron ppm	Mode	Biased K-eff
K200580D1	S20058	2.0	5.80	341.48	0	Single Assembly	0.99767
K251340D1	S25134	2.5	13.40	341.48	0	Single Assembly	0.99793
K302000D1	S320	3.0	20.00	341.48	0	Single Assembly	0.99720
K352630D1	S35263	3.5	26.30	341.48	0	Single Assembly	0.99648
K403200D1	S40320	4.0	32.00	341.48	0	Single Assembly	0.99665
K453750D1	S45375	4.5	37.50	*341.48*	*0*	Single Assembly	0.99750
K504300D1	S50430	5.0	43.00	341.48	0	Single Assembly	0.99728
K200580D2	S20058	2.0	5.80	341.48	300	Single Assembly	0.92157
K251340D2	S25134	2.5	13.40	341.48	300	Single Assembly	0.92623
K302000D2	S320	3.0	20.00	341.48	300	Single Assembly	0.92744
K352630D2	S35263	3.5	26.30	341.48	300	Single Assembly	0.92913
K403200D2	S40320	4.0	32.00	341.48	300	Single Assembly	0.93231
K453750D2	S45375	4.5	37.50	341.48	300	Single Assembly	0.93384
K504300D2	S50430	5.0	43.00	341.48	300	Single Assembly	0.93516

Note that at zero soluble boron, all of the reactivity values are less than 0.998, while at 300 ppm soluble boron, all of the reactivity values are less than 0.95. This is in accordance with 10 CFR 50.68 (Ref.2), if credit is taken for soluble boron, the k-effective of the spent fuel storage racks loaded with fuel of the maximum fuel assembly reactivity must not exceed 0.95, at a 95% probability, 95% confidence level, if flooded with borated water, and the k-effective must remain below 1.0 (subcritical) at a 95% probability, 95% confidence level, if flooded with unborated water. The above burnup values must be increased by the measured burnup uncertainty. The uncertainty in measured burnup was extracted from Ref. 61 for ABB/CE fuel assemblies. For burnups less then 30 gwd/mtu, the burnup must be increased by 2.5%. For burnups in excess of 30 gwd/mtu, the burnup must be increased by 750 mwd/mtu. The burnups required to store fuel

in the Unit 2 SFP crediting 350 ppm of soluble boron including all biases and uncertainties are detailed in the following table and in Figure 8.

Enrichment (w/o)	Burnup (GWD/MTU)
2.0	6.00
2.5	13.75
3.0	20.50
3.5	27.00
4.0	32.75
4.5	38.25
5.0	43.75

(12.D) Comparison of Two-Dimensional to Three-Dimensional Models

To estimate the conservatism of utilizing an infinite two-dimensional assembly array with worst-case biases and uncertainties, the reactivity of the SFP as a function of soluble boron concentration was determined for the actual three-dimensional SFP configuration versus an infinite two-dimensional assembly array with the worst-case bias and uncertainty including burnup related biases and uncertainties and nominal bias and uncertainty excluding burnup related bias and uncertainty. The results are detailed in the following table and in Figure 7.

KENO Case	Enr w/o	Burnup gwd/t	Tmod K	Boron ppm	Mode	Biased K-eff
K500000D1	5.0	0.00	341.48	0	Single Assembly / Worst-Case Bias	1.27241
K500000D2	5.0	0.00	341.48	300	Single Assembly / Worst-Case Bias	1.19573
K500000D4	5.0	0.00	341.48	1930	Single Assembly / Worst-Case Bias	0.94694
K500000D3	5.0	0.00	341.48	2000	Single Assembly / Worst-Case Bias	0.94036
K500000D1	5.0	0.00	341.48	0	Single Assembly / Nominal Bias	1.23056
K500000D2	5.0	0.00	*341.48*	*300*	Single Assembly / Nominal Bias	1.15388
K500000D6	5.0	0.00	341.48	1590	Single Assembly / Nominal Bias	0.94353
K500000D3	5.0	0.00	341.48	2000	Single Assembly / Nominal Bias	0.89851
KU2SFPA	5.0	0.00	341.48	0	Unit 2 SFP / Worst-Case Bias	1.25677
KU2SFPB	5.0	0.00	341.48	300	Unit 2 SFP / Worst-Case Bias	1.09386
KU2SFPF	5.0	0.00	341.48	730	Unit 2 SFP / Worst-Case Bias	0.94672
KU2SFPC	5.0	0.00	341.48	2000	Unit 2 SFP / Worst-Case Bias	0.72165
KU2SFPA	5.0	0.00	341.48	0	Unit 2 SFP / Nominal Bias	1.21492
KU2SFPB	5.0	0.00	341.48	300	Unit 2 SFP / Nominal Bias	1.05201
KU2SFPJ	5.0	0.00	341.48	590	Unit 2 SFP / Nominal Bias	0.94597
KU2SFPC	5.0	0.00	341.48	2000	Unit 2 SFP / Nominal Bias	0.67980

Note that the conservatism in reactivity for a two-dimensional infinite array versus a three-dimensional Unit 2 specific model increases from 1.56% Δk at 0 ppm, to 10.18% Δk at 300 ppm, to 21.87% Δk at 2000 ppm. In addition, for the zero burnup cases, an additional reactivity conservatism of 4.185% Δk exists. Thus for the three-dimensional Unit 2 specific model, an entire SFP of 5.0 w/o fresh fuel becomes subcritical (k-effective < 1) for soluble boron concentrations in excess of 500 ppm assuming no credit for boraflex in the Unit 2 SFP racks. For the two-dimensional infinite array model, ~1600 ppm would be required to maintain subcriticality.

(12.E) Configuration Control

Three checkerboard patterns were modeled in an effort to store more reactive fuel in the Unit 2 SFP.

Pattern 1

```
x   x   x   x
  x   x   x
x   x   x   x
  x   x   x
x   x   x   x
```

Pattern 2:

```
x x x x x x x x x x x
x   x   x   x   x   x
x x x x x x x x x x x
x   x   x   x   x   x
x x x x x x x x x x x
```

Pattern 3:

```
a b a b a b a
b a b a b a b
a b a b a b a
```

The results are detailed in the following table:

Case	w/o	gwd/t	K	ppm		K-eff
KU2CONA	5	0	341.48	0	Pattern 1	0.95666
KU2CONB	5	0	341.48	300	Pattern 1	0.84793
KU2CONC	5	0	341.48	0	Pattern 2	1.15017
KU2COND1	5	20	341.48	0	Pattern 3: a=fresh, b=burned	1.19211
KU2COND2	5	40	341.48	0	Pattern 3: a=fresh, b=burned	1.14593
KU2COND3	5	60	*341.48*	0	Pattern 3: a=fresh, b=burned	1.10819
KU2CONE1	4	20	341.48	0	Pattern 3: a=fresh, b=burned	1.14127
KU2CONE2	4	40	341.48	0	Pattern 3: a=fresh, b=burned	1.09295
KU2CONE3	4	60	341.48	0	Pattern 3: a=fresh, b=burned	1.05891

Note that only pattern 1 meets the requirements of 10 CFR 50.68 (Ref.2). If credit is taken for soluble boron, the k-effective of the spent fuel storage racks loaded with fuel of the maximum fuel assembly reactivity must not exceed 0.95, at a 95% probability, 95% confidence level, if flooded with borated water, and the k-effective must remain below 1.0 (subcritical) at a 95% probability, 95% confidence level, if flooded with unborated water. Thus to store any fuel with insufficient burnup to satisfy reactivity requirements, that fuel assembly must be surrounded on all four adjacent faces by empty rack cells or other nonreactive materials (e.g., wall, water,...).

(12.F) Reconstitution and Inspection

A finite radial and axial model of the Unit 2 SFP of nominal dimensions containing the maximum enrichment of 5.0 w/o VAP fuel at a soluble boron concentration of 0, 300, and 2000 ppm was modeled with sequential assemblies in the row closest to the SFP wall on spacers to simulate the reconstitution/inspection process. There is no reactivity difference between reconstituting an entire row of assemblies or normal storage of said assemblies. Since Boraflex is not credited in this analysis, placing assemblies on spacers has no reactivity effect.

KENO Case	Enr w/o	Burnup gwd/t	Tmod K	Boron ppm	Mode	Biased K-eff
KU2SFPA	5.0	0.00	341.48	0	Unit 2 SFP / No Reconstitution	1.25677
KU2SFPB	5.0	0.00	341.48	300	Unit 2 SFP / No Reconstitution	1.09386
KU2SFPC	5.0	0.00	341.48	2000	Unit 2 SFP / No Reconstitution	0.72165
KU2SFPAR	5.0	0.00	341.48	0	Unit 2 SFP / Reconstitution	1.25400
KU2SFPBR	5.0	0.00	341.48	300	Unit 2 SFP / Reconstitution	1.09365
KU2SFPCR	5.0	0.00	*341.48*	*2000*	Unit 2 SFP / Reconstitution	0.72347

(12.G) Additional Margin Provided by Inclusion of Additional Isotopes

While only the 50 isotopes for which benchmark data existed were included in the burnup credit calculations, there is no valid reason to exclude additional fission product isotopes. Reactivity calculations were performed to include 101 isotopes, and the additional margin that would be generated by this inclusion was calculated as a function of enrichment and burnup.

Enrichment	Boron	Burnup	50 Isotopes	101 Isotopes	
w/o	ppm	gwd/mtu	K-effective	K-effective	Delta K-effective
5	0	10	1.13638	1.12996	-0.00642
5	0	20	1.07119	1.06249	-0.00870
5	0	30	1.01281	1.00313	-0.00968
5	0	40	0.95358	0.94032	-0.01326
5	0	50	0.89641	0.88183	-0.01458
5	0	60	0.84339	0.82754	-0.01585
5	0	70	0.79503	0.78126	-0.01377
4	0	10	1.08330	1.07849	-0.00481
4	0	20	1.01347	1.00744	-0.00603
4	0	30	0.94894	0.93814	-0.01080
4	0	40	0.88840	0.87704	-0.01136
4	0	50	0.83200	0.81838	-0.01362
4	0	60	0.78548	0.77035	-0.01513
4	0	70	0.74660	0.73326	-0.01334
3	0	10	1.01050	1.00342	-0.00708
3	0	20	0.93591	0.92802	-0.00789
3	0	30	0.87020	0.86187	-0.00833
3	0	40	0.81338	0.80172	-0.01166
3	0	50	0.76783	0.75627	-0.01156
3	0	60	0.73518	0.72120	-0.01398
3	0	70	0.71073	0.69729	-0.01344
2	0	10	0.90578	0.90008	-0.00570
2	0	20	0.83855	0.83024	-0.00831
2	0	30	0.78440	0.77555	-0.00885
2	0	40	0.74665	0.73641	-0.01024
2	0	50	0.71990	0.70752	-0.01238
2	0	60	0.70267	0.69013	-0.01254
2	0	70	0.69082	0.67796	-0.01286

Note that the additional margin provided by the expanded list of isotopes generally increases as a function of burnup and enrichment, exceeding 1.5% Δk for high enrichments (4-5 w/o) and high burnup (60 gwd/mtu) fuel.

13. CONCLUSIONS

The purpose of this report is to document the Calvert Cliffs Nuclear Power Plant (CCNPP) Spent Fuel Pool (SFP) Rack Criticality Methodology that ensures that the spent fuel rack multiplication factor, k-eff, is less than the 10 CFR 50.68 (Ref.2) regulatory limit with Value Added Pellet (VAP) fuel ranging in enrichment from 2.0 to 5.0 w/o with burnup credit and with partial credit for soluble boron in the Unit 2 SFP. The soluble boron credit will be limited to 300 ppm per the restrictions of the Unit 1 criticality analysis in Ref.43. Note that 300 ppm is a minimum boron concentration requirement. 15% should be added to this value to account for all uncertainties. Thus a boron level of 350 ppm with uncertainties is required to credit soluble boron in the SFP.

The burnups required to store fuel in the Unit 2 SFP crediting 350 ppm of soluble boron including all biases and uncertainties are the following:

Enrichment (w/o)	Burnup (GWD/MTU)
2.0	6.00
2.5	13.75
3.0	20.50
3.5	27.00
4.0	32.75
4.5	38.25
5.0	43.75

A graphical representation of the above is presented in Figure 8, while a second-order regression analysis is listed in Attachment S. Note that these minimum burnup values are less than those reported in Ref.42 Thus, all assemblies currently qualified to be stored in the Unit 2 Spent Fuel Pool may continue to be safely stored in the Unit 2 Spent Fuel Pool. In addition, each assembly offloaded from either reactor or from an ISFSI DSC must be evaluated against the above burnup restrictions to determine if it can be safely stored in the Unit 2 SFP. No similar restrictions exist on the Unit 1 SFP.

A finite radial and axial model of the Unit 2 SFP of nominal dimensions containing the maximum enrichment of 5.0 w/o VAP fuel at a soluble boron concentration of 0, 300, and 2000 ppm was modeled with sequential assemblies in the row closest to the SFP wall on spacers to simulate the reconstitution/inspection process. There is no reactivity difference between reconstituting an entire row of assemblies or normal storage of said assemblies. Since Boraflex is not credited in this analysis, placing assemblies on spacers has no reactivity effect.

Dropping an assembly of 5.0 w/o VAP fuel onto the SFP racks was analyzed, even though it is not a credible accident. Per Ref.4, the double contingency principle was applied. It required two unlikely, independent, concurrent events to produce a criticality accident. The double contingency principle means that realistic conditions may be assumed. For example, if soluble boron is normally present in the SFP water, the loss of soluble boron is considered as one accident condition and a second concurrent accident need not be assumed. Therefore, total credit for the presence of soluble boron may be assumed in evaluating this accident condition. Per Technical Assumption 7.H, the normal SFP boron concentration is conservatively assumed to be 2000 ppm. A finite radial and axial configuration of the Unit 2 SFP of nominal dimensions containing the maximum enrichment of 5.0 w/o fuel was modeled as a function of soluble boron concentration (0, 300, 2000 ppm) for the dropped assembly accident with and without reconstitution. The dropped assembly is effectively decoupled from the assemblies stored in the SFP storage racks as was previously noted in Ref.32. Taking credit for 2000 ppm per the double

contingency principle drops the k-effective value to well below the regulatory requirement for all cases.

Several checkerboard patterns were modeled in an effort to store more reactive fuel in the Unit 2 SFP. Note that only one pattern meets the requirements of 10 CFR 50.68 (Ref.2). If credit is taken for soluble boron, the k-effective of the spent fuel storage racks loaded with fuel of the maximum fuel assembly reactivity must not exceed 0.95, at a 95% probability, 95% confidence level, if flooded with borated water, and the k-effective must remain below 1.0 (subcritical) at a 95% probability, 95% confidence level, if flooded with unborated water. Thus to store any fuel with insufficient burnup to satisfy reactivity requirements, that fuel assembly must be surrounded on all four adjacent faces by empty rack cells or other nonreactive materials (e.g., wall, water,...).

The above results include the following conservatisms:

(01) SAS2H isotopics were modeled with conservative fuel temperature, moderator temperature, soluble boron concentration, specific power, and refueling downtime inputs. For 5 w/o fuel at 50 GWD/MTU, the conservatism was in excess of 0.4% Δk for Tfuel, 0.5% Δk for Tmod, and 2.6% Δk for cooling time (100 hours vs 5 years). The conservatisms were higher for lower enrichments but lower for lower burnups.

(02) Integral burnable absorbers, boraflex poison sheets, and control element assemblies were conservatively neglected in this work.

(03) A reactivity uncertainty due to uncertainty in the fuel depletion calculation should be developed and combined with other calculational uncertainties. An uncertainty equal to 5% of the reactivity decrement to the burnup of interest is an acceptable assumption. Based on computations presented in this work, a worst case uncertainty value of 0.02089 was used in all burnup related reactivity calculations, even though SAS2H generated reactivity was determined to be 0.358% more reactive than those adjusted to radiochemical assay isotopics.

(04) For conservatism, an axial burnup bias of 3.3% Δk was utilized for all burnup cases. The most conservative Calvert Cliffs specific reactivity bias was calculated to be -0.579% Δk. Thus for Calvert Cliffs specific fuel, use of 26-node axial burnup profiles is less conservative than uniform axial burnups

(05) Inclusion of additional isotopes in the SAS2H and KENO executions can add significantly more margin to the reactivity results. While no benchmarks exist for these additional isotopes, comparison of existing benchmark cases to SAS2H/KENO computations indicates that the computation results are conservative. Note that the additional margin provided by an expanded list of isotopes (101 vs 50) generally increases as a function of burnup and enrichment, exceeding 1.5% Δk for high enrichments (4-5 w/o) and high burnup (60 gwd/mtu) fuel.

(06) The worst case composite bias and uncertainty value was 0.06129 ΔK for zero soluble boron and zero burnup. This value was conservatively applied to all calculated reactivity values.

(07) The conservatism in reactivity for a two-dimensional infinite array versus a three-dimensional Unit 2 specific model increases from 1.56% Δk at 0 ppm, to 10.18% Δk at 300 ppm, to 21.87% Δk at 2000 ppm. In addition, for the zero burnup cases, an additional reactivity conservatism of 4.185% Δk exists. Thus for the three-dimensional Unit 2 specific model, an entire SFP of 5.0 w/o fresh fuel becomes subcritical (k-effective < 1) for soluble boron concentrations in excess of 500 ppm assuming no credit for boraflex in the Unit 2 SFP racks and no credit for burnup. For the two-dimensional infinite array model, ~1600 ppm would be required to maintain subcriticality under the same conditions.

ATTACHMENT A
CALCULATION LIST

KENO Reactivity Results														
KENO Case	SAS2H Case	Enr w/o	Burnup gwd/t	Tmod K	SHD	Pitch in	Steel cm	Clad	Boron ppm	Planar Geom Notes	Axial	Unbiased K-eff	Delta K-eff	Biased K-eff
SAS2H Cooling Time														
K205000AA	S250A	2.0	50	277.15	0.945	10.09375	0.1524	zirlo	0	Single assembly - 100 days decay	Infinite	0.70641	0.00075	
K205000AB	S250B	2.0	50	277.15	0.945	10.09375	0.1524	zirlo	0	Single assembly - 1 year decay	Infinite	0.69684	0.00059	
K205000AC	S250C	2.0	50	277.15	0.945	10.09375	0.1524	zirlo	0	Single assembly - 2 year decay	Infinite	0.69026	0.00068	
K205000AD	S250D	2.0	50	277.15	0.945	10.09375	0.1524	zirlo	0	Single assembly - 5 year decay	Infinite	0.67068	0.00065	
K502000AA	S520A	5.0	20	277.15	0.945	10.09375	0.1524	zirlo	0	Single assembly - 100 days decay	Infinite	1.05935	0.00083	
K502000AB	S520B	5.0	20	277.15	0.945	10.09375	0.1524	zirlo	0	Single assembly - 1 year decay	Infinite	1.05345	0.00080	
K502000AC	S520C	5.0	20	277.15	0.945	10.09375	0.1524	zirlo	0	Single assembly - 2 year decay	Infinite	1.05450	0.00079	
K502000AD	S520D	5.0	20	277.15	0.945	10.09375	0.1524	zirlo	0	Single assembly - 5 year decay	Infinite	1.05015	0.00095	
K505000AA	S550A	5.0	50	277.15	0.945	10.09375	0.1524	zirlo	0	Single assembly - 100 days decay	Infinite	0.88271	0.00077	
K505000AB	S550B	5.0	50	277.15	0.945	10.09375	0.1524	zirlo	0	Single assembly - 1 year decay	Infinite	0.87514	0.00077	
K505000AC	S550C	5.0	50	277.15	0.945	10.09375	0.1524	zirlo	0	Single assembly - 2 year decay	Infinite	0.87105	0.00083	
K505000AD	S550D	5.0	50	277.15	0.945	10.09375	0.1524	zirlo	0	Single assembly - 5 year decay	Infinite	0.85665	0.00071	
SAS2H Tfuel														
K205000AA	S250A	2.0	50	277.15	0.945	10.09375	0.1524	zirlo	0	Single assembly - Tfuel=1285.42K	Infinite	0.70641	0.00075	
K205000AE	S250E	2.0	50	277.15	0.945	10.09375	0.1524	zirlo	0	Single assembly - Tfuel=1085.42K	Infinite	0.69927	0.00065	
K205000AF	S250F	2.0	50	277.15	0.945	10.09375	0.1524	zirlo	0	Single assembly - Tfuel=885.42K	Infinite	0.69036	0.00064	
K502000AA	S520A	5.0	20	277.15	0.945	10.09375	0.1524	zirlo	0	Single assembly - Tfuel=1285.42K	Infinite	1.05935	0.00083	
K502000AE	S520E	5.0	20	277.15	0.945	10.09375	0.1524	zirlo	0	Single assembly - Tfuel=1085.42K	Infinite	1.05864	0.00083	
K502000AF	S520F	5.0	20	277.15	0.945	10.09375	0.1524	zirlo	0	Single assembly - Tfuel=885.42K	Infinite	1.05793	0.00083	
K505000AA	S550A	5.0	50	277.15	0.945	10.09375	0.1524	zirlo	0	Single assembly - Tfuel=1285.42K	Infinite	0.88271	0.00077	
K505000AE	S550E	5.0	50	277.15	0.945	10.09375	0.1524	zirlo	0	Single assembly - Tfuel=1085.42K	Infinite	0.87832	0.00081	
K505000AF	S550F	5.0	50	277.15	0.945	10.09375	0.1524	zirlo	0	Single assembly - Tfuel=885.42K	Infinite	0.87249	0.00076	
SAS2H Boron Concentration														
K205000AA	S250A	2.0	50	277.15	0.945	10.09375	0.1524	zirlo	0	Single assembly - PPM=950	Infinite	0.70641	0.00075	
K205000AG	S250G	2.0	50	277.15	0.945	10.09375	0.1524	zirlo	0	Single assembly - PPM=1100	Infinite	0.71116	0.00061	
K205000AH	S250H	2.0	50	277.15	0.945	10.09375	0.1524	zirlo	0	Single assembly - PPM=800	Infinite	0.70343	0.00065	
K502000AA	S520A	5.0	20	277.15	0.945	10.09375	0.1524	zirlo	0	Single assembly - PPM=950	Infinite	1.05935	0.00083	
K502000AG	S520G	5.0	20	277.15	0.945	10.09375	0.1524	zirlo	0	Single assembly - PPM=1100	Infinite	1.05882	0.00085	
K502000AH	S520H	5.0	20	277.15	0.945	10.09375	0.1524	zirlo	0	Single assembly - PPM=800	Infinite	1.05837	0.00082	
K505000AA	S550A	5.0	50	277.15	0.945	10.09375	0.1524	zirlo	0	Single assembly - PPM=950	Infinite	0.88271	0.00077	
K505000AG	S550G	5.0	50	277.15	0.945	10.09375	0.1524	zirlo	0	Single assembly - PPM=1100	Infinite	0.88656	0.00087	
K505000AH	S550H	5.0	50	277.15	0.945	10.09375	0.1524	zirlo	0	Single assembly - PPM=800	Infinite	0.88274	0.00072	

SAS2H Tmod														
K205000AA	S250A	2.0	50	277.15	0.945	10.09375	0.1524	zirlo	0	Single assembly - Tmod=601F	Infinite	0.70641	0.00075	
K205000AI	S250I	2.0	50	277.15	0.945	10.09375	0.1524	zirlo	0	Single assembly - Tmod=580F	Infinite	0.69791	0.00070	
K205000AJ	S250J	2.0	50	277.15	0.945	10.09375	0.1524	zirlo	0	Single assembly - Tmod=560F	Infinite	0.69044	0.00061	
K502000AA	S520A	5.0	20	277.15	0.945	10.09375	0.1524	zirlo	0	Single assembly - Tmod=601F	Infinite	1.05935	0.00083	
K502000AI	S520I	5.0	20	277.15	0.945	10.09375	0.1524	zirlo	0	Single assembly - Tmod=580F	Infinite	1.05764	0.00087	
K502000AJ	S520J	5.0	20	277.15	0.945	10.09375	0.1524	zirlo	0	Single assembly - Tmod=560F	Infinite	1.05770	0.00085	
K505000AA	S550A	5.0	50	277.15	0.945	10.09375	0.1524	zirlo	0	Single assembly - Tmod=601F	Infinite	0.88271	0.00077	
K505000AI	S550I	5.0	50	277.15	0.945	10.09375	0.1524	zirlo	0	Single assembly - Tmod=580F	Infinite	0.87720	0.00077	
K505000AJ	S550J	5.0	50	277.15	0.945	10.09375	0.1524	zirlo	0	Single assembly - Tmod=560F	Infinite	0.87276	0.00072	
SAS2H Assembly Power														
K205000AA	S250A	2.0	50	277.15	0.945	10.09375	0.1524	zirlo	0	Single assembly - AP=22.583MW	Infinite	0.70641	0.00075	
K205000AK	S250K	2.0	50	277.15	0.945	10.09375	0.1524	zirlo	0	Single assembly - AP=20.0MW	Infinite	0.70793	0.00066	
K205000AL	S250L	2.0	50	277.15	0.945	10.09375	0.1524	zirlo	0	Single assembly - AP=17.5MW	Infinite	0.70753	0.00068	
K205000AM	S250M	2.0	50	277.15	0.945	10.09375	0.1524	zirlo	0	Single assembly - AP=15.0MW	Infinite	0.70754	0.00066	
K205000AN	S250N	2.0	50	277.15	0.945	10.09375	0.1524	zirlo	0	Single assembly - AP=12.442MW	Infinite	0.70774	0.00063	
K502000AA	S520A	5.0	20	277.15	0.945	10.09375	0.1524	zirlo	0	Single assembly - AP=22.583MW	Infinite	1.05935	0.00083	
K502000AK	S520K	5.0	20	277.15	0.945	10.09375	0.1524	zirlo	0	Single assembly - AP=20.0MW	Infinite	1.05903	0.00091	
K502000AL	S520L	5.0	20	277.15	0.945	10.09375	0.1524	zirlo	0	Single assembly - AP=17.5MW	Infinite	1.05801	0.00093	
K502000AM	S520M	5.0	20	277.15	0.945	10.09375	0.1524	zirlo	0	Single assembly - AP=15.0MW	Infinite	1.05983	0.00091	
K502000AN	S520N	5.0	20	277.15	0.945	10.09375	0.1524	zirlo	0	Single assembly - AP=12.442MW	Infinite	1.06091	0.00081	
K505000AA	S550A	5.0	50	277.15	0.945	10.09375	0.1524	zirlo	0	Single assembly - AP=22.583MW	Infinite	0.88271	0.00077	
K505000AK	S550K	5.0	50	277.15	0.945	10.09375	0.1524	zirlo	0	Single assembly - AP=20.0MW	Infinite	0.88415	0.00073	
K505000AL	S550L	5.0	50	277.15	0.945	10.09375	0.1524	zirlo	0	Single assembly - AP=17.5MW	Infinite	0.88372	0.00076	
K505000AM	S550M	5.0	50	277.15	0.945	10.09375	0.1524	zirlo	0	Single assembly - AP=15.0MW	Infinite	0.88420	0.00071	
K505000AN	S550N	5.0	50	277.15	0.945	10.09375	0.1524	zirlo	0	Single assembly - AP=12.442MW	Infinite	0.88363	0.00071	
KENO Biases and Uncertainties as a Function of Tmod and Clad Material														
K500000B1		5.0	0	277.15	0.945	10.09375	0.1524	zirlo	0	Single assembly	Infinite	1.19925	0.00107	
K500000B2		5.0	0	277.15	0.945	10.09375	0.1524	optin	0	Single assembly	Infinite	1.19707	0.00099	
K500000B3		5.0	0	277.15	0.945	10.09375	0.1524	zirc4	0	Single assembly	Infinite	1.19639	0.00091	
K500000B4		5.0	0	341.48	0.945	10.09375	0.1524	zirlo	0	Single assembly	Infinite	1.20803	0.00084	
K500000B5		5.0	0	341.48	0.945	10.09375	0.1524	optin	0	Single assembly	Infinite	1.20813	0.00103	
K500000B6		*5.0*	*0*	*341.48*	*0.945*	*10.09375*	*0.1524*	*zirc4*	*0*	*Single assembly*	*Infinite*	*1.21112*	*0.00091*	***
K500000B7		5.0	0	341.48	0.945	10.09375	0.1524	alloy a	0	Single assembly	Infinite	1.20980	0.00091	
K500000B8		5.0	0	341.48	0.945	10.09375	0.1524	lt zirlo	0	Single assembly	Infinite	1.20870	0.00095	
K500000B9		5.0	0	341.48	0.945	10.09375	0.1524	m5	0	Single assembly	Infinite	1.20890	0.00090	
K500000C1		5.0	0	277.15	0.945	10.09375	0.1524	zirlo	300	Single assembly	Infinite	1.12220	0.00094	

K500000C2		5.0	0	277.15	0.945	10.09375	0.1524	optin	300	Single assembly	Infinite	1.12203	0.00095	
K500000C3		5.0	0	277.15	0.945	10.09375	0.1524	zirc4	300	Single assembly	Infinite	1.12104	0.00107	
K500000C4		5.0	0	341.48	0.945	10.09375	0.1524	zirlo	300	Single assembly	Infinite	1.13323	0.00091	
K500000C5		5.0	0	341.48	0.945	10.09375	0.1524	optin	300	Single assembly	Infinite	1.13396	0.00083	
K500000C6		*5.0*	*0*	*341.48*	*0.945*	*10.09375*	*0.1524*	*zirc4*	*300*	*Single assembly*	*Infinite*	*1.13444*	*0.00094*	***
K500000C7		5.0	0	341.48	0.945	10.09375	0.1524	alloy a	300	Single assembly	Infinite	1.13241	0.00094	
K500000C8		5.0	0	341.48	0.945	10.09375	0.1524	lt zirlo	300	Single assembly	Infinite	1.13259	0.00091	
K500000C9		5.0	0	341.48	0.945	10.09375	0.1524	m5	300	Single assembly	Infinite	1.13359	0.00106	
K504000C1	S540	5.0	40	277.15	0.945	10.09375	0.1524	zirlo	300	Single assembly	Infinite	0.87878	0.00076	
K504000C2	S540	5.0	40	277.15	0.945	10.09375	0.1524	optin	300	Single assembly	Infinite	0.87862	0.00085	
K504000C3	S540	5.0	40	277.15	0.945	10.09375	0.1524	zirc4	300	Single assembly	Infinite	0.87750	0.00077	
K504000C4	S540	5.0	40	341.48	0.945	10.09375	0.1524	zirlo	300	Single assembly	Infinite	0.89027	0.00071	
K504000C5	S540	5.0	40	341.48	0.945	10.09375	0.1524	optin	300	Single assembly	Infinite	0.89083	0.00078	
K504000C6	*S540*	*5.0*	*40*	*341.48*	*0.945*	*10.09375*	*0.1524*	*zirc4*	*300*	*Single assembly*	*Infinite*	*0.89089*	*0.00077*	***
K504000C7	S540	5.0	40	341.48	0.945	10.09375	0.1524	alloy a	300	Single assembly	Infinite	0.89039	0.00076	
K504000C8	S540	5.0	40	341.48	0.945	10.09375	0.1524	lt zirlo	300	Single assembly	Infinite	,89004	0.00082	
K504000C9	S540	5.0	40	341.48	0.945	10.09375	0.1524	m5	300	Single assembly	Infinite	0.89018	0.00086	
KENO Biases and Uncertainties as a Function of Stack Height Density														
K500000BA		5.0	0	341.48	0.965	10.09375	0.1524	zirc4	0	Single assembly	Infinite	1.21021	0.00090	0.00090
K500000CA		5.0	0	341.48	0.965	10.09375	0.1524	zirc4	300	Single assembly	Infinite	1.13606	0.00084	0.00340
K504000CA	S540SHD	5.0	40	341.48	0.965	10.09375	0.1524	zirc4	300	Single assembly	Infinite	0.89768	0.00085	0.00841
KENO Biases and Uncertainties as a Function of Assembly Pitch														
K500000BB		5.0	0	341.48	0.945	10.125	0.1524	zirc4	0	Single assembly	Infinite	1.20356	0.00088	-0.00577
K500000BC		5.0	0	341.48	0.945	10.0625	0.1524	zirc4	0	Single assembly	Infinite	1.21278	0.00101	0.00358
K500000CB		5.0	0	341.48	0.945	10.125	0.1524	zirc4	300	Single assembly	Infinite	1.12857	0.00091	-0.00402
K500000CC		5.0	0	341.48	0.945	10.0625	0.1524	zirc4	300	Single assembly	Infinite	1.13705	0.00094	0.00449
K504000CB	S540	5.0	40	341.48	0.945	10.125	0.1524	zirc4	300	Single assembly	Infinite	0.88473	0.00077	-0.00462
K504000CC	S540	5.0	40	341.48	0.945	10.0625	0.1524	zirc4	300	Single assembly	Infinite	0.89382	0.00084	0.00454
KENO Biases and Uncertainties as a Function of Steel Thickness														
K500000BD		5.0	0	341.48	0.945	10.09375	0.1270	zirc4	0	Single assembly	Infinite	1.22267	0.00100	0.01346
K500000BE		5.0	0	341.48	0.945	10.09375	0.1778	zirc4	0	Single assembly	Infinite	1.19742	0.00109	-0.01170
K500000CD		5.0	0	341.48	0.945	10.09375	0.1270	zirc4	300	Single assembly	Infinite	1.14037	0.00088	0.00775
K500000CE		5.0	0	341.48	0.945	10.09375	0.1778	zirc4	300	Single assembly	Infinite	1.12599	0.00098	-0.00653
K504000CD	S540	5.0	40	341.48	0.945	10.09375	0.1270	zirc4	300	Single assembly	Infinite	0.89639	0.00071	0.00698
K504000CE	S540	5.0	40	341.48	0.945	10.09375	0.1778	zirc4	300	Single assembly	Infinite	0.88471	0.00083	-0.00458
KENO Biases and Uncertainties as a Function of Assembly Eccentric Positioning														
K500000BF		5.0	0	341.48	0.945	10.09375	0.1524	zirc4	0	10x10	Infinite	1.20934	0.00095	0.00008

K500000BG		5.0 ecc	0	341.48	0.945	10.09375	0.1524	zirc4	0	10x10 ecc in	Infinite	1.21883	0.00099	0.00961
K500000BH		5.0 ecc	0	341.48	0.945	10.09375	0.1524	zirc4	0	10x10 ecc out	Infinite	1.21889	0.00092	0.00960
K500000CF		5.0	0	341.48	0.945	10.09375	0.1524	zirc4	300	10x10	Infinite	1.13528	0.00096	0.00274
K500000CG		5.0 ecc	0	341.48	0.945	10.09375	0.1524	zirc4	300	10x10 ecc in	Infinite	1.14187	0.00104	0.00941
K500000CH		5.0 ecc	0	341.48	0.945	10.09375	0.1524	zirc4	300	10x10 ecc out	Infinite	1.14386	0.00086	0.01122
K504000CF	S540	5.0	40	341.48	0.945	10.09375	0.1524	zirc4	300	10x10	Infinite	0.89070	0.00077	0.00135
K504000CG	S540	5.0 ecc	40	341.48	0.945	10.09375	0.1524	zirc4	300	10x10 ecc in	Infinite	0.89731	0.00081	0.00800
K504000CH	S540	5.0 ecc	40	341.48	0.945	10.09375	0.1524	zirc4	300	10x10 ecc out	Infinite	0.89682	0.00088	0.00758
KENO Biases and Uncertainties as a Function of Enrichment														
K500000BI		5.05	0	341.48	0.945	10.09375	0.1397	zirc4	0	Single assembly	Infinite	1.21080	0.00096	0.00155
K500000CI		5.05	0	341.48	0.945	10.09375	0.1397	zirc4	300	Single assembly	Infinite	1.13474	0.00086	0.00210
K504000CI	S540ENR	5.05	40	341.48	0.945	10.09375	0.1397	zirc4	300	Single assembly	Infinite	0.89238	0.00078	0.00304
KENO Biases and Uncertainties as a Function of Gap Contents														
K500000BJ		5.00	0	341.48	0.945	10.09375	0.1397	zirc4	0	Single assembly-Water in gap	Infinite	1.20915	0.00089	-0.00017
K500000CJ		5.00	0	341.48	0.945	10.09375	0.1397	zirc4	300	Single assembly-Water in gap	Infinite	1.13618	0.00088	0.00356
K504000CJ	S540ENR	5.00	40	341.48	0.945	10.09375	0.1397	zirc4	300	Single assembly-Water in gap	Infinite	0.89204	0.00075	0.00267
Enrichment vs Burnup at 0 PPM														
K200000D1		2.0	0	341.48	0.945	10.09375	0.1524	zirc4	0	Single assembly	Infinite	0.97726	0.00082	1.03855
K201000D1	S210	2.0	10	341.48	0.945	10.09375	0.1524	zirc4	0	Single assembly	Infinite	0.90578	0.00074	0.96707
K202000D1	S220	2.0	20	341.48	0.945	10.09375	0.1524	zirc4	0	Single assembly	Infinite	0.83855	0.00071	0.89984
K203000D1	S230	2.0	30	341.48	0.945	10.09375	0.1524	zirc4	0	Single assembly	Infinite	0.78440	0.00087	0.84569
K204000D1	S240	2.0	40	341.48	0.945	10.09375	0.1524	zirc4	0	Single assembly	Infinite	0.74665	0.00066	0.80794
K205000D1	S250	2.0	50	341.48	0.945	10.09375	0.1524	zirc4	0	Single assembly	Infinite	0.71990	0.00068	0.78119
K206000D1	S260	2.0	60	341.48	0.945	10.09375	0.1524	zirc4	0	Single assembly	Infinite	0.70267	0.00059	0.76396
K207000D1	S270	2.0	70	341.48	0.945	10.09375	0.1524	zirc4	0	Single assembly	Infinite	0.69082	0.00060	0.75211
														0.01439
K300000D1		3.0	0	341.48	0.945	10.09375	0.1524	zirc4	0	Single assembly	Infinite	1.09184	0.00091	1.15313
K301000D1	S310	3.0	10	341.48	0.945	10.09375	0.1524	zirc4	0	Single assembly	Infinite	1.01050	0.00083	1.07179
K302000D1	S320	3.0	20	341.48	0.945	10.09375	0.1524	zirc4	0	Single assembly	Infinite	0.93591	0.00077	0.99720
K303000D1	S330	3.0	30	341.48	0.945	10.09375	0.1524	zirc4	0	Single assembly	Infinite	0.87020	0.00069	0.93149
K304000D1	S340	3.0	40	341.48	0.945	10.09375	0.1524	zirc4	0	Single assembly	Infinite	0.81338	0.00070	0.87467
K305000D1	S350	3.0	50	341.48	0.945	10.09375	0.1524	zirc4	0	Single assembly	Infinite	0.76783	0.00074	0.82912
K306000D1	S360	3.0	60	341.48	0.945	10.09375	0.1524	zirc4	0	Single assembly	Infinite	0.73518	0.00070	0.79647
K307000D1	S370	3.0	70	341.48	0.945	10.09375	0.1524	zirc4	0	Single assembly	Infinite	0.71073	0.00063	0.77202
														0.01913
K400000D1		4.0	0	341.48	0.945	10.09375	0.1524	zirc4	0	Single assembly	Infinite	1.15989	0.00096	1.22118
K401000D1	S410	4.0	10	341.48	0.945	10.09375	0.1524	zirc4	0	Single assembly	Infinite	1.08330	0.00092	1.14459

K402000D1	S420	4.0	20	341.48	0.945	10.09375	0.1524	zirc4	0	Single assembly	Infinite	1.01347	0.00082	1.07476
K403000D1	S430	4.0	30	341.48	0.945	10.09375	0.1524	zirc4	0	Single assembly	Infinite	0.94894	0.00083	1.01023
K404000D1	S440	4.0	40	341.48	0.945	10.09375	0.1524	zirc4	0	Single assembly	Infinite	0.88840	0.00076	0.94969
K405000D1	S450	4.0	50	341.48	0.945	10.09375	0.1524	zirc4	0	Single assembly	Infinite	0.83200	0.00071	0.89329
K406000D1	S460	4.0	60	341.48	0.945	10.09375	0.1524	zirc4	0	Single assembly	Infinite	0.78548	0.00073	0.84677
K407000D1	S470	4.0	70	341.48	0.945	10.09375	0.1524	zirc4	0	Single assembly	Infinite	0.74660	0.00070	0.80789
														0.02075
K500000D1		5.0	0	341.48	0.945	10.09375	0.1524	zirc4	0	Single assembly	Infinite	1.21112	0.00091	1.27241
K501000D1	S510	5.0	10	341.48	0.945	10.09375	0.1524	zirc4	0	Single assembly	Infinite	1.13638	0.00085	1.19767
K502000D1	S520	5.0	20	341.48	0.945	10.09375	0.1524	zirc4	0	Single assembly	Infinite	1.07119	0.00088	1.13248
K503000D1	S530	5.0	30	341.48	0.945	10.09375	0.1524	zirc4	0	Single assembly	Infinite	1.01281	0.00079	1.07410
K504000D1	S540	5.0	40	341.48	0.945	10.09375	0.1524	zirc4	0	Single assembly	Infinite	0.95358	0.00083	1.01487
K505000D1	S550	5.0	50	341.48	0.945	10.09375	0.1524	zirc4	0	Single assembly	Infinite	0.89641	0.00079	0.95770
K506000D1	S560	5.0	60	341.48	0.945	10.09375	0.1524	zirc4	0	Single assembly	Infinite	0.84339	0.00071	0.90468
K507000D1	S570	5.0	70	341.48	0.945	10.09375	0.1524	zirc4	0	Single assembly	Infinite	0.79503	0.00072	0.85632
														0.02089
K200580D1	S20058	2.0	5.80	341.48	0.945	10.09375	0.1524	zirc4	0	Single assembly	Infinite	0.93638	0.00079	0.99767
K251340D1	S25134	2.5	13.40	341.48	0.945	10.09375	0.1524	zirc4	0	Single assembly	Infinite	0.93664	0.00078	0.99793
K302000D1	S320	3.0	20.00	341.48	0.945	10.09375	0.1524	zirc4	0	Single assembly	Infinite	0.93591	0.00077	0.99720
K352630D1	S35263	3.5	26.30	341.48	0.945	10.09375	0.1524	zirc4	0	Single assembly	Infinite	0.93519	0.00089	0.99648
K403200D1	S40320	4.0	32.00	341.48	0.945	10.09375	0.1524	zirc4	0	Single assembly	Infinite	0.93536	0.00080	0.99665
K453750D1	S45375	4.5	37.50	341.48	0.945	10.09375	0.1524	zirc4	0	Single assembly	Infinite	0.93621	0.00075	0.99750
K504300D1	S50430	5.0	43.00	341.48	0.945	10.09375	0.1524	zirc4	0	Single assembly	Infinite	0.93599	0.00075	0.99728
Enrichment vs Burnup at 300 PPM														
K200000D2		2.0	0	341.48	0.945	10.09375	0.1524	zirc4	300	Single assembly	Infinite	0.89457	0.00083	0.95586
K201000D2	S210	2.0	10	341.48	0.945	10.09375	0.1524	zirc4	300	Single assembly	Infinite	0.83281	0.00074	0.89410
K202000D2	S220	2.0	20	341.48	0.945	10.09375	0.1524	zirc4	300	Single assembly	Infinite	0.76997	0.00079	0.83126
K203000D2	S230	2.0	30	341.48	0.945	10.09375	0.1524	zirc4	300	Single assembly	Infinite	0.72224	0.00065	0.78353
K204000D2	S240	2.0	40	341.48	0.945	10.09375	0.1524	zirc4	300	Single assembly	Infinite	0.68733	0.00059	0.74862
K205000D2	S250	2.0	50	341.48	0.945	10.09375	0.1524	zirc4	300	Single assembly	Infinite	0.66433	0.00072	0.72562
K206000D2	S260	2.0	60	341.48	0.945	10.09375	0.1524	zirc4	300	Single assembly	Infinite	0.64749	0.00064	0.70878
K207000D2	S270	2.0	70	341.48	0.945	10.09375	0.1524	zirc4	300	Single assembly	Infinite	0.63731	0.00056	0.69860
														0.01293
K300000D2		3.0	0	341.48	0.945	10.09375	0.1524	zirc4	300	Single assembly	Infinite	1.00921	0.00081	1.07050
K301000D2	S310	3.0	10	341.48	0.945	10.09375	0.1524	zirc4	300	Single assembly	Infinite	0.93514	0.00077	0.99643
K302000D2	S320	3.0	20	341.48	0.945	10.09375	0.1524	zirc4	300	Single assembly	Infinite	0.86615	0.00085	0.92744
K303000D2	S330	3.0	30	341.48	0.945	10.09375	0.1524	zirc4	300	Single assembly	Infinite	0.80550	0.00075	0.86679

K304000D2	S340	3.0	40	341.48	0.945	10.09375	0.1524	zirc4	300	Single assembly	Infinite	0.75140	0.00072	0.81269
K305000D2	S350	3.0	50	341.48	0.945	10.09375	0.1524	zirc4	300	Single assembly	Infinite	0.71084	0.00069	0.77213
K306000D2	S360	3.0	60	341.48	0.945	10.09375	0.1524	zirc4	300	Single assembly	Infinite	0.67942	0.00068	0.74071
K307000D2	S370	3.0	70	341.48	0.945	10.09375	0.1524	zirc4	300	Single assembly	Infinite	0.65791	0.00058	0.71920
														0.01763
K400000D2		4.0	0	341.48	0.945	10.09375	0.1524	zirc4	300	Single assembly	Infinite	1.08296	0.00085	1.14425
K401000D2	S410	4.0	10	341.48	0.945	10.09375	0.1524	zirc4	300	Single assembly	Infinite	1.00944	0.00095	1.07073
K402000D2	S420	4.0	20	341.48	0.945	10.09375	0.1524	zirc4	300	Single assembly	Infinite	0.94612	0.00079	1.00741
K403000D2	S430	4.0	30	341.48	0.945	10.09375	0.1524	zirc4	300	Single assembly	Infinite	0.88401	0.00078	0.94530
K404000D2	S440	4.0	40	341.48	0.945	10.09375	0.1524	zirc4	300	Single assembly	Infinite	0.82508	0.00075	0.88637
K405000D2	S450	4.0	50	341.48	0.945	10.09375	0.1524	zirc4	300	Single assembly	Infinite	0.77122	0.00070	0.83251
K406000D2	S460	4.0	60	341.48	0.945	10.09375	0.1524	zirc4	300	Single assembly	Infinite	0.72752	0.00074	0.78881
K407000D2	S470	4.0	70	341.48	0.945	10.09375	0.1524	zirc4	300	Single assembly	Infinite	0.69218	0.00069	0.75347
														0.01962
K500000D2		5.0	0	341.48	0.945	10.09375	0.1524	zirc4	300	Single assembly	Infinite	1.13444	0.00094	1.19573
K501000D2	S510	5.0	10	341.48	0.945	10.09375	0.1524	zirc4	300	Single assembly	Infinite	1.06482	0.00093	1.12611
K502000D2	S520	5.0	20	341.48	0.945	10.09375	0.1524	zirc4	300	Single assembly	Infinite	1.00457	0.00081	1.06586
K503000D2	S530	5.0	30	341.48	0.945	10.09375	0.1524	zirc4	300	Single assembly	Infinite	0.94771	0.00075	1.00900
K504000D2	S540	5.0	40	341.48	0.945	10.09375	0.1524	zirc4	300	Single assembly	Infinite	0.89059	0.00077	0.95188
K505000D2	S550	5.0	50	341.48	0.945	10.09375	0.1524	zirc4	300	Single assembly	Infinite	0.83586	0.00080	0.89715
K506000D2	S560	5.0	60	341.48	0.945	10.09375	0.1524	zirc4	300	Single assembly	Infinite	0.78435	0.00071	0.84564
K507000D2	S570	5.0	70	341.48	0.945	10.09375	0.1524	zirc4	300	Single assembly	Infinite	0.73910	0.00068	0.80039
														0.01985
K200580D2	S20058	2.0	5.80	341.48	0.945	10.09375	0.1524	zirc4	300	Single assembly	Infinite	0.86028	0.00071	0.92157
K251340D2	S25134	2.5	13.40	341.48	0.945	10.09375	0.1524	zirc4	300	Single assembly	Infinite	0.86494	0.00077	0.92623
K302000D2	S320	3.0	20.00	341.48	0.945	10.09375	0.1524	zirc4	300	Single assembly	Infinite	0.86615	0.00085	0.92744
K352630D2	S35263	3.5	26.30	341.48	0.945	10.09375	0.1524	zirc4	300	Single assembly	Infinite	0.86784	0.00074	0.92913
K403200D2	S40320	4.0	32.00	341.48	0.945	10.09375	0.1524	zirc4	300	Single assembly	Infinite	0.87102	0.00078	0.93231
K453750D2	S45375	4.5	37.50	341.48	0.945	10.09375	0.1524	zirc4	300	Single assembly	Infinite	0.87255	0.00078	0.93384
K504300D2	S50430	5.0	43.00	341.48	0.945	10.09375	0.1524	zirc4	300	Single assembly	Infinite	0.87387	0.00083	0.93516
Enrichment vs Reactivity at 2000 PPM														
K200000D3		2.0	0	341.48	0.945	10.09375	0.1524	zirc4	2000	Single assembly	Infinite	0.62679	0.00066	0.68808
K300000D3		3.0	0	341.48	0.945	10.09375	0.1524	zirc4	2000	Single assembly	Infinite	0.74302	0.00073	0.80431
K400000D3		4.0	0	341.48	0.945	10.09375	0.1524	zirc4	2000	Single assembly	Infinite	0.82161	0.00096	0.88290
K500000D3		5.0	0	341.48	0.945	10.09375	0.1524	zirc4	2000	Single assembly	Infinite	0.87907	0.00094	0.94036
Axial Profiles at 0 PPM														
K5062AAD1	s562aa2.xxx	5.0	62	341.48	0.945	10.09375	0.1524	zirc4	0	Single assm-18 axial nodes	Water	0.86254	0.00104	0.03226

K5062AAE1	s562aa1.xxx	5.0	62	341.48	0.945	10.09375	0.1524	zirc4	0	Single assm-1 axial node	Water	0.83204	0.00072	
K5046ABD1	s546ab2.xxx	5.0	46	341.48	0.945	10.09375	0.1524	zirc4	0	Single assm-18 axial nodes	Water	0.93104	0.00087	0.01751
K5046ABE1	s546ab1.xxx	5.0	46	341.48	0.945	10.09375	0.1524	zirc4	0	Single assm-1 axial node	Water	0.91513	0.00073	
K5042ACD1	s542ac2.xxx	5.0	42	341.48	0.945	10.09375	0.1524	zirc4	0	Single assm-18 axial nodes	Water	0.94813	0.00091	0.01060
K5042ACE1	s542ac1.xxx	5.0	42	341.48	0.945	10.09375	0.1524	zirc4	0	Single assm-1 axial node	Water	0.93931	0.00087	
K5038ADD1	s538ad2.xxx	5.0	38	341.48	0.945	10.09375	0.1524	zirc4	0	Single assm-18 axial nodes	Water	0.97777	0.00090	0.01623
K5038ADE1	s538ad1.xxx	5.0	38	341.48	0.945	10.09375	0.1524	zirc4	0	Single assm-1 axial node	Water	0.96331	0.00087	
K5034AED1	s534ae2.xxx	5.0	34	341.48	0.945	10.09375	0.1524	zirc4	0	Single assm-18 axial nodes	Water	0.99441	0.00089	0.01255
K5034AEE1	s534ae1.xxx	5.0	34	341.48	0.945	10.09375	0.1524	zirc4	0	Single assm-1 axial node	Water	0.98361	0.00086	
K5030AFD1	s530af2.xxx	5.0	30	341.48	0.945	10.09375	0.1524	zirc4	0	Single assm-18 axial nodes	Water	1.01763	0.00096	0.00918
K5030AFE1	s530af1.xxx	5.0	30	341.48	0.945	10.09375	0.1524	zirc4	0	Single assm-1 axial node	Water	1.01030	0.00089	
K5026AGD1	s526ag2.xxx	5.0	26	341.48	0.945	10.09375	0.1524	zirc4	0	Single assm-18 axial nodes	Water	1.03809	0.00111	0.00688
K5026AGE1	s526ag1.xxx	5.0	26	341.48	0.945	10.09375	0.1524	zirc4	0	Single assm-1 axial node	Water	1.03312	0.00080	
K5022AHD1	s522ah2.xxx	5.0	22	341.48	0.945	10.09375	0.1524	zirc4	0	Single assm-18 axial nodes	Water	1.05695	0.00096	0.00193
K5022AHE1	s522ah1.xxx	5.0	22	341.48	0.945	10.09375	0.1524	zirc4	0	Single assm-1 axial node	Water	1.05677	0.00079	
K5018AID1	s518ai2.xxx	5.0	18	341.48	0.945	10.09375	0.1524	zirc4	0	Single assm-18 axial nodes	Water	1.09833	0.00102	0.01682
K5018AIE1	s518ai1.xxx	5.0	18	341.48	0.945	10.09375	0.1524	zirc4	0	Single assm-1 axial node	Water	1.08348	0.00095	
K5014AJD1	s514aj2.xxx	5.0	14	341.48	0.945	10.09375	0.1524	zirc4	0	Single assm-18 axial nodes	Water	1.09717	0.00092	-0.00834
K5014AJE1	s514aj1.xxx	5.0	14	341.48	0.945	10.09375	0.1524	zirc4	0	Single assm-1 axial node	Water	1.10729	0.00086	
K5010AKD1	s510ak2.xxx	5.0	10	341.48	0.945	10.09375	0.1524	zirc4	0	Single assm-18 axial nodes	Water	1.12772	0.00092	-0.00294
K5010AKE1	s510ak1.xxx	5.0	10	341.48	0.945	10.09375	0.1524	zirc4	0	Single assm-1 axial node	Water	1.13244	0.00086	
K5006ALD1	s506al2.xxx	5.0	6	341.48	0.945	10.09375	0.1524	zirc4	0	Single assm-18 axial nodes	Water	1.15379	0.00092	-0.00360
K5006ALE1	s506al1.xxx	5.0	6	341.48	0.945	10.09375	0.1524	zirc4	0	Single assm-1 axial node	Water	1.15923	0.00092	
K5006ALF1	s506al2.yyy	5.0	6	341.48	0.945	10.09375	0.1524	zirc4	0	Single assm-18 axial nodes	Water	1.15383	0.00083	-0.00343
K5006ALG1	s506al1.yyy	5.0	6	341.48	0.945	10.09375	0.1524	zirc4	0	Single assm-1 axial node	Water	1.15898	0.00089	
K5006ALH1	s506	5.0	6	341.48	0.945	10.09375	0.1524	zirc4	0	Single assm-1 axial node	Water	1.16104	0.00104	
Axial Profiles at 0 PPM														
K5062BAD1	s562ba2.xxx	5.0	62	341.48	0.945	10.09375	0.1524	zirc4	0	Single assm-18 axial nodes	Water	0.86091	0.00095	0.03054
K5062AAE1	s562aa1.xxx	5.0	62	341.48	0.945	10.09375	0.1524	zirc4	0	Single assm-1 axial node	Water	0.83204	0.00072	
K5046BBD1	s546bb2.xxx	5.0	46	341.48	0.945	10.09375	0.1524	zirc4	0	Single assm-18 axial nodes	Water	0.92725	0.00096	0.01381
K5046ABE1	s546ab1.xxx	5.0	46	341.48	0.945	10.09375	0.1524	zirc4	0	Single assm-1 axial node	Water	0.91513	0.00073	
K5042BCD1	s542bc2.xxx	5.0	42	341.48	0.945	10.09375	0.1524	zirc4	0	Single assm-18 axial nodes	Water	0.94408	0.00079	0.00643
K5042ACE1	s542ac1.xxx	5.0	42	341.48	0.945	10.09375	0.1524	zirc4	0	Single assm-1 axial node	Water	0.93931	0.00087	
K5038BDD1	s538bd2.xxx	5.0	38	341.48	0.945	10.09375	0.1524	zirc4	0	Single assm-18 axial nodes	Water	0.97221	0.00096	0.01073
K5038ADE1	s538ad1.xxx	5.0	38	341.48	0.945	10.09375	0.1524	zirc4	0	Single assm-1 axial node	Water	0.96331	0.00087	
K5034BED1	s534be2.xxx	5.0	34	341.48	0.945	10.09375	0.1524	zirc4	0	Single assm-18 axial nodes	Water	0.99202	0.00086	0.01013
K5034AEE1	s534ae1.xxx	5.0	34	341.48	0.945	10.09375	0.1524	zirc4	0	Single assm-1 axial node	Water	0.98361	0.00086	

K5030BFD1	s530bf2.xxx	5.0	30	341.48	0.945	10.09375	0.1524	zirc4	0	Single assm-18 axial nodes	Water	1.01689	0.00102	0.00850
K5030AFE1	s530af1.xxx	5.0	30	341.48	0.945	10.09375	0.1524	zirc4	0	Single assm-1 axial node	Water	1.01030	0.00089	
K5026BGD1	s526bg2.xxx	5.0	26	341.48	0.945	10.09375	0.1524	zirc4	0	Single assm-18 axial nodes	Water	1.03869	0.00104	0.00741
K5026AGE1	s526ag1.xxx	5.0	26	341.48	0.945	10.09375	0.1524	zirc4	0	Single assm-1 axial node	Water	1.03312	0.00080	
K5022BHD1	s522bh2.xxx	5.0	22	341.48	0.945	10.09375	0.1524	zirc4	0	Single assm-18 axial nodes	Water	1.05485	0.00105	-0.00008
K5022AHE1	s522ah1.xxx	5.0	22	341.48	0.945	10.09375	0.1524	zirc4	0	Single assm-1 axial node	Water	1.05677	0.00079	
K5018BID1	s518bi2.xxx	5.0	18	341.48	0.945	10.09375	0.1524	zirc4	0	Single assm-18 axial nodes	Water	1.10153	0.00089	0.01989
K5018AIE1	s518ai1.xxx	5.0	18	341.48	0.945	10.09375	0.1524	zirc4	0	Single assm-1 axial node	Water	1.08348	0.00095	
K5014BJD1	s514bj2.xxx	5.0	14	341.48	0.945	10.09375	0.1524	zirc4	0	Single assm-18 axial nodes	Water	1.11182	0.00105	0.00644
K5014AJE1	s514aj1.xxx	5.0	14	341.48	0.945	10.09375	0.1524	zirc4	0	Single assm-1 axial node	Water	1.10729	0.00086	
K5010BKD1	s510bk2.xxx	5.0	10	341.48	0.945	10.09375	0.1524	zirc4	0	Single assm-18 axial nodes	Water	1.12731	0.00090	-0.00337
K5010AKE1	s510ak1.xxx	5.0	10	341.48	0.945	10.09375	0.1524	zirc4	0	Single assm-1 axial node	Water	1.13244	0.00086	
K5006BLD1	s506bl2.xxx	5.0	6	341.48	0.945	10.09375	0.1524	zirc4	0	Single assm-18 axial nodes	Water	1.15490	0.00087	-0.00254
K5006ALE1	s506al1.xxx	5.0	6	341.48	0.945	10.09375	0.1524	zirc4	0	Single assm-1 axial node	Water	1.15923	0.00092	
Axial Profiles at 300 PPM														
K5062AAD3	s562aa2.xxx	5.0	62	341.48	0.945	10.09375	0.1524	zirc4	300	Single assm-18 axial nodes	Water	0.80241	0.00087	0.03047
K5062AAE3	s562aa1.xxx	5.0	62	341.48	0.945	10.09375	0.1524	zirc4	300	Single assm-1 axial node	Water	0.77352	0.00071	
K5046ABD3	s546ab2.xxx	5.0	46	341.48	0.945	10.09375	0.1524	zirc4	300	Single assm-18 axial nodes	Water	0.86800	0.00100	0.01656
K5046ABE3	s546ab1.xxx	5.0	46	341.48	0.945	10.09375	0.1524	zirc4	300	Single assm-1 axial node	Water	0.85319	0.00075	
K5042ACD3	s542ac2.xxx	5.0	46	341.48	0.945	10.09375	0.1524	zirc4	300	Single assm-18 axial nodes	Water	0.88407	0.00089	0.00944
K5042ACE3	s542ac1.xxx	5.0	46	341.48	0.945	10.09375	0.1524	zirc4	300	Single assm-1 axial node	Water	0.87627	0.00075	
K5038ADD3	s538ad2.xxx	5.0	38	341.48	0.945	10.09375	0.1524	zirc4	300	Single assm-18 axial nodes	Water	0.91655	0.00088	0.02030
K5038ADE3	s538ad1.xxx	5.0	38	341.48	0.945	10.09375	0.1524	zirc4	300	Single assm-1 axial node	Water	0.89790	0.00077	
K5034AED3	s534ae2.xxx	5.0	38	341.48	0.945	10.09375	0.1524	zirc4	300	Single assm-18 axial nodes	Water	0.93206	0.00085	0.01245
K5034AEE3	s534ae1.xxx	5.0	38	341.48	0.945	10.09375	0.1524	zirc4	300	Single assm-1 axial node	Water	0.92130	0.00084	
K5030AFD3	s530af2.xxx	5.0	30	341.48	0.945	10.09375	0.1524	zirc4	300	Single assm-18 axial nodes	Water	0.95155	0.00098	0.00996
K5030AFE3	s530af1.xxx	5.0	30	341.48	0.945	10.09375	0.1524	zirc4	300	Single assm-1 axial node	Water	0.94349	0.00092	
K5026AGD3	s526ag2.xxx	5.0	26	341.48	0.945	10.09375	0.1524	zirc4	300	Single assm-18 axial nodes	Water	0.97262	0.00096	0.00789
K5026AGE3	s526ag1.xxx	5.0	26	341.48	0.945	10.09375	0.1524	zirc4	300	Single assm-1 axial node	Water	0.96659	0.00090	
K5022AHD3	s522ah2.xxx	5.0	22	341.48	0.945	10.09375	0.1524	zirc4	300	Single assm-18 axial nodes	Water	0.98880	0.00104	0.00109
K5022AHE3	s522ah1.xxx	5.0	22	341.48	0.945	10.09375	0.1524	zirc4	300	Single assm-1 axial node	Water	0.98965	0.00090	
K5018AID3	s518ai2.xxx	5.0	18	341.48	0.945	10.09375	0.1524	zirc4	300	Single assm-18 axial nodes	Water	1.02935	0.00103	0.01528
K5018AIE3	s518ai1.xxx	5.0	18	341.48	0.945	10.09375	0.1524	zirc4	300	Single assm-1 axial node	Water	1.01598	0.00088	
K5014AJD3	s514aj2.xxx	5.0	14	341.48	0.945	10.09375	0.1524	zirc4	300	Single assm-18 axial nodes	Water	1.03210	0.00085	-0.00236
K5014AJE3	s514aj1.xxx	5.0	14	341.48	0.945	10.09375	0.1524	zirc4	300	Single assm-1 axial node	Water	1.03628	0.00097	
K5010AKD3	s510ak2.xxx	5.0	10	341.48	0.945	10.09375	0.1524	zirc4	300	Single assm-18 axial nodes	Water	1.05620	0.00090	-0.00409
K5010AKE3	s510ak1.xxx	5.0	10	341.48	0.945	10.09375	0.1524	zirc4	300	Single assm-1 axial node	Water	1.06210	0.00091	

K5006ALD3	s506al2.xxx	5.0	6	341.48	0.945	10.09375	0.1524	zirc4	300	Single assm-18 axial nodes	Water	1.08098	0.00096	-0.00286
K5006ALE3	s506al1.xxx	5.0	6	341.48	0.945	10.09375	0.1524	zirc4	300	Single assm-1 axial node	Water	1.08583	0.00103	
K5006ALF3	s506al2.yyy	5.0	6	341.48	0.945	10.09375	0.1524	zirc4	300	Single assm-18 axial nodes	Water	1.08256	0.00088	-0.00215
K5006ALG3	s506al1.yyy	5.0	6	341.48	0.945	10.09375	0.1524	zirc4	300	Single assm-1 axial node	Water	1.08642	0.00083	
K5006ALH3	s506	5.0	6	341.48	0.945	10.09375	0.1524	zirc4	300	Single assm-1 axial node	Water	1.08621	0.00087	
Axial Profiles at 300 PPM														
K5062BAD3	s562ba2.xxx	5.0	62	341.48	0.945	10.09375	0.1524	zirc4	300	Single assm-18 axial nodes	Water	0.80133	0.00103	0.02955
K5062AAE3	s562aa1.xxx	5.0	62	341.48	0.945	10.09375	0.1524	zirc4	300	Single assm-1 axial node	Water	0.77352	0.00071	
K5046BBD3	s546bb2.xxx	5.0	46	341.48	0.945	10.09375	0.1524	zirc4	300	Single assm-18 axial nodes	Water	0.86749	0.00093	0.01598
K5046ABE3	s546ab1.xxx	5.0	46	341.48	0.945	10.09375	0.1524	zirc4	300	Single assm-1 axial node	Water	0.85319	0.00075	
K5042BCD3	s542bc2.xxx	5.0	46	341.48	0.945	10.09375	0.1524	zirc4	300	Single assm-18 axial nodes	Water	0.88241	0.00084	0.00773
K5042ACE3	s542ac1.xxx	5.0	46	341.48	0.945	10.09375	0.1524	zirc4	300	Single assm-1 axial node	Water	0.87627	0.00075	
K5038BDD3	s538bd2.xxx	5.0	38	341.48	0.945	10.09375	0.1524	zirc4	300	Single assm-18 axial nodes	Water	0.90892	0.00106	0.01285
K5038ADE3	s538ad1.xxx	5.0	38	341.48	0.945	10.09375	0.1524	zirc4	300	Single assm-1 axial node	Water	0.89790	0.00077	
K5034BED3	s534be2.xxx	5.0	38	341.48	0.945	10.09375	0.1524	zirc4	300	Single assm-18 axial nodes	Water	0.92553	0.00096	0.00603
K5034AEE3	s534ae1.xxx	5.0	38	341.48	0.945	10.09375	0.1524	zirc4	300	Single assm-1 axial node	Water	0.92130	0.00084	
K5030BFD3	s530bf2.xxx	5.0	30	341.48	0.945	10.09375	0.1524	zirc4	300	Single assm-18 axial nodes	Water	0.95246	0.00094	0.01083
K5030AFE3	s530af1.xxx	5.0	30	341.48	0.945	10.09375	0.1524	zirc4	300	Single assm-1 axial node	Water	0.94349	0.00092	
K5026BGD3	s526bg2.xxx	5.0	26	341.48	0.945	10.09375	0.1524	zirc4	300	Single assm-18 axial nodes	Water	0.97153	0.00094	0.00678
K5026AGE3	s526ag1.xxx	5.0	26	341.48	0.945	10.09375	0.1524	zirc4	300	Single assm-1 axial node	Water	0.96659	0.00090	
K5022BHD3	s522bh2.xxx	5.0	22	341.48	0.945	10.09375	0.1524	zirc4	300	Single assm-18 axial nodes	Water	0.98935	0.00094	0.00154
K5022AHE3	s522ah1.xxx	5.0	22	341.48	0.945	10.09375	0.1524	zirc4	300	Single assm-1 axial node	Water	0.98965	0.00090	
K5018BID3	s518bi2.xxx	5.0	18	341.48	0.945	10.09375	0.1524	zirc4	300	Single assm-18 axial nodes	Water	1.02929	0.00100	0.01519
K5018AIE3	s518ai1.xxx	5.0	18	341.48	0.945	10.09375	0.1524	zirc4	300	Single assm-1 axial node	Water	1.01598	0.00088	
K5014BJD3	s514bj2.xxx	5.0	14	341.48	0.945	10.09375	0.1524	zirc4	300	Single assm-18 axial nodes	Water	1.04213	0.00085	0.00767
K5014AJE3	s514aj1.xxx	5.0	14	341.48	0.945	10.09375	0.1524	zirc4	300	Single assm-1 axial node	Water	1.03628	0.00097	
K5010BKD3	s510bk2.xxx	5.0	10	341.48	0.945	10.09375	0.1524	zirc4	300	Single assm-18 axial nodes	Water	1.05793	0.00091	-0.00235
K5010AKE3	s510ak1.xxx	5.0	10	341.48	0.945	10.09375	0.1524	zirc4	300	Single assm-1 axial node	Water	1.06210	0.00091	
K5006BLD3	s506bl2.xxx	5.0	6	341.48	0.945	10.09375	0.1524	zirc4	300	Single assm-18 axial nodes	Water	1.08307	0.00092	-0.00081
K5006ALE3	s506al1.xxx	5.0	6	341.48	0.945	10.09375	0.1524	zirc4	300	Single assm-1 axial node	Water	1.08583	0.00103	
Axial Profiles at 0 PPM														
K4062AAD1	s462aa2.xxx	4.0	62	341.48	0.945	10.09375	0.1524	zirc4	0	Single assm-18 axial nodes	Water	0.80208	0.00096	0.03046
K4062AAE1	s462aa1.xxx	4.0	62	341.48	0.945	10.09375	0.1524	zirc4	0	Single assm-1 axial node	Water	0.77332	0.00074	
K4046ABD1	s446ab2.xxx	4.0	46	341.48	0.945	10.09375	0.1524	zirc4	0	Single assm-18 axial nodes	Water	0.87055	0.00079	0.02128
K4046ABE1	s446ab1.xxx	4.0	46	341.48	0.945	10.09375	0.1524	zirc4	0	Single assm-1 axial node	Water	0.85093	0.00087	
K4042ACD1	s442ac2.xxx	4.0	42	341.48	0.945	10.09375	0.1524	zirc4	0	Single assm-18 axial nodes	Water	0.88373	0.00096	0.01195
K4042ACE1	s442ac1.xxx	4.0	42	341.48	0.945	10.09375	0.1524	zirc4	0	Single assm-1 axial node	Water	0.87350	0.00076	

K4038ADD1	s438ad2.xxx	4.0	38	341.48	0.945	10.09375	0.1524	zirc4	0	Single assm-18 axial nodes	Water	0.91851	0.00094	0.02367
K4038ADE1	s438ad1.xxx	4.0	38	341.48	0.945	10.09375	0.1524	zirc4	0	Single assm-1 axial node	Water	0.89658	0.00080	
K4034AED1	s434ae2.xxx	4.0	34	341.48	0.945	10.09375	0.1524	zirc4	0	Single assm-18 axial nodes	Water	0.93496	0.00096	0.01739
K4034AEE1	s434ae1.xxx	4.0	34	341.48	0.945	10.09375	0.1524	zirc4	0	Single assm-1 axial node	Water	0.91931	0.00078	
K4030AFD1	s430af2.xxx	4.0	30	341.48	0.945	10.09375	0.1524	zirc4	0	Single assm-18 axial nodes	Water	0.95822	0.00100	0.01559
K4030AFE1	s430af1.xxx	4.0	30	341.48	0.945	10.09375	0.1524	zirc4	0	Single assm-1 axial node	Water	0.94456	0.00093	
K4026AGD1	s426ag2.xxx	4.0	26	341.48	0.945	10.09375	0.1524	zirc4	0	Single assm-18 axial nodes	Water	0.98197	0.00011	0.01089
K4026AGE1	s426ag1.xxx	4.0	26	341.48	0.945	10.09375	0.1524	zirc4	0	Single assm-1 axial node	Water	0.97207	0.00088	
K4022AHD1	s422ah2.xxx	4.0	22	341.48	0.945	10.09375	0.1524	zirc4	0	Single assm-18 axial nodes	Water	1.00104	0.00099	0.00479
K4022AHE1	s422ah1.xxx	4.0	22	341.48	0.945	10.09375	0.1524	zirc4	0	Single assm-1 axial node	Water	0.99814	0.00090	
K4018AID1	s418ai2.xxx	4.0	18	341.48	0.945	10.09375	0.1524	zirc4	0	Single assm-18 axial nodes	Water	1.04820	0.00099	0.02645
K4018AIE1	s418ai1.xxx	4.0	18	341.48	0.945	10.09375	0.1524	zirc4	0	Single assm-1 axial node	Water	1.02363	0.00089	
K4014AJD1	s414aj2.xxx	4.0	14	341.48	0.945	10.09375	0.1524	zirc4	0	Single assm-18 axial nodes	Water	1.04819	0.00097	-0.00135
K4014AJE1	s414aj1.xxx	4.0	14	341.48	0.945	10.09375	0.1524	zirc4	0	Single assm-1 axial node	Water	1.05138	0.00087	
K4010AKD1	s410ak2.xxx	4.0	10	341.48	0.945	10.09375	0.1524	zirc4	0	Single assm-18 axial nodes	Water	1.07393	0.00093	-0.00241
K4010AKE1	s410ak1.xxx	4.0	10	341.48	0.945	10.09375	0.1524	zirc4	0	Single assm-1 axial node	Water	1.07813	0.00086	
K4006ALD1	s406al2.xxx	4.0	6	341.48	0.945	10.09375	0.1524	zirc4	0	Single assm-18 axial nodes	Water	1.10190	0.00096	-0.00406
K4006ALE1	s406al1.xxx	4.0	6	341.48	0.945	10.09375	0.1524	zirc4	0	Single assm-1 axial node	Water	1.10783	0.00091	
Axial Profiles at 0 PPM														
K4062BAD1	s462ba2.xxx	4.0	62	341.48	0.945	10.09375	0.1524	zirc4	0	Single assm-18 axial nodes	Water	0.80215	0.00104	0.03061
K4062AAE1	s462aa1.xxx	4.0	62	341.48	0.945	10.09375	0.1524	zirc4	0	Single assm-1 axial node	Water	0.77332	0.00074	
K4046BBD1	s446bb2.xxx	4.0	46	341.48	0.945	10.09375	0.1524	zirc4	0	Single assm-18 axial nodes	Water	0.86715	0.00094	0.01803
K4046ABE1	s446ab1.xxx	4.0	46	341.48	0.945	10.09375	0.1524	zirc4	0	Single assm-1 axial node	Water	0.85093	0.00087	
K4042BCD1	s442bc2.xxx	4.0	42	341.48	0.945	10.09375	0.1524	zirc4	0	Single assm-18 axial nodes	Water	0.88253	0.00087	0.01066
K4042ACE1	s442ac1.xxx	4.0	42	341.48	0.945	10.09375	0.1524	zirc4	0	Single assm-1 axial node	Water	0.87350	0.00076	
K4038BDD1	s438bd2.xxx	4.0	38	341.48	0.945	10.09375	0.1524	zirc4	0	Single assm-18 axial nodes	Water	0.91317	0.00103	0.01842
K4038ADE1	s438ad1.xxx	4.0	38	341.48	0.945	10.09375	0.1524	zirc4	0	Single assm-1 axial node	Water	0.89658	0.00080	
K4034BED1	s434be2.xxx	4.0	34	341.48	0.945	10.09375	0.1524	zirc4	0	Single assm-18 axial nodes	Water	0.93255	0.00097	0.01499
K4034AEE1	s434ae1.xxx	4.0	34	341.48	0.945	10.09375	0.1524	zirc4	0	Single assm-1 axial node	Water	0.91931	0.00078	
K4030BFD1	s430bf2.xxx	4.0	30	341.48	0.945	10.09375	0.1524	zirc4	0	Single assm-18 axial nodes	Water	0.95916	0.00095	0.01648
K4030AFE1	s430af1.xxx	4.0	30	341.48	0.945	10.09375	0.1524	zirc4	0	Single assm-1 axial node	Water	0.94456	0.00093	
K4026BGD1	s426bg2.xxx	4.0	26	341.48	0.945	10.09375	0.1524	zirc4	0	Single assm-18 axial nodes	Water	0.97947	0.00095	0.00923
K4026AGE1	s426ag1.xxx	4.0	26	341.48	0.945	10.09375	0.1524	zirc4	0	Single assm-1 axial node	Water	0.97207	0.00088	
K4022BHD1	s422bh2.xxx	4.0	22	341.48	0.945	10.09375	0.1524	zirc4	0	Single assm-18 axial nodes	Water	1.00094	0.00091	0.00461
K4022AHE1	s422ah1.xxx	4.0	22	341.48	0.945	10.09375	0.1524	zirc4	0	Single assm-1 axial node	Water	0.99814	0.00090	
K4018BID1	s418bi2.xxx	4.0	18	341.48	0.945	10.09375	0.1524	zirc4	0	Single assm-18 axial nodes	Water	1.04896	0.00082	0.02704
K4018AIE1	s418ai1.xxx	4.0	18	341.48	0.945	10.09375	0.1524	zirc4	0	Single assm-1 axial node	Water	1.02363	0.00089	

K4014BJD1	s414bj2.xxx	4.0	14	341.48	0.945	10.09375	0.1524	zirc4	0	Single assm-18 axial nodes	Water	1.05918	0.00096	0.00963
K4014AJE1	s414aj1.xxx	4.0	14	341.48	0.945	10.09375	0.1524	zirc4	0	Single assm-1 axial node	Water	1.05138	0.00087	
K4010BKD1	s410bk2.xxx	4.0	10	341.48	0.945	10.09375	0.1524	zirc4	0	Single assm-18 axial nodes	Water	1.07496	0.00080	-0.00151
K4010AKE1	s410ak1.xxx	4.0	10	341.48	0.945	10.09375	0.1524	zirc4	0	Single assm-1 axial node	Water	1.07813	0.00086	
K4006BLD1	s406bl2.xxx	4.0	6	341.48	0.945	10.09375	0.1524	zirc4	0	Single assm-18 axial nodes	Water	1.10342	0.00103	-0.00247
K4006ALE1	s406al1.xxx	4.0	6	341.48	0.945	10.09375	0.1524	zirc4	0	Single assm-1 axial node	Water	1.10783	0.00091	
Axial Profiles at 300 PPM														
K4062AAD3	s462aa2.xxx	4.0	62	341.48	0.945	10.09375	0.1524	zirc4	300	Single assm-18 axial nodes	Water	0.74486	0.00082	0.02898
K4062AAE3	s462aa1.xxx	4.0	62	341.48	0.945	10.09375	0.1524	zirc4	300	Single assm-1 axial node	Water	0.71743	0.00073	
K4046ABD3	s446ab2.xxx	4.0	46	341.48	0.945	10.09375	0.1524	zirc4	300	Single assm-18 axial nodes	Water	0.80845	0.00085	0.02062
K4046ABE3	s446ab1.xxx	4.0	46	341.48	0.945	10.09375	0.1524	zirc4	300	Single assm-1 axial node	Water	0.78950	0.00082	
K4042ACD3	s442ac2.xxx	4.0	46	341.48	0.945	10.09375	0.1524	zirc4	300	Single assm-18 axial nodes	Water	0.82387	0.00091	0.01367
K4042ACE3	s442ac1.xxx	4.0	46	341.48	0.945	10.09375	0.1524	zirc4	300	Single assm-1 axial node	Water	0.81182	0.00071	
K4038ADD3	s438ad2.xxx	4.0	38	341.48	0.945	10.09375	0.1524	zirc4	300	Single assm-18 axial nodes	Water	0.85491	0.00094	0.02418
K4038ADE3	s438ad1.xxx	4.0	38	341.48	0.945	10.09375	0.1524	zirc4	300	Single assm-1 axial node	Water	0.83250	0.00083	
K4034AED3	s434ae2.xxx	4.0	38	341.48	0.945	10.09375	0.1524	zirc4	300	Single assm-18 axial nodes	Water	0.86937	0.00095	0.01549
K4034AEE3	s434ae1.xxx	4.0	38	341.48	0.945	10.09375	0.1524	zirc4	300	Single assm-1 axial node	Water	0.85565	0.00082	
K4030AFD3	s430af2.xxx	4.0	30	341.48	0.945	10.09375	0.1524	zirc4	300	Single assm-18 axial nodes	Water	0.89376	0.00101	0.01475
K4030AFE3	s430af1.xxx	4.0	30	341.48	0.945	10.09375	0.1524	zirc4	300	Single assm-1 axial node	Water	0.88083	0.00081	
K4026AGD3	s426ag2.xxx	4.0	26	341.48	0.945	10.09375	0.1524	zirc4	300	Single assm-18 axial nodes	Water	0.91168	0.00090	0.00858
K4026AGE3	s426ag1.xxx	4.0	26	341.48	0.945	10.09375	0.1524	zirc4	300	Single assm-1 axial node	Water	0.90474	0.00074	
K4022AHD3	s422ah2.xxx	4.0	22	341.48	0.945	10.09375	0.1524	zirc4	300	Single assm-18 axial nodes	Water	0.93452	0.00099	0.00863
K4022AHE3	s422ah1.xxx	4.0	22	341.48	0.945	10.09375	0.1524	zirc4	300	Single assm-1 axial node	Water	0.92765	0.00077	
K4018AID3	s418ai2.xxx	4.0	18	341.48	0.945	10.09375	0.1524	zirc4	300	Single assm-18 axial nodes	Water	0.97727	0.00106	0.02703
K4018AIE3	s418ai1.xxx	4.0	18	341.48	0.945	10.09375	0.1524	zirc4	300	Single assm-1 axial node	Water	0.95210	0.00080	
K4014AJD3	s414aj2.xxx	4.0	14	341.48	0.945	10.09375	0.1524	zirc4	300	Single assm-18 axial nodes	Water	0.97598	0.00081	-0.00250
K4014AJE3	s414aj1.xxx	4.0	14	341.48	0.945	10.09375	0.1524	zirc4	300	Single assm-1 axial node	Water	0.98007	0.00078	
K4010AKD3	s410ak2.xxx	4.0	10	341.48	0.945	10.09375	0.1524	zirc4	300	Single assm-18 axial nodes	Water	1.00175	0.00083	-0.00208
K4010AKE3	s410ak1.xxx	4.0	10	341.48	0.945	10.09375	0.1524	zirc4	300	Single assm-1 axial node	Water	1.00557	0.00091	
K4006ALD3	s406al2.xxx	4.0	6	341.48	0.945	10.09375	0.1524	zirc4	300	Single assm-18 axial nodes	Water	1.02825	0.00085	-0.00290
K4006ALE3	s406al1.xxx	4.0	6	341.48	0.945	10.09375	0.1524	zirc4	300	Single assm-1 axial node	Water	1.03299	0.00099	
Axial Profiles at 300 PPM														
K4062BAD3	s462ba2.xxx	4.0	62	341.48	0.945	10.09375	0.1524	zirc4	300	Single assm-18 axial nodes	Water	0.74379	0.00093	0.02802
K4062AAE3	s462aa1.xxx	4.0	62	341.48	0.945	10.09375	0.1524	zirc4	300	Single assm-1 axial node	Water	0.71743	0.00073	
K4046BBD3	s446bb2.xxx	4.0	46	341.48	0.945	10.09375	0.1524	zirc4	300	Single assm-18 axial nodes	Water	0.80520	0.00092	0.01744
K4046ABE3	s446ab1.xxx	4.0	46	341.48	0.945	10.09375	0.1524	zirc4	300	Single assm-1 axial node	Water	0.78950	0.00082	
K4042BCD3	s442bc2.xxx	4.0	46	341.48	0.945	10.09375	0.1524	zirc4	300	Single assm-18 axial nodes	Water	0.81795	0.00107	0.00791

K4042ACE3	s442ac1.xxx	4.0	46	341.48	0.945	10.09375	0.1524	zirc4	300	Single assm-1 axial node	Water	0.81182	0.00071	
K4038BDD3	s438bd2.xxx	4.0	38	341.48	0.945	10.09375	0.1524	zirc4	300	Single assm-18 axial nodes	Water	0.84721	0.00096	0.01650
K4038ADE3	s438ad1.xxx	4.0	38	341.48	0.945	10.09375	0.1524	zirc4	300	Single assm-1 axial node	Water	0.83250	0.00083	
K4034BED3	s434be2.xxx	4.0	38	341.48	0.945	10.09375	0.1524	zirc4	300	Single assm-18 axial nodes	Water	0.86626	0.00074	0.01217
K4034AEE3	s434ae1.xxx	4.0	38	341.48	0.945	10.09375	0.1524	zirc4	300	Single assm-1 axial node	Water	0.85565	0.00082	
K4030BFD3	s430bf2.xxx	4.0	30	341.48	0.945	10.09375	0.1524	zirc4	300	Single assm-18 axial nodes	Water	0.89257	0.00104	0.01359
K4030AFE3	s430af1.xxx	4.0	30	341.48	0.945	10.09375	0.1524	zirc4	300	Single assm-1 axial node	Water	0.88083	0.00081	
K4026BGD3	s426bg2.xxx	4.0	26	341.48	0.945	10.09375	0.1524	zirc4	300	Single assm-18 axial nodes	Water	0.91314	0.00088	0.01002
K4026AGE3	s426ag1.xxx	4.0	26	341.48	0.945	10.09375	0.1524	zirc4	300	Single assm-1 axial node	Water	0.90474	0.00074	
K4022BHD3	s422bh2.xxx	4.0	22	341.48	0.945	10.09375	0.1524	zirc4	300	Single assm-18 axial nodes	Water	0.93016	0.00102	0.00430
K4022AHE3	s422ah1.xxx	4.0	22	341.48	0.945	10.09375	0.1524	zirc4	300	Single assm-1 axial node	Water	0.92765	0.00077	
K4018BID3	s418bi2.xxx	4.0	18	341.48	0.945	10.09375	0.1524	zirc4	300	Single assm-18 axial nodes	Water	0.97695	0.00104	0.02669
K4018AIE3	s418ai1.xxx	4.0	18	341.48	0.945	10.09375	0.1524	zirc4	300	Single assm-1 axial node	Water	0.95210	0.00080	
K4014BJD3	s414bj2.xxx	4.0	14	341.48	0.945	10.09375	0.1524	zirc4	300	Single assm-18 axial nodes	Water	0.98657	0.00083	0.00811
K4014AJE3	s414aj1.xxx	4.0	14	341.48	0.945	10.09375	0.1524	zirc4	300	Single assm-1 axial node	Water	0.98007	0.00078	
K4010BKD3	s410bk2.xxx	4.0	10	341.48	0.945	10.09375	0.1524	zirc4	300	Single assm-18 axial nodes	Water	1.00358	0.00085	-0.00023
K4010AKE3	s410ak1.xxx	4.0	10	341.48	0.945	10.09375	0.1524	zirc4	300	Single assm-1 axial node	Water	1.00557	0.00091	
K4006BLD3	s406bl2.xxx	4.0	6	341.48	0.945	10.09375	0.1524	zirc4	300	Single assm-18 axial nodes	Water	1.03200	0.00091	0.00091
K4006ALE3	s406al1.xxx	4.0	6	341.48	0.945	10.09375	0.1524	zirc4	300	Single assm-1 axial node	Water	1.03299	0.00099	
Axial Profiles at 0 PPM														
K3062AAD1	s362aa2.xxx	3.0	62	341.48	0.945	10.09375	0.1524	zirc4	0	Single assm-18 axial nodes	Water	0.74309	0.00090	0.01704
K3062AAE1	s362aa1.xxx	3.0	62	341.48	0.945	10.09375	0.1524	zirc4	0	Single assm-1 axial node	Water	0.72764	0.00069	
K3046ABD1	s346ab2.xxx	3.0	46	341.48	0.945	10.09375	0.1524	zirc4	0	Single assm-18 axial nodes	Water	0.79727	0.00083	0.01459
K3046ABE1	s346ab1.xxx	3.0	46	341.48	0.945	10.09375	0.1524	zirc4	0	Single assm-1 axial node	Water	0.78431	0.00080	
K3042ACD1	s342ac2.xxx	3.0	42	341.48	0.945	10.09375	0.1524	zirc4	0	Single assm-18 axial nodes	Water	0.81294	0.00083	0.01380
K3042ACE1	s342ac1.xxx	3.0	42	341.48	0.945	10.09375	0.1524	zirc4	0	Single assm-1 axial node	Water	0.80075	0.00078	
K3038ADD1	s338ad2.xxx	3.0	38	341.48	0.945	10.09375	0.1524	zirc4	0	Single assm-18 axial nodes	Water	0.84467	0.00096	0.02465
K3038ADE1	s338ad1.xxx	3.0	38	341.48	0.945	10.09375	0.1524	zirc4	0	Single assm-1 axial node	Water	0.82169	0.00071	
K3034AED1	s334ae2.xxx	3.0	34	341.48	0.945	10.09375	0.1524	zirc4	0	Single assm-18 axial nodes	Water	0.86022	0.00086	0.01684
K3034AEE1	s334ae1.xxx	3.0	34	341.48	0.945	10.09375	0.1524	zirc4	0	Single assm-1 axial node	Water	0.84505	0.00081	
K3030AFD1	s330af2.xxx	3.0	30	341.48	0.945	10.09375	0.1524	zirc4	0	Single assm-18 axial nodes	Water	0.88332	0.00090	0.01609
K3030AFE1	s330af1.xxx	3.0	30	341.48	0.945	10.09375	0.1524	zirc4	0	Single assm-1 axial node	Water	0.86888	0.00075	
K3026AGD1	s326ag2.xxx	3.0	26	341.48	0.945	10.09375	0.1524	zirc4	0	Single assm-18 axial nodes	Water	0.90835	0.00086	0.01730
K3026AGE1	s326ag1.xxx	3.0	26	341.48	0.945	10.09375	0.1524	zirc4	0	Single assm-1 axial node	Water	0.89268	0.00077	
K3022AHD1	s322ah2.xxx	3.0	22	341.48	0.945	10.09375	0.1524	zirc4	0	Single assm-18 axial nodes	Water	0.92670	0.00080	0.00914
K3022AHE1	s322ah1.xxx	3.0	22	341.48	0.945	10.09375	0.1524	zirc4	0	Single assm-1 axial node	Water	0.91917	0.00081	
K3018AID1	s318ai2.xxx	3.0	18	341.48	0.945	10.09375	0.1524	zirc4	0	Single assm-18 axial nodes	Water	0.97541	0.00107	0.02942

K3018AIE1	s318ai1.xxx	3.0	18	341.48	0.945	10.09375	0.1524	zirc4	0	Single assm-1 axial node	Water	0.94783	0.00077	
K3014AJD1	s314aj2.xxx	3.0	14	341.48	0.945	10.09375	0.1524	zirc4	0	Single assm-18 axial nodes	Water	0.97395	0.00087	-0.00052
K3014AJE1	s314aj1.xxx	3.0	14	341.48	0.945	10.09375	0.1524	zirc4	0	Single assm-1 axial node	Water	0.97620	0.00086	
K3010AKD1	s310ak2.xxx	3.0	10	341.48	0.945	10.09375	0.1524	zirc4	0	Single assm-18 axial nodes	Water	1.00359	0.00079	-0.00079
K3010AKE1	s310ak1.xxx	3.0	10	341.48	0.945	10.09375	0.1524	zirc4	0	Single assm-1 axial node	Water	1.00603	0.00086	
K3006ALD1	s306al2.xxx	3.0	6	341.48	0.945	10.09375	0.1524	zirc4	0	Single assm-18 axial nodes	Water	1.03277	0.00100	-0.00169
K3006ALE1	s306al1.xxx	3.0	6	341.48	0.945	10.09375	0.1524	zirc4	0	Single assm-1 axial node	Water	1.03625	0.00079	
Axial Profiles at 0 PPM														
K3062BAD1	s362ba2.xxx	3.0	62	341.48	0.945	10.09375	0.1524	zirc4	0	Single assm-18 axial nodes	Water	0.74092	0.00073	0.01470
K3062AAE1	s362aa1.xxx	3.0	62	341.48	0.945	10.09375	0.1524	zirc4	0	Single assm-1 axial node	Water	0.72764	0.00069	
K3046BBD1	s346bb2.xxx	3.0	46	341.48	0.945	10.09375	0.1524	zirc4	0	Single assm-18 axial nodes	Water	0.79649	0.00075	0.01373
K3046ABE1	s346ab1.xxx	3.0	46	341.48	0.945	10.09375	0.1524	zirc4	0	Single assm-1 axial node	Water	0.78431	0.00080	
K3042BCD1	s342bc2.xxx	3.0	42	341.48	0.945	10.09375	0.1524	zirc4	0	Single assm-18 axial nodes	Water	0.80923	0.00080	0.01006
K3042ACE1	s342ac1.xxx	3.0	42	341.48	0.945	10.09375	0.1524	zirc4	0	Single assm-1 axial node	Water	0.80075	0.00078	
K3038BDD1	s338bd2.xxx	3.0	38	341.48	0.945	10.09375	0.1524	zirc4	0	Single assm-18 axial nodes	Water	0.83911	0.00099	0.01912
K3038ADE1	s338ad1.xxx	3.0	38	341.48	0.945	10.09375	0.1524	zirc4	0	Single assm-1 axial node	Water	0.82169	0.00071	
K3034BED1	s334be2.xxx	3.0	34	341.48	0.945	10.09375	0.1524	zirc4	0	Single assm-18 axial nodes	Water	0.85793	0.00084	0.01453
K3034AEE1	s334ae1.xxx	3.0	34	341.48	0.945	10.09375	0.1524	zirc4	0	Single assm-1 axial node	Water	0.84505	0.00081	
K3030BFD1	s330bf2.xxx	3.0	30	341.48	0.945	10.09375	0.1524	zirc4	0	Single assm-18 axial nodes	Water	0.88298	0.00099	0.01584
K3030AFE1	s330af1.xxx	3.0	30	341.48	0.945	10.09375	0.1524	zirc4	0	Single assm-1 axial node	Water	0.86888	0.00075	
K3026BGD1	s326bg2.xxx	3.0	26	341.48	0.945	10.09375	0.1524	zirc4	0	Single assm-18 axial nodes	Water	0.90498	0.00094	0.01401
K3026AGE1	s326ag1.xxx	3.0	26	341.48	0.945	10.09375	0.1524	zirc4	0	Single assm-1 axial node	Water	0.89268	0.00077	
K3022BHD1	s322bh2.xxx	3.0	22	341.48	0.945	10.09375	0.1524	zirc4	0	Single assm-18 axial nodes	Water	0.92658	0.00087	0.00909
K3022AHE1	s322ah1.xxx	3.0	22	341.48	0.945	10.09375	0.1524	zirc4	0	Single assm-1 axial node	Water	0.91917	0.00081	
K3018BID1	s318bi2.xxx	3.0	18	341.48	0.945	10.09375	0.1524	zirc4	0	Single assm-18 axial nodes	Water	0.97460	0.00099	0.02853
K3018AIE1	s318ai1.xxx	3.0	18	341.48	0.945	10.09375	0.1524	zirc4	0	Single assm-1 axial node	Water	0.94783	0.00077	
K3014BJD1	s314bj2.xxx	3.0	14	341.48	0.945	10.09375	0.1524	zirc4	0	Single assm-18 axial nodes	Water	0.98446	0.00096	0.01008
K3014AJE1	s314aj1.xxx	3.0	14	341.48	0.945	10.09375	0.1524	zirc4	0	Single assm-1 axial node	Water	0.97620	0.00086	
K3010BKD1	s310bk2.xxx	3.0	10	341.48	0.945	10.09375	0.1524	zirc4	0	Single assm-18 axial nodes	Water	1.00535	0.00084	0.00102
K3010AKE1	s310ak1.xxx	3.0	10	341.48	0.945	10.09375	0.1524	zirc4	0	Single assm-1 axial node	Water	1.00603	0.00086	
K3006BLD1	s306bl2.xxx	3.0	6	341.48	0.945	10.09375	0.1524	zirc4	0	Single assm-18 axial nodes	Water	1.03359	0.00078	-0.00109
K3006ALE1	s306al1.xxx	3.0	6	341.48	0.945	10.09375	0.1524	zirc4	0	Single assm-1 axial node	Water	1.03625	0.00079	
Axial Profiles at 300 PPM														
K3062AAD3	s362aa2.xxx	3.0	62	341.48	0.945	10.09375	0.1524	zirc4	300	Single assm-18 axial nodes	Water	0.68572	0.00082	0.01423
K3062AAE3	s362aa1.xxx	3.0	62	341.48	0.945	10.09375	0.1524	zirc4	300	Single assm-1 axial node	Water	0.67297	0.00066	
K3046ABD3	s346ab2.xxx	3.0	46	341.48	0.945	10.09375	0.1524	zirc4	300	Single assm-18 axial nodes	Water	0.73814	0.00084	0.01619
K3046ABE3	s346ab1.xxx	3.0	46	341.48	0.945	10.09375	0.1524	zirc4	300	Single assm-1 axial node	Water	0.72350	0.00071	

K3042ACD3	s342ac2.xxx	3.0	46	341.48	0.945	10.09375	0.1524	zirc4	300	Single assm-18 axial nodes	Water	0.75227	0.00068	0.01345
K3042ACE3	s342ac1.xxx	3.0	46	341.48	0.945	10.09375	0.1524	zirc4	300	Single assm-1 axial node	Water	0.74023	0.00073	
K3038ADD3	s338ad2.xxx	3.0	38	341.48	0.945	10.09375	0.1524	zirc4	300	Single assm-18 axial nodes	Water	0.78138	0.00079	0.02391
K3038ADE3	s338ad1.xxx	3.0	38	341.48	0.945	10.09375	0.1524	zirc4	300	Single assm-1 axial node	Water	0.75899	0.00073	
K3034AED3	s334ae2.xxx	3.0	38	341.48	0.945	10.09375	0.1524	zirc4	300	Single assm-18 axial nodes	Water	0.79473	0.00089	0.01495
K3034AEE3	s334ae1.xxx	3.0	38	341.48	0.945	10.09375	0.1524	zirc4	300	Single assm-1 axial node	Water	0.78137	0.00070	
K3030AFD3	s330af2.xxx	3.0	30	341.48	0.945	10.09375	0.1524	zirc4	300	Single assm-18 axial nodes	Water	0.81765	0.00105	0.01616
K3030AFE3	s330af1.xxx	3.0	30	341.48	0.945	10.09375	0.1524	zirc4	300	Single assm-1 axial node	Water	0.80341	0.00087	
K3026AGD3	s326ag2.xxx	3.0	26	341.48	0.945	10.09375	0.1524	zirc4	300	Single assm-18 axial nodes	Water	0.83919	0.00085	0.01544
K3026AGE3	s326ag1.xxx	3.0	26	341.48	0.945	10.09375	0.1524	zirc4	300	Single assm-1 axial node	Water	0.82538	0.00078	
K3022AHD3	s322ah2.xxx	3.0	22	341.48	0.945	10.09375	0.1524	zirc4	300	Single assm-18 axial nodes	Water	0.85846	0.00097	0.00869
K3022AHE3	s322ah1.xxx	3.0	22	341.48	0.945	10.09375	0.1524	zirc4	300	Single assm-1 axial node	Water	0.85156	0.00082	
K3018AID3	s318ai2.xxx	3.0	18	341.48	0.945	10.09375	0.1524	zirc4	300	Single assm-18 axial nodes	Water	0.90243	0.00091	0.02705
K3018AIE3	s318ai1.xxx	3.0	18	341.48	0.945	10.09375	0.1524	zirc4	300	Single assm-1 axial node	Water	0.87730	0.00101	
K3014AJD3	s314aj2.xxx	3.0	14	341.48	0.945	10.09375	0.1524	zirc4	300	Single assm-18 axial nodes	Water	0.90353	0.00083	0.00036
K3014AJE3	s314aj1.xxx	3.0	14	341.48	0.945	10.09375	0.1524	zirc4	300	Single assm-1 axial node	Water	0.90487	0.00087	
K3010AKD3	s310ak2.xxx	3.0	10	341.48	0.945	10.09375	0.1524	zirc4	300	Single assm-18 axial nodes	Water	0.92889	0.00077	-0.00224
K3010AKE3	s310ak1.xxx	3.0	10	341.48	0.945	10.09375	0.1524	zirc4	300	Single assm-1 axial node	Water	0.93267	0.00077	
K3006ALD3	s306al2.xxx	3.0	6	341.48	0.945	10.09375	0.1524	zirc4	300	Single assm-18 axial nodes	Water	0.95490	0.00079	-0.00331
K3006ALE3	s306al1.xxx	3.0	6	341.48	0.945	10.09375	0.1524	zirc4	300	Single assm-1 axial node	Water	0.95977	0.00077	
Axial Profiles at 300 PPM														
K3062BAD3	s362ba2.xxx	3.0	62	341.48	0.945	10.09375	0.1524	zirc4	300	Single assm-18 axial nodes	Water	0.68415	0.00087	0.01271
K3062AAE3	s362aa1.xxx	3.0	62	341.48	0.945	10.09375	0.1524	zirc4	300	Single assm-1 axial node	Water	0.67297	0.00066	
K3046BBD3	s346bb2.xxx	3.0	46	341.48	0.945	10.09375	0.1524	zirc4	300	Single assm-18 axial nodes	Water	0.73730	0.00091	0.01542
K3046ABE3	s346ab1.xxx	3.0	46	341.48	0.945	10.09375	0.1524	zirc4	300	Single assm-1 axial node	Water	0.72350	0.00071	
K3042BCD3	s342bc2.xxx	3.0	46	341.48	0.945	10.09375	0.1524	zirc4	300	Single assm-18 axial nodes	Water	0.74910	0.00081	0.01041
K3042ACE3	s342ac1.xxx	3.0	46	341.48	0.945	10.09375	0.1524	zirc4	300	Single assm-1 axial node	Water	0.74023	0.00073	
K3038BDD3	s338bd2.xxx	3.0	38	341.48	0.945	10.09375	0.1524	zirc4	300	Single assm-18 axial nodes	Water	0.77575	0.00093	0.01842
K3038ADE3	s338ad1.xxx	3.0	38	341.48	0.945	10.09375	0.1524	zirc4	300	Single assm-1 axial node	Water	0.75899	0.00073	
K3034BED3	s334be2.xxx	3.0	38	341.48	0.945	10.09375	0.1524	zirc4	300	Single assm-18 axial nodes	Water	0.79238	0.00078	0.01249
K3034AEE3	s334ae1.xxx	3.0	38	341.48	0.945	10.09375	0.1524	zirc4	300	Single assm-1 axial node	Water	0.78137	0.00070	
K3030BFD3	s330bf2.xxx	3.0	30	341.48	0.945	10.09375	0.1524	zirc4	300	Single assm-18 axial nodes	Water	0.81780	0.00086	0.01612
K3030AFE3	s330af1.xxx	3.0	30	341.48	0.945	10.09375	0.1524	zirc4	300	Single assm-1 axial node	Water	0.80341	0.00087	
K3026BGD3	s326bg2.xxx	3.0	26	341.48	0.945	10.09375	0.1524	zirc4	300	Single assm-18 axial nodes	Water	0.83862	0.00097	0.01499
K3026AGE3	s326ag1.xxx	3.0	26	341.48	0.945	10.09375	0.1524	zirc4	300	Single assm-1 axial node	Water	0.82538	0.00078	
K3022BHD3	s322bh2.xxx	3.0	22	341.48	0.945	10.09375	0.1524	zirc4	300	Single assm-18 axial nodes	Water	0.85879	0.00086	0.00891
K3022AHE3	s322ah1.xxx	3.0	22	341.48	0.945	10.09375	0.1524	zirc4	300	Single assm-1 axial node	Water	0.85156	0.00082	

K3018BID3	s318bi2.xxx	3.0	18	341.48	0.945	10.09375	0.1524	zirc4	300	Single assm-18 axial nodes	Water	0.90273	0.00109	0.02753
K3018AIE3	s318ai1.xxx	3.0	18	341.48	0.945	10.09375	0.1524	zirc4	300	Single assm-1 axial node	Water	0.87730	0.00101	
K3014BJD3	s314bj2.xxx	3.0	14	341.48	0.945	10.09375	0.1524	zirc4	300	Single assm-18 axial nodes	Water	0.91129	0.00085	0.00814
K3014AJE3	s314aj1.xxx	3.0	14	341.48	0.945	10.09375	0.1524	zirc4	300	Single assm-1 axial node	Water	0.90487	0.00087	
K3010BKD3	s310bk2.xxx	3.0	10	341.48	0.945	10.09375	0.1524	zirc4	300	Single assm-18 axial nodes	Water	0.92854	0.00092	-0.00244
K3010AKE3	s310ak1.xxx	3.0	10	341.48	0.945	10.09375	0.1524	zirc4	300	Single assm-1 axial node	Water	0.93267	0.00077	
K3006BLD3	s306bl2.xxx	3.0	6	341.48	0.945	10.09375	0.1524	zirc4	300	Single assm-18 axial nodes	Water	0.95819	0.00091	0.00010
K3006ALE3	s306al1.xxx	3.0	6	341.48	0.945	10.09375	0.1524	zirc4	300	Single assm-1 axial node	Water	0.95977	0.00077	
Axial Profiles at 0 PPM														
K501S0A	s501s02.xxx	5.0	48.013	341.48	0.945	10.09375	0.1524	zirc4	0	Single assm-18 axial nodes	Water	0.89127	0.00085	-0.01135
K501S0B	s501s01.xxx	5.0	48.013	341.48	0.945	10.09375	0.1524	zirc4	0	Single assm-1 axial node	Water	0.90432	0.00085	
K502S0A	s502s02.xxx	5.0	46.688	341.48	0.945	10.09375	0.1524	zirc4	0	Single assm-18 axial nodes	Water	0.90032	0.00088	-0.00875
K502S0B	s502s01.xxx	5.0	46.688	341.48	0.945	10.09375	0.1524	zirc4	0	Single assm-1 axial node	Water	0.91074	0.00079	
K503S1A	s503s12.xxx	5.0	49.523	341.48	0.945	10.09375	0.1524	zirc4	0	Single assm-18 axial nodes	Water	0.88684	0.00077	-0.00838
K503S1B	s503s11.xxx	5.0	49.523	341.48	0.945	10.09375	0.1524	zirc4	0	Single assm-1 axial node	Water	0.89679	0.00080	
K504V0A	s504v02.xxx	5.0	14.895	341.48	0.945	10.09375	0.1524	zirc4	0	Single assm-18 axial nodes	Water	1.09373	0.00090	-0.00649
K504V0B	s504v01.xxx	5.0	14.895	341.48	0.945	10.09375	0.1524	zirc4	0	Single assm-1 axial node	Water	1.10196	0.00084	
K505T0A	s505t02.xxx	5.0	35.696	341.48	0.945	10.09375	0.1524	zirc4	0	Single assm-18 axial nodes	Water	0.96314	0.00077	-0.01075
K505T0B	s505t01.xxx	5.0	35.696	341.48	0.945	10.09375	0.1524	zirc4	0	Single assm-1 axial node	Water	0.97553	0.00087	
K506V1A	s506v12.xxx	5.0	20.408	341.48	0.945	10.09375	0.1524	zirc4	0	Single assm-18 axial nodes	Water	1.05680	0.00087	-0.00934
K506V1B	s506v11.xxx	5.0	20.408	341.48	0.945	10.09375	0.1524	zirc4	0	Single assm-1 axial node	Water	1.06800	0.00099	
K507V0A	s507v02.xxx	5.0	22.090	341.48	0.945	10.09375	0.1524	zirc4	0	Single assm-18 axial nodes	Water	1.04669	0.00101	-0.00761
K507V0B	s507v01.xxx	5.0	22.090	341.48	0.945	10.09375	0.1524	zirc4	0	Single assm-1 axial node	Water	1.05614	0.00083	
K508S2A	s508s22.xxx	5.0	51.485	341.48	0.945	10.09375	0.1524	zirc4	0	Single assm-18 axial nodes	Water	0.87445	0.00085	-0.00863
K508S2B	s508s21.xxx	5.0	51.485	341.48	0.945	10.09375	0.1524	zirc4	0	Single assm-1 axial node	Water	0.88469	0.00076	
K509V0A	s509v02.xxx	5.0	18.880	341.48	0.945	10.09375	0.1524	zirc4	0	Single assm-18 axial nodes	Water	1.06785	0.00085	-0.00579
K509V0B	s509v01.xxx	5.0	18.880	341.48	0.945	10.09375	0.1524	zirc4	0	Single assm-1 axial node	Water	1.07543	0.00094	
K510T0A	s510t02.xxx	5.0	35.485	341.48	0.945	10.09375	0.1524	zirc4	0	Single assm-18 axial nodes	Water	0.96462	0.00082	-0.01080
K510T0B	s510t01.xxx	5.0	35.485	341.48	0.945	10.09375	0.1524	zirc4	0	Single assm-1 axial node	Water	0.97705	0.00081	
K511V1A	s511v12.xxx	5.0	25.651	341.48	0.945	10.09375	0.1524	zirc4	0	Single assm-18 axial nodes	Water	1.02649	0.00099	-0.00581
K511V1B	s511v11.xxx	5.0	25.651	341.48	0.945	10.09375	0.1524	zirc4	0	Single assm-1 axial node	Water	1.03419	0.00090	
K512T0A	s512t02.xxx	5.0	41.171	341.48	0.945	10.09375	0.1524	zirc4	0	Single assm-18 axial nodes	Water	0.93159	0.00082	-0.01016
K512T0B	s512t01.xxx	5.0	41.171	341.48	0.945	10.09375	0.1524	zirc4	0	Single assm-1 axial node	Water	0.94338	0.00081	
K513T1A	s513t12.xxx	5.0	42.997	341.48	0.945	10.09375	0.1524	zirc4	0	Single assm-18 axial nodes	Water	0.92007	0.00079	-0.01064
K513T1B	s513t11.xxx	5.0	42.997	341.48	0.945	10.09375	0.1524	zirc4	0	Single assm-1 axial node	Water	0.93228	0.00078	
K514T2A	s514t22.xxx	5.0	35.350	341.48	0.945	10.09375	0.1524	zirc4	0	Single assm-18 axial nodes	Water	0.96551	0.00084	-0.01111
K514T2B	s514t21.xxx	5.0	35.350	341.48	0.945	10.09375	0.1524	zirc4	0	Single assm-1 axial node	Water	0.97838	0.00092	

K515V0A	s515v02.xxx	5.0	19.295	341.48	0.945	10.09375	0.1524	zirc4	0	Single assm-18 axial nodes	Water	1.06410	0.00088	-0.00902
K515V0B	s515v01.xxx	5.0	19.295	341.48	0.945	10.09375	0.1524	zirc4	0	Single assm-1 axial node	Water	1.07477	0.00077	
K516T2A	s516t22.xxx	5.0	46.518	341.48	0.945	10.09375	0.1524	zirc4	0	Single assm-18 axial nodes	Water	0.90079	0.00085	-0.00887
K516T2B	s516t21.xxx	5.0	46.518	341.48	0.945	10.09375	0.1524	zirc4	0	Single assm-1 axial node	Water	0.91128	0.00077	
K517V1A	s517v12.xxx	5.0	26.726	341.48	0.945	10.09375	0.1524	zirc4	0	Single assm-18 axial nodes	Water	1.01743	0.00080	-0.00914
K517V1B	s517v11.xxx	5.0	26.726	341.48	0.945	10.09375	0.1524	zirc4	0	Single assm-1 axial node	Water	1.02815	0.00078	
K518T2A	s518t22.xxx	5.0	49.829	341.48	0.945	10.09375	0.1524	zirc4	0	Single assm-18 axial nodes	Water	0.88105	0.00076	-0.01169
K518T2B	s518t21.xxx	5.0	49.829	341.48	0.945	10.09375	0.1524	zirc4	0	Single assm-1 axial node	Water	0.89428	0.00078	
K519V1A	s519v12.xxx	5.0	27.257	341.48	0.945	10.09375	0.1524	zirc4	0	Single assm-18 axial nodes	Water	1.01588	0.00086	-0.00765
K519V1B	s519v11.xxx	5.0	27.257	341.48	0.945	10.09375	0.1524	zirc4	0	Single assm-1 axial node	Water	1.02522	0.00083	
K520T2A	s520t22.xxx	5.0	48.874	341.48	0.945	10.09375	0.1524	zirc4	0	Single assm-18 axial nodes	Water	0.88802	0.00083	-0.00977
K520T2B	s520t21.xxx	5.0	48.874	341.48	0.945	10.09375	0.1524	zirc4	0	Single assm-1 axial node	Water	0.89937	0.00075	
K524V1A	s524v12.xxx	5.0	26.492	341.48	0.945	10.09375	0.1524	zirc4	0	Single assm-18 axial nodes	Water	1.01997	0.00079	-0.00935
K524V1B	s524v11.xxx	5.0	26.492	341.48	0.945	10.09375	0.1524	zirc4	0	Single assm-1 axial node	Water	1.03091	0.00080	
K525T2A	s525t22.xxx	5.0	47.452	341.48	0.945	10.09375	0.1524	zirc4	0	Single assm-18 axial nodes	Water	0.89696	0.00076	-0.00864
K525T2B	s525t21.xxx	5.0	47.452	341.48	0.945	10.09375	0.1524	zirc4	0	Single assm-1 axial node	Water	0.90720	0.00084	
K526V1A	s526v12.xxx	5.0	27.861	341.48	0.945	10.09375	0.1524	zirc4	0	Single assm-18 axial nodes	Water	1.01223	0.00087	-0.00680
K526V1B	s526v11.xxx	5.0	27.861	341.48	0.945	10.09375	0.1524	zirc4	0	Single assm-1 axial node	Water	1.02083	0.00093	
K527T2A	s527t22.xxx	5.0	50.026	341.48	0.945	10.09375	0.1524	zirc4	0	Single assm-18 axial nodes	Water	0.88127	0.00076	-0.01105
K527T2B	s527t21.xxx	5.0	50.026	341.48	0.945	10.09375	0.1524	zirc4	0	Single assm-1 axial node	Water	0.89381	0.00073	
K528V1A	s528v12.xxx	5.0	27.664	341.48	0.945	10.09375	0.1524	zirc4	0	Single assm-18 axial nodes	Water	1.01291	0.00086	-0.00847
K528V1B	s528v11.xxx	5.0	27.664	341.48	0.945	10.09375	0.1524	zirc4	0	Single assm-1 axial node	Water	1.02300	0.00076	
K533V2A	s533v22.xxx	5.0	27.782	341.48	0.945	10.09375	0.1524	zirc4	0	Single assm-18 axial nodes	Water	1.01279	0.00085	-0.00699
K533V2B	s533v21.xxx	5.0	27.782	341.48	0.945	10.09375	0.1524	zirc4	0	Single assm-1 axial node	Water	1.02151	0.00088	
K534T2A	s534t22.xxx	5.0	49.939	341.48	0.945	10.09375	0.1524	zirc4	0	Single assm-18 axial nodes	Water	0.88212	0.00079	-0.01008
K534T2B	s534t21.xxx	5.0	49.939	341.48	0.945	10.09375	0.1524	zirc4	0	Single assm-1 axial node	Water	0.89385	0.00086	
K535V2A	s535v22.xxx	5.0	27.639	341.48	0.945	10.09375	0.1524	zirc4	0	Single assm-18 axial nodes	Water	1.01361	0.00082	-0.00797
K535V2B	s535v21.xxx	5.0	27.639	341.48	0.945	10.09375	0.1524	zirc4	0	Single assm-1 axial node	Water	1.02327	0.00087	
K536T2A	s536t22.xxx	5.0	49.592	341.48	0.945	10.09375	0.1524	zirc4	0	Single assm-18 axial nodes	Water	0.88620	0.00079	-0.00679
K536T2B	s536t21.xxx	5.0	49.592	341.48	0.945	10.09375	0.1524	zirc4	0	Single assm-1 axial node	Water	0.89460	0.00082	
K542V2A	s542v22.xxx	5.0	27.667	341.48	0.945	10.09375	0.1524	zirc4	0	Single assm-18 axial nodes	Water	1.01453	0.00078	-0.00660
K542V2B	s542v21.xxx	5.0	27.667	341.48	0.945	10.09375	0.1524	zirc4	0	Single assm-1 axial node	Water	1.02275	0.00084	
K543T2A	s543t22.xxx	5.0	49.325	341.48	0.945	10.09375	0.1524	zirc4	0	Single assm-18 axial nodes	Water	0.88586	0.00077	-0.00952
K543T2B	s543t21.xxx	5.0	49.325	341.48	0.945	10.09375	0.1524	zirc4	0	Single assm-1 axial node	Water	0.89691	0.00076	
K544V2A	s544v22.xxx	5.0	27.779	341.48	0.945	10.09375	0.1524	zirc4	0	Single assm-18 axial nodes	Water	1.01270	0.00091	-0.00864
K544V2B	s544v21.xxx	5.0	27.779	341.48	0.945	10.09375	0.1524	zirc4	0	Single assm-1 axial node	Water	1.02305	0.00080	
K552V2A	s552v22.xxx	5.0	27.236	341.48	0.945	10.09375	0.1524	zirc4	0	Single assm-18 axial nodes	Water	1.01566	0.00094	-0.00780

K552V2B	s552v21.xxx	5.0	27.236	341.48	0.945	10.09375	0.1524	zirc4	0	Single assm-1 axial node	Water	1.02526	0.00086	
K553T0A	s553t02.xxx	5.0	40.843	341.48	0.945	10.09375	0.1524	zirc4	0	Single assm-18 axial nodes	Water	0.93400	0.00086	-0.00914
K553T0B	s553t01.xxx	5.0	40.843	341.48	0.945	10.09375	0.1524	zirc4	0	Single assm-1 axial node	Water	0.94473	0.00073	
K554S0A	s554s02.xxx	5.0	46.417	341.48	0.945	10.09375	0.1524	zirc4	0	Single assm-18 axial nodes	Water	0.90097	0.00075	-0.01068
K554S0B	s554s01.xxx	5.0	46.417	341.48	0.945	10.09375	0.1524	zirc4	0	Single assm-1 axial node	Water	0.91314	0.00074	
K555V0A	s555v02.xxx	5.0	22.094	341.48	0.945	10.09375	0.1524	zirc4	0	Single assm-18 axial nodes	Water	1.04789	0.00085	-0.00777
K555V0B	s555v01.xxx	5.0	22.094	341.48	0.945	10.09375	0.1524	zirc4	0	Single assm-1 axial node	Water	1.05741	0.00090	
K556T1A	s556t12.xxx	5.0	42.987	341.48	0.945	10.09375	0.1524	zirc4	0	Single assm-18 axial nodes	Water	0.92007	0.00077	-0.01120
K556T1B	s556t11.xxx	5.0	42.987	341.48	0.945	10.09375	0.1524	zirc4	0	Single assm-1 axial node	Water	0.93279	0.00075	
K557T2A	s557t22.xxx	5.0	48.568	341.48	0.945	10.09375	0.1524	zirc4	0	Single assm-18 axial nodes	Water	0.88947	0.00075	-0.01021
K557T2B	s557t21.xxx	5.0	48.568	341.48	0.945	10.09375	0.1524	zirc4	0	Single assm-1 axial node	Water	0.90122	0.00079	
K558V1A	s558v12.xxx	5.0	27.667	341.48	0.945	10.09375	0.1524	zirc4	0	Single assm-18 axial nodes	Water	1.01443	0.00081	-0.00667
K558V1B	s558v11.xxx	5.0	27.667	341.48	0.945	10.09375	0.1524	zirc4	0	Single assm-1 axial node	Water	1.02275	0.00084	
K559T2A	s559t22.xxx	5.0	49.583	341.48	0.945	10.09375	0.1524	zirc4	0	Single assm-18 axial nodes	Water	0.88405	0.00080	-0.00905
K559T2B	s559t21.xxx	5.0	49.583	341.48	0.945	10.09375	0.1524	zirc4	0	Single assm-1 axial node	Water	0.89462	0.00072	
K560V2A	s560v22.xxx	5.0	27.735	341.48	0.945	10.09375	0.1524	zirc4	0	Single assm-18 axial nodes	Water	1.01220	0.00087	-0.00956
K560V2B	s560v21.xxx	5.0	27.735	341.48	0.945	10.09375	0.1524	zirc4	0	Single assm-1 axial node	Water	1.02346	0.00083	
K561T0A	s561t02.xxx	5.0	43.765	341.48	0.945	10.09375	0.1524	zirc4	0	Single assm-18 axial nodes	Water	0.91574	0.00086	-0.01120
K561T0B	s561t01.xxx	5.0	43.765	341.48	0.945	10.09375	0.1524	zirc4	0	Single assm-1 axial node	Water	0.92865	0.00085	
K562J0A	s562j02.xxx	5.0	50.648	341.48	0.945	10.09375	0.1524	zirc4	0	Single assm-18 axial nodes	Water	0.88103	0.00074	-0.00700
K562J0B	s562j01.xxx	5.0	50.648	341.48	0.945	10.09375	0.1524	zirc4	0	Single assm-1 axial node	Water	0.88951	0.00074	
Whole Unit 2 SFP Models with Biases and Uncertainties Including Burnup														
KU2SFPA		5.0	0	341.48	0.945	10.09375	0.1524	zirc4	0	Unit 2 SFP	Finite	1.19548	0.00093	1.25677
KU2SFPB		5.0	0	341.48	0.945	10.09375	0.1524	zirc4	300	Unit 2 SFP	Finite	1.03257	0.00092	1.09386
KU2SFPG		5.0	0	341.48	0.945	10.09375	0.1524	zirc4	710	Unit 2 SFP	Finite	0.89142	0.00083	0.95271
KU2SFPH		5.0	0	341.48	0.945	10.09375	0.1524	zirc4	720	Unit 2 SFP	Finite	0.89027	0.00092	0.95156
KU2SFPF		5.0	0	341.48	0.945	10.09375	0.1524	zirc4	730	Unit 2 SFP	Finite	0.88543	0.00090	0.94672
KU2SFPE		5.0	0	341.48	0.945	10.09375	0.1524	zirc4	760	Unit 2 SFP	Finite	0.87970	0.00102	0.94099
KU2SFPD		5.0	0	341.48	0.945	10.09375	0.1524	zirc4	960	Unit 2 SFP	Finite	0.82810	0.00104	0.88939
KU2SFPC		5.0	0	341.48	0.945	10.09375	0.1524	zirc4	2000	Unit 2 SFP	Finite	0.66036	0.00070	0.72165
Whole Unit 2 SFP Models with Biases and Uncertainties Excluding Burnup														
KU2SFPA		5.0	0	341.48	0.945	10.09375	0.1524	zirc4	0	Unit 2 SFP	Finite	1.19548	0.00093	1.21492
KU2SFPB		5.0	0	341.48	0.945	10.09375	0.1524	zirc4	300	Unit 2 SFP	Finite	1.03257	0.00092	1.05201
KU2SFPJ		5.0	0	341.48	0.945	10.09375	0.1524	zirc4	590	Unit 2 SFP	Finite	0.92653	0.00103	0.94597
KU2SFPI		5.0	0	341.48	0.945	10.09375	0.1524	zirc4	600	Unit 2 SFP	Finite	0.92342	0.00089	0.94286
KU2SFPG		5.0	0	341.48	0.945	10.09375	0.1524	zirc4	710	Unit 2 SFP	Finite	0.89142	0.00083	0.91086
KU2SFPH		5.0	0	341.48	0.945	10.09375	0.1524	zirc4	720	Unit 2 SFP	Finite	0.89027	0.00092	0.90971

KU2SFPF		5.0	0	341.48	0.945	10.09375	0.1524	zirc4	730	Unit 2 SFP	Finite	0.88543	0.00090	0.90487
KU2SFPE		5.0	0	341.48	0.945	10.09375	0.1524	zirc4	760	Unit 2 SFP	Finite	0.87970	0.00102	0.89914
KU2SFPD		5.0	0	341.48	0.945	10.09375	0.1524	zirc4	960	Unit 2 SFP	Finite	0.82810	0.00104	0.84754
KU2SFPC		5.0	0	341.48	0.945	10.09375	0.1524	zirc4	2000	Unit 2 SFP	Finite	0.66036	0.00070	0.67980
Single Assembly Model with Biases and Uncertainties Including Burnup														
K500000D1		5.0	0	341.48	0.945	10.09375	0.1524	zirc4	0	Single assembly	Infinite	1.21112	0.00091	1.27241
K500000D2		5.0	0	341.48	0.945	10.09375	0.1524	zirc4	300	Single assembly	Infinite	1.13444	0.00094	1.19573
K500000D4		5.0	0	341.48	0.945	10.09375	0.1524	zirc4	1930	Single assembly	Infinite	0.88565	0.00086	0.94694
K500000D3		5.0	0	341.48	0.945	10.09375	0.1524	zirc4	2000	Single assembly	Infinite	0.87907	0.00094	0.94036
Single Assembly Model with Biases and Uncertainties Excluding Burnup														
K500000D1		5.0	0	341.48	0.945	10.09375	0.1524	zirc4	0	Single assembly	Infinite	1.21112	0.00091	1.23056
K500000D2		5.0	0	341.48	0.945	10.09375	0.1524	zirc4	300	Single assembly	Infinite	1.13444	0.00094	1.15388
K500000D6		5.0	0	341.48	0.945	10.09375	0.1524	zirc4	1590	Single assembly	Infinite	0.92409	0.00094	0.94353
K500000D5		5.0	0	341.48	0.945	10.09375	0.1524	zirc4	1670	Single assembly	Infinite	0.91631	0.00094	0.93575
K500000D4		5.0	0	341.48	0.945	10.09375	0.1524	zirc4	1930	Single assembly	Infinite	0.88565	0.00086	0.90509
K500000D3		5.0	0	341.48	0.945	10.09375	0.1524	zirc4	2000	Single assembly	Infinite	0.87907	0.00094	0.89851
Configuration Control														
KU2CONA		5.0	0	341.48	0.945	10.09375	0.1524	zirc4	0	Unit 2 SFP Configuration Control	Finite	0.89537	0.00108	0.95666
KU2CONB		5.0	0	341.48	0.945	10.09375	0.1524	zirc4	300	Unit 2 SFP Configuration Control	Finite	0.78664	0.00095	0.84793
KU2CONC		5.0	0	341.48	0.945	10.09375	0.1524	zirc4	0	Unit 2 SFP Configuration Control	Finite	1.08888	0.00105	1.15017
KU2COND1	S520	5.0	20	341.48	0.945	10.09375	0.1524	zirc4	0	Unit 2 SFP Configuration Control	Finite	1.13082	0.00111	1.19211
KU2COND2	S540	5.0	40	341.48	0.945	10.09375	0.1524	zirc4	0	Unit 2 SFP Configuration Control	Finite	1.08464	0.00103	1.14593
KU2COND3	S560	5.0	60	341.48	0.945	10.09375	0.1524	zirc4	0	Unit 2 SFP Configuration Control	Finite	1.04690	0.00100	1.10819
KU2CONE1	S420	4.0	20	341.48	0.945	10.09375	0.1524	zirc4	0	Unit 2 SFP Configuration Control	Finite	1.07998	0.00107	1.14127
KU2CONE2	S440	4.0	40	341.48	0.945	10.09375	0.1524	zirc4	0	Unit 2 SFP Configuration Control	Finite	1.03166	0.00096	1.09295
KU2CONE3	S460	4.0	60	341.48	0.945	10.09375	0.1524	zirc4	0	Unit 2 SFP Configuration Control	Finite	0.99762	0.00119	1.05891
Assembly Reconstitution														
KU2SFPAR		5.0	0	341.48	0.945	10.09375	0.1524	zirc4	0	Unit 2 SFP with Recon	Finite	1.19271	0.00098	1.25400
KU2SFPBR		5.0	0	341.48	0.945	10.09375	0.1524	zirc4	300	Unit 2 SFP with Recon	Finite	1.03236	0.00088	1.09365
KU2SFPCR		5.0	0	341.48	0.945	10.09375	0.1524	zirc4	2000	Unit 2 SFP with Recon	Finite	0.66218	0.00069	0.72347
Dropped Assembly														
KU2SFPAD		5.0	0	341.48	0.945	10.09375	0.1524	zirc4	0	Unit 2 SFP Dropped Assembly	Finite	1.19382	0.00090	1.25511
KU2SFPBD		5.0	0	341.48	0.945	10.09375	0.1524	zirc4	300	Unit 2 SFP Dropped Assembly	Finite	1.03258	0.00106	1.09387
KU2SFPCD		5.0	0	341.48	0.945	10.09375	0.1524	zirc4	2000	Unit 2 SFP Dropped Assembly	Finite	0.65990	0.00085	0.72119
Dropped Assembly During Reconstitution														
KU2SFPARD		5.0	0	341.48	0.945	10.09375	0.1524	zirc4	0	Unit 2 SFP Recon/Dropped Assm	Finite	1.19334	0.00102	1.25463
KU2SFPBRD		5.0	0	341.48	0.945	10.09375	0.1524	zirc4	300	Unit 2 SFP Recon/Dropped Assm	Finite	1.03280	0.00100	1.09409

KU2SFPCRD		5.0	0	341.48	0.945	10.09375	0.1524	zirc4	2000	Unit 2 SFP Recon/Dropped Assm	Finite	0.66264	0.00068	0.72393
Isotopic Comparison														
K501000D1	S510	5.0	10	341.48	0.945	10.09375	0.1524	zirc4	0	Single assembly - 50 Isotopes	Infinite	1.13638	0.00085	
K501000F1	X510	5.0	10	341.48	0.945	10.09375	0.1524	zirc4	0	Single assembly - 101 Isotopes	Infinite	1.12996	0.00091	-0.00642
K502000D1	S520	5.0	20	341.48	0.945	10.09375	0.1524	zirc4	0	Single assembly - 50 Isotopes	Infinite	1.07119	0.00088	
K502000F1	X520	5.0	20	341.48	0.945	10.09375	0.1524	zirc4	0	Single assembly - 101 Isotopes	Infinite	1.06249	0.00084	-0.00870
K503000D1	S530	5.0	30	341.48	0.945	10.09375	0.1524	zirc4	0	Single assembly - 50 Isotopes	Infinite	1.01281	0.00079	
K503000F1	X530	5.0	30	341.48	0.945	10.09375	0.1524	zirc4	0	Single assembly - 101 Isotopes	Infinite	1.00313	0.00086	-0.00968
K504000D1	S540	5.0	40	341.48	0.945	10.09375	0.1524	zirc4	0	Single assembly - 50 Isotopes	Infinite	0.95358	0.00083	
K504000F1	X540	5.0	40	341.48	0.945	10.09375	0.1524	zirc4	0	Single assembly - 101 Isotopes	Infinite	0.94032	0.00081	-0.01326
K505000D1	S550	5.0	50	341.48	0.945	10.09375	0.1524	zirc4	0	Single assembly - 50 Isotopes	Infinite	0.89641	0.00079	
K505000F1	X550	5.0	50	341.48	0.945	10.09375	0.1524	zirc4	0	Single assembly - 101 Isotopes	Infinite	0.88183	0.00073	-0.01458
K506000D1	S560	5.0	60	341.48	0.945	10.09375	0.1524	zirc4	0	Single assembly - 50 Isotopes	Infinite	0.84339	0.00071	
K506000F1	X560	5.0	60	341.48	0.945	10.09375	0.1524	zirc4	0	Single assembly - 101 Isotopes	Infinite	0.82754	0.00075	-0.01585
K507000D1	S570	5.0	70	341.48	0.945	10.09375	0.1524	zirc4	0	Single assembly - 50 Isotopes	Infinite	0.79503	0.00072	
K507000F1	X570	5.0	70	341.48	0.945	10.09375	0.1524	zirc4	0	Single assembly - 101 Isotopes	Infinite	0.78126	0.00071	-0.01377
K401000D1	S410	4.0	10	341.48	0.945	10.09375	0.1524	zirc4	0	Single assembly - 50 Isotopes	Infinite	1.08330	0.00092	
K401000F1	X410	4.0	10	341.48	0.945	10.09375	0.1524	zirc4	0	Single assembly - 101 Isotopes	Infinite	1.07849	0.00090	-0.00481
K402000D1	S420	4.0	20	341.48	0.945	10.09375	0.1524	zirc4	0	Single assembly - 50 Isotopes	Infinite	1.01347	0.00082	
K402000F1	X420	4.0	20	341.48	0.945	10.09375	0.1524	zirc4	0	Single assembly - 101 Isotopes	Infinite	1.00744	0.00080	-0.00603
K403000D1	S430	4.0	30	341.48	0.945	10.09375	0.1524	zirc4	0	Single assembly - 50 Isotopes	Infinite	0.94894	0.00083	
K403000F1	X430	4.0	30	341.48	0.945	10.09375	0.1524	zirc4	0	Single assembly - 101 Isotopes	Infinite	0.93814	0.00089	-0.01080
K404000D1	S440	4.0	40	341.48	0.945	10.09375	0.1524	zirc4	0	Single assembly - 50 Isotopes	Infinite	0.88840	0.00076	
K404000F1	X440	4.0	40	341.48	0.945	10.09375	0.1524	zirc4	0	Single assembly - 101 Isotopes	Infinite	0.87704	0.00079	-0.01136
K405000D1	S450	4.0	50	341.48	0.945	10.09375	0.1524	zirc4	0	Single assembly - 50 Isotopes	Infinite	0.83200	0.00071	
K405000F1	X450	4.0	50	341.48	0.945	10.09375	0.1524	zirc4	0	Single assembly - 101 Isotopes	Infinite	0.81838	0.00073	-0.01362
K406000D1	S460	4.0	60	341.48	0.945	10.09375	0.1524	zirc4	0	Single assembly - 50 Isotopes	Infinite	0.78548	0.00073	
K406000F1	X460	4.0	60	341.48	0.945	10.09375	0.1524	zirc4	0	Single assembly - 101 Isotopes	Infinite	0.77035	0.00069	-0.01513
K407000D1	S470	4.0	70	341.48	0.945	10.09375	0.1524	zirc4	0	Single assembly - 50 Isotopes	Infinite	0.74660	0.00070	
K407000F1	X470	4.0	70	341.48	0.945	10.09375	0.1524	zirc4	0	Single assembly - 101 Isotopes	Infinite	0.73326	0.00062	-0.01334
K301000D1	S310	3.0	10	341.48	0.945	10.09375	0.1524	zirc4	0	Single assembly - 50 Isotopes	Infinite	1.01050	0.00083	
K301000F1	X310	3.0	10	341.48	0.945	10.09375	0.1524	zirc4	0	Single assembly - 101 Isotopes	Infinite	1.00342	0.00092	-0.00708
K302000D1	S320	3.0	20	341.48	0.945	10.09375	0.1524	zirc4	0	Single assembly - 50 Isotopes	Infinite	0.93591	0.00077	
K302000F1	X320	3.0	20	341.48	0.945	10.09375	0.1524	zirc4	0	Single assembly - 101 Isotopes	Infinite	0.92802	0.00082	-0.00789
K303000D1	S330	3.0	30	341.48	0.945	10.09375	0.1524	zirc4	0	Single assembly - 50 Isotopes	Infinite	0.87020	0.00069	

K303000F1	X330	3.0	30	341.48	0.945	10.09375	0.1524	zirc4	0	Single assembly - 101 Isotopes	Infinite	0.86187	0.00070	-0.00833
K304000D1	S340	3.0	40	341.48	0.945	10.09375	0.1524	zirc4	0	Single assembly - 50 Isotopes	Infinite	0.81338	0.00070	
K304000F1	X340	3.0	40	341.48	0.945	10.09375	0.1524	zirc4	0	Single assembly - 101 Isotopes	Infinite	0.80172	0.00074	-0.01166
K305000D1	S350	3.0	50	341.48	0.945	10.09375	0.1524	zirc4	0	Single assembly - 50 Isotopes	Infinite	0.76783	0.00074	
K305000F1	X350	3.0	50	341.48	0.945	10.09375	0.1524	zirc4	0	Single assembly - 101 Isotopes	Infinite	0.75627	0.00071	-0.01156
K306000D1	S360	3.0	60	341.48	0.945	10.09375	0.1524	zirc4	0	Single assembly - 50 Isotopes	Infinite	0.73518	0.00070	
K306000F1	X360	3.0	60	341.48	0.945	10.09375	0.1524	zirc4	0	Single assembly - 101 Isotopes	Infinite	0.72120	0.00067	-0.01398
K307000D1	S370	3.0	70	341.48	0.945	10.09375	0.1524	zirc4	0	Single assembly - 50 Isotopes	Infinite	0.71073	0.00063	
K307000F1	X370	3.0	70	341.48	0.945	10.09375	0.1524	zirc4	0	Single assembly - 101 Isotopes	Infinite	0.69729	0.00069	-0.01344
K201000D1	S210	2.0	10	341.48	0.945	10.09375	0.1524	zirc4	0	Single assembly - 50 Isotopes	Infinite	0.90578	0.00074	
K201000F1	X210	2.0	10	341.48	0.945	10.09375	0.1524	zirc4	0	Single assembly - 101 Isotopes	Infinite	0.90008	0.00076	-0.00570
K202000D1	S220	2.0	20	341.48	0.945	10.09375	0.1524	zirc4	0	Single assembly - 50 Isotopes	Infinite	0.83855	0.00071	
K202000F1	X220	2.0	20	341.48	0.945	10.09375	0.1524	zirc4	0	Single assembly - 101 Isotopes	Infinite	0.83024	0.00071	-0.00831
K203000D1	S230	2.0	30	341.48	0.945	10.09375	0.1524	zirc4	0	Single assembly - 50 Isotopes	Infinite	0.78440	0.00087	
K203000F1	X230	2.0	30	341.48	0.945	10.09375	0.1524	zirc4	0	Single assembly - 101 Isotopes	Infinite	0.77555	0.00075	-0.00885
K204000D1	S240	2.0	40	341.48	0.945	10.09375	0.1524	zirc4	0	Single assembly - 50 Isotopes	Infinite	0.74665	0.00066	
K204000F1	X240	2.0	40	341.48	0.945	10.09375	0.1524	zirc4	0	Single assembly - 101 Isotopes	Infinite	0.73641	0.00065	-0.01024
K205000D1	S250	2.0	50	341.48	0.945	10.09375	0.1524	zirc4	0	Single assembly - 50 Isotopes	Infinite	0.71990	0.00068	
K205000F1	X250	2.0	50	341.48	0.945	10.09375	0.1524	zirc4	0	Single assembly - 101 Isotopes	Infinite	0.70752	0.00064	-0.01238
K206000D1	S260	2.0	60	341.48	0.945	10.09375	0.1524	zirc4	0	Single assembly - 50 Isotopes	Infinite	0.70267	0.00059	
K206000F1	X260	2.0	60	341.48	0.945	10.09375	0.1524	zirc4	0	Single assembly - 101 Isotopes	Infinite	0.69013	0.00065	-0.01254
K207000D1	S270	2.0	70	341.48	0.945	10.09375	0.1524	zirc4	0	Single assembly - 50 Isotopes	Infinite	0.69082	0.00060	
K207000F1	X270	2.0	70	341.48	0.945	10.09375	0.1524	zirc4	0	Single assembly - 101 Isotopes	Infinite	0.67796	0.00067	-0.01286
K500000D1		5.0	0	341.48	0.945	10.09375	0.1524	zirc4	0	Single assembly	Infinite	1.21112	0.00091	
K501000D1	S510	5.0	10	341.48	0.945	10.09375	0.1524	zirc4	0	Single assembly - 50 Isotopes	Infinite	1.13638	0.00085	
K501000DA	S510mod	5.0	10	341.48	0.945	10.09375	0.1524	zirc4	0	Single assembly - 38 Isotopes	Infinite	1.14193	0.00092	0.00555
K502000D1	S520	5.0	20	341.48	0.945	10.09375	0.1524	zirc4	0	Single assembly - 50 Isotopes	Infinite	1.07119	0.00088	
K502000DA	S520mod	5.0	20	341.48	0.945	10.09375	0.1524	zirc4	0	Single assembly - 38 Isotopes	Infinite	1.08389	0.00083	0.01270
K503000D1	S530	5.0	30	341.48	0.945	10.09375	0.1524	zirc4	0	Single assembly - 50 Isotopes	Infinite	1.01281	0.00079	
K503000DA	S530mod	5.0	30	341.48	0.945	10.09375	0.1524	zirc4	0	Single assembly - 38 Isotopes	Infinite	1.02581	0.00082	0.01300
K504000D1	S540	5.0	40	341.48	0.945	10.09375	0.1524	zirc4	0	Single assembly - 50 Isotopes	Infinite	0.95358	0.00083	
K504000DA	S540mod	5.0	40	341.48	0.945	10.09375	0.1524	zirc4	0	Single assembly - 38 Isotopes	Infinite	0.97189	0.00073	0.01831
K505000D1	S550	5.0	50	341.48	0.945	10.09375	0.1524	zirc4	0	Single assembly - 50 Isotopes	Infinite	0.89641	0.00079	
K505000DA	S550mod	5.0	50	341.48	0.945	10.09375	0.1524	zirc4	0	Single assembly - 38 Isotopes	Infinite	0.91505	0.00094	0.01864
K506000D1	S560	5.0	60	341.48	0.945	10.09375	0.1524	zirc4	0	Single assembly - 50 Isotopes	Infinite	0.84339	0.00071	

K506000DA	S560mod	5.0	60	341.48	0.945	10.09375	0.1524	zirc4	0	Single assembly - 38 Isotopes	Infinite	0.86469	0.00068	0.02130
K507000D1	S570	5.0	70	341.48	0.945	10.09375	0.1524	zirc4	0	Single assembly - 50 Isotopes	Infinite	0.79503	0.00072	
K507000DA	S570mod	5.0	70	341.48	0.945	10.09375	0.1524	zirc4	0	Single assembly - 38 Isotopes	Infinite	0.81685	0.00067	0.02182
K507000DB	S570mod	5.0	70	341.48	0.945	10.09375	0.1524	zirc4	0	Single assembly-50 Isotopes-50%	Infinite	0.80674	0.00074	0.01171
K507000DD	S570mod	5.0	70	341.48	0.945	10.09375	0.1524	zirc4	0	Single assembly-50 Isotopes-75%	Infinite	0.79973	0.00076	0.00470
K507000DE	S570mod	5.0	70	341.48	0.945	10.09375	0.1524	zirc4	0	Single assembly-50 Isotopes-90%	Infinite	0.79727	0.00071	0.00224
K507000DF	S570mod	5.0	70	341.48	0.945	10.09375	0.1524	zirc4	0	Single assembly-50 Isotopes-95%	Infinite	0.79587	0.00069	0.00084
K507000DC	S570mod	5.0	70	341.48	0.945	10.09375	0.1524	zirc4	0	Single assembly-38 Isotopes-99%	Infinite	0.79587	0.00074	0.00084
														0.01979
K501000D1	S510	5.0	10	341.48	0.945	10.09375	0.1524	zirc4	0	Single assembly - 50 Isotopes	Infinite	1.13638	0.00085	
K501000FA	S510mod	5.0	10	341.48	0.945	10.09375	0.1524	zirc4	0	Single assembly - 85 Isotopes	Infinite	1.13661	0.00086	0.00023
K502000D1	S520	5.0	20	341.48	0.945	10.09375	0.1524	zirc4	0	Single assembly - 50 Isotopes	Infinite	1.07119	0.00088	
K502000FA	S520mod	5.0	20	341.48	0.945	10.09375	0.1524	zirc4	0	Single assembly - 85 Isotopes	Infinite	1.07402	0.00088	0.00283
K503000D1	S530	5.0	30	341.48	0.945	10.09375	0.1524	zirc4	0	Single assembly - 50 Isotopes	Infinite	1.01281	0.00079	
K503000FA	S530mod	5.0	30	341.48	0.945	10.09375	0.1524	zirc4	0	Single assembly - 85 Isotopes	Infinite	1.01601	0.00080	0.00320
K504000D1	S540	5.0	40	341.48	0.945	10.09375	0.1524	zirc4	0	Single assembly - 50 Isotopes	Infinite	0.95358	0.00083	
K504000FA	S540mod	5.0	40	341.48	0.945	10.09375	0.1524	zirc4	0	Single assembly - 85 Isotopes	Infinite	0.95673	0.00081	0.00315
K505000D1	S550	5.0	50	341.48	0.945	10.09375	0.1524	zirc4	0	Single assembly - 50 Isotopes	Infinite	0.89641	0.00079	
K505000FA	S550mod	5.0	50	341.48	0.945	10.09375	0.1524	zirc4	0	Single assembly - 85 Isotopes	Infinite	0.90193	0.00076	0.00552
K506000D1	S560	5.0	60	341.48	0.945	10.09375	0.1524	zirc4	0	Single assembly - 50 Isotopes	Infinite	0.84339	0.00071	
K506000FA	S560mod	5.0	60	341.48	0.945	10.09375	0.1524	zirc4	0	Single assembly - 85 Isotopes	Infinite	0.84868	0.00070	0.00529
K507000D1	S570	5.0	70	341.48	0.945	10.09375	0.1524	zirc4	0	Single assembly - 50 Isotopes	Infinite	0.79503	0.00072	
K507000FA	S570mod	5.0	70	341.48	0.945	10.09375	0.1524	zirc4	0	Single assembly - 85 Isotopes	Infinite	0.80151	0.00062	0.00648
K5062AADA	s562aa2.xxx	5.0	62	341.48	0.945	10.09375	0.1524	zirc4	0	Single assm-18 axial nodes	Water	0.87753	0.00087	0.02577
K5062AAEA	s562aa1.xxx	5.0	62	341.48	0.945	10.09375	0.1524	zirc4	0	Single assm-1 axial node	Water	0.85176	0.00068	
Isotopic Bias Calculation with SAS2H Validation Data														
K506000D1	S560	5.0	60	341.48	0.945	10.09375	0.1524	zirc4	0	Single assembly - 50 Isotopes	Infinite	0.84339	0.00071	-0.00358
K506000G1	Hand	5.0	60	341.48	0.945	10.09375	0.1524	zirc4	0	Single assembly - 50 Isotopes - Val	Infinite	0.83981	0.00071	
Reactivity Comparison with Moderator as UEF/LEF and Actual UEF/LEF														
KU2SFPA		5.0	0	341.48	0.945	10.09375	0.1524	zirc4	0	Unit 2 SFP-H2O in UEF/LEF	Finite	1.19548	0.00093	
KU2SFPX		5.0	0	341.48	0.945	10.09375	0.1524	zirc4	0	Unit 2 SFP-Actual UEF/LEF	Finite	1.19449	0.00101	

ATTACHMENT B
BIAS AND UNCERTAINTY RESULTS

Summary of Bias and Uncertainty Results:											
			0 PPM	0 PPM	300 PPM	300 PPM	300 PPM	300 PPM			
			No Burnup	No Burnup	No Burnup	No Burnup	With Burnup	With Burnup			
			Bias	Uncertainty	Bias	Uncertainty	Bias	Uncertainty			
Calculational Methodology			0.00080	0.00760	0.00080	0.00760	0.00080	0.00760			
SAS2H									Worst Case		
Water in Gap			0.00000	0.00000	0.00000	0.00356	0.00000	0.00267			
Temperature									Worst Case - 68C		
Fuel Cladding Composition									Worst Case - zirc4		
Stack Height Density			0.00000	0.00090	0.00000	0.00340	0.00000	0.00841	Nominal		
Storage Cell Pitch			0.00000	0.00358	0.00000	0.00449	0.00000	0.00454	Nominal		
Fuel Enrichment			0.00000	0.00155	0.00000	0.00210	0.00000	0.00304	Nominal		
Soluble Boron Concentration									Worst Case		
Steel Thickness			0.00000	0.01346	0.00000	0.00775	0.00000	0.00698	Nominal		
Poison Loading									Worst Case - 0.000 gm/cm2		
Eccentric Positioning			0.00000	0.00961	0.00000	0.01122	0.00000	0.00800	Nominal		
Fuel Depletion			0.00000	0.02089	0.00000	0.01985	0.00000	0.01985	Nominal		
Axial Burnup Distribution			0.03250	0.00000	0.03250	0.00000	0.03250	0.00000	Nominal		
Total with Burnup			0.03330	0.02799	0.03330	0.02620	0.03330	0.02593			
				0.06129		0.05950		0.05923	Bias and Uncertainty		
Total without Burnup			0.00080	0.01864	0.00080	0.01710	0.00080	0.01668			
				0.01944		0.01790		0.01748	Bias and Uncertainty		

Summary of Bias and Uncertainty Results:											
			0 PPM	0 PPM	300 PPM	300 PPM	300 PPM	300 PPM			
			No Burnup	No Burnup	No Burnup	No Burnup	With Burnup	With Burnup			
			Bias	Uncertainty	Bias	Uncertainty	Bias	Uncertainty			
Calculational Methodology			0.00080	0.00760	0.00080	0.00760	0.00080	0.00760			
No Volatiles			0.00000	0.00084	0.00000	0.00084	0.00000	0.00084			
Water in Gap			0.00000	0.00000	0.00000	0.00356	0.00000	0.00267			
Temperature									Worst Case - 68C		
Fuel Cladding Composition									Worst Case - zirc4		
Stack Height Density			0.00000	0.00090	0.00000	0.00340	0.00000	0.00841	Nominal		
Storage Cell Pitch			0.00000	0.00358	0.00000	0.00449	0.00000	0.00454	Nominal		
Fuel Enrichment			0.00000	0.00155	0.00000	0.00210	0.00000	0.00304	Nominal		
Soluble Boron Concentration									Worst Case		
Steel Thickness			0.00000	0.01346	0.00000	0.00775	0.00000	0.00698	Nominal		
Poison Loading									Worst Case - 0.000 gm/cm2		
Eccentric Positioning			0.00000	0.00961	0.00000	0.01122	0.00000	0.00800	Nominal		
Fuel Depletion			0.00000	0.02089	0.00000	0.01985	0.00000	0.01985	Nominal		
Axial Burnup Distribution			0.03250	0.00000	0.03250	0.00000	0.03250	0.00000	Nominal		
Total with Burnup			0.03330	0.02800	0.03330	0.02621	0.03330	0.02594			
				0.06130		0.05951		0.05924	Bias and Uncertainty		
Total without Burnup			0.00080	0.01864	0.00080	0.01710	0.00080	0.01670			
				0.01944		0.01790		0.01750			

ATTACHMENT C
DENSITY CALCULATIONS

Densities

	A	B	C	D	E	F	G	H
1	**Carborundum Material Densities:**							
2	F =	B4C density fraction = B10L / PST / B10A * MWB4C / AWB4 / DB4C						
3	F =				0.240685	0.213007	0.191706	
4								
5	B10L = B10 Loading (gm/cm2)				0.020	0.017700	0.015930	Ref.15
6	PST = Poison Sheet Thickness (cm) = 0.090" * 2.54 =				0.2286	0.2286	0.2286	Ref.15
7	B10A = Abundance of B10 in a/f				0.19900	0.19900	0.19900	Ref.19
8	B11A = B11 abundance in a/f				0.80100	0.80100	0.80100	Ref.19
9	AWB10 = B10 atomic weight in gm/mole				10.012937	10.012937	10.012937	Ref.19
10	AWB11 = B11 atomic weight in gm/mole				11.009306	11.009306	11.009306	Ref.19
11	AWB = B atomic weight in gm/mole				10.81103	10.81103	10.81103	calculated
12	AWC = Atomic Weight of C				12.01100	12.01100	12.01100	Ref.19
13	MWB4C = Molecular Weight of B4C				55.2551	55.2551	55.2551	calculated
14	AWB4 = Atomic Weight of Natural B in B4C				43.2441	43.2441	43.2441	calculated
15	DB4C = Density of B4C in gm/cc				2.52	2.52	2.52	Ref.21
16	B10W = B10 abundance in w/f				0.18431	0.18431	0.18431	Ref.21
17								
18	**ZIRLO Material Densities**							
19	N(ATOMS/B-CM) = DZ * f * NA / AW / C							
20								
21		f(w/o)	AW(gm/mole)	N				
22	Sn	1.00	118.71	3.2594E-04				
23	Fe	0.11	55.847	7.6211E-05				
24	Nb	1.00	92.90638	4.1647E-04				
25	Zr	97.89	91.224	4.1520E-02				
26		100.00						
27								
28	f = Zirlo composition in w/o							Refs.17-18
29	DZ = Zirlo density in gm/cc				6.425			Ref.18
30	AW = Atomic weight in gm/mole							Ref.19
31	NA = Avogadro's Number in atoms/mole				6.022E+23			Ref.20
32	C = barns/cm2				1.00E+24			Ref.20
33								
34	**OPTIN Material Densities**							
35	N(ATOMS/B-CM) = DZ * f * NA / AW / C							
36								
37		f(w/o)	AW(gm/mole)	N				
38	Sn	1.25	118.71	4.1535E-04				
39	Fe	0.21	55.847	1.4832E-04				
40	Cr	0.10	51.996	7.5862E-05				
41	O	0.12	15.9994	2.9585E-04				
42	Zr	98.32	91.224	4.2514E-02				
43		100.00						
44								
45	f = Optin composition in w/o							Refs.17-18
46	DZ = Optin density in gm/cc				6.550			Ref.18
47	AW = Atomic weight in gm/mole							Ref.19
48	NA = Avogadro's Number in atoms/mole				6.022E+23			Ref.20
49	C = barns/cm2				1.00E+24			Ref.20
50								

Densities

	A	B	C	D	E	F	G	H
51	**Soluble Boron Density**							
52								
53	D(H3BO3) = f * D(H2O) * MW(H3BO3) / AWB = Density of H3BO3 in gm/cc							
54								
55	B10A = B10 abundance in w/o				19.9			Ref.19
56	B11A = B11 abundance in w/o				80.1			Ref.19
57	AWB10 = B10 atomic weight in gm/mole				10.012937			Ref.19
58	AWB11 = B11 atomic weight in gm/mole				11.009306			Ref.19
59	AWB = B atomic weight in gm/mole				10.81103			calculated
60	AWH = H atomic weight in gm/mole				1.00780			Ref.19
61	AWO = O atomic weight in gm/mole				15.99940			Ref.19
62	MWH3BO3 = H3BO3 molecular weight in gm/mole				61.83263			calculated
63								
64	f	DH2O	DH3BO3					
65	0.000100	1.0000	0.00057194					
66	0.000200	1.0000	0.001143881					
67	0.000300	1.0000	0.001715821					
68	0.000400	1.0000	0.002287761					
69	0.000500	1.0000	0.002859702					
70	0.002000	1.0000	0.011438806					
71	0.000100	1.0000	0.00057194					
72	0.000200	0.9785	0.001119287					
73	0.000300	0.9785	0.001678931					
74	0.000400	0.9785	0.002238574					
75	0.000500	0.9785	0.002798218					
76	0.000590	0.9785	0.003301897					
77	0.000600	0.9785	0.003357862					
78	0.000710	0.9785	0.003973469					
79	0.000720	0.9785	0.004029434					
80	0.000730	0.9785	0.004085398					
81	0.000760	0.9785	0.004253291					
82	0.000960	0.9785	0.005372578					
83	0.001590	0.9785	0.008898333					
84	0.001670	0.9785	0.009346048					
85	0.001930	0.9785	0.010801121					
86	0.002000	0.9785	0.011192872					
87								
88	**Fuel Isotopic Fractions**							
89	U235	U238	U235	U238	O16			
90	2.000000	98.0000	1.7629	86.3826	11.8545			
91	2.500000	97.5000	2.2036	85.9412	11.8552			
92	3.000000	97.0000	2.6443	85.4998	11.8559			
93	3.500000	96.5000	3.085	85.0585	11.8565			
94	4.000000	96.0000	3.5257	84.6171	11.8572			
95	4.500000	95.5000	3.9664	84.1758	11.8579			
96	5.000000	95.0000	4.4071	83.7344	11.8585			
97								
98								
99								
100								

Densities

	A	B	C	D	E	F	G	H
101	**Upper End Fitting:**							
102	Length	8.12	in	20.6248	cm	UFSAR Fig.3.3-1		
103	Width	8.12	in	20.6248	cm	UFSAR Fig.3.3-1		
104	Height	15.295	in	38.8493	cm	Ref.25		
105	Total Volume	1008.46665	in3	16525.8075	cc			
106	Inconel X-750	1100	gm			Ref.26		
107	SS-304	5080	gm			Ref.26		
108	Zirc-4	680	gm			Ref.26		
109	SS-302	7980	gm			Ref.26		
110	Inconel X-750	8.30	gm/cc-ref			Ref.21		
111	SS-304	7.94	gm/cc-ref			Ref.21		
112	Zirc-4	6.56	gm/cc-ref			Ref.21		
113	SS-302	7.94	gm/cc-ref			Ref.21		
114	Inconel X-750	132.5301	cc	0.008020	vol frac			
115	SS-304	639.7985	cc	0.038715	vol frac			
116	Zirc-4	103.6585	cc	0.006273	vol frac			
117	SS-302	1005.0378	cc	0.060816	vol frac			
118	Water Vol	14644.7826	cc	0.886177	vol frac			
119								
120								
121	**Lower End Fitting:**							
122	Length	8.12	in	20.6248	cm	UFSAR Fig.3.3-1		
123	Width	8.12	in	20.6248	cm	UFSAR Fig.3.3-1		
124	Height	5.246	in	13.32484	cm	Ref.25		
125	Volume	345.89186	in3	5668.152086	cc			
126	Inconel-625	1360	gm			Ref.26		
127	SS-304	5000	gm			Ref.26		
128	Inconel	8.30	gm/cc-ref			Ref.21		
129	SS-304	7.94	gm/cc-ref			Ref.21		
130	Inconel	163.8554	cc	0.028908	vol frac			
131	SS-304	629.7229	cc	0.111098	vol frac			
132	Water Vol	4874.5737	cc	0.859993	vol frac			

ATTACHMENT D
FUEL DATA SPREADSHEET

Fuel

217			Assemblies per core	UFSAR 3.1
77			CEAs per core	UFSAR 3.1
176			Rods per assembly	UFSAR 3.1
5			Guide tubes per assembly	UFSAR 3.1
136.7	347.218	in-cm	Active core height	UFSAR 3.1
1.035	2.6289	in-cm	Guide tube ID	BGE Drwg E-550-701-303 - Ref.27
1.115	2.8321	in-cm	Guide tube oD	BGE Drwg E-550-701-303 - Ref.27
0.580	1.4732	in-cm	Fuel rod pitch	UFSAR Figure 3.3-1
0.20	0.508	in-cm	Assembly spacing, fuel ros surface-surface	UFSAR Table 3.3-5
8.12	20.6248	in-cm	Assembly pitch (14*0.58")	UFSAR Figure 3.3-1
0.06	0.1524	in-cm	Assembly gap (8.18"-8.12")	UFSAR Figure 3.3-1
548		deg F	Tcold	UFSAR Figure 4-9
572.5		deg F	Tave	UFSAR Figure 4-9
599.4		deg F	Thot	UFSAR Figure 4-9
532		deg F	Thzp	UFSAR Figure 4-9
Standard Fuel Design				
0.3795	0.96393	in-cm	Pellet diameter (A-C U1)	UFSAR Table 3.3-1
15.4626		in3	Pin fuel volume	
0.3805	0.96647	in-cm	Pellet diameter (A-C U2)	UFSAR Table 3.3-2
15.5442		in3	Pin fuel volume	
0.3765	0.95631	in-cm	Pellet diameter (D-S U1, D-R U2)	UFSAR Table 3.3-1/2
15.2191		in3	Pin fuel volume	
0.388	0.98552	in-cm	Clad ID (A-C U1-U2)	UFSAR Table 3.3-1/2
0.384	0.97536	in-cm	Clad ID	UFSAR Table 3.3-1/2
0.440	1.1176	in-cm	Clad OD	UFSAR Table 3.3-1/2
10.170		gm/cc	Stack height density (max)	UFSAR Table 3.3-1/2
0.9279			Stack height density (% TD)	
VAP Fuel Design				
0.381	0.96774	in-cm	Pellet diameter	UFSAR Table 3.3-1/2
15.585		in3	Pin fuel volume	
0.388	0.98552	in-cm	Clad ID	UFSAR Table 3.3-1/2
0.440	1.1176	in-cm	Clad OD	UFSAR Table 3.3-1/2
10.310		gm/cc	Stack height density	UFSAR Table 3.3-1/2
0.9407			Stack height density (% TD)	
SAS2H Larger Unit Cell Effective Radii for 176 pin assembly (Standard and VAP Fuel Design)				
1.31445		cm	Clad ID/2 = 1.035"/2 = 0.5175" (H2O)	
1.41605		cm	Clad OD/2 = 1.115"/2 = 0.5575" (Zirc)	
1.66233		cm	SQRT[4*(0.58)^2/pi] = 0.65446" (H2O)	
5.20391		cm	SQRT[196*(0.58)^2/5/pi] = 2.04878" (Fuel)	
5.22314		cm	SQRT[(8.15)^2/5/pi] = 2.05635" (H2O)	In ORNL/TM-12667, uses 8.18".
SAS2H Larger Unit Cell Effective Radii for 172 pin assembly (Standard and VAP Fuel Design)				
1.31445		cm	Clad ID/2 = 1.035"/2 = 0.5175" (H2O)	
1.41605		cm	Clad OD/2 = 1.115"/2 = 0.5575" (Zirc)	
1.66233		cm	SQRT[4*(0.58)^2/pi] = 0.65446" (H2O)	
5.15054		cm	SQRT[192*(0.58)^2/5/pi] = 2.02777" (Fuel)	
5.22314		cm	SQRT[(8.15)^2/5/pi] = 2.05635" (H2O)	In ORNL/TM-12667, uses 8.18".

ATTACHMENT E
SFP SINGLE RACK PLANAR GEOMETRY

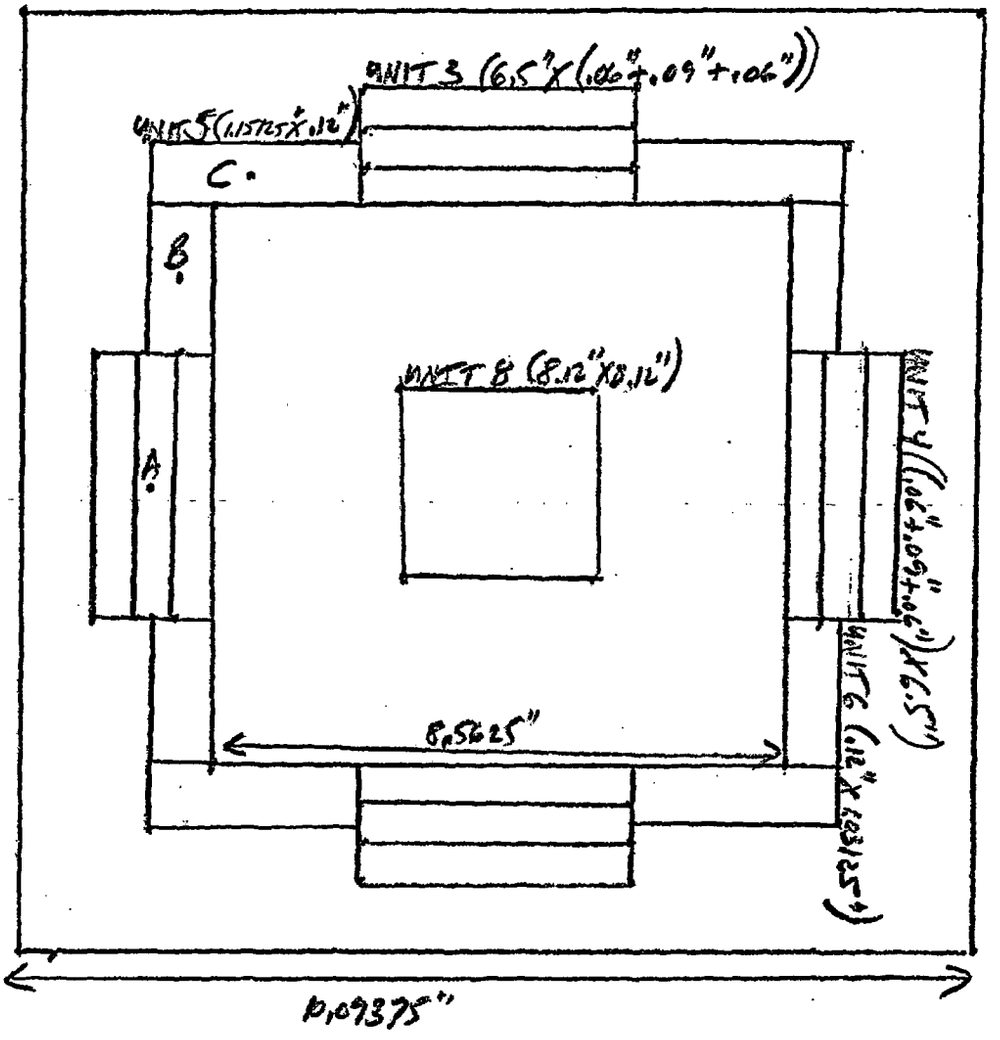

A: $X = 8.5625"/2 + .06" + .09"/2 = 4.38625" = 11.141075$ CM

B: $X = 8.5625"/2 + .12"/2 = 4.34125" = 11.026775$ CM

$Y = (8.5625" + 6.5")/4 = 3.765625" = 9.5616875$ CM

C: $X = (8.5625" + 6.5" + .24")/4 = 3.825625" = 9.7170875$ CM

$Y = 8.5625"/2 + .06" = 4.34125" = 11.026775$ CM

STORAGE CELL PITCH UNCERTAINTY

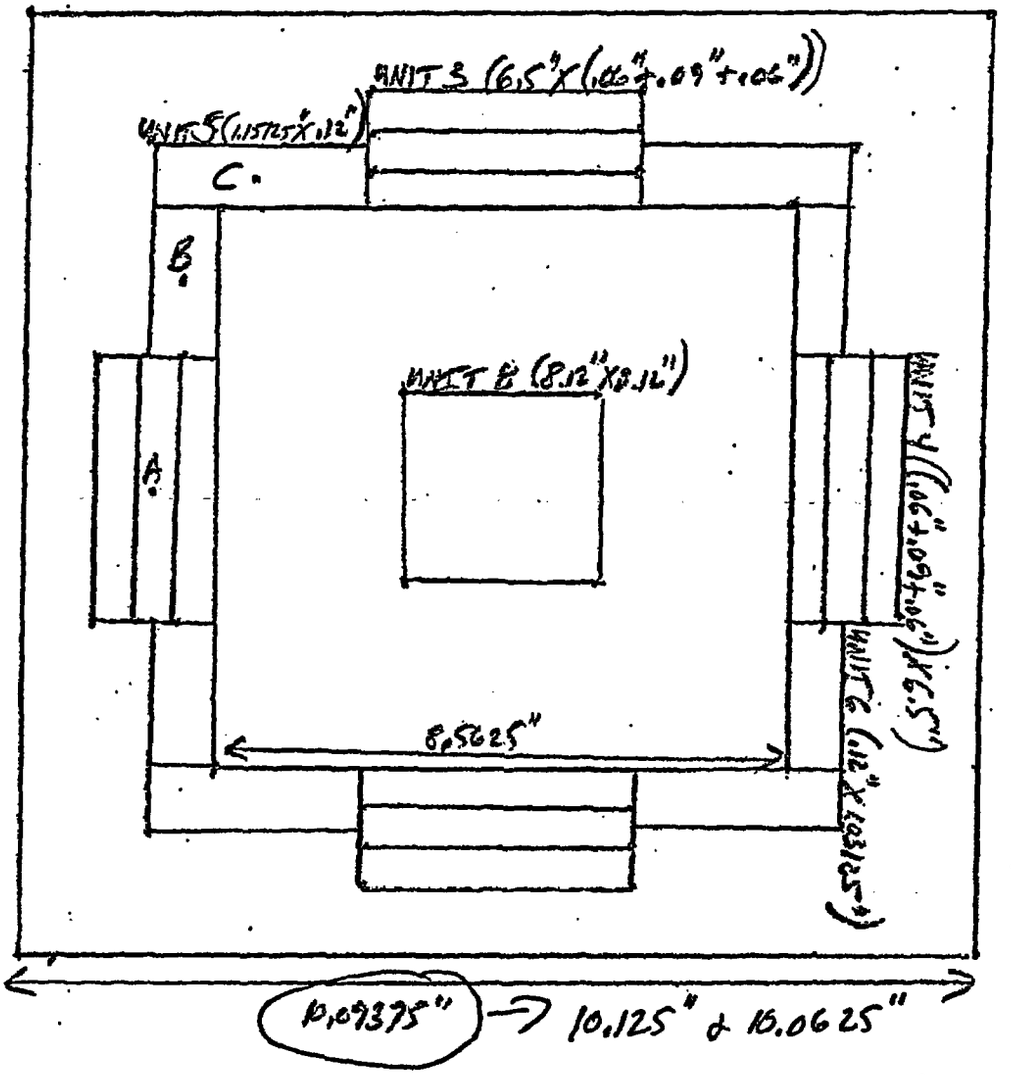

A: $X = 8.5625"/2 + .06" + .09"/2 = 4.38625" = 11.141075$ CM

B: $X = 8.5625"/2 + .12"/2 = 4.34125" = 11.026775$ CM

$Y = (8.5625" + 6.5")/4 = 3.765625" = 9.564687$ CM

C: $X = (8.5625" + 6.5" + .24")/4 = 2.825625" = 7.1770875$ CM

$Y = 8.5625"/2 + .06" = 4.34125" = 11.026775$ CM

STEEL THICKNESS UNCERTAINTY (±0.010)

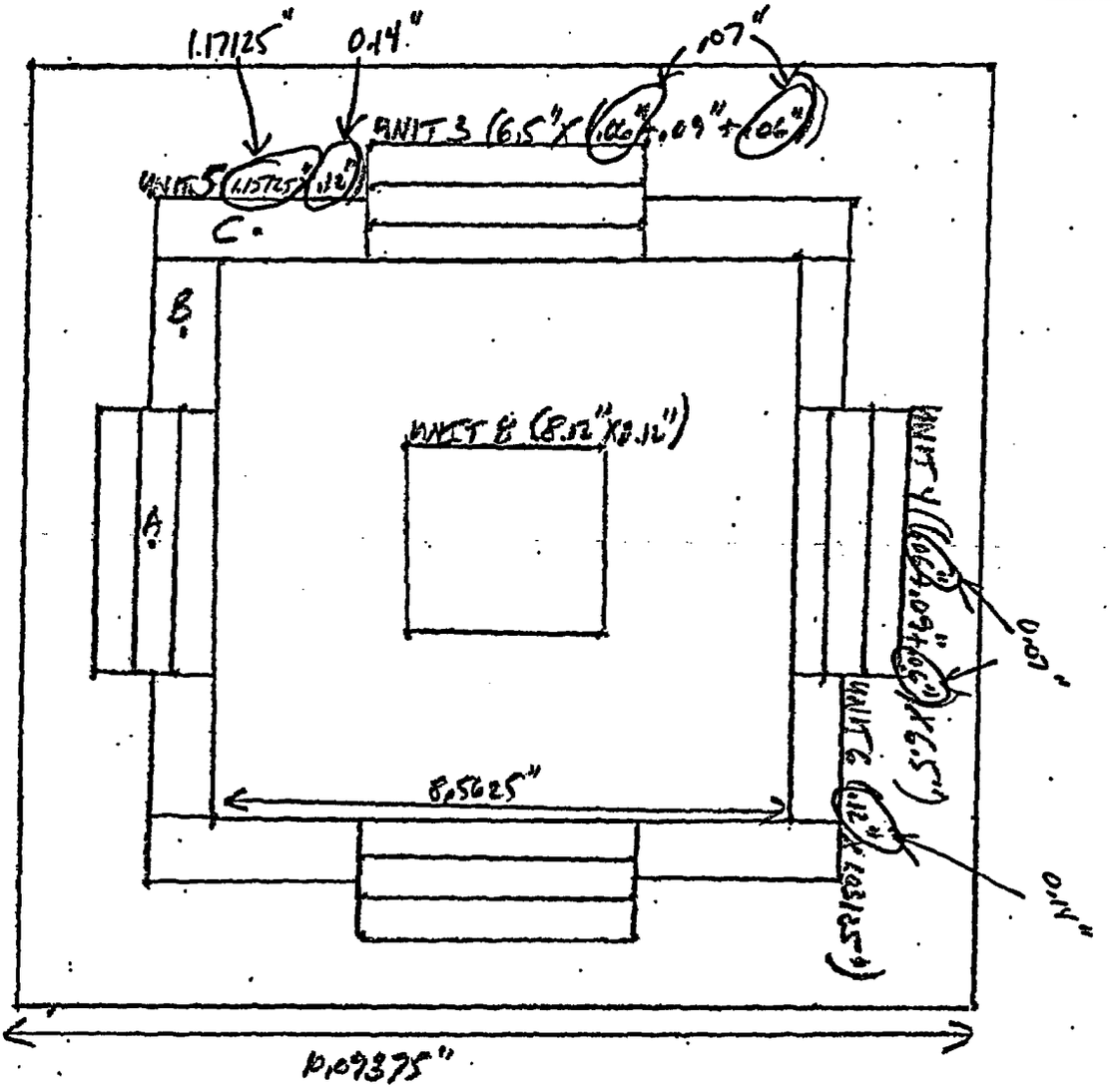

A: $X = 8.5625"/2 + \underbrace{.07" + .06" + .09"}_{.22"}/2 = \underbrace{4.39625"}_{4.39250"} = \underbrace{11.141075}_{11.166875}$ CM

B: $X = 8.5625"/2 + \underbrace{.12"}_{0.14"}/2 = \underbrace{4.34125"}_{4.35125"} = \underbrace{11.026775}_{11.052175}$ CM

$Y = (8.5625" + 6.5")/4 = 3.765625" = 9.561875$ CM

C: $X = (8.5625" + 6.5" + \underbrace{.21"}_{0.28"})/4 = \underbrace{3.82625"}_{3.835625"} = \underbrace{9.717075}_{9.742475}$ CM

$Y = 8.5625"/2 + \underbrace{.06"}_{.07"} = \underbrace{4.34125"}_{4.35125"} = \underbrace{11.026775}_{11.052175}$ CM

STEEL THICKNESS UNCERTAINTY (−0.010)

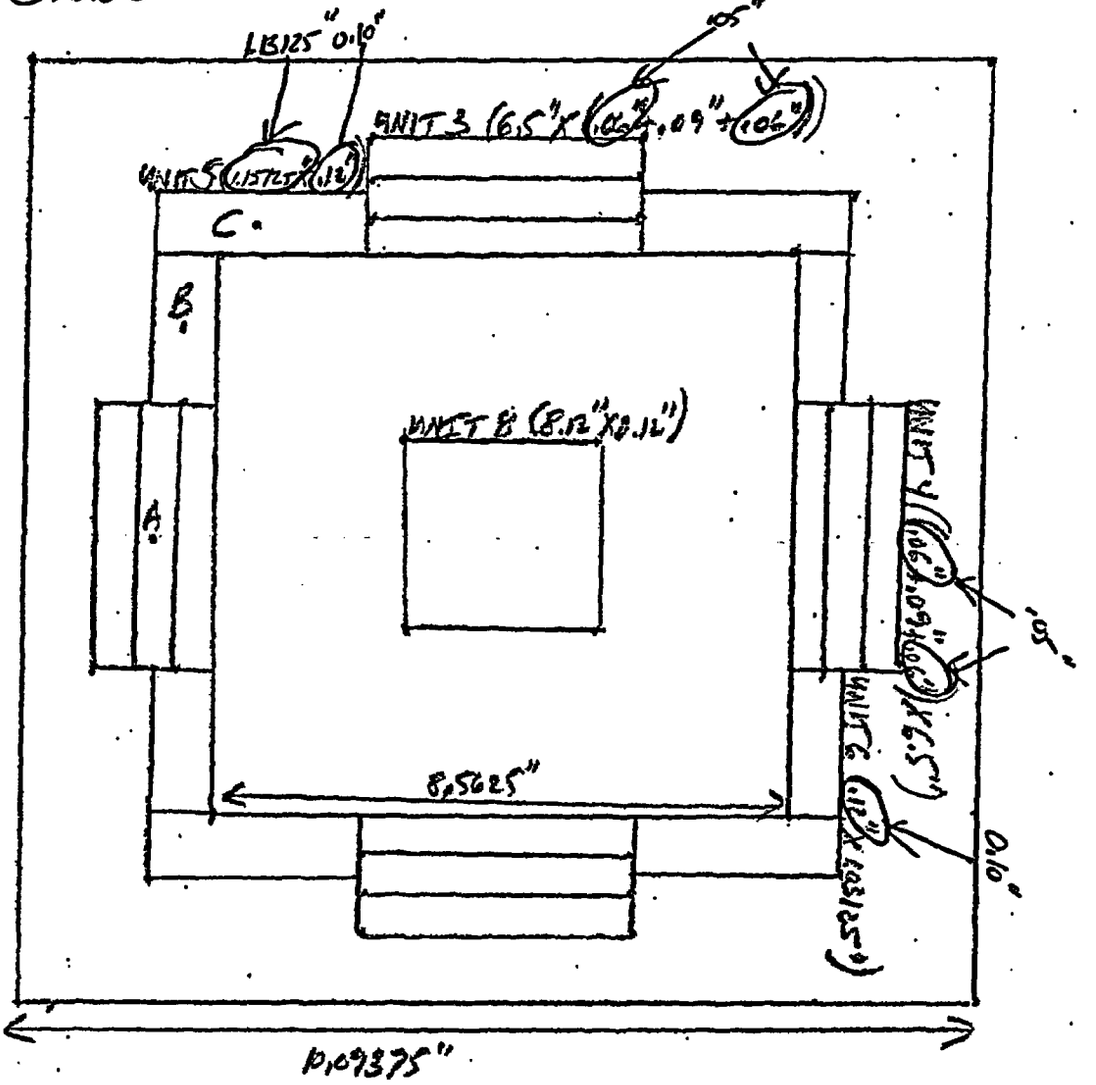

A: $X = 8.5625"/2 + .05" + .06" + .09"/2 = 4.38625" = 11.141075$ CM (4.37625", 11.115675)

B: $X = 8.5625"/2 + .10" + .11"/2 = 4.34125" = 11.026775$ CM (4.33125, 11.001375)

$Y = (8.5625" + 6.5")/4 = 3.765625" = 9.564675$ CM

C: $X = (8.5625" + 6.5" + .20" + .24")/4 = 3.815625" = 9.691675$ CM (3.8256625")

$Y = 8.5625"/2 + .06" + .05" = 4.34125" = 11.026775$ CM (4.33125", 11.001375)

ECCENTRIC POSITIONING

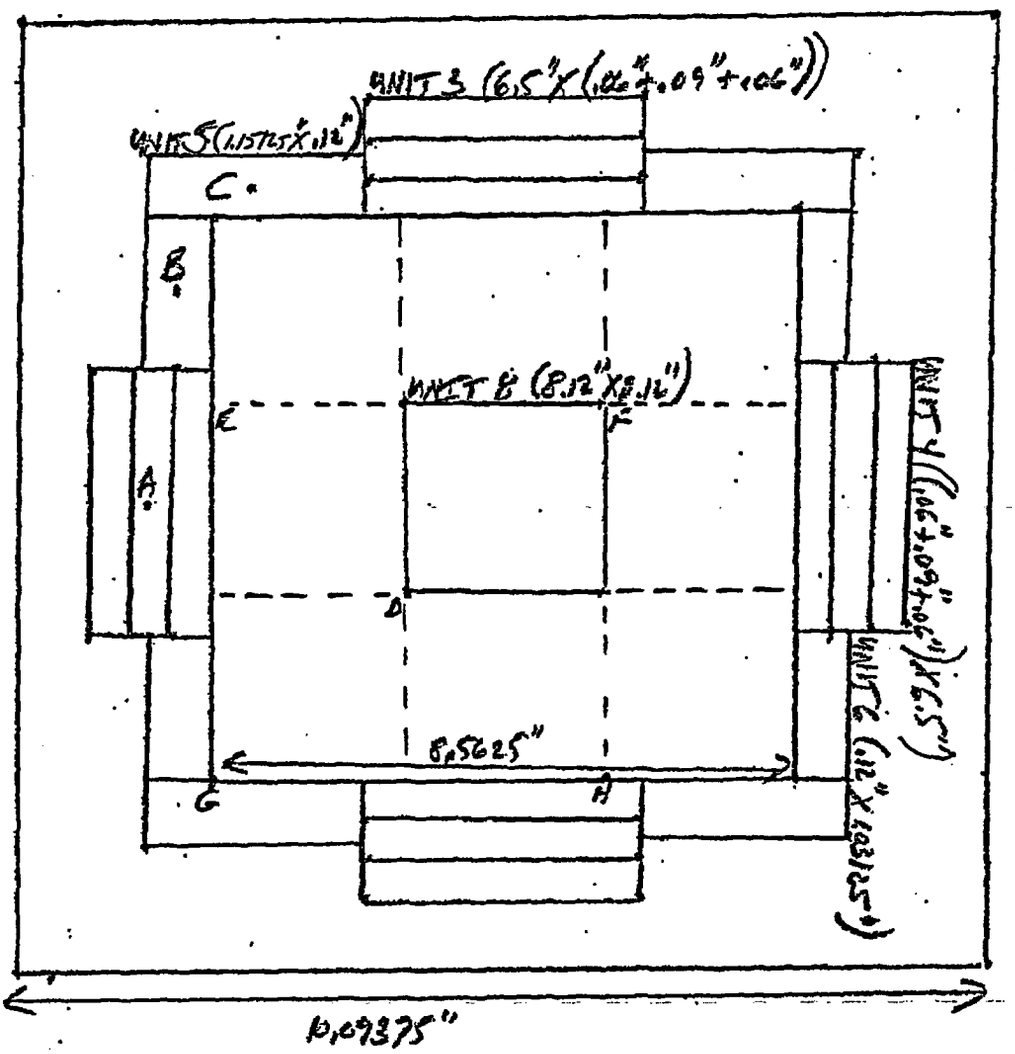

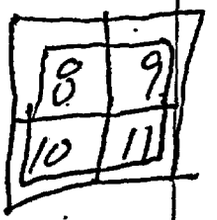

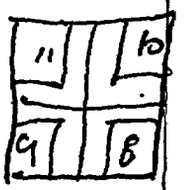

A: $X = 8.5625"/2 + .06" + .09"/2 = 4.38625" = 11.141075$ CM

B: $X = 8.5625"/2 + .12"/2 = 4.34125" = 11.026775$ CM

$Y = (8.5625" + 6.5")/4 = 3.765625" = 9.566875$ CM

C: $X = (8.5625" + 6.5" + .12")/4 = 3.825625" = 9.717075$ CM

$Y = 8.5625"/2 + .06" = 4.34125" = 11.026775$ CM

D $X = Y = -10.3125$

E $X = -10.874375$ $Y = -9.750425$

F $X = Y = -9.750425$

G $X = Y = -10.874375$

H $X = -9.750425$ $Y = -10.874375$

ATTACHMENT F
UNIT 2 SFP PLANAR GEOMETRY

UNIT 2 SFP

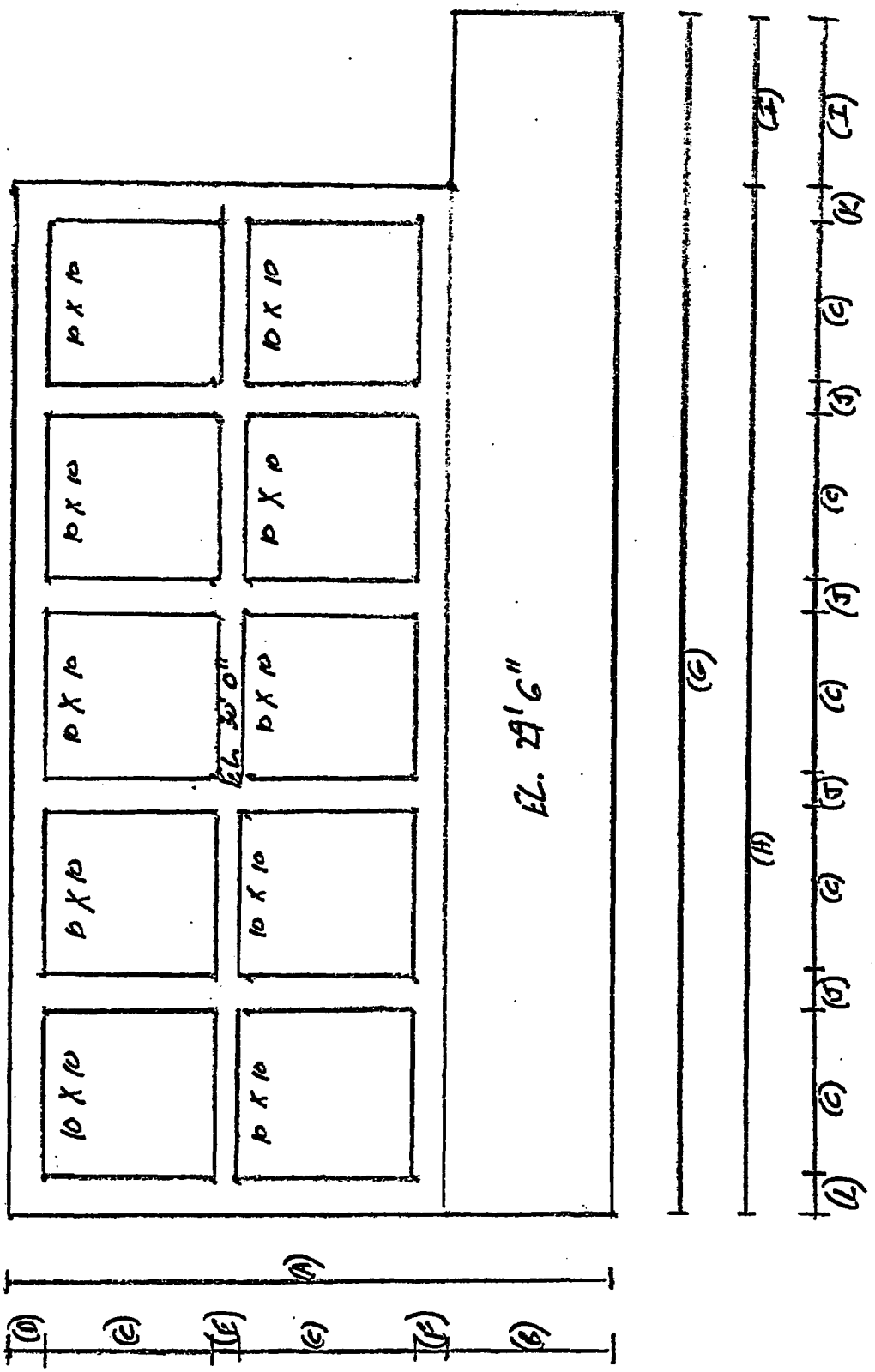
10 X 10
10 X 10
10 X 10
10 X 10
10 X 10
10 X 10
10 X 10
10 X 10
10 X 10
10 X 10
32'0"
EL. 29'6"
(A)
(B)
(C)
(D)
(E)
(F)
(G)
(H)
(I)
(J)
(K)
(L)
(M)

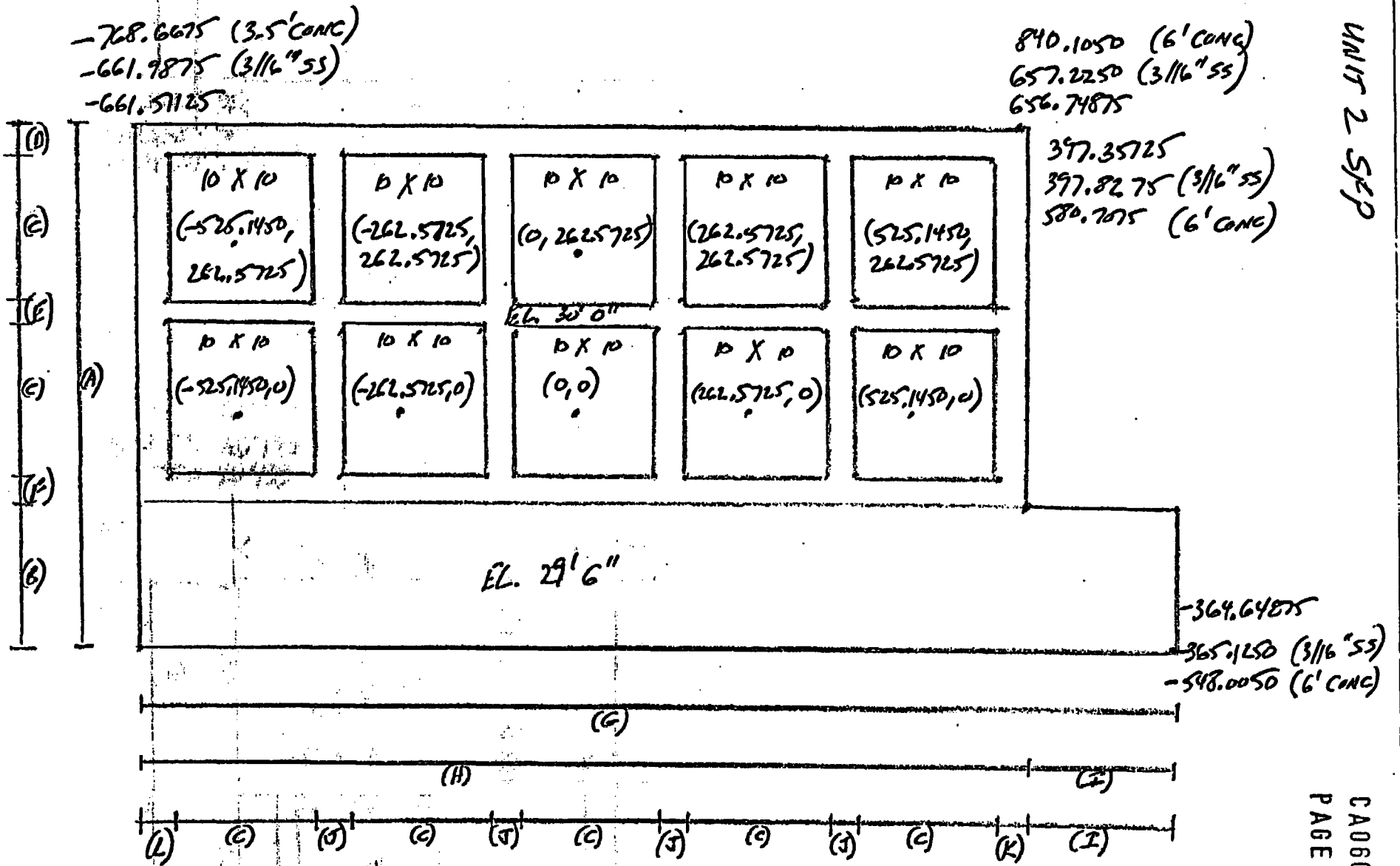

UNIT 2 SKP

CA06015 REV 0
PAGE 111

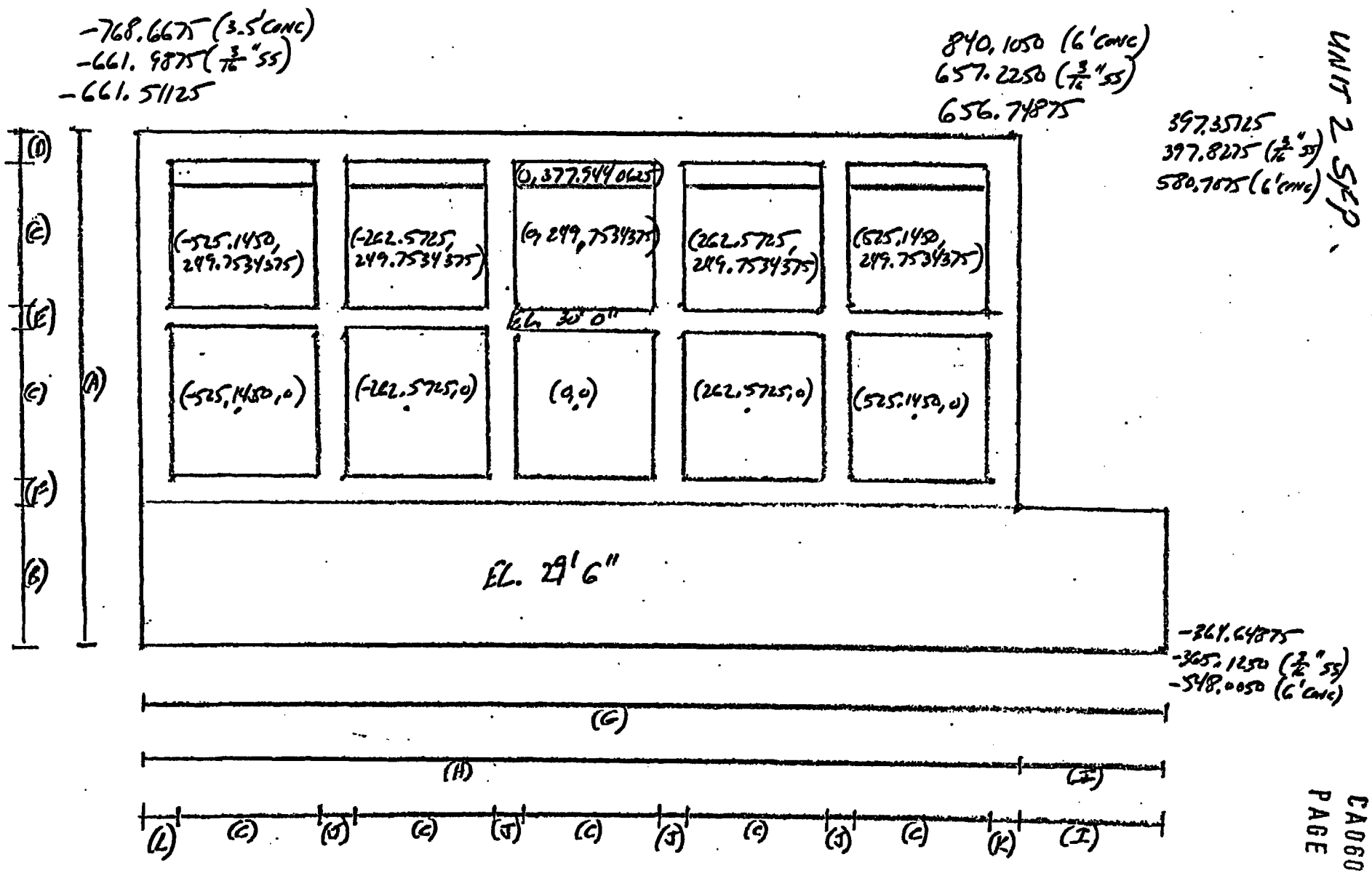

CA0615 REV 0
PAGE 112

(A) 25' 0"	Refs. 23-24
(B) 83.625"	Ref. 24
(C) 10 * 10.09375" = 100.9375"	Ref. 15
(D) 2.5" + 0.09375" = 2.59375"	Ref. 24
(E) 2.25" + 2 * 0.09375" = 2.4375"	Ref. 24
(F) A-B-2C-D-E = 9.46875"	Refs. 23-24
(G) 54' 0"	Ref. 23
(H) 43' 3"	Ref. 24
(I) G-H = 10' 9"	Refs. 23-24
(J) 2.25" + 2 * 0.09375" = 2.4375"	Ref. 24
(K) 1.25" + 0.09375" = 1.34375"	Ref. 24
(L) 3.125" + 0.09375" = 3.2187 5"	Refs. 23-24
(M) ELEVATIONS	Ref. 23

ATTACHMENT G
UNIT 2 SFP AXIAL GEOMETRY

AXIAL GEOMETRY
(Reference 25)

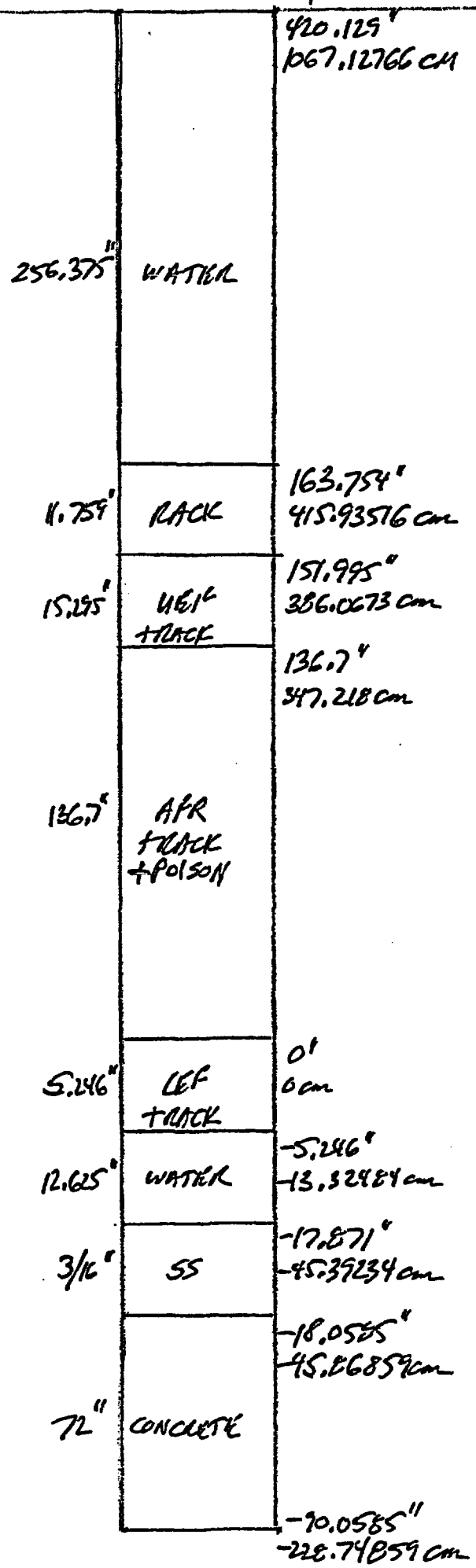

RECONSTITUTION AXIAL GEOMETRY

(Reference 25)

		420.129" 1067.12766 cm
247.634"	WATER	
		172.495" 438.1373 cm
8.741"	WATER + UEF	
		163.754" 415.93516 cm
6.554"	RACK + UEF	
		157.20" 399.288 cm
20.5"	RACK + AIR	
		136.70" 347.218 cm
116.200"	RACK + POISON + AIR	
		20.5" 52.0700 cm
5.246"	RACK + POISON + LEF	
		15.254" 38.74516 cm
15.254"	RACK + POISON + SPACER	
		0" 0 cm
5.246"	RACK + SPACER	
		-5.246" -13.32484 cm
11.625"	WATER	
		-17.871" -45.39234 cm
3/16"	SS	
		-18.0585" -45.86859 cm
72"	Concrete	
		-90.0585" -228.74859 cm

OP LIMIT – 67'
CL Norm – 66.5'

SPENT FUEL POOL DIAGRAM

47' 0" Full Max Up (2)
46' 0.625" (2) BOTTOM ASSM IN SFHM AT NORMAL UP LIMIT

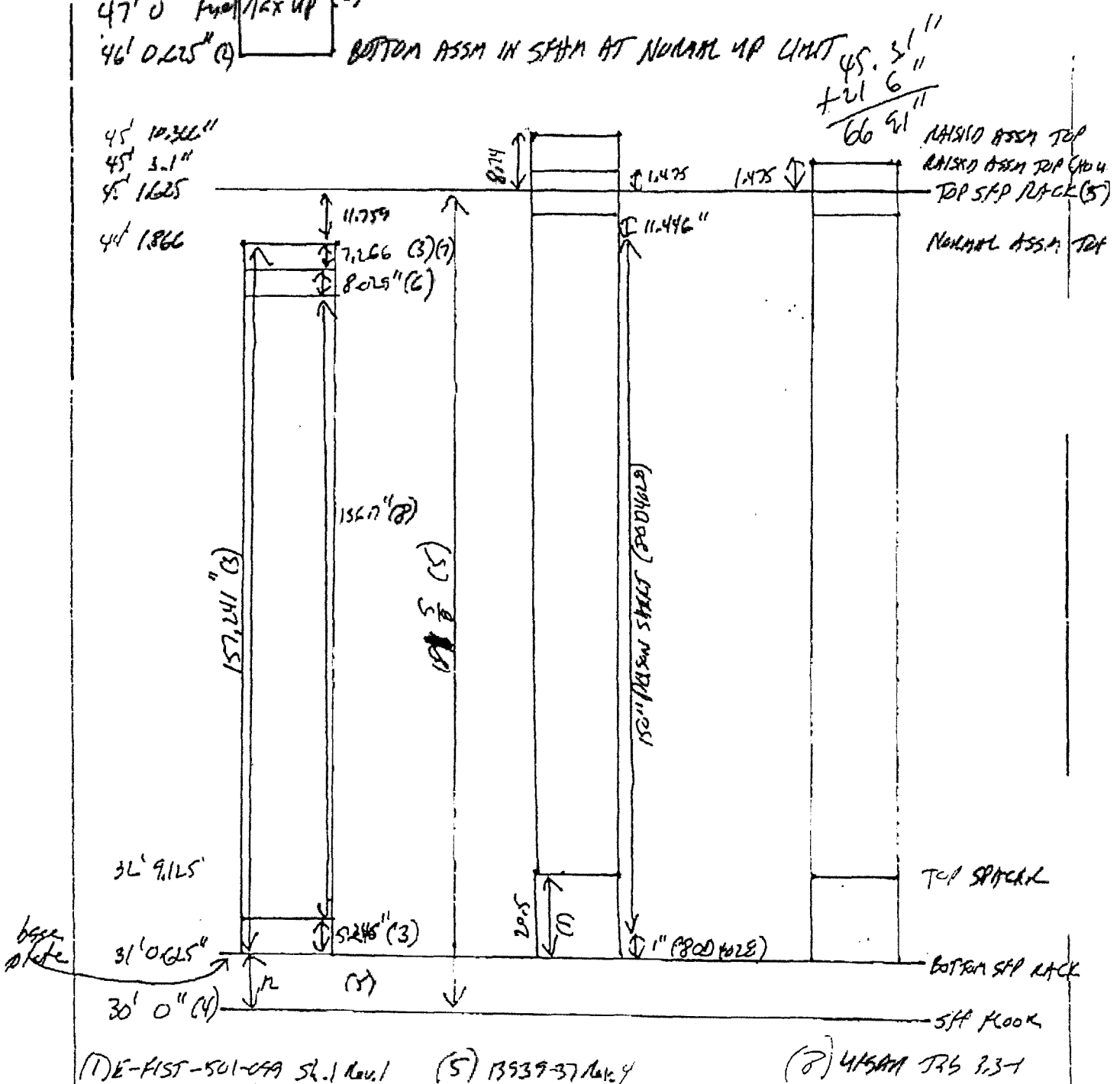

(1) E-FIST-501-059 Sh. 1 Rev. 1
(2) 15534-0001 Sh. 3 Rev.
(3) 12131-0250 Rev. 0
(4) 63876 Rev. 1
(5) 13539-37 Rev. 4
CC 0114-E000-RC3 Rev. 2
NUH-SL-574
(7) IE-FCI-11.000-A-2 Rev. 4
(8) WASAM TRS 2.3-1

ATTACHMENT H
KENO PLOTS

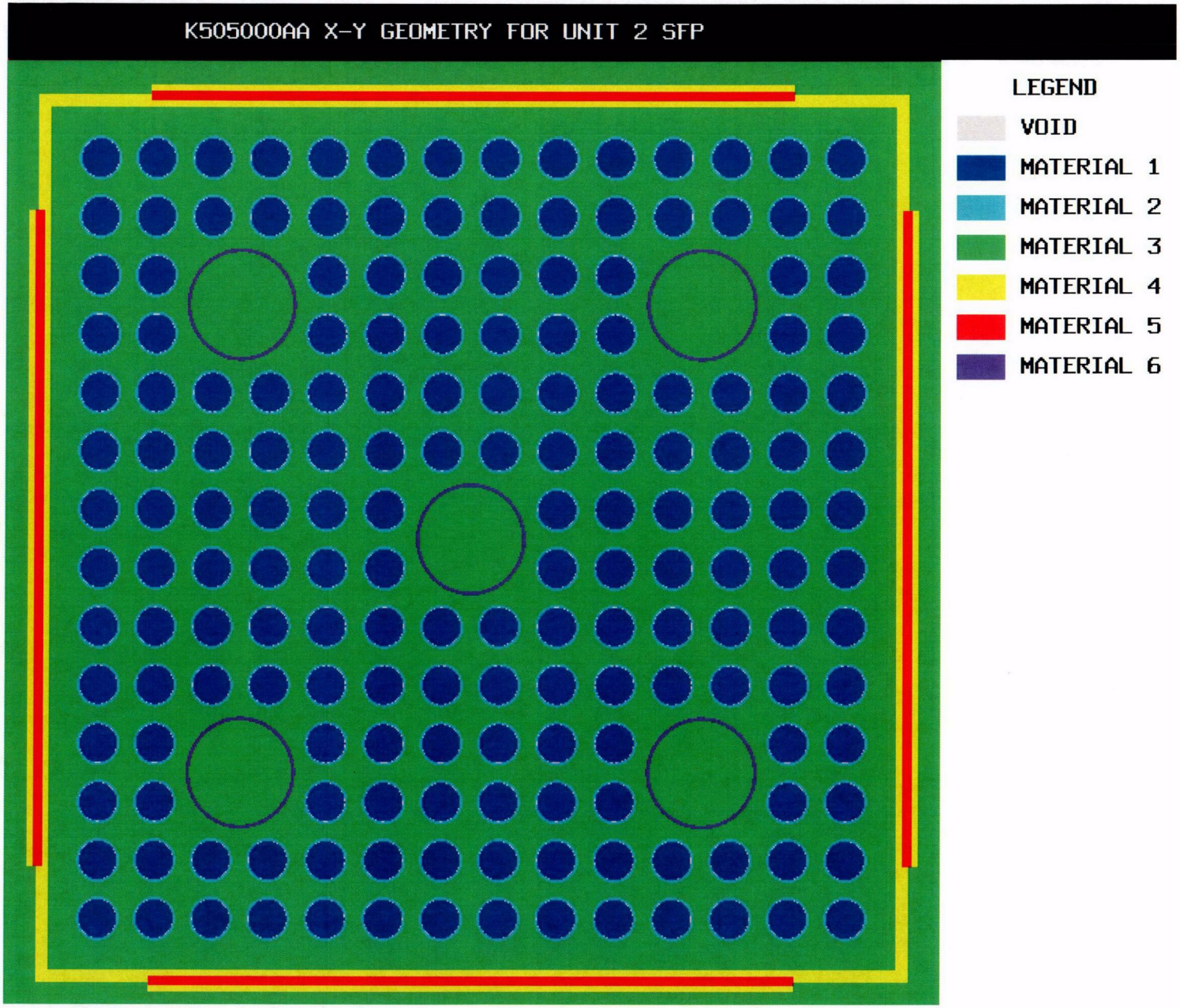
K505000AA X-Y GEOMETRY FOR UNIT 2 SFP
LEGEND
VOID
MATERIAL 1
MATERIAL 2
MATERIAL 3
MATERIAL 4
MATERIAL 5
MATERIAL 6

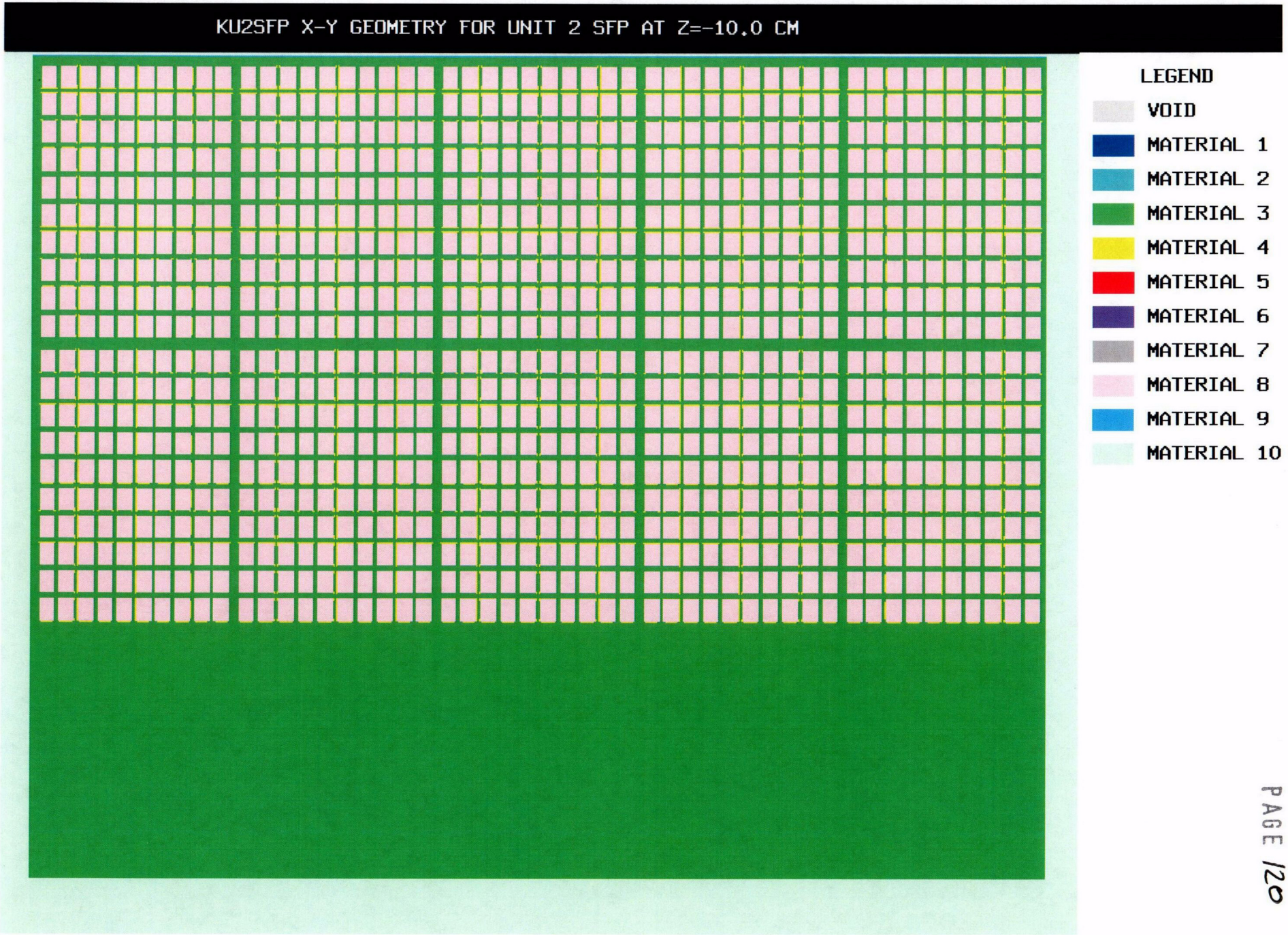
KU2SFP X-Y GEOMETRY FOR UNIT 2 SFP AT Z=-10.0 CM
LEGEND
VOID
MATERIAL 1
MATERIAL 2
MATERIAL 3
MATERIAL 4
MATERIAL 5
MATERIAL 6
MATERIAL 7
MATERIAL 8
MATERIAL 9
MATERIAL 10

KU2CON X-Y GEOMETRY FOR UNIT 2 SFP AT Z=10.0 CM

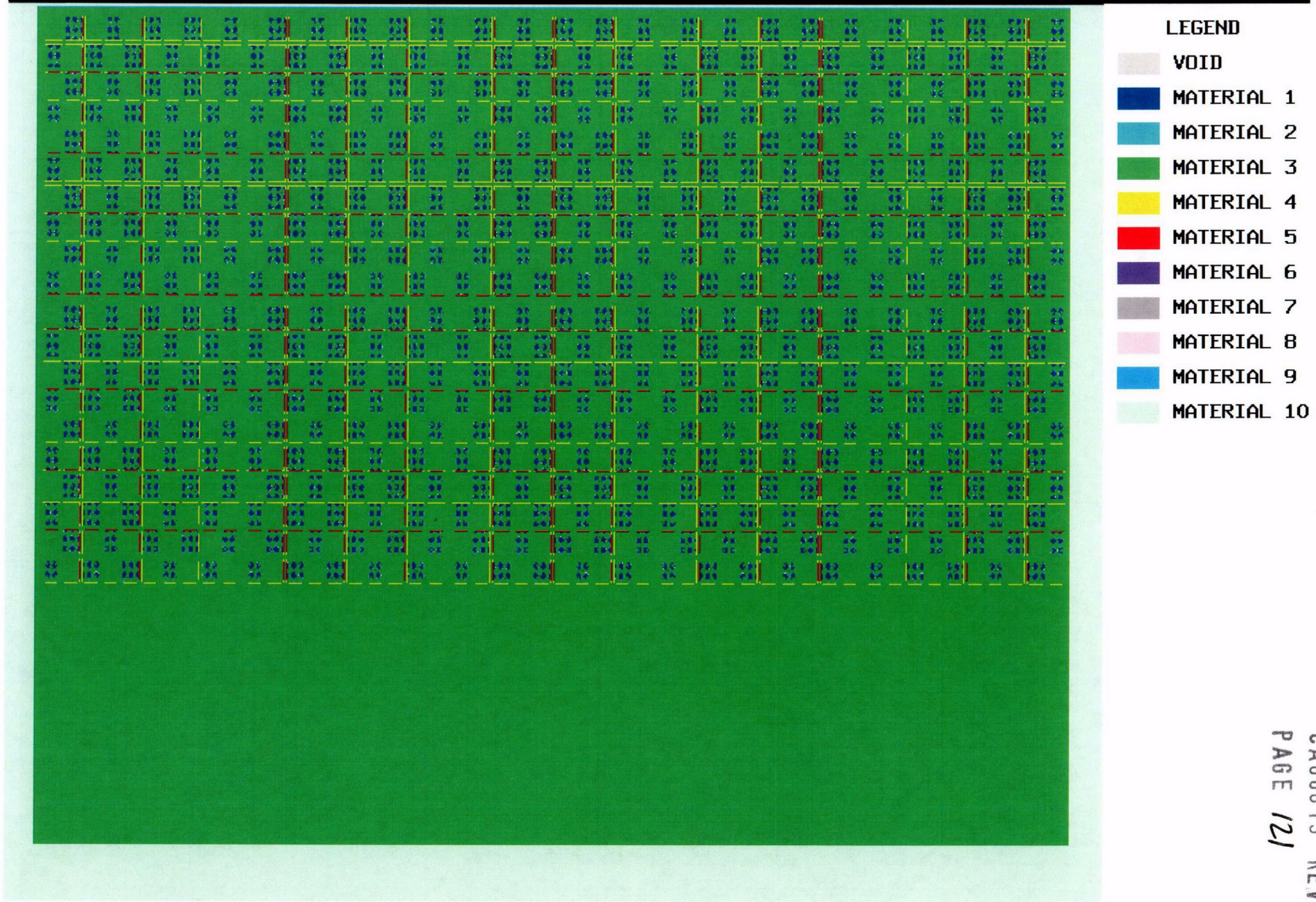

KU2CON X-Y GEOMETRY FOR UNIT 2 SFP AT Z=10.0 CM

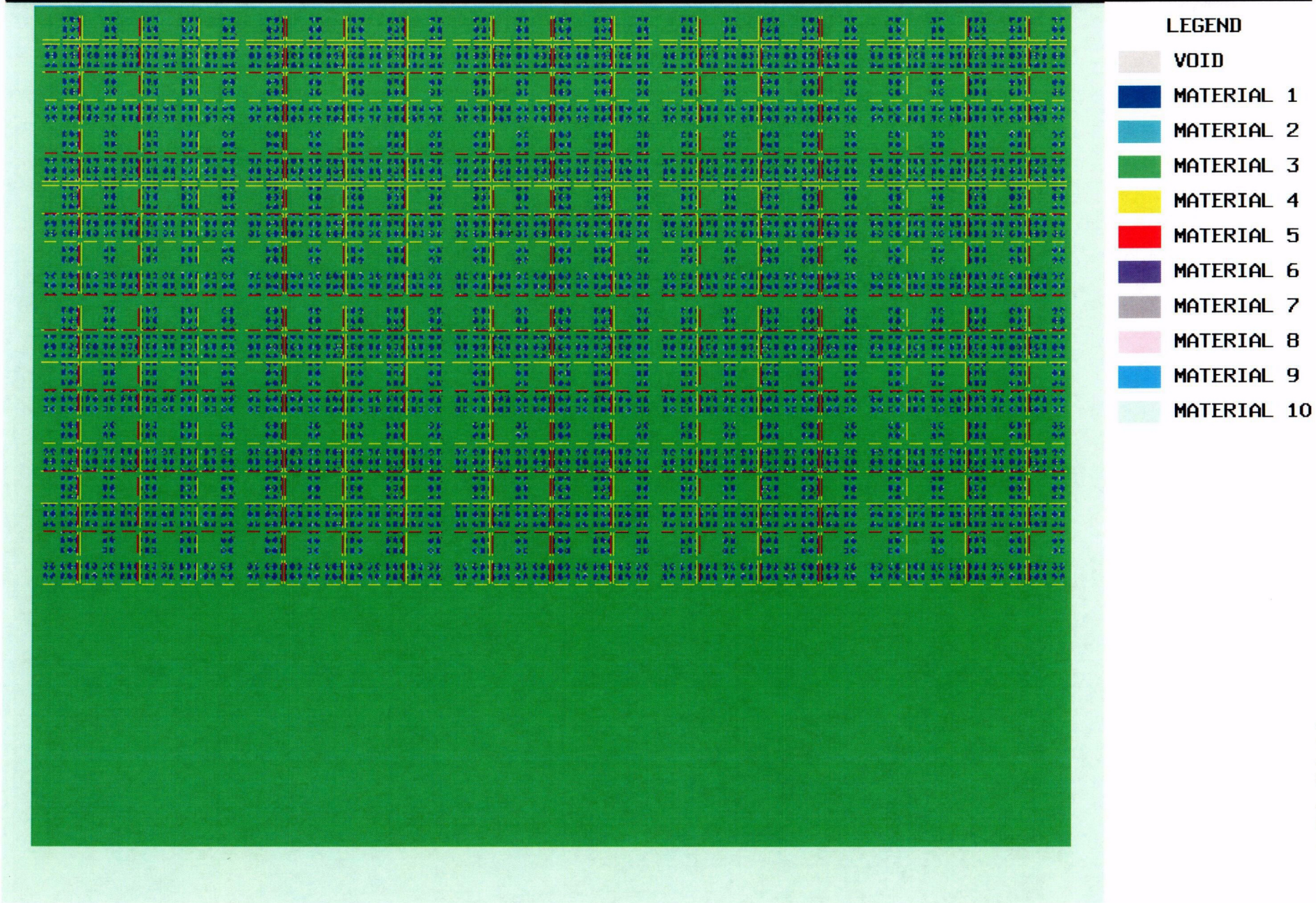

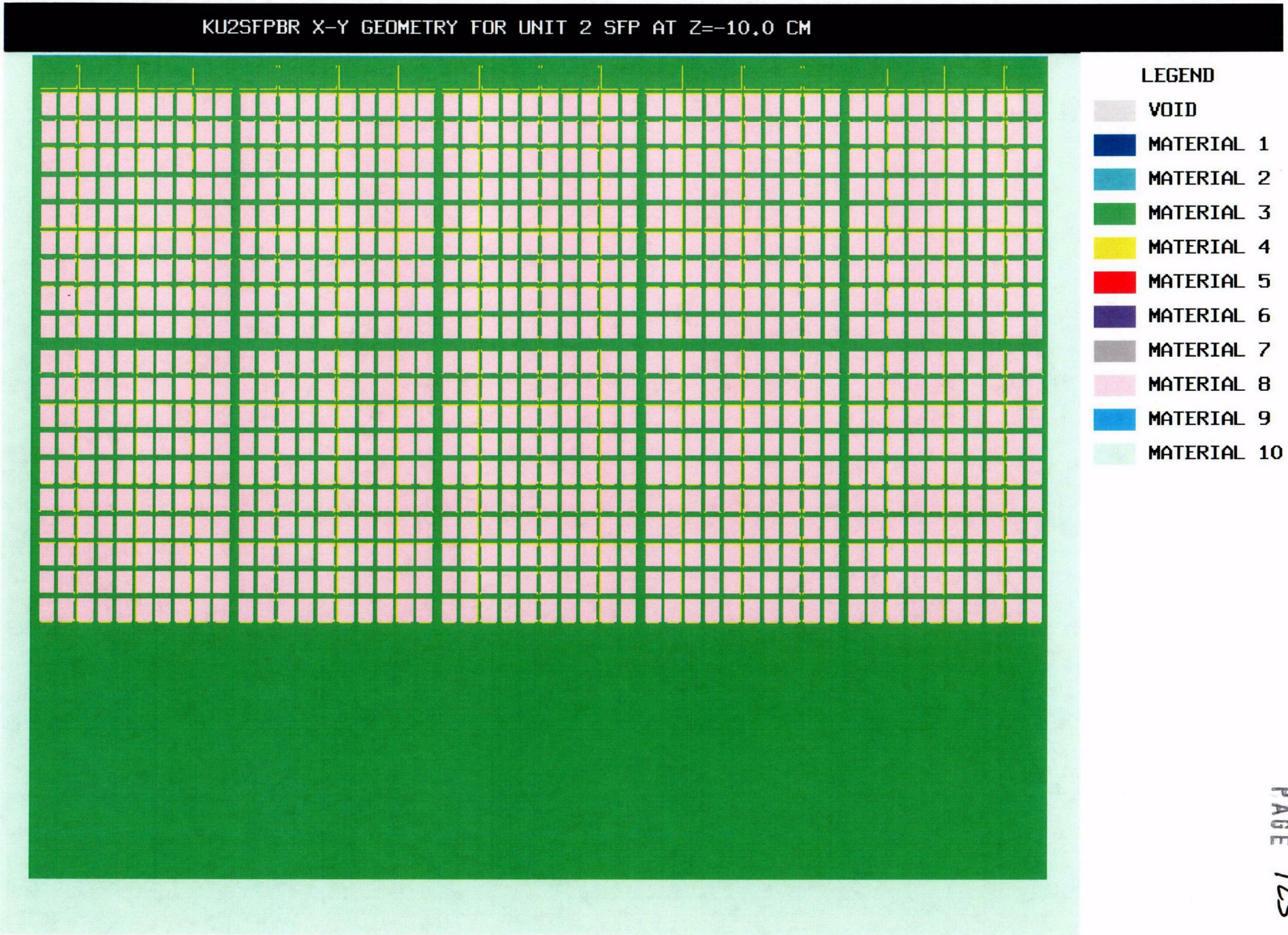
KU2SFPBR X-Y GEOMETRY FOR UNIT 2 SFP AT Z=-10.0 CM
LEGEND
VOID
MATERIAL 1
MATERIAL 2
MATERIAL 3
MATERIAL 4
MATERIAL 5
MATERIAL 6
MATERIAL 7
MATERIAL 8
MATERIAL 9
MATERIAL 10